Charakterisierung der humanen Glutaminyl-Cyclase im Vergleich mit dem analogen Enzym aus *Carica papaya*

Kumulative Dissertation

zur Erlangung des akademischen Grades

doctor rerum naturalium (Dr. rer. nat.)

vorgelegt der

Mathematisch-Naturwissenschaftlich-Technischen Fakultät
(mathematisch-naturwissenschaftlicher Bereich)
der Martin-Luther-Universität Halle-Wittenberg

von

Herrn Dipl.-Biochem. Stephan Schilling

geb. am: 30.05.1976 in: Halle (Saale)

Gutachterin bzw. Gutachter:

1. Prof. Dr. C. Wasternack
2. PD Dr. H.-U. Demuth
3. Prof. Dr. D. Schomburg

Halle (Saale), 05.05.2004

Inhaltsverzeichnis

Anhang

Abkürzungsverzeichnis

AD	„Alzheimer`s Disease", Alzheimersche Erkrankung
AMC	7-Amino-4-methyl-cumarin
ApAP	*Aeromonas proteolytica* Aminopeptidase
APA	Aminopeptidase A, Glutamyl-Aminopeptidase
APN	Aminopeptidase N, Alanyl-Aminopeptidase
APP	„Amyloid Precursor Protein"
βNA	2-Naphthylamin
CD	Circulardichroismus
DTT	Dithiothreitol
EC	Glutamyl-Cyclase; Glutamyl-Cyclase Aktivität
FPP	„Fertilization Promoting Peptide"
FTIR	„Fourier Transform Infrared Spectroscopy"
GDH	Glutamat-Dehydrogenase
GnRH	„Gonadotropin Releasing-Hormone", Gonadoliberin
MCP	„Monocyte Chemotactic Protein"
pGAP	Pyroglutamyl-Aminopeptidase
pGlu, pE	Pyroglutamat, Pyroglutamyl-
pNA	4-Nitroanilin
PMSF	Phenylmethansulfonylfluorid
QC	Glutaminyl-Cyclase
TRH	„Thyrotropin Releasing-Hormone", Thyreoliberin

1 Einleitung – Ziel der Arbeit

Glutaminyl-Cyclasen (QC; EC 2.3.2.5) sind im Tier- und Pflanzenreich weit verbreitete Enzyme der Familie der Acyltransferasen. Sie katalysieren die Bildung von Pyroglutamyl-Peptiden oder -Proteinen aus N-terminalem Glutamin. Bei der Reaktion wird Ammoniak freigesetzt (Abb. 1.1).
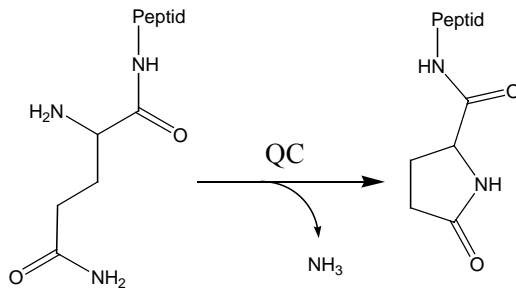

Abb. 1.1: Die Zyklisierung von N-terminalen Glutaminylresten, katalysiert durch Glutaminyl-Cyclasen (QCs). Produkt der Reaktion ist ein 5-gliedriger Lactamring (generisch auch Pyroglutamat oder 5-Oxo-Prolin genannt), der die basischen Eigenschaften eines Peptid-N-Terminus nicht mehr aufweist.

Eine QC wurde erstmals von Messer (1963) beschrieben, der das Protein aus dem Latex der tropischen Pflanze *Carica papaya* isolierte. Das analoge Enzym tierischen Ursprungs konnte später im Hypophysengewebe von Säugern nachgewiesen werden (Busby *et al.*, 1987; Fischer und Spiess, 1987). Die Primärstrukturen der QCs aus *C. papaya*, Mensch und Rind wurden aufgeklärt (Song *et al.*, 1994; Pohl *et al.*, 1991; Dahl *et al.*, 2000). Obgleich die Enzyme tierischen und pflanzlichen Ursprungs offenbar Ähnlichkeiten in der Spezifität und im katalytischen Verhalten aufweisen (siehe Abschnitt 3, S. 14), haben die Sequenzuntersuchungen gezeigt, dass zwischen der QC aus *C. papaya* und den Enzymen der Säuger keine Homologie besteht (Bateman *et al.*, 2001). Es wird auch vermutet, dass die physiologischen Funktionen der pflanzlichen und tierischen QCs nicht übereinstimmen. Während die QC aus *C. papaya* vermutlich durch die Produktion von Ammonium-Ionen in die pflanzliche Pathogen-Abwehr involviert ist, spielen die tierischen QCs eine Rolle bei der Synthese von Pyroglutamyl-Peptiden wie z.B. Hormonen bzw. Neuropeptiden (siehe Abschnitt 4, S. 21). Die Evolution der QCs tierischer und pflanzlicher Herkunft führte offenbar zu funktionell ähnlichen Enzymen, die sich jedoch strukturell und physiologisch unterscheiden.

In jüngerer Zeit gibt es zunehmend Berichte, die Pyroglutamyl-Peptiden eine Rolle bei der Entstehung und Progression humaner pathophysiologischer Prozesse, wie zum Beispiel der Alzheimerschen Erkrankung und anderer Amyloidosen, zuweisen (siehe Abschnitt 5, S. 24). In vielen dieser Fälle scheint die Pyroglutamyl-Bildung jedoch aus N-terminalen Glutaminsäure-

Resten und nicht aus Glutamin zu erfolgen. Deshalb wurde eine QC-Katalyse der pGlu-Bildung aus Glutamat bisher in Frage gestellt (Garden *et al.*, 1999).

Ziel der vorgelegten Arbeit war es, die katalytischen Eigenschaften einer tierischen und einer pflanzlichen QC zu charakterisieren. Durch die vergleichende Betrachtung der humanen QC und der QC aus *C. papaya* sollten katalytische Unterschiede, welche durch die unterschiedliche Struktur dieser Proteine bedingt sein könnten, identifiziert werden. Im Vordergrund stand dabei auch, ob die menschliche QC auf Grund ihrer katalytischen Spezifität eine Rolle bei der Entstehung von amyloidogenen Ablagerungen spielen könnte.

2 Vorkommen, Biosynthese und Struktur der Glutaminyl-Cyclasen (QCs)

Die QC aus *C. papaya* kommt hauptsächlich im Latex vor, einem Sekret, welches bei Verwundung der Pflanze austritt und als Schutz vor Infektionen dient. Es wurde daher vermutet, dass die QC von den Latex-produzierenden Zellen sezerniert wird (Zerhouni *et al.*, 1997). Diese Vermutung konnte durch die Aufklärung der Primärstruktur und einer N-terminalen Signalsequenz, die den cotranslationalen Transport ins endoplasmatische Retikulum (ER) bewirkt, bestätigt werden (Dahl *et al.*, 2000). Offenbar wird das Enzym nach Translokation über den Golgi-Apparat und sekretorische Vesikel von der Zelle sezerniert. Die Isolation einer Papaya-QC cDNA führte auch zur Identifizierung homologer mRNA-Sequenzen in anderen Pflanzenarten, so z.B. der Tomate und *Arabidopsis thaliana* (Dahl *et al.*, 2000). Die Sequenzidentität zu anderen pflanzlichen QCs liegt zwischen 54 % und 64 %. Diese hohe Konservierung der Sequenz lässt funktionsfähige QCs auch in diesen Pflanzen erwarten. Eine Isolation oder ein Nachweis der katalytischen Aktivität einer QC in anderen Pflanzenarten erfolgte bisher jedoch noch nicht.

Obgleich zwischen den QCs tierischer und pflanzlicher Herkunft keine Homologien bestehen, ähnelt sich offensichtlich ihr intrazelluläres Vorkommen. Die QCs der Vertebraten, deren Sequenz anscheinend hoch konserviert ist (Bateman *et al.*, 2001), werden ebenfalls durch eine Signalsequenz in das ER transportiert. Erste immunologische Untersuchungen zur intrazellulären Lokalisation des Enzyms aus Rinderhypophyse haben gezeigt, dass das Protein nach Passage des Golgi-Apparats in sekretorischen Vesikeln nahe der Zellmembran lokalisiert ist (Bockers *et al.*, 1995). Wahrscheinlich wird die QC nach Empfang eines extrazellulären Signals zusammen mit den Produkten ihrer Katalyse, den Pyroglutamyl-Peptiden, von der Zelle sezerniert. Es wird vermutet, dass die reife QC auch in anderen Organen über diesen Sekretionsweg, der als reguliert-sekretorisch bezeichnet wird („Regulated Secretory Pathway", RSP), gebildet wird.

Tierische und pflanzliche QC ähneln sich jedoch nicht nur hinsichtlich ihres Vorkommens. Beide Enzyme sind monomere Glykoproteine mit einem Zuckeranteil von ca. 4 kDa (Pohl *et al.*, 1991; Zerhouni *et al.*, 1998) und weisen ein ähnliches Molekulargewicht von ca. 33 kDa (*C. papaya*) bzw. 40-42 kDa (humane QC) auf (Schilling *et al.*, 2002b; Zerhouni *et al.*, 1998; Pohl *et al.*, 1991). Untersuchungen der Sekundärstruktur beider Proteine haben jedoch gezeigt, dass im Faltungsmuster deutliche Unterschiede, bedingt durch unterschiedliche Primärstrukturen, bestehen. CD- und FTIR- Untersuchungen der Papaya-QC zeigten fast ausschließlich β-Faltblattstruktur (Oberg *et al.*, 1998). Es wird vermutet, dass das Protein eine sehr kompakte Struktur besitzt, gekennzeichnet durch sehr kurze, unflexible „loops" an der Oberfläche (Oberg *et al.*, 1998). Infolgedessen besitzt das Enzym eine außerordentliche Stabilität gegenüber proteolytischem Abbau sowie thermischer und chemischer Denaturierung. Offenbar ist diese katalytische Stabilität in dem an Proteasen reichen Latex notwendig (Oberg *et al.*, 1998).

Im Gegensatz zur Papaya-QC konnte für eine rekombinant exprimierte humane QC im Rahmen dieser Arbeit ein hoher α-helikaler Anteil nachgewiesen werden (Schilling *et al.*, 2002a). Auf Grund der verschiedenen Sekundärstrukturen beider Enzymformen ist davon auszugehen, dass auch die Tertiärstruktur deutliche Unterschiede aufweist. Da die pflanzliche QC keine Homologie zu anderen Enzymen besitzt und offenbar einer unikaten Strukurfamilie angehört (Dahl *et al.*, 2000), kann ein verlässliches Modell der dreidimensionalen Struktur nicht erstellt werden. Die Identifizierung einer hohen Strukturhomologie der humanen QC zu bakteriellen Zn-abhängigen Aminopeptidasen des „Clans" MH[1] führte hingegen zu ersten Vorstellungen über die Tertiärstruktur der tierischen QCs (Bateman *et al.*, 2001). Das meistuntersuchte Enzym dieser Familie ist die Leucin-Aminopeptidase aus *Aeromonas proteolytica* (ApAP) (Bennett und Holz, 1997; Prescott *et al.*, 1985; Prescott und Wilkes, 1966; Prescott *et al.*, 1971; Wagner *et al.*, 1972; Wilkes *et al.*, 1973; Prescott und Wilkes, 1976). Die Struktur dieser monomeren Peptidase, die auch hinsichtlich ihrer Größe in etwa den tierischen QCs entspricht, ist durch ein gedrehtes, 8-strängiges β-Faltblatt geprägt (Chevrier *et al.*, 1994) (Abb. 2.1A). Die Peptidkette ist in eine einzelne α/β-globuläre Domäne gefaltet. Das teils parallel, teils antiparallel angeordnete zentrale Faltblatt bildet den hydrophoben Kern des Proteins, umgeben von α-Helices. Dieses Strukturmerkmal ist charakteristisch für Proteine der Zn-Hydrolase-Superfamilie und dient häufig als Anhaltspunkt, um die Strukturen der Hydrolasen miteinander zu vergleichen und Untersuchungen über deren evolutionäre Veränderungen durchzuführen (Lowther und Matthews, 2002). Das aktive Zentrum der Peptidase, in dem zwei Zink-Ionen gebunden sind, befindet sich an der Oberfläche des Proteins und ist für Lösungsmittelmoleküle gut zugänglich.

---

[1]Protease-Klassifikation nach Barrett und Rawlings (http://merops.sanger.ac.uk)

Fünf Aminosäureseitenketten, entsprechend dem Motiv His-Asp-Glu-Asp-His, welches für den „Clan" MH kennzeichnend ist, bilden ein verdrehtes, tetraedrisches Koordinationsmuster der beiden Zn-Ionen. Gemeinsame Koordinationspartner sind ein Wassermolekül und ein Aspartatrest. Das aktive Zentrum ist in einer Region in der Nähe des carboxyterminalen Endes des Faltblattes lokalisiert. Die gebundenen Metallionen, bezeichnet als Zn_1 und Zn_2, haben einen Abstand von 3,5 Å zueinander. Das Wassermolekül attackiert bei der Katalyse die zu spaltende Peptidbindung.
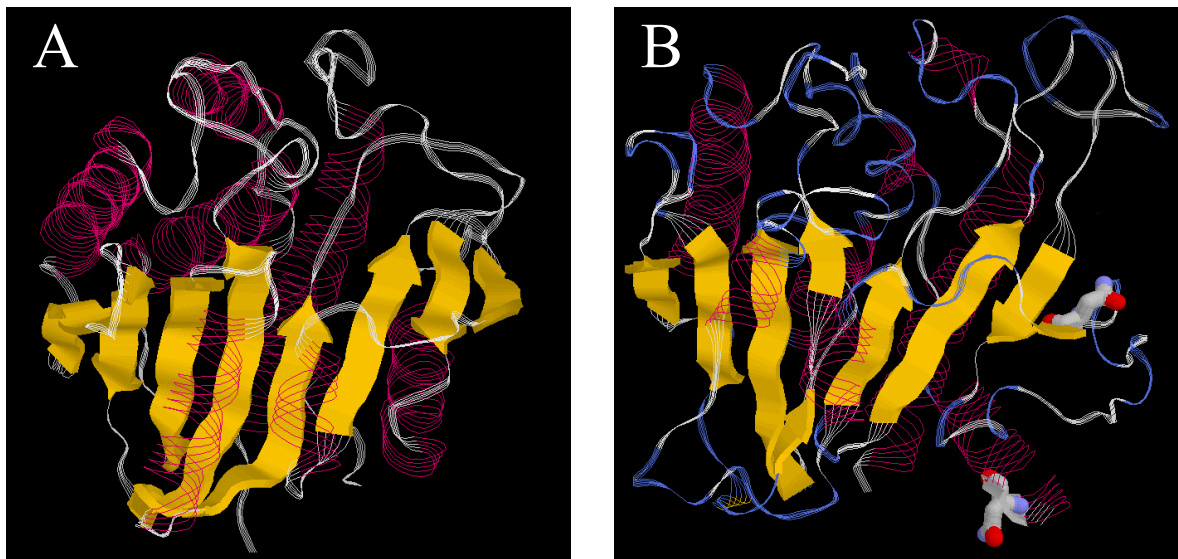

Abb. 2.1: Vergleich der Tertiärstruktur der Leucin-Aminopeptidase aus *Vibrio proteolyticus* (*Aeromonas proteolytica*) (A) mit der mutmaßlichen Struktur der humanen QC (B). Letztere wurde *in silico* anhand von Sequenz und Struktur der bakteriellen Peptidase modelliert. Gemeinsames Strukturmerkmal ist ein zentrales, 8-strängiges β-Faltblatt, welches charakteristisch für die Metallopeptidase-Superfamilie ist. Die humane QC weist zwei N-Glykosylierungsstellen auf. Die entsprechenden Asparaginyl-Seitenketten sind hervorgehoben und liegen an der Oberfläche des Enzyms. Das Modell der humanen QC wurde mit dem Programm 3D-pssm (www.sbg.bio.ic.ac.uk) in Zusammenarbeit mit Herrn Dr. J.-U. Rahfeld erstellt.

Durch einen Vergleich der Struktur der ApAP mit der modellierten Struktur der humanen QC (Abb. 2.1B) wird die Homologie veranschaulicht. Wie im Fall der ApAP ist die Peptidkette der humanen QC in eine α/β-globuläre Domäne gefaltet. Das ebenfalls 8-strängige zentrale β-Faltblatt und die umgebenden Helices verdeutlichen die Zugehörigkeit des Proteins zur Metallopeptidase-Superfamilie. Die Validität des Strukturmodells der humanen QC kann zudem durch einige experimentelle Ergebnisse belegt werden. Wie in eigenen Untersuchungen zur heterologen Expression der humanen QC in *Pichia pastoris* gezeigt werden konnte, führt die N-Glykosylierung an den Seitenketten der beiden Asparaginyl-Reste N49 und N296 zu einem

Enzym, welches eine nahezu identische katalytische Aktivität wie eine gereinigte QC aus Rinderhypophyse aufweist (Schilling *et al*., 2002a). Eine Deglykosylierung des Proteins hatte keinen Einfluss auf die Enzymkatalyse. Anscheinend wird die strukturelle Beschaffenheit des Proteins durch die Abspaltung der Oligosaccharide nicht beeinflusst. Dies wird auch durch die Expression von enzymatisch aktiver QC in *E. coli* bestätigt, wobei keine Glykosylierung erfolgt (Schilling *et al*., 2002a; Bateman *et al*., 2001). Die fehlende Glykosylierung führt jedoch zu einer stark herabgesetzten Löslichkeit des Proteins (unpublizierte eigene Ergebnisse). Da die rekombinante humane QC im nativen Zustand enzymatisch deglykosyliert werden konnte, scheinen beide Glykosylierungsstellen an der Oberfläche des Proteins an exponierten Stellen vorzuliegen (Schilling *et al*., 2002a). Wie in Abb. 2.1B gezeigt, spiegelt das Strukturmodell diese Beobachtung wider, da die Asparaginylreste 49 und 296 an der Oberfläche des Proteins lokalisiert sind.

Einen weiteren Hinweis auf die Richtigkeit des Modells der humanen QC und somit für ihre strukturelle Verwandtschaft mit Zn-abhängigen Peptidasen lieferte in der vorliegenden Arbeit die Identifikation einer für die katalytisch aktive Struktur essentiellen Disulfidbrücke (Schilling *et al*., 2002a). Die humane QC wie auch die ApAP besitzen in ihrer Primärstruktur lediglich zwei Cysteinreste (vgl. Abb. 2.2). Im Fall der ApAP bildet die Disulfidbrücke eine strukturelle Komponente bei der Ausbildung einer hydrophoben Tasche, in der eine Wechselwirkung mit der ersten Aminosäureseitenkette des Substrates erfolgt. Dadurch wird die Spezifität des Enzyms bewirkt und die strukturelle Integrität des aktiven Zentrums stabilisiert (Chevrier *et al*., 1994) (s. auch Abb. 3.3, S. 19). Durch Modellierung der Struktur der humanen QC anhand der ApAP-Struktur werden auch die beiden Cysteine der QC in eine Nähe zueinander gebracht, die auf die Bildung einer Disulfidbrücke unter oxidativen Bedingungen schließen lässt. Im Fall der QC liegt die Disulfidbrücke in der Nähe des hydrophoben Kerns des Proteins, bei der ApAP dagegen eher an der Proteinoberfläche. Da eine Spaltung der Bindung mittels DTT zur Inaktivierung der QC führte, scheint der Disulfidbrücke auch eine Rolle bei der Stabilisierung der Struktur des aktiven Zentrums zuzukommen (Schilling *et al*., 2002a). Interessanterweise ist die mit der Inaktivierung verbundene Strukturänderung des gesamten Proteins gering (Schilling *et al*., 2002a), was durch eine lokale strukturelle Änderung in der Nähe des aktiven Zentrums begründet sein könnte.

Als wichtigster experimenteller Hinweis auf die Verwandtschaft der humanen QC zu Zn-abhängigen Aminopeptidasen kann die Identifizierung der Metallabhängigkeit der QC-Katalyse angesehen werden (Schilling *et al*., 2003b). Dieser Zusammenhang macht es außerordentlich wahrscheinlich, dass die tierischen QCs evolutionär aus einer bakteriellen Peptidase hervorgegangen sind. Das mutmaßliche aktive Zentrum der humanen QC ist in Analogie zur ApAP in Abb. 2.2B gekennzeichnet.
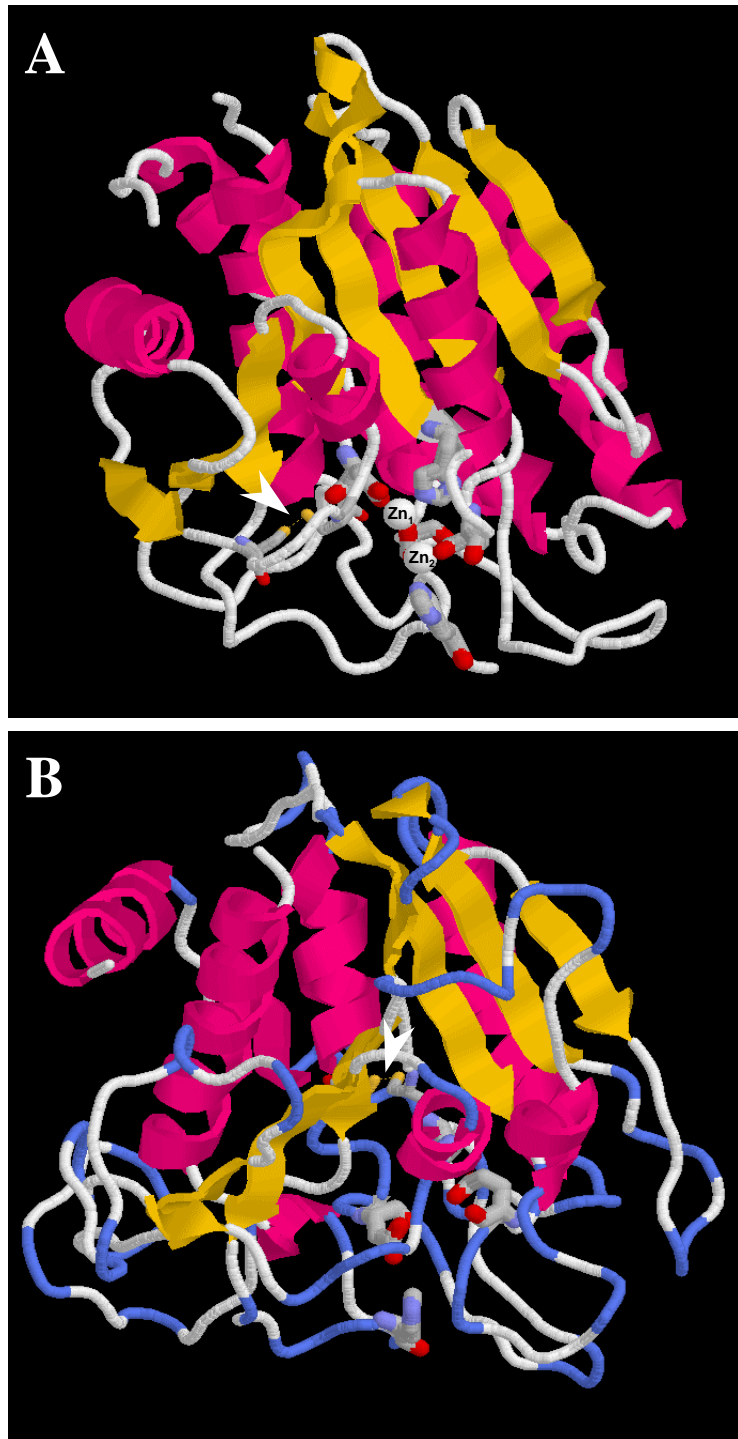
Abb. 2.2: Tertiärstruktur der ApAP (A) und der mutmaßlichen Struktur der humanen QC (B), dargestellt in annähernd vergleichbarer Perspektive, im Vordergrund die aktiven Zentren. Die metallbindenden Aminosäureseitenketten der Enzyme sind gekennzeichnet. Das typische Bindungsmotiv His-Asp-Glu-Asp-His der Aminopeptidasen bildet zusammen mit einem Wassermolekül ein nahezu tetraedrisches Koordinationsmuster der beiden Zink-Ionen der ApAP aus (Chevrier *et al.*, 1994). Vier der fünf komplexierenden Aminosäureseitenketten kennzeichnen auch das wahrscheinliche aktive Zentrum der QC. Die Lage der fünften Aminosäure ist dem Modell nicht mit Verlässlichkeit zu entnehmen. Die einzigen beiden Cysteinreste in den Enzymen bilden eine Disulfidbrücke in der Nähe des aktiven Zentrums (weiße Pfeilspitze).

Obwohl das in Abb. 2.1 und 2.2 gezeigte Modell der humanen QC durch die experimentellen Ergebnisse gestützt wird, ist eine genaue Aussage über die Strukturverhältnisse im aktiven Zentrum der QC im Sinne einer Aufklärung des enzymatischen Mechanismus (siehe Abschnitt 3, S. 12) nicht möglich. Ein hauptsächliches Problem stellt in diesem Zusammenhang die Zahl der am Enzym gebundenen Metallionen dar. Es ist noch unklar, ob die QC wie die verwandten Peptidasen zwei Zn-Ionen bindet oder nur eines. Einen Hinweis für die mögliche Bindung zweier Metallionen lieferte der Sequenzvergleich der QC mit zwei Vertretern des „Clans" MH (Schilling *et al.*, 2003b). Wie gezeigt werden konnte, sind die in den Metalloenzymen für die Metallbindung verantwortlichen Reste auch in der QC-Primärstruktur vorhanden. Weiterhin ist das Metallbindungsmotiv His-Asp-Glu-Asp-His auch in QCs anderer tierischer Organismen konserviert, wie ein Sequenzvergleich zeigt (Abb. 2.3). Gegen eine Bindung von zwei Zn-Ionen spricht die beobachtete Inhibierung der QC-Aktivität durch Zn-Konzentrationen über 0,1 mM. Eine Inhibierung durch Metallionen ist für die Vertreter des Clans MH untypisch, ist aber für Metalloenzyme, die nur ein Zn-Ion in ihrem aktiven Zentrum besitzen, beschrieben worden (Lowther und Matthews, 2002).

Ein weiteres Indiz für die Bindung von nur einem Metallion könnten mechanistische Überlegungen liefern (siehe Abb. 3.4, S. 20). Da die QC kein gebundenes Wassermolekül für die Reaktion benötigt, sondern das Nucleophil vom Substrat selbst zur Verfügung gestellt wird (nämlich die α-Aminogruppe des N-terminalen Gln), ist die Notwendigkeit eines zweiten Zn-Ions für die Katalyse nur schwer vorstellbar. Auf Grund dieser ungeklärten Metallbindung in der QC ist eine verlässliche Voraussage der dreidimensionalen (3D-) Struktur des aktiven Zentrums des Enzyms nicht möglich, da wie im Fall der ApAP flexible Regionen der Peptidkette an seiner Ausbildung beteiligt sind. Die Klärung der Metallbindung würde die Frage beantworten, ob einige der Regionen mit flexibler Struktur fixiert werden können.

Bedingt durch die Strukturhomologie der humanen QC zu bakteriellen Zn-abhängigen Aminopeptidasen, existieren im Gegensatz zur pflanzlichen QC erste Vorstellungen über die Faltung der Peptidkette in eine 3D-Proteinstruktur. Interessant ist in diesem Zusammenhang, dass die Proteine tierischer und pflanzlicher Herkunft trotz offensichtlich deutlicher Unterschiede in ihrer Struktur Ähnlichkeiten in ihrer Spezifität aufweisen (siehe Abschnitt 3, S. 12). Eine verlässliche Klärung, inwieweit die strukturelle Divergenz durch Unterschiede im katalytischen Mechanismus reflektiert wird, erfordert die Aufklärung der 3D-Proteinstruktur. Der Nachweis einer metallabhängigen Katalyse der humanen QC ließ jedoch erste Vermutungen zu möglichen Unterschieden im Mechanismus der tierischen und pflanzlichen QCs zu, da die QC aus *C. papaya* metallunabhängig katalysiert (Schilling *et al.*, 2003b) (Abschnitt 3, S. 12).

```
QC Mensch        ----SAWPEEKNYHQPAILNSSALRQIAEGTSISEMWQNDLQPLLIERYPGSPGSYAARQ
QC Rind          ----VDWTQEKNYHQPALLNVSSLRQVAEGTSISEMWQNDLRPLLIERYPGSPGSFAARQ
QC Maus          ----AAWTQEKNHHQPAHLNSSSLQQVAEGTSISEMWQNDLRPLLIERYPGSPGSYSARQ
B. jararaca      REDRADWTQEKYSHRPTILNATCILQVTSQTNVSRMWQNDLHPILIERYPGSPGSYAVRQ
C. elegans       -----QWRTNQRTHQLSLLPESSTLRLCRDFTNTTRFKEILAPIMVPRIVDTKQHRQVGD
D. melanogaster  --CFELVDIPKISYNPSELSEPRFLEYSN-LSDKLHLREAIDKILIPVVGTTNHSIVRE
L. mayor         -----GWELSYEQYHAAHLNEA----INPDSGWNKSTKNLLLPFNRTRVPGSEGSREIQR
                      :. : *  .                .    ::  :  :    *   .:

QC Mensch        HIMQRIQR-LQADWVLEIDTFLSQTPY-GYRSFSNIISTLNPTAKRHLVLACHYDSKYFS
QC Rind          HIMQRIQR-LQADWVLEVDTFLSQTPY-GYRSFSNIISTLNPTAKRHLVLACHYDSKYFP
QC Maus          HIMQRIQR-LQAEWVVEVDTFLSRTPY-GYRSFSNIISTLNPEAKRHLVLACHYDSKYFP
B. jararaca      HIKHRLQG-LQAGWLVEEDTFQSHTPY-GYRTFSNIISTLNPLAKRHLVIACHYDSKYFP
C. elegans       YLQSFLH---NLGFATEWDAFTDTTPL-GTRNFRNLIATFDESAPRRLVLACHYDSKIIP
D. melanogaster  YIVQSLR---DLDWDVEVNSFHDHAPIKGKLHFHNIIATLNPNAERYLVLSCHYDSKYMP
L. mayor         FIIEHFNNTLAGEWAVETQAFEEN----GYR-FNNLVMTLQNNASEYLVLAAHYDTKIAP
                  .:   :.      :  * ::* .     *   * *:: *::  *  . **::.***:* .

QC Mensch        -HWNNRVFVGATDSAVPCAMMLELARALD-------KKLLSLKT---VSDS-KPDLSLQ
QC Rind          -HWDDRVFVGATDSAVPCAMMLELARALD-------KQLFSLKN---ISDS-RPDLSLQ
QC Maus          -RWDSRVFVGATDSAVPCAMMLELARALD-------KKLHSLKD---VSGS-KPDLSLR
B. jararaca      PQLDGKVFVGATDSAVPCAMMLELARSLD-------RPLSFLKQ---SSLPPKADLSLK
C. elegans       ----SQVMIAATDSAVPCAMMLDIAQTLA-------PYMY--KR---VAQQ----IGLQ
D. melanogaster  ----GVEFLGATDSAVPCAMLLNLAQVLQ-------EQLKPLK------KS---KLSLM
L. mayor         ---TG--MVGAIDSAASCAALLYTAQFLTHIACHERTKEYNDLESNTVVSNS---TLGVK
                     .  ::.* *** .** :*  *:  *           :            :.:

QC Mensch        LIFFDGEEAFLHWSPQDSLYGSRHLAAKMASTPHPPGA-----RGTSQLHGMDLLVLLDL
QC Rind          LIFFDGEEAFHLWSPQDSLYGSRHLASKMASTPHPPGA-----RDTNQLHGMDLLVLLDL
QC Maus          LIFFDGEEAFHHWSPQDSLYGSRHLAQKMASSPHPPGS-----RGTNQLDGMDLLVLLDL
B. jararaca      LIFFDGEEAFVRWSPSDSLYGSRSLAQKMASTPHPPGA-----RNTYQIRGIDLFVLLDL
C. elegans       LIFFDGEEAFRDWTATDSLYGSRHLAQKWEQKWYPSSSSLNNFELSKELDRIDVLMLLDL
D. melanogaster  LLFFDGEEAFEEWGPKDSIYGARHLAKK-W--HH-EG----------KLDRIDMLVLLDL
L. mayor         IVFFDGEEAIEEWGPEDSIYGARRLAAQ----WLADG----------TMTRIRLLFLLDL
                 ::*******:  *  . **:**:* ** :         .          : : ::.****

QC Mensch        IGAPN--PTFPNFFPN-SARWFERLQAIEHELH-----ELGLLKDHSL----EG-----R
QC Rind          IGAPF--PTFPNFFPN-TARWFGRLEAIEHGLR-----ELGLLKDHSS----ER-----W
QC Maus          IGAAN--PTFPNFFPK-TTRWFNRLQAIEKELY-----ELGLLKDHSL----ER-----K
B. jararaca      IGARN--PVFPVYFLN-TARWFGRLEAIERNLN-----DLGLLNNYSS----ER-----Q
C. elegans       LGAAN--PSIGNTIGMGANDLFSQLADVESNLR-----TSGCLSSLR------R-----N
D. melanogaster  LGAPD--PAFYSFFEN-TESWYMRIQSVETRLA-----KLQLLERYASSGVAQRDPT--R
L. mayor         LGSGEEEPLVPSYYAE-THQEYQLLNRIEDDLLFRRGDEINGESALAAEVARQRKHLDPT
                 :*:     *  .     :    :   :  :* *              .

QC Mensch        YFQNYSYG-GVIQDDHIPFLRRGVPVLHLIPSPFPEVWHTMDDNEENLDESTIDNLNKIL
QC Rind          YFRNYGYG-GVIQDDHIPFLRRGVPVLHLISSPFPEVWHTMDDNEENLDRTTIDNLNKIL
QC Maus          YFQNFGYG-NIIQDDHIPFLRKGVPVLHLIASPFPEVWHTMDDNEENLHASTIDNLNKII
B. jararaca      YFRSNLRR-HPVEDDHIPFLRRGVPILHLIPSPFPRVWHTMEDNEENLDKPTIDNLSKIL
C. elegans       VFNKQLSY-NQVEDDHIPFLKRGVPILHLITVPFPSVWHRSSDNANALHYPTIDHMTAVI
D. melanogaster  YFQSQAMRSSFIEDDHIPFLRRNVPILHLIPVPFPSVWHTPDDNASVIDYATTDNLALII
L. mayor         DYRFLGLGHSVIGDDHTPFLAAGVPVLHAIPLPFPSTWHTVDDDFRHLDAAETRHWALLV
                 :.        : *** *** .**:** *. *** .** .*: :.  :   ::

QC Mensch        QVFVLEYLHL-----
QC Rind          QVFVLEYLHL-----
QC Maus          QVFVLEYLHL-----
B. jararaca      QVFVLEYLNLG----
C. elegans       RVFVAKYLGIAPA--
D. melanogaster  RLFALEYLLAGTEAK
L. mayor         CEFVVQSLRSRNQ--
                  *. : *
```

Abb. 2.3: Sequenzvergleich der QCs einiger Vertebraten und Invertebraten. Innerhalb der Säuger ist die Primärstruktur konserviert. Charakteristisch für alle QCs ist eine Konservierung der mutmaßlich metallbindenden Aminosäuren (His-Asp-Glu-Asp-His, gekennzeichnet)(*D. melanogaster*, *Drosophila melanogaster*; *B. jararaca*, *Bothrops jararaca*; *L. mayor*, *Leishmania mayor*; *C. elegans*, *Caenorhabditis elegans*).

3 Der Reaktionsmechanismus der QCs

3.1 Nachweismethoden der Reaktion

Die durch die QC katalysierte Zyklisierung N-terminaler Glutaminylreste (siehe Abb. 1.1, S. 4) führt zu strukturellen Unterschieden zwischen Substrat und Produkt, die im sichtbaren Bereich des Lichts kaum Änderungen hervorrufen. Daher ist die Reaktion auf direktem und kontinuierlichem Weg nur schwer verfolgbar. Die Bildung des 5-gliedrigen Lactamringes aus der Seitenkette des Glutamins führt zwar zu geringen Unterschieden in der UV-Absorption bei 210-220 nm, was durch den elektronischen n→π* Übergang der Amidbindung verursacht wird. Diese Unterschiede ließen die kontinuierliche Untersuchung der QC-Katalyse anhand von Di- und Tripeptid-Substraten zu (Gololobov *et al.*, 1996; Gololobov *et al.*, 1994). Auf Grund der starken Absorption von Peptiden, Proteinen und DNA bei dieser Wellenlänge ist aber die Anwendbarkeit dieser Methode auf kurzkettige, aromatenfreie Substrate und gereinigte Enzymproben beschränkt. Zudem ist die Messung in diesem Wellenlängenbereich, bedingt durch die Absorption von gelöstem Sauerstoff, mit großen Fehlern und präparativem Aufwand verbunden. Dadurch ist die Analyse einer Vielzahl von Proben in kurzer Zeit, beispielsweise bei der Charakterisierung von Inhibitoren, nicht möglich. Andere Testmethoden zum Nachweis der QC-Katalyse basierten auf der Trennung von Substrat und Produkt mittels HPLC und gekoppelter photometrischer oder fluorimetrischer Detektion (Consalvo *et al.*, 1988; Fischer und Spiess, 1987) oder auf dem immunochemischen Nachweis des Produktes der Katalyse (TRH) mittels „Radioimmunoassay" (RIA) (Busby *et al.*, 1987; Koger *et al.*, 1989). In einer weiteren Methode wurde das durch die Zyklisierung gebildete Ammoniak mit α-Ketoglutarat und NADH/H$^+$ durch Glutamat-Dehydrogenase zu Glutamat und NAD$^+$ umgesetzt. Die Oxidation von NADH/H$^+$ zu NAD$^+$ führt dabei zu spektroskopisch leicht nachweisbaren Änderungen, wodurch der Substratumsatz verfolgt und quantifiziert werden kann (Bateman, 1989). Obwohl die zuvor genannten Nachweismethoden sensitiv sind, ist die ihnen zugrunde liegende diskontinuierliche Arbeitsweise mit einem hohen Arbeits- und Zeitaufwand verbunden. Ihre Anwendbarkeit wird dadurch stark beeinträchtigt.

Diese Nachteile stimulierten die Entwicklung kontinuierlicher Methoden des Nachweises der QC-Aktivität im Rahmen dieser Arbeit (Schilling *et al.*, 2002b; Schilling *et al.*, 2003a). Einerseits basierten diese auf dem bereits zuvor beschriebenen Nachweis von Ammoniak durch Kopplung mit Glutamat-Dehydrogenase (GDH) (Schilling *et al.*, 2003a), andererseits wurde eine bakterielle Pyroglutamyl-Aminopeptidase (pGAP) als Hilfsenzym genutzt (Schilling *et al.*, 2002b). Auf Grund der verschiedenen Hilfsenzyme basieren die Methoden auf unterschiedlichen

Mechanismen. Während im gekoppelten Test mit GDH das durch die Gln-Zyklisierung frei werdende Ammoniak bestimmt wird, spaltet die pGAP in der Detektionsreaktion pGlu-Dipeptid-Surrogate, die durch die Katalyse der QC aus Gln-Substraten gebildet werden (Schilling *et al.*, 2002b). Die Katalyse der pGAP führt dabei zur Abspaltung von chromophoren oder fluorogenen Gruppen, wie z.B. 4-Nitroanilin oder 7-Amino-4-methyl-cumarin, was in einem Anstieg der Fluoreszenz oder der Absorption resultiert (Fujiwara und Tsuru, 1978).

Diese gekoppelten Tests für die QC-katalysierte Reaktion ergeben auf Grund der verschiedenen Hilfsenzyme GDH, einer Oxidoreduktase, und pGAP, einer Hydrolase, unterschiedliche Anwendungsbereiche. Beispielsweise erwies sich die Kopplung der QC-Katalyse mit GDH als vorteilhaft bei der Untersuchung der Substratspezifität der humanen und pflanzlichen QC (Schilling *et al.*, 2003a). Da Ammoniak bei der Umsetzung der meisten Substrate der QC frei wird, konnte eine Vielzahl von Peptiden bezüglich ihrer Substrateigenschaften verglichen werden (s. Abschnitt 3.2, S. 14). Als nachteilig erwies sich die Detektion des Ammoniaks jedoch bei der Proteinreinigung oder der Detektion der QC-Aktivität in Rohhomogenaten oder Expressionsmedien. Da diese Proben häufig Ammonium-Ionen enthalten, wurde ein Nachweis der relativ geringen umgesetzten Substratmengen erschwert. Im Gegensatz dazu ist der gekoppelte Enzymtest mittels pGAP unempfindlich gegenüber Verunreinigungen durch Ammonium-Ionen. Deshalb wurde diese Methode für die Detektion der QC während der Expression und Reinigung des humanen und pflanzlichen Enzyms eingesetzt (Schilling *et al.*, 2002b; Schilling *et al.*, 2002a). Des weiteren ermöglichten die Eigenschaften der pGAP Untersuchungen zur pH-Abhängigkeit der Katalyse und Inhibierung der humanen und pflanzlichen QC. Da die pGAP über einen breiten pH-Bereich aktiv und stabil ist und eine hohe Spezifität zu den fluorogenen Substraten aufweist, beeinflussen geringe pH-bedingte Veränderungen der Aktivität die Methode nicht. Jedoch ist die Untersuchung der QC-Aktivität durch Kopplung mit pGAP auf Substrate wie Gln-pNA, Gln-AMC und Gln-βNA beschränkt. Dies steht im Gegensatz zu einer Vielzahl möglicher Peptidsubstrate für den gekoppelten Test mit GDH. Eine detaillierte Untersuchung der Substratspezifität der QC wäre anhand dieser Methode deshalb nicht möglich.

Die Vor- und Nachteile der gekoppelten kontinuierlichen Tests der QC sind zusammenfassend in Tabelle 3.1 dargestellt. Dabei wird deutlich, dass sich ihre Anwendbarkeit wechselseitig ergänzt. Auf Grund dieser Komplementarität konnten viele Untersuchungen mit der pflanzlichen und humanen QC durchgeführt werden. Zudem ermöglichte die Anwendung von Mikrotiterplatten-Messgeräten die Analyse einer Vielzahl von Proben innerhalb kürzester Zeit, wodurch diese Methoden im Vergleich zu den zuvor beschriebenen diskontinuierlichen Tests zu bevorzugen sind. Die Anwendung dieser neuen Nachweismethoden war essentieller Bestandteil aller

Untersuchungen und führte letztendlich auch zu den mechanistischen Schlussfolgerungen, die im folgenden Abschnitt beschrieben werden.

Tabelle 3.1: Vergleich gekoppelter, kontinuierlicher Testmethoden zum Nachweis und zur Charakterisierung der QC. Für eine genaue Beschreibung der experimentellen Bedingungen wird auf die Literatur verwiesen (Schilling *et al.*, 2003a; Schilling *et al.*, 2002b; Schilling und Demuth, 2004).

$$Gln\text{-}Peptid \xrightarrow{\ QC\ } pGlu\text{-}Peptid \quad + \quad Ammoniak$$

Grundlage	Spaltung des pGlu-Peptides	Umsetzung von Ammoniak
Hilfsenzym	Pyroglutamyl-Aminopeptidase	Glutamat-Dehydrogenase
Detektion	Spektrophotometrisch (pNA), Fluorimetrisch (AMC, βNA)	Spektrophotometrisch (NADH/H$^+$)
Substrate	Gln-pNA, Gln-AMC, Gln-βNA	keine Beschränkung in Bezug auf Substrate
Vorteile	robuste Eigenschaften des Hilfsenzyms, geringe Hilfsenzymmenge	nahezu für alle QC-Substrate anwendbar
Nachteile	Eingeschränktes Substratspektrum	Störung durch Ammonium-Ionen, hohe Hilfsenzymkonzentration und Hilfsenzymsubstrate nötig
Anwendung	Aktivitätsbestimmung der QC in Homogenaten, Proteinreinigung, Untersuchung der pH-Abhängigkeit, Inhibitorcharakterisierung	Untersuchung der Substratspezifität
Referenz	(Schilling *et al.*, 2002b; Schilling *et al.*, 2003b; Schilling *et al.*, 2002a)	(Schilling *et al.*, 2003a)

3.2 Katalyse und Inhibierung

Die Aufklärung der Wirkungsweise von Enzymen ist eine essentielle Voraussetzung für die Entwicklung von potenten Inhibitoren der Katalyse, da durch Kenntnis der Intermediate der Enzymkatalyse Strukturen für mögliche Inhibitoren abgeleitet bzw. bekannte Inhibitorstrukturen optimiert werden können. Die humane QC ist auf Grund ihrer physiologischen und möglicherweise pathophysiologischen Funktion ein potentielles Zielenzym für die Wirkstoffentwicklung (s. Abschnitt 5, S. 24). Daher ist das Verstehen des Katalysemechanismus dieses Enzyms von großer Bedeutung.

Bei der theoretischen Betrachtung möglicher Mechanismen der QC-Katalyse standen zwei grundlegend verschiedene Wirkungsweisen des Enzyms im Mittelpunkt (Gololobov *et al.*, 1994) (Abb. 3.1). Zum einen könnte die Katalyse über die Bildung eines kovalent verknüpften Intermediats (Acyl-Enzym-Intermediat) erfolgen (Abb. 3.1A). Bei diesem Mechanismus wird ein nucleophiler Rest des aktiven Zentrums, z.B. ein aktivierter Cysteinrest, die γ-Amidgruppe des N-terminalen Glutamins des Substrates attackieren. Das Acyl-Enzym-Intermediat bildet sich und Ammoniak wird freigesetzt (Acylierung). In einem zweiten Schritt greift die α-Aminogruppe des Glutamins die γ-Carbonylfunktion nucleophil an. Das Produkt wird freigesetzt und der Ausgangszustand bildet sich zurück (Deacylierung). Die Katalyse der QC würde in diesem Fall in Analogie zu den Katalysemechanismen von Serin/Cysteinproteasen, Transglutaminasen, γ-Glutamyl-Transpeptidasen oder γ-Glutamyl-Cyclotransferasen verlaufen.

Einem alternativen Mechanismus liegt eine nicht-kovalente Katalyse durch die QC zugrunde (Abb. 3.1B). Durch den intramolekularen Angriff der α-Aminogruppe an der γ-Carbonylfunktion des N-terminalen Glutamins im Substrat bildet sich ein tetraedrisches, nicht-kovalent enzymgebundenes Intermediat, welches in die Produkte Ammoniak und pGlu-Peptid zerfällt. Das Enzym würde die katalytische Funktion in diesem Fall durch die Bindung des Substrates, welche einen nucleophilen Angriff begünstigt, und die Stabilisierung des intermediär gebildeten tetraedrischen Intermediats ausüben.

Erste Untersuchungen an der QC aus Schweinehypophyse ließen die Vermutung zu, dass das Enzym Thiolgruppen besitzen könnte, welche für die Katalyse essentiell sind (Busby *et al.*, 1987). Diese ersten Ergebnisse einer kovalenten Enzymmodifizierung konnten jedoch nicht bestätigt werden (Temple *et al.*, 1998; Bateman *et al.*, 2001) und durch die Identifizierung einer Disulfidbrücke in der humanen QC, die unter Einbeziehung der Cysteinreste entsteht, ist eine kovalente Katalyse unter Beteiligung von Cystein ausgeschlossen (Schilling *et al.*, 2002a). Papaya-QC wie auch die QC der Säuger zeigte keine Inhibierung durch Serin-modifizierende Inhibitoren wie PMSF (Busby *et al.*, 1987). Auch Cystein- oder Histidin-modifizierende Reagenzien inhibierten das pflanzliche Enzym nicht (Bateman *et al.*, 2001; Zerhouni *et al.*, 1998; Messer und Ottesen, 1964). Es erscheint daher sehr wahrscheinlich, dass die Papaya-QC ebenfalls nicht-kovalent katalysiert (Gololobov *et al.*, 1994).

Indizien für einen analogen Mechanismus der Katalyse der pflanzlichen und tierischen QC - trotz vollkommen verschiedener Proteinstruktur (s. Abschnitt 2, S. 5) - erbrachte auch ein detaillierter Vergleich der Substratspezifität beider Enzyme (Schilling *et al.*, 2003a). Papaya und humane QC katalysieren stereospezifisch die Zyklisierung N-terminaler L-Glutaminylreste. Beide Enzymspezies setzten Oligopeptide mit sehr ähnlicher Spezifität um und zeigen die höchste Selektivität gegenüber Substraten mit aromatischen Aminosäuren in der zweiten Position.

Zudem weisen die QC-Formen eine ähnliche pH-Abhängigkeit der katalytischen Parameter k_{cat} und K_m auf. In beiden Fällen zeigt k_{cat} im pH-Bereich zwischen pH 5,5 und 8,5 keine Veränderung (Schilling *et al.*, 2003b; Gololobov *et al.*, 1994). Der Zerfall des Enzym-Substrat-Komplexes wird demnach durch Änderungen des pH-Wertes nicht beeinflusst. Im Gegensatz dazu wies die pH-Abhängigkeit der Michaelis-Konstanten K_M darauf hin, dass humane QC und Papaya-QC das Substrat nur im N-terminal unprotonierten Zustand binden. Die pH-Abhängigkeit der katalytischen Aktivität ist daher in beiden Fällen vom Protonierungszustand des Substrates abhängig, was ähnliche Mechanismen der Substraterkennung in Bezug auf die α-Aminogruppe und den katalytischen Umsatz wahrscheinlich macht. Beide Enzyme zeigten auch einen sehr ähnlichen, substratabhängigen Einfluss der Ionenstärke des Mediums auf die Katalyse (Schilling *et al.*, 2003a). Überdies setzten Papaya und humane QC L-β-Homoglutaminyl-Peptide mit gleicher Spezifität um, was darauf hindeutete, dass die generellen strukturellen Anforderungen an ein Substrat, d.h. eine Amino- und Amidgruppe in einem spezifischen sterischen Verhältnis zueinander, bei beiden Enzymen sehr ähnlich sind (Schilling *et al.*, 2003a).
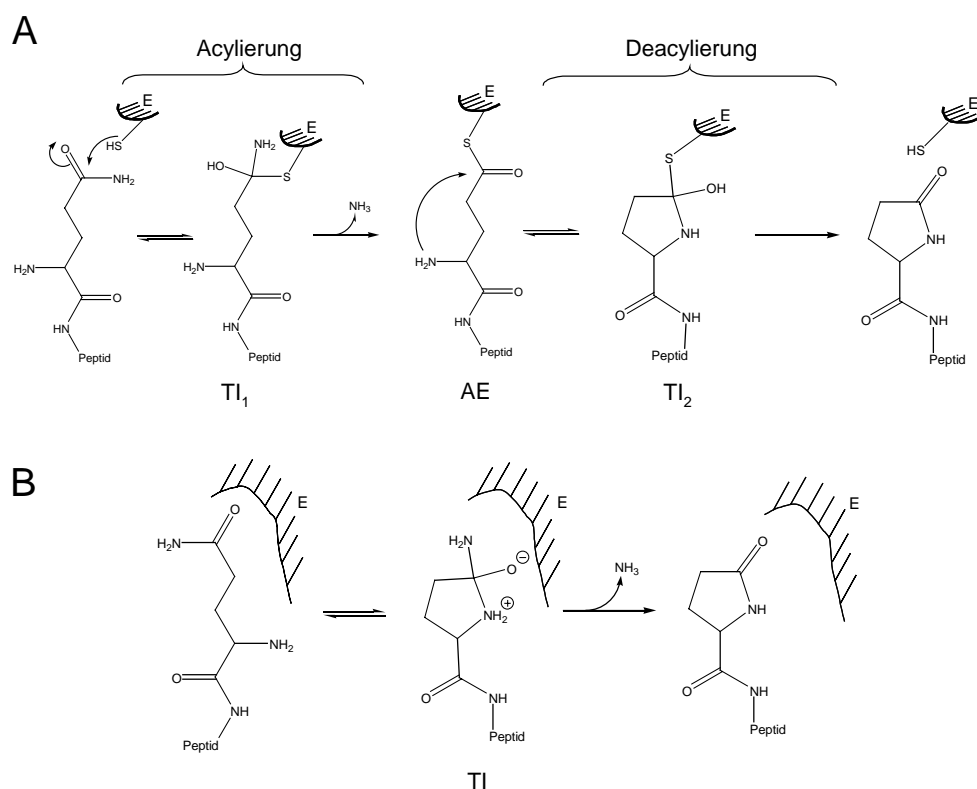

Abb. 3.1: Schematische Darstellung zweier möglicher Mechanismen der QC-Katalyse (in Anlehnung an Gololobov *et al.*, 1994). A) Katalyse durch nucleophilen Angriff einer Cysteinseitenkette der QC unter Bildung eines Acyl-Enzym-Intermediats (AE) in Analogie zu Proteasen oder Transglutaminasen. B) Nicht-kovalente Katalyse. Das Enzym beschleunigt die Bildung des tetraedrischen Intermediats (TI), welches durch intramolekularen nucleophilen Angriff der α-Aminogruppe an der γ-Carbonylfunktion entsteht. Neuere experimentelle Befunde stehen in Einklang mit einer Katalyse der pflanzlichen und tierischen QC analog zu B (siehe Text).

Trotz der aufgeführten Gemeinsamkeiten, die für einen generell identischen Katalysemechanismus analog zu Abb. 3.1B sprechen, haben die Untersuchungen auch Unterschiede offengelegt. Im Vergleich zur humanen QC katalysiert die Papaya-QC die Zyklisierung von Dipeptiden, Glutaminylestern und fluorogenen Substraten mit höherer Effizienz (Abb. 3.2) (Schilling *et al.*, 2003a). Mit steigender Kettenlänge des Substrates steigt jedoch die Selektivität der humanen QC im Gegensatz zur Papaya-QC (Abb. 3.2). Unterschiede zwischen der QC pflanzlichen und tierischen Ursprungs wurden nicht nur bezüglich der Kettenlänge des Substrates deutlich. Die humane QC war im Vergleich zur Papaya-QC spezifischer in Bezug auf die Struktur der Peptidkette, was z.B. durch geringere Spezifitätskonstanten gegenüber Peptiden mit Prolin in zweiter Position oder partiell zyklischen Peptiden deutlich wurde. Während die Gegensätze in der Sekundärspezifität wahrscheinlich auf strukturbedingte Unterschiede der sekundären Substratbindungsstellen in den Enzymen tierischen und pflanzlichen Ursprungs zurückzuführen sind, wurden auch katalytische Unterschiede identifiziert, die auf verschiedene Wechselwirkungen des N-terminalen Glutamins im Substrat mit dem aktiven Zentrum des Enzyms schließen lassen.

Beispielsweise setzte die humane QC im Gegensatz zur Papaya-QC γ-methylierte Glutaminylreste nicht um. γ-Glutamyl-hydrazide inhibierten jedoch ausschließlich die metallabhängige humane QC. Dies deutet darauf hin, dass sich die Art der Wechselwirkung der
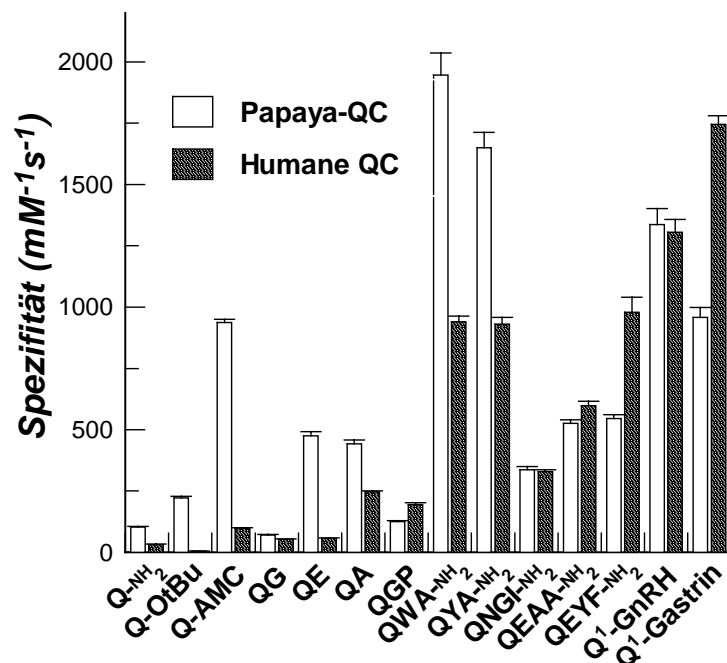

Abb. 3.2: Vergleich der Umsetzung ausgewählter Peptidsubstrate durch die humane QC und Papaya-QC hinsichtlich der Spezifitätskonstante k_{cat}/K_m. Die Daten der Abbildung wurden der eigenen Arbeit (Schilling *et al.*, 2003a) entnommen und zur besseren Übersicht graphisch dargestellt. Die Abkürzungen entsprechen dem Einbuchstabencode der Aminosäuren. Weitere Abkürzungen sind: Q-NH$_2$=Glutaminamid, Q-OtBu=Glutaminyl-*tert*-Butylester, Q-AMC=(*N*-Glutaminyl)-7-Amino-4-methyl-cumarin, GnRH=Gonadoliberin.

γ-Amidfunktion des Substrates mit dem Enzym und somit der spezifische Mechanismus der Stabilisierung des enzymgebundenen tetraedrischen Intermediats (s. Abb. 3.1B) unterscheidet (Schilling *et al.*, 2003a). Diese Ergebnisse werden durch die unterschiedliche Inhibierbarkeit beider Enzymformen bestätigt. Beispielsweise wird die Aktivität der pflanzlichen QC durch Peptide mit N-terminalem Prolin kompetitiv gehemmt und die der humanen QC nicht (Gololobov *et al.*, 1996). Es wird vermutet, dass Prolin der Struktur des tetraedrischen Intermediats im Zuge der Katalyse der Papaya-QC ähnelt und daher durch das aktive Zentrum des Enzyms gebunden wird. Die Inhibierung der Papaya-QC durch Prolinpeptide wurde auch als Hinweis für eine nicht-kovalente Katalyse gewertet (Abb 3.1B) (Gololobov *et al.*, 1996).

Im Gegensatz zur Papaya-QC wird die Aktivität der humanen QC nicht durch Prolin oder Prolin-haltige Peptide beeinflusst. Bereits in frühen Arbeiten wurde eine Inhibierung der tierischen QC durch den heterozyklischen Chelator 1,10-Phenanthrolin gezeigt (Busby *et al.*, 1987). Da der Komplexbildner EDTA jedoch keinen Einfluss auf die Enzymaktivität hatte, und durch 1,10-Phenanthrolin inaktiviertes Enzym mittels Dialyse gegen chelatorfreie Puffer reaktiviert werden konnte, wurde die katalytische Funktion eines Metallions zunächst ausgeschlossen (Busby *et al.*, 1987; Bateman *et al.*, 2001). Die kompetitive Inhibierung der humanen QC durch Imidazol und Imidazolderivate sowie die Hemmung durch weitere heterozyklische Chelatoren und die Reaktivierung der QC mittels Zn-Ionen führten jedoch in den eigenen Untersuchungen zur Identifizierung der QC als Metalloenzym (Schilling *et al.*, 2003b). Wie gezeigt werden konnte, unterscheiden sich die Chelatoren und die Imidazolderivate im Inhibierungsmechanismus. Während Imidazole eine rein kompetitive Hemmung der Aktivität bewirken, ergeben sich bei der Hemmung durch Komplexbildner nichtlineare Substratumsatz-Kurven, also eine zeitabhängige Verstärkung der Hemmung (Schilling *et al.*, 2003b). Offenbar sind Chelatoren wie Dipicolinsäure und 1,10-Phenanthrolin auf Grund ihrer planaren Struktur im Gegensatz zu EDTA in der Lage, das enzymgebundene Metallion vom aktiven Zentrum zu lösen.

Die Metallionen im aktiven Zentrum der QC sind vermutlich auch Interaktionspartner für die oben genannten kompetitiven Inhibitoren, die auf der Grundstruktur Imidazol basieren. Ein unprotonierter Ringstickstoff des Imidazols ist Bedingung für die inhibitorische Aktivität der Imidazolderivate, was auf eine Interaktion des Imidazolrings mit einem Metallion im aktiven Zentrum hinweist (Schilling *et al.*, 2003b). Die Analyse der Struktur-Wirkungsbeziehung verschiedener Imidazolderivate deutet auch auf eine essentielle Interaktion des aktiven Zentrums mit dem basischen Ringstickstoff im Inhibitor hin. Substituenten in Nachbarschaft zum interagierenden Stickstoff beeinflussen die Bindung der Inhibitoren an das aktive Zentrum. Im Gegensatz dazu konnten N1-Derivate des Imidazols als potente Inhibitoren der humanen QC identifiziert werden (Schilling *et al.*, 2003b).

Die Ergebnisse der Untersuchungen zur Substrat- und Inhibitorspezifität und die strukturelle Verwandtschaft der tierischen QC zu Zn-abhängigen Aminopeptidasen des „Clans" MH (s. Abschnitt 2, S. 8) führten zu ersten Hypothesen über den Mechanismus der Katalyse (Schilling *et al.*, 2003b).

Bei den verwandten Metalloaminopeptidasen werden den katalytisch aktiven Metallionen folgende Aufgaben zugeschrieben: a) die zu spaltende Peptidbindung durch Wechselwirkung mit dem Carbonylsauerstoff zu polarisieren, b) die Nucleophilie des angreifenden Wassermoleküls zu erhöhen und c) das durch den nucleophilen Angriff entstandene tetraedrische Intermediat durch Bindung des Oxanions zu stabilisieren. Im Fall der Aminopeptidase aus *Aeromonas proteolytica* (ApAP), die die höchste Strukturhomologie zu den tierischen QCs aufweist, werden die zuvor genannten und auch für andere Metallopeptidasen gültigen Aufgaben hauptsächlich von einem Zink-Ion des aktiven Zentrums übernommen. Das andere Metallion fixiert während der Katalyse den N-terminalen Aminostickstoff (Abb. 3.3).
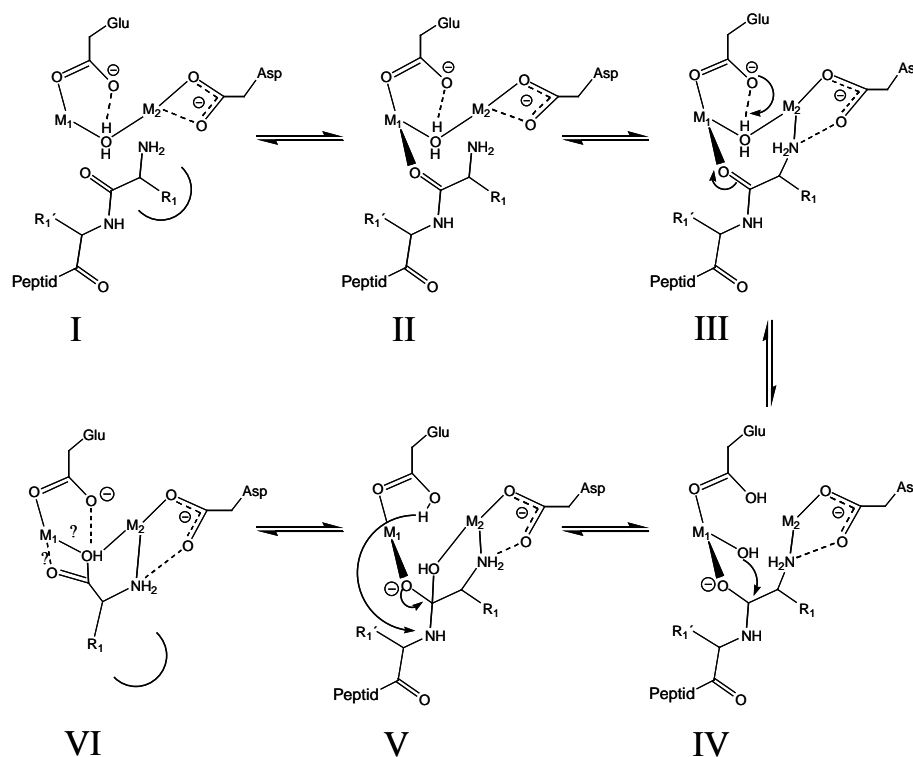

Abb. 3.3: Schematische Darstellung des Katalysemechanismus der Zn-abhängigen Leucin-Aminopeptidase aus *Aeromonas proteolytica* (ApAP) in Anlehnung an Lowther und Matthews, 2002. Nach initialer Bindung der N-terminalen Aminosäureseitenkette (R_1) durch eine hydrophobe Tasche der ApAP (I) bindet die Carbonylgruppe der zu spaltenden Bindung an ein Zn-Ion (M_1) (II), gefolgt von der Bindung der N-terminalen Aminogruppe an das andere Zn-Ion (M_2) (III). Durch diese Interaktion löst sich das gebundene Wassermolekül vom Zink-Ion, beschleunigt durch einen Glutamatrest, der als Base fungiert (IV). Anschließend greift das an Zn_1 gebundene Nucleophil die polarisierte Carbonylgruppe unter Bildung eines tetraedrischen Intermediats an (V). Der Zerfall des Intermediats ist der geschwindigkeitsbestimmende Schritt der katalysierten Reaktion und wird vermutlich durch den Protonentransfer vom Glutamatrest bewirkt (VI).

Durch die letztgenannte Interaktion ist auch die pH-Abhängigkeit der Katalyse begründet, welche zeigt, dass N-terminal protonierte Substratmoleküle durch diese Aminopeptidase nicht umgesetzt werden (Baker und Prescott, 1983).

Die durch QC katalysierte Reaktion unterscheidet sich vom Katalysemechanismus der Aminopeptidase in verschiedener Hinsicht. Zum einen ist die Zyklisierung im Gegensatz zur Hydrolyse eine intramolekulare Reaktion. Zum anderen erscheint eine Aktivierung des angreifenden Nucleophils, was bei Aminopeptidasen ein essentieller Bestandteil des Katalyseapparates ist, im Fall der QC-Katalyse nicht notwendig, da der freie N-terminale Stickstoff eine starke Nucleophilie aufweist. Trotz dieser Unterschiede könnten sich Teilreaktionen der Katalysemechanismen von humaner QC und Zn-abhängigen Aminopeptidasen gleichen. In beiden Fällen verläuft die Reaktion über einen Additions-Eliminierungs-Mechanismus (S_N2_t) an einer Amidgruppierung. Im Fall der QC ist dies die γ-Amidfunktion des N-terminalen Glutamins.
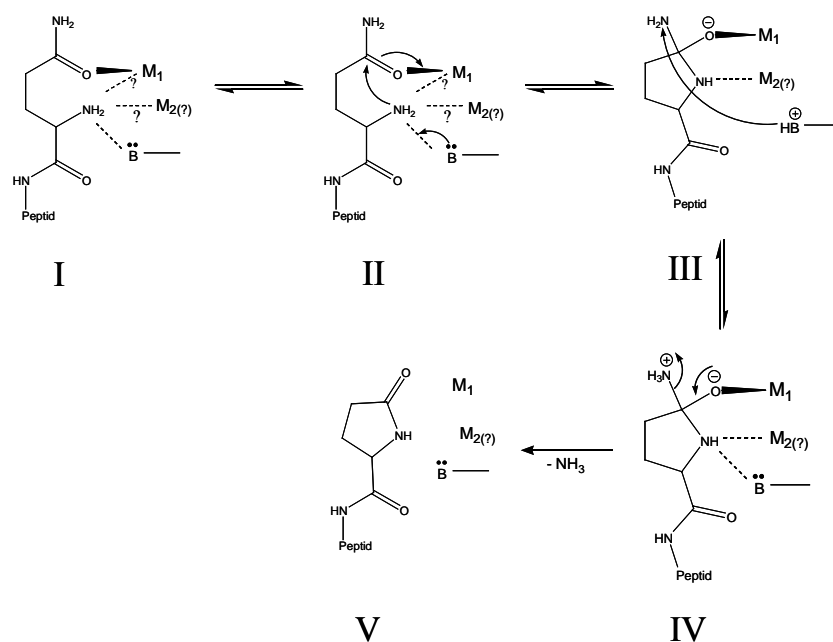

Abb. 3.4: Hypothetische Beteiligung der Metallionen an der Katalyse durch humane QC. In Analogie zur Aminopeptidase könnte ein Zn-Ion der QC die γ-Carbonylgruppe binden (I). Das fragliche zweite Zn-Ion könnte daher die α-Aminogruppe des Substrates binden. Eine andere Möglichkeit der Bindung besteht jedoch in einer Wechselwirkung mit Zn_1, was das Nucleophil in räumliche Nähe zum Carbonylkohlenstoff bringen würde (vgl. Intermediat IV, Abb. 3.3). Nach erfolgter Polarisation der Carbonylgruppe greift der Aminostickstoff nucleophil an (II). Es bildet sich ein durch das Zn-Ion stabilisiertes, tetraedrisches Intermediat (III). Der Protonenübergang zwischen der Aminogruppe des Rings und des abzuspaltenden Ammoniaks könnte ebenfalls über eine generelle Basenkatalyse erfolgen (B in II, III), was letztendlich zum Zerfall des tetraedrischen Intermediats führt (III-V).

Ein Metallion im aktiven Zentrum der QC könnte daher, analog der Katalyse durch Aminopeptidasen, a) die γ-Amidgruppe des Substrates polarisieren und dadurch die Elektrophilie des Carbonylkohlenstoffs erhöhen und b) das durch den Angriff der α-Aminogruppe entstehende tetraedrische Intermediat durch eine Metall-Oxanion-Wechselwirkung stabilisieren (Abb. 3.4). Eine derartige Wechselwirkung ist durch die Inhibierung der humanen QC durch γ-Glutamyl-Hydrazide wahrscheinlich, bei der vermutlich die γ-Hydrazid-Gruppierung mit dem Metallion eine Komplexbindung eingeht (Schilling *et al*., 2003a).

Für den intramolekularen nucleophilen Angriff der α-Aminogruppe auf den γ-Carbonylkohlenstoff ist ein unprotonierter α-Aminostickstoff eine Voraussetzung. Ein Merkmal der Katalyse könnte daher sein, dass nur Substratmoleküle, die unprotoniert sind und daher umgesetzt werden können, gebunden werden. Diese Fixierung des Substrat-N-Terminus durch die QC könnte durch eine Metall-Stickstoff-Wechselwirkung analog der Interaktion im Aminopeptidase-Vorläufer übernommen worden sein. Dies könnte auch die gleichartige pH-Abhängigkeit der Substratbindung der ApAP und der QC erklären (Baker und Prescott, 1983; Lowther und Matthews, 2002; Schilling *et al*., 2003a) (Abb. 3.4).

Obwohl die Arbeiten zur Metallabhängigkeit und der Substrat- und Inhibitorspezifität der QCs erste Vorstellungen über Katalysemechanismen, wie z.B. die Art der Involvierung der Metallionen, der humanen QC zulassen, ist eine detaillierte Rekonstruktion der katalytischen Schritte der Reaktion noch nicht möglich. Nicht zuletzt durch die noch ungeklärte Stöchiometrie des Zinkgehalts der QC bleibt unklar, ob α-Amino- und γ-Amidgruppe des Substrates mit demselben oder verschiedenen Metallionen in Wechselwirkung treten. Im ersten Fall würden sterisch günstige Verhältnisse für einen nucleophilen Angriff analog Aminopeptidasen vorliegen (vgl. Abb. 3.3, Intermediat IV). Genauere Einblicke in die Katalyse durch QC könnte daher die Aufklärung der Metallbindung und der 3D-Struktur der QC liefern. Die Vorstellungen zum Katalysemechanismus der Aminopeptidasen könnten auch bei einer Auswertung dieser Daten ein wertvolles Hilfsmittel sein.

4 Die physiologische Funktion der QC

Das ubiquitäre Vorkommen von QCs im Pflanzen- und Tierreich und vermutlich auch in einigen Mikroorganismen (Chen und Russell, 1989) lässt eine wichtige Rolle des Enzyms in verschiedenen regulatorischen Prozessen vermuten. Obwohl die pflanzliche QC bereits vor 40 Jahren entdeckt wurde, ist ihre physiologische Funktion noch nicht endgültig geklärt. Das

Vorkommen im Latex von *C. papaya* deutet auf eine Rolle in einem pflanzlichen Schutzmechanismus vor pathogenen Mikroorganismen hin.

Tabelle 4.1: Ausgewählte Pyroglutamyl-Peptide tierischen Ursprungs und ihre physiologische Funktion (zusammengestellt nach diversen Literaturangaben).

Peptid	Ort der Bildung	Funktion
Gastrin 17 pEGPWLEEEEEAYGWMDF$_a$	G-Zellen der Schleimhaut des Magenantrums	- stimuliert Magensäuresekretion der Zellen des Magenfundus und regt Produktion von Pankreassaft an - aktiviert Magen/Darm-Muskulatur - erhöhte Produktion bei Zolliger-Ellison-Syndrom (Neoplasma des Pankreas)
Neurotensin pELYENKPRRPYIL	N-Zellen des Dünndarms, auch im Gehirn nachgewiesen	- Hemmung der Salzsäuresekretion des Magens - bewirkt Kontraktion der glatten Muskulatur des Darmes und Freisetzung von Glukagon (Regulation des Fettmetabolismus)
FPP ("Fertilization Promoting Peptide") pEEP$_a$	Prostata	- hohe Konzentrationen im Seminalplasma, Beeinflussung der Samenreifung - Verhinderung des spontanen Acrosomen-verlusts
TRH („Thyrotropin Releasing Hormone") pEHP$_a$	Hypothalamus, Pankreas, Prostata, Plazenta	- bewirkt Synthese und Freisetzung von Thyrotropin (TSH) in der Hypophyse - fungiert als Neurotransmitter/Neuro-modulator im zentralen Nervensystem - beeinflußt Freisetzung von Prolactin, Insulin, Adrenalin und anderen Hormonen
GnRH („Gonadotropin Releasing Hormone") pEHWSYGLRP$_a$	Hypothalamus	- Stimulus für Ausschüttung von Gonadotropinen (LH und FSH), zyklische Freisetzung wichtig für Sexualfunktion
Orexin A (Hypocretin-1) pEPLPDCCRQKTCSCRLYEL LHGAGNHAAGILTL	Hypothalamus	- Regulation des Tageszyklus (bei Fehlen von Orexinen dauerhafte Müdigkeit, Narkolepsie) - stimuliert Magensäureproduktion, Darmmotilität, Nahrungsaufnahme - vermutlich übergeordnete Funktion der Energiehomöostase
MCP-1, MCP-2 ("Monocyte Chemotactic Protein" 1 und 2) pEPDAI….(MCP-1) pEPDSV....(MCP-2)	Monocyten, Makrophagen, Keratinocyten	- chemotaktischer Faktor für Monocyten - bewirkt Anheftung der Monocyten an Gefäßwände, Verlassen der Blutbahn und Aktivierung; chemotaktischer Faktor für T-Gedächtniszellen

Der Latex der Pflanze, der auch für seine hohen Konzentrationen an Proteasen wie Papain oder Chymopapain bekannt ist, dient *C. papaya* als initialer fungizider und bakterizider Wundverschluss. Direkt nach der Verwundung steigt die Ammonium-Ionen-Konzentration im Sekret auf bis zu 10 mM. Andere Arbeiten konnten zeigen, dass dies wachstumshemmend auf Mikroorganismen wirken kann. Es wird daher vermutet, dass der QC die Rolle der Ammoniakfreisetzung zukommen könnte und das Enzym dadurch in die Pathogenabwehr einbezogen ist (Giordani *et al.*, 1996; El Moussaoui *et al.*, 2001). Physiologische Substrate des Pflanzenenzyms konnten jedoch noch nicht identifiziert werden. Des weiteren ist die Funktion der QC in anderen Pflanzen, in welchen die mRNA der QC durch Sequenzvergleiche identifiziert werden konnte (Dahl *et al.*, 2000), noch ungeklärt. Erste Ergebnisse deuten darauf hin, dass der QC eine Funktion beim Schutz von Samenspeicherproteinen und bei der Samenreifung zukommen könnte (Yamada *et al.*, 1999).

Im Gegensatz zur pflanzlichen QC existieren für die tierische QC genauere Vorstellungen über eine physiologische Funktion. Aus tierischen Geweben konnten bereits zahlreiche regulatorische Peptide isoliert werden, die N-terminal einen Pyroglutamylrest aufweisen (Awade *et al.*, 1994; Abraham und Podell, 1981). Obschon ein Nachweis über eine direkte Beteiligung der QC an der Synthese dieser Peptide in vielen Fällen noch aussteht, deutet die zelluläre Lokalisation des Enzyms und der mutmaßlichen Substrate im regulierten Sekretionsweg auf eine Rolle bei der Synthese dieser Hormone und Neuropeptide hin.

Erste Studien zum Vorkommen der QC in Hypothalamus und Hypophyse haben gezeigt, dass das Enzym mit den Pyroglutamyl-Hormonen TRH und GnRH in sekretorischen Vesikeln kolokalisiert ist (Bockers *et al.*, 1995). Offenbar ist die Expression aber auf zellulärer Ebene reguliert, da bestimmte Bereiche des Hypothalamus und der Hypophyse keine QC aufweisen. Das Vorkommen hauptsächlich im Gehirn und in peripheren Drüsenorganen, also Geweben mit endokriner oder exokriner Funktion, bestätigt die gewebs- und zelltypspezifische Expression der QC (Pohl *et al.*, 1991). Einige Beispiele für Pyroglutamyl-Peptide und -Proteine und deren Funktion sind in Tabelle 4.1 zusammengefasst. Eine Umsetzung ihrer Präkursoren durch die QC wurde in vielen Fällen bereits *in vitro* belegt (Schilling *et al.*, 2003a).

Für einige der in Tabelle 4.1 aufgeführten Peptide, wie z.B. TRH oder MCP-2, konte gezeigt werden, dass ihre biologische Wirksamkeit vom N-terminalen Pyroglutamyl-Rest abhängig ist. Eine Veränderung des N-Terminus, z.B. das Unterbleiben der Zyklisierung des Glutamins, führt zu einem Verlust der Bindung dieser Hormone an ihre spezifischen Rezeptoren bzw. zum Unterbleiben einer zellulären Reaktion (Van Coillie *et al.*, 1998; Abraham und Podell, 1981). Neben der Generierung der aktiven Konformation bewirkt die Pyroglutamylbildung auch eine Erhöhung der Stabilität der Hormone. Durch die Bildung des Pyroglutamyl-Lactamringes

verliert der Peptid-N-Terminus seine basischen Eigenschaften und somit ein essentielles Erkennungsmerkmal für viele Aminopeptidasen. Der N-Terminus ist daher gegenüber unspezifischer Proteolyse weitgehend resistent, was auch eine Möglichkeit der Regulation des Abbaus dieser Peptide darstellt.

Die wahrscheinliche Beteiligung an der Synthese einer Vielzahl von Peptiden mit regulativer Funktion legt eine essentielle Rolle der QC im Hormonanabolismus und somit für die Steuerung körpereigener Regelkreisläufe nahe. Es eröffnet sich dadurch die Möglichkeit, in patho-physiologische Prozesse einzugreifen.

5 Humane QC – Zielenzym für die Wirkstoffentwicklung

5.1 Pyroglutamyl-Peptide in pathophysiologischen Prozessen

Obwohl die physiologische Funktion der Pyroglutamylbildung und somit der QC die Generierung der biologisch aktiven Struktur von Hormonen zu sein scheint, treten in jüngerer Zeit zunehmend Berichte auf, die Pyroglutamylpeptide in Zusammenhang mit pathophysiologischen Prozessen, vorwiegend amyloidogenen Erkrankungen, bringen (Saido *et al.*, 1995; Vidal *et al.*, 1999). In diesem Zusammenhang ist die Alzheimersche Krankheit (AD) als die wahrscheinlich bekannteste amyloidogene histopathologische Veränderung hervorzuheben.

AD ist eine neurodegenerative Erkrankung, die durch eine fortschreitende Ablagerung von amyloidogenen Peptiden im Gehirn, sogenanntem Amyloid-β oder βA4, und einen dadurch hervorgerufenen Abbau von Gehirnsubstanz gekennzeichnet ist (Selkoe, 2001; Selkoe, 1998; Glenner und Wong, 1984a; Glenner und Wong, 1984b; Terry und Katzman, 1983). Die Ablagerungen, sogenannte Plaques, bestehen hauptsächlich aus dem 4 kDa-Peptid βA4. Diese amyloidogene Molekülspezies wird durch Prozessierung des „Amyloid Precursor Proteins" (APP) gebildet (Kang *et al.*, 1987; Goldgaber *et al.*, 1987). APP, ein Transmembranprotein, dessen physiologische Funktion noch nicht vollständig geklärt ist (Selkoe, 2001), kommt ubiquitär im Organismus vor, vorwiegend jedoch in neuronalen Zellen. Auf Grund verschiedener Spleißvarianten der mRNA, was in Proteinen mit 695, 751 oder 770 Aminosäuren resultiert, und diverser posttranslationaler Modifikationen, wie z.B. N- und O-Glykosylierung sowie Phosphorylierung, stellen die APP-Moleküle eine äußerst heterogene Molekülspezies dar (Selkoe *et al.*, 1988; Hung und Selkoe, 1994).

Während und nach dem Transport des APP durch den sekretorischen Weg kann das Protein unterschiedlich gespalten werden (Goate *et al*., 1991). Die entsprechenden proteolytischen Aktivitäten werden α-, β- oder γ-Sekretase genannt. Die Aktivität der α-Sekretase führt zur Abspaltung des löslichen, extrazellulären Teils des Proteins (Esch *et al*., 1990). Der Transmembranteil, das sogenannte C-83 Fragment, bleibt dabei zurück („non-amyloidogenic pathway"). Ein anderer Weg der Prozessierung beinhaltet die Spaltung durch β- und γ-Sekretase („amyloidogenic pathway"). Die Spaltung durch die β-Sekretaseaktivität resultiert in einem etwas kleineren sezernierten Fragment (β-APPs) und einem größeren Transmembranteil (C-99). Das C-99 Fragment wird im folgenden durch die γ-Sekretaseaktivität innerhalb des Transmembranteils gespalten. Aus dieser Spaltung, die prinzipiell an zwei Stellen erfolgen kann, resultieren die amyloidogenen Aβ-Peptide mit 40 oder 42 Aminosäuren (Aβ1-40, 1-42). Der molekulare Ursprung der β- und γ-Sekretaseaktivität steht im Mittelpunkt der derzeitigen Forschung. Eine Aspartyl-Protease mit β-Sekretaseaktivität konnte identifiziert werden (Vassar *et al*., 1999; Sinha *et al*., 1999; Yan *et al*., 1999). Es gibt zudem auch Hinweise auf andere Proteasen, vor allem Cysteinproteasen, mit dieser Aktivität (Munger *et al*., 1995). Eine γ-Sekretase konnte bisher nicht isoliert werden. Vielmehr weisen neuere Erkenntnisse darauf hin, dass diese Spaltung von einem Multienzymkomplex („γ-Secretase-complex"), der als essentiellen Bestandteil das 44 kDa Protein Presenilin enthält, vermittelt wird (Takasugi *et al*., 2003; Thinakaran *et al*., 1997; Tomita *et al*., 2001; Takasugi *et al*., 2002; Francis *et al*., 2002).

Untersuchungen der Plaques von Patienten mit Down Syndrom und AD ergaben, dass die Ablagerungen aus verschiedenen Formen des βA4 bestehen. Einerseits weisen die Peptide auf Grund der γ-Sekretasespaltung unterschiedliche C-Termini auf. Vor allem das βA4(1-42) scheint eine besondere Neigung zur Aggregation aufzuweisen (Pike *et al*., 1995). Ein vermehrtes Entstehen des Peptides wird mit einer beschleunigten Progression der Erkrankung in Verbindung gebracht (Levy *et al*., 1990; Scheuner *et al*., 1996).

In letzter Zeit traten aber auch verstärkt Berichte auf, die Inhomogenitäten des N-Terminus des βA4 beschreiben (Mori *et al*., 1992; Pike *et al*., 1995). Neben einer Bindungsveränderung des N-terminalen Aspartats, der sogenannten iso-Asp Bildung, beschreiben diese Untersuchungen das Vorkommen von N-terminal verkürzten βA4-Spezies, die einen Pyroglutamylrest aufweisen (Saido *et al*., 1995). Weitergehende Untersuchungen haben gezeigt, dass diese Formen des βA4, insbesondere βA4pE(3-40/42), den Hauptanteil der abgelagerten Amyloide bilden (Kuo *et al*., 1997; Hosoda *et al*., 1998). Auf Grund des hohen Anteils von 25–50 % dieser pGlu-βA4 Peptide an den Plaques wird vermutet, dass diese Peptide eine entscheidende Rolle bei der Ausbildung der Erkrankung spielen könnten (Russo *et al*., 1997).

Tatsächlich konnten Untersuchungen zum Aggregationsverhalten von pGlu-βA4 zeigen, dass diese Formen des βA4 eine ausgeprägte, stabile β-Faltblattstruktur aufweisen und dadurch stärker zur Aggregation neigen als Peptide vergleichbarer Länge ohne eine pGlu-Modifikation des N-Terminus (He und Barrow, 1999). Befunde zur Toxizität ergaben, dass die pGlu-βA4 Formen einen stärkeren Einfluss auf die Zellvitalität ausübten als andere βA4 Spezies (Russo *et al.*, 2002). Auf Grund dieser Eigenschaften und des dominanten Vorkommens von βA4pE(3-42) in Plaques von Down-Syndrom-Patienten wird daher vermutet, dass diese Molekülspezies die initialen Ablagerungen bilden könnte und daher die Entstehung und das Fortschreiten der Krankheit beschleunigt (Russo *et al.*, 1997; Harigaya *et al.*, 2000; Saido *et al.*, 1996). Eine Hemmung der Bildung dieser Peptide könnte somit eine Möglichkeit darstellen, die Ausprägung der Krankheit zu verlangsamen (Hosoda *et al.*, 1998).

Neben der Verstärkung der Aggregation und Toxizität wird vermutet, dass die pGlu-Modifikation des N-Terminus zu einer erhöhten Stabilität des βA4 gegen proteolytischen Abbau führt (Saido, 1998). Erste Ergebnisse weisen einen verringerten Abbau der pGlu-Amyloidpeptide in Zellkultur nach (Russo *et al.*, 2002). Befunde anderer Arbeiten zeigten zudem, dass verschiedene proteolytische Enzymaktivitäten, wie z.B. Pyroglutamyl-Aminopeptidase und Glutamyl-Aminopeptidase, mit steigendem Alter abnehmen, was einen verlangsamten Abbau der Glutamyl- und Pyroglutamylformen des βA4 bedingen könnte (Kuda *et al.*, 1997; Agirregoitia *et al.*, 2003). Die sogenannte „Aminopeptidase-Hypothese" geht davon aus, dass die Entstehung der sporadischen Form der Alzheimer Erkrankung auf eine generelle Dysfunktion des N-terminalen Abbaus von βA4 durch Aminopeptidasen zurückzuführen ist (Saido, 1998). Durch den verringerten Abbau entsteht eine erhöhte Konzentration von Intermediaten, die zur Aggregation neigen bzw. in besonders toxische Formen überführt werden können. Dem βA4pE(3-42) wird dabei eine entscheidende Funktion unterstellt (Saido, 1998; Abb. 5.1).

Es ist jedoch noch unklar, wie die pGlu-Modifikation *in vivo* entsteht. Nach Abspaltung der beiden N-terminalen Aminosäuren des βA4(1-42) bildet ein Glutamylrest den N-Terminus des Peptids. Im Gegensatz zur Pyroglutamylbildung aus N-terminalem Glutamin konnte eine enzymatische Zyklisierung von Glutamat unter physiologischen Bedingungen bisher nicht beschrieben werden. Es wurde daher vermutet, dass sich die Pyroglutamylpeptide durch spontane Dehydratation bilden (Hashimoto *et al.*, 2002). Da die QC jedoch das einzige bekannte Enzym ist, welches die Pyroglutamylbildung am N-Terminus von Peptiden katalysiert, wurde durch uns ein möglicher Einfluss des Enzyms auf die pGlu-βA4-Bildung geprüft (Schilling *et al.*, eingereicht).

Um die Entstehung des Pyroglutamylrestes am N-Terminus zu untersuchen, wurden verschiedene Derivate des Glutamats auf Umsatz sowohl durch QC als auch durch spontane

Zyklisierung getestet. Wie in Analogie zu den Ergebnissen der Substratspezifitätsuntersuchungen (s. Kapitel 3, S. 17) zu erwarten war, stellten die Peptide mit einem N-terminalen Glutaminylrest, d.h. βA4Gln^3(3-x), gute Substrate der QC dar. Es konnte zudem gezeigt werden, dass die beiden N-terminalen Reste (Asp-Ala), die nach der Spaltung durch β-Sekretase den Glu-Rest an Position 3 maskieren, für Aminopeptidasen zugänglich sind. Esterderivate des N-terminalen Glutamats zyklisierten ohne katalytischen Einfluss der QC.
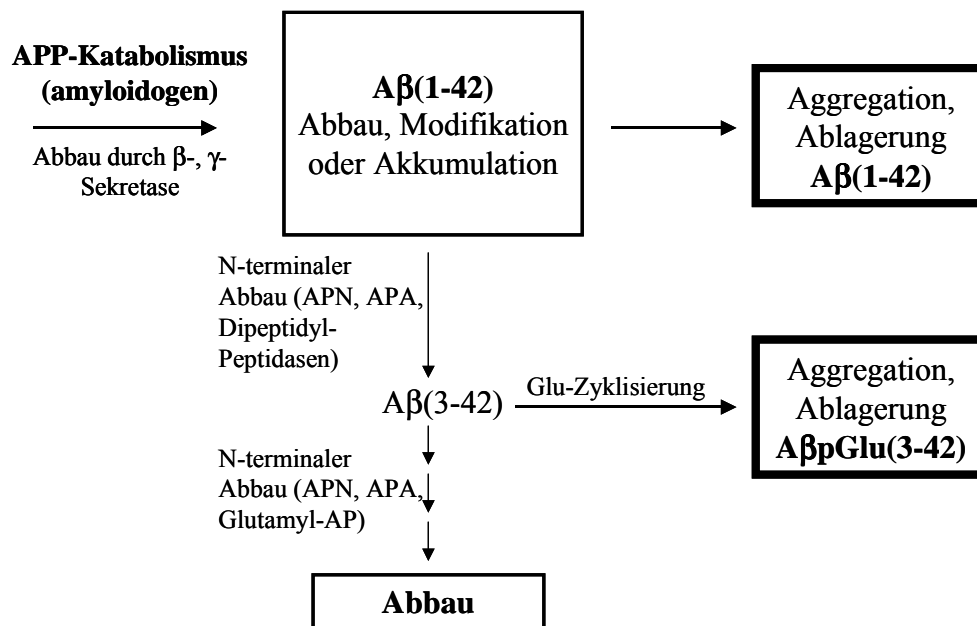
Abb. 5.1: Die Aminopeptidase-Hypothese des Aβ-Katabolismus (Saido, 1998). Die Hypothese beruht auf einem verlangsamten Abbau des Aβ42 durch Aminopeptidasen, was zur Plaqueentstehung führt. Die Vermutungen werden zum einen dadurch gestützt, dass die initialen Ablagerungen fast ausschließlich aus Formen des Aβ(1-42) und AβpGlu(3-42) bestehen. Zum anderen wurden mit steigendem Lebensalter und in Patienten mit Alzheimerscher Erkrankung geringere Peptidaseaktivitäten bestimmt. Eine Verringerung der Aminopeptidaseaktivität führt zu einem Ansteigen der Konzentrationen von Aβ(1-42) und AβpGlu(3-42). Weiterhin geht die Hypothese davon aus, dass eine Verkürzung des N-Terminus um 4 Aminosäuren und mehr zu einem Abbau des Aβ führt, da diese Peptide nicht oder nur in geringer Menge in Ablagerungen zu finden sind.

Von besonderer Bedeutung ist jedoch das unerwartete Ergebnis, dass humane und Papaya-QC auch N-terminale Glutamylreste des βA4 zu Pyroglutamat zyklisieren (Schilling *et al.*, eingereicht). Die spezifische Umsetzung konnte durch Zugabe von QC-Inhibitoren und hitzeinaktiviertem Enzym belegt werden. Der N-terminale Glutamylrest neigt zudem nicht zur spontanen Zyklisierung (Schilling *et al.*, eingereicht).

Die pH-Abhängigkeit der Umsetzung des fluorogenen Substrates Glu-βNA wies zudem darauf hin, dass die Katalyse offenbar durch mehr Faktoren beeinflusst wird als die Zyklisierung von Glutaminyl-Peptiden. Das pH-Optimum der Gln-Zyklisierung liegt bei pH 8 (Schilling *et al.*,

2003a). Im Gegensatz dazu besitzt die Umsetzung von N-terminalem Glutamat ein Aktivitätsoptimum der Katalyse im schwach sauren Bereich. Die beobachteten Unterschiede sind vermutlich auf den katalytischen Einfluss des Protonierungszustandes der γ-Carbonylgruppe des Glutamats zurückzuführen (Abb. 5.2). Für die enzymatische Katalyse der Gln-Zyklisierung konnte gezeigt werden, dass die Substratbindung von einer unprotonierten α-Aminogruppe abhängt. Im Gegensatz dazu wird die Verschiebung des Aktivitätsoptimums für Glu-Peptide in den sauren Bereich dadurch erklärt, dass unter leicht sauren Bedingungen eine Molekülspezies entsteht, die einen unprotonierten N-Terminus, jedoch eine protonierte γ-Carboxylfunktion aufweist.
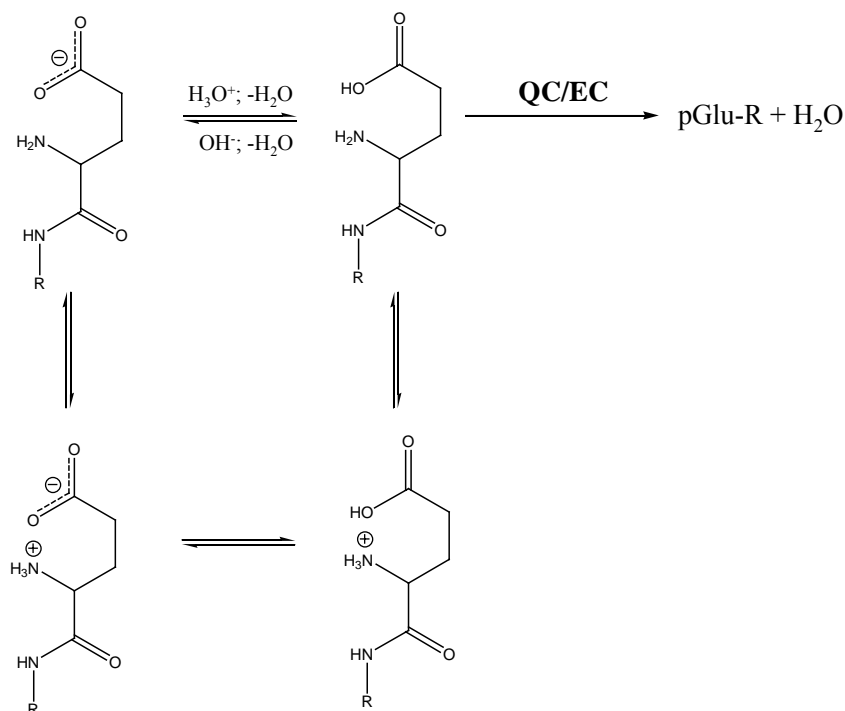

Abb. 5.2: Abhängigkeit der QC-katalysierten Umsetzung N-terminaler Glutamylreste vom Protonierungszustand des Substrates. Nur Substrate mit ungeladener N-terminaler Aminosäure können vom Enzym umgesetzt werden. Durch die unterschiedlichen pK_a-Werte von α-Aminogruppe (≈7,5; 25°C) und γ-Carboxylgruppe (≈4,3; 25°C) von Glutamat in Peptidsubstraten ist die höchste Konzentration der ungeladenen N-terminalen Molekülspezies im pH-Bereich um pH 6 zu finden. Das ermittelte pH-Optimum der Spezifitätskonstante k_{cat}/K_m für die QC-katalysierte Umsetzung von Glu-βNA bei pH 6,0 kann als ein Beleg dafür gelten (Schilling *et al.*, eingereicht).

Die Protonierung der Carboxylgruppe erscheint hier essentiell, da sich dadurch die Carbonylaktivität der Gruppe erhöht. Das Carboxylat-Ion weist keine elektrophilen Eigenschaften auf. Zudem zeigten Untersuchungen an Inhibitoren, dass negative Ladungen der Moleküle zu einer deutlich verschlechterten Bindung am Enzym führen (Schilling *et al.*, 2003b).

Eine elektrostatische Abstoßung vom aktiven Zentrum könnte daher zusätzlich für die geringere Glutamyl-Cyclase Aktivität (EC) der QC im basischen pH-Bereich verantwortlich sein.

Obwohl die dargelegten Untersuchungen eine Beteiligung der QC an der Bildung der pGlu-Aβ-Peptide nahe legen, bedarf es noch eines Nachweises *in vivo*. Einige Fakten weisen darauf hin, dass die QC-Aktivität die vorgeschlagene Schlüsselrolle (Harigaya *et al.*, 2000) bei der Plaqueentstehung spielen könnte:

1) Die QC wird in allen Regionen des Gehirns exprimiert. Eine besonders hohe Expression wurde im Hypothalamus und Hippocampus nachgewiesen, in welchen sich neben den kortikalen Regionen auch Ablagerungen des βA4 bilden.

2) Die intrazelluläre Lokalisation der humanen QC und des APP im sekretorischen Weg stimmen überein (Selkoe, 2001). Zudem konnte gezeigt werden, dass ein großer Teil des APP bereits im sekretorischen Weg durch β-Sekretaseaktivität prozessiert wird (Haass *et al.*, 1995a; Haass *et al.*, 1995b; Hartmann *et al.*, 1997; Selkoe, 1998; Xia *et al.*, 1998). Es ist daher wahrscheinlich, dass die QC bereits vor der Sezernierung mit ihren vermeintlichen Substraten kolokalisiert ist. Neueste Ergebnisse weisen sogar auf die maximale β-Sekretaseaktivität und Lokalisation des APP in sekretorischen Vesikeln hin, dem Ort der intrazellulär höchsten QC-Konzentration (Bockers *et al.*, 1995; Hook und Reisine, 2003).

3) Das Milieu der intrazellulären Kompartimente ER, Golgi und sekretorische Vesikel ist schwach sauer. Diese Bedingungen begünstigen eine Zyklisierung des N-terminalen Glutamats durch QC (Schilling *et al.*, eingereicht).

4) Der Acetylcholinesterase-Inhibitor Rivastigmine (SDZ ENA 713, Novartis) erhöhte die Pyroglutamyl-Aminopeptidaseaktivität im Gehirn der Maus in einer dosisabhängigen Weise. Es wird vermutet, dass der Inhibitor nicht nur durch Verbesserung der synaptischen Transmission, sondern mittelbar durch Stimulierung des Abbaus der Pyroglutamyl-Formen des βA4 wirkt.

5) Die Gabe des Antibiotikums Cliochinol, ein Abkömmling des heterozyklischen Chelators 8-Hydroxychinolin, bewirkte einen Rückgang der amyloidogenen Ablagerungen im Gehirn der Maus (Cherny *et al.*, 2001). Der Wirkmechanismus der Substanz ist noch nicht geklärt. Es wurde vermutet, dass die Komplexierung von Kupfer, welches Bestandteil der Plaques ist, zur Destabilisierung der Ablagerungen führt. Da 8-Hydroxychinolin jedoch auch die humane QC hemmt (unpublizierte Ergebnisse), scheint ein Einfluss auf die Bildung von pGlu-βA4 ebenfalls nicht ausgeschlossen zu sein.

Sollten sich diese Indizien durch den Nachweis der Bildung von pGlu-Amyloid-Peptiden, katalysiert durch QC, *in vivo* bestätigen, könnte die Hemmung der EC-Aktivität eine neue

Möglichkeit eröffnen, die Entstehung und Progression der Alzheimerschen Erkrankung zu verlangsamen. Potentielle Wirkstoffe könnten in diesem Zusammenhang N1-Imidazolderivate sein, die als kompetitive Inhibitoren der QC fungieren (Schilling *et al.*, 2003b).

5.2 Potentielle Ziele der Wirkstoffentwicklung

Eine Beteiligung der QC-Aktivität an der Synthese der Pyroglutamyl-Peptidhormone und der Nachweis der essentiellen Funktion des N-Terminus für die biologische Wirksamkeit dieser Peptide (s. Abschnitt 4, S. 21) eröffnet weitere Möglichkeiten des Einsatzes von QC-Effektoren mit einer pharmakologischen Zielsetzung. Vorstellbar wäre in diesem Zusammenhang beispielsweise eine Beeinflussung der Synthese der Hormone FPP oder Gastrin (vgl. Tabelle 4.1). Eine Hemmung der QC-Aktivität in den Zielzellen könnte zur Sezernierung von unreifen Hormonen führen, die nicht oder nur partiell in der Lage sind, ihre biologische Funktion zu erfüllen. Des weiteren könnte dadurch auch der proteolytische Abbau der Peptide beschleunigt werden, was die pharmakologische Wirkung verstärken würde. In den beiden beschriebenen Fällen wäre ein erwünschtes Resultat eine Unterdrückung der Fertilität der Spermien beziehungsweise die Verringerung der Salzsäureproduktion des Magens.

Als primäres Interesse der Entwicklung von QC-Inhibitoren als Wirkstoffe kann jedoch die Unterdrückung der Bildung der toxischen Pyroglutamyl-Peptide des βA4 angesehen werden (Schilling *et al.*, eingereicht). Durch eine Hemmung der QC-Aktivität in neuronalen Zellen und im zentralen Nervensystem (ZNS) von Alzheimer oder Down Syndrom Patienten könnte die vermutlich entscheidende Blockierung des N-Terminus durch Zyklisierung unterbleiben. Die βA4-Spezies würden dadurch N-terminal nicht gegen Proteolyse stabilisiert. Ein verstärkter Abbau der Peptide wäre das Resultat, was wiederum zu einer Verlangsamung der Plaqueentstehung beitragen würde.

Eine dauerhafte Inhibierung der QC-Aktivität erscheint jedoch nicht unbedingt notwendig, um einen Effekt auf die Plaqueentstehung zu erreichen. Auf Grund der geringen Umsatzgeschwindigkeit der QC-katalysierten Glutamatzyklisierung im Vergleich zur physiologischen Umsetzung von N-terminalem Glutamin könnte bereits eine teilweise Inhibierung der QC/EC-Aktivität durch potente reversible Inhibitoren einen therapeutischen Effekt haben. Wird davon ausgegangen, dass die Bildung der ersten Ablagerungen über Jahrzehnte verläuft, würde bereits eine partielle Hemmung der QC den Beginn der Erkrankung bedeutend verzögern. Zudem kann die Kombinationstherapie von QC-Inhibitoren und Effektoren der Sekretaseaktivitäten oder anderer hydrolytischer Enzyme dazu beitragen, mögliche Nebenwirkungen jeder einzelnen Effektorspezies zu verringern und doch einen maximalen

Therapieeffekt zu erhalten. Die Vermeidung unerwünschter Nebeneffekte erfordert auch den effizienten Transport der Wirkstoffe zum Wirkort („drug targeting").

Eine mögliche Grundstruktur für die zu entwickelnden Wirkstoffe könnten Imidazol-N1-Derivate darstellen (Schilling *et al.*, 2003b). Obgleich diese Verbindungen noch hinsichtlich ihrer Toxizität, der inhibitorischen Potenz und der Bioverfügbarkeit untersucht und optimiert werden müssen, zeigt die Vielzahl der bereits jetzt zugelassenen Pharmaka auf Imidazolbasis, dass eine Wirkstoffentwicklung auf dieser Strukturbasis („lead structure") möglich ist.

Da zur Untersuchung der Funktion der QC-Aktivität im Rahmen dieser Arbeit nur *in vitro* Daten vorliegen, konzentrieren sich aktuelle Untersuchungen auf den Nachweis der Zyklisierung von N-terminalem Glutamat in Zellsystemen. Hierbei geht es um die Klärung der Frage, ob die Zyklisierung durch Applikation von QC-Inhibitoren *in situ* unterdrückt werden kann. Es ist geplant, auf der Basis dieser Ergebnisse erste membrangängige Inhibitoren als potentielle Wirkstoffe zu selektieren und erste präklinische Untersuchungen, z.B. an transgenen Mäusen (Tg2576), einem Tiermodell der Alzheimerschen Krankheit, durchzuführen.

6 Zusammenfassung

Bioaktive Peptide, wie z.B. die Säugerhormone Thyreoliberin oder Gastrin, weisen N-terminal einen Pyroglutamylrest (pGlu) auf. In vielen Fällen ist dieser essentiell für die Ausbildung der physiologisch aktiven Struktur dieser Peptide. Wie gezeigt werden konnte, entsteht die N-terminale Modifikation dieser Hormone durch Zyklisierung eines Glutaminylrestes eines Vorgängermoleküls. Glutaminyl-Cyclasen (QC; EC 2.3.2.5) sind im Tier- und Pflanzenreich vorkommende Enzyme, welche diese Umsetzung katalysieren. Die bisher bekannten QCs der Säuger und Pflanzen sind monomere Glykoproteine mit ähnlicher molekularer Masse von ca. 40 und 33 kDa. Die Enzyme werden über den sekretorischen Expressionsweg gebildet und von den Zellen sezerniert. Diese scheinbare Homologie zwischen Säuger- und pflanzlicher QC spiegelt sich jedoch nicht in der Primärstruktur wider. Während die pflanzlichen Glutaminyl-Cyclasen offenbar eine eigene Enzymfamilie darstellen, zeigen die hoch homologen QCs der Säuger strukturelle Ähnlichkeiten zu bakteriellen Aminopeptidasen.

Neben tierischen Hormonen weisen auch amyloidogene Peptide an ihrem N-Terminus Pyroglutamylreste auf. Bis zu 50 % der Ablagerungen des Peptids βA4 im Gehirn von Patienten mit Alzheimerscher Erkrankung oder Down Syndrom zeigen diese N-terminale Modifikation. Der Präkursor des Pyroglutamats dieser Peptide ist jedoch nicht Glutamin, sondern Glutamat. Eine Involvierung der QC in die Bildung dieser besonders toxischen Peptide, die verstärkt zur Aggregation neigen, wurde daher noch nicht untersucht.

Ein Ziel der vorliegenden Arbeit war die vergleichende Betrachtung der katalytischen Eigenschaften der humanen QC und der pflanzlichen QC aus *Carica papaya*. Es sollte untersucht werden, ob sich die strukturellen Unterschiede in differenten enzymologischen Charakteristika widerspiegeln.

Ein weiteres Ziel dieser Arbeit war zu prüfen, ob humane QC und QC aus *C. papaya* N-terminale Glutamylreste unter Wasserfreisetzung zyklisieren. Die humane QC würde dadurch ein potentielles Zielenzym für eine Wirkstoffentwicklung zur Behandlung neurodegenerativer Erkrankungen darstellen.

Zur Bearbeitung der Aufgaben wurden neue, kontinuierliche Testmethoden zum Nachweis der QC-Aktivität entwickelt und die heterologe Expression der humanen QC in der Hefe *Pichia pastoris* etabliert. Die pflanzliche QC wurde aus Papaya Latex gereinigt. Die folgenden Ergebnisse können zusammenfassend formuliert werden:

1. Humane QC und Papaya-QC zeigen eine sehr ähnliche katalytische Spezifität gegenüber Oligopeptiden und eine ähnliche pH-Abhängigkeit des Substratumsatzes. In beiden Fällen beeinflusst der Protonierungszustand des Substrates die Substratbindung.

Unterschiede bestehen hauptsächlich in der Umsetzung von Dipeptid-Substraten und nicht-physiologischen Dipeptid-Analoga sowie in der Inhibitorspezifität.

2. Imidazol-N1-Derivate wurden als potente kompetitive Inhibitoren der humanen QC identifiziert. Die Charakterisierung ihrer Bindung zum Enzym weist auf eine essentielle Interaktion zwischen basischem Ringstickstoff und dem aktiven Zentrum des Proteins hin. Die Aktivität der pflanzlichen QC wurde durch die Inhibitoren nicht beeinflußt.

3. Die Inhibierung der humanen QC durch heterozyklische Chelatoren identifiziert das Protein als metallabhängiges Enzym. Inaktiviertes Enzym konnte mittels Zink-Ionen reaktiviert werden. Ein Metallion im aktiven Zentrum ist somit auch potentieller Wechselwirkungspartner für die inhibitorisch wirkenden Imidazolderivate. Die Chelatoren beeinflussten die Katalyse der Papaya-QC nicht.

4. Die Identifikation einer essentiellen Disulfidbrücke in der humanen QC und die Metallabhängigkeit bestätigen die strukturelle Verwandtschaft der Säuger-QC zu bakteriellen Zn-abhängigen Aminopeptidasen.

5. Humane und Papaya-QC katalysieren die Umsetzung N-terminaler Glutamylreste.

Die Ergebnisse weisen auf eine generell ähnliche Wirkungsweise der analogen QC tierischen und pflanzlichen Ursprungs hin. Die unterschiedliche Inhibierbarkeit beider QCs ist z.Zt. nur mit möglichen strukturellen und daraus resultierenden mechanistischen Differenzen erklärbar. Es ist jedoch noch unklar, wie die pflanzliche QC die Reaktion beschleunigt. Die Metallabhängigkeit der Katalyse tierischer QCs weist in Analogie zu Aminopeptidasen auf eine Interaktion des Metallions mit der γ-Carbonylgruppe des N-terminalen Glutamins im Substrat hin, was zur Beschleunigung der intramolekularen Reaktion führt.

Die Umsetzung der N-terminalen Glutaminyl- oder Glutamylreste der amyloidogenen βA4 Peptide durch die humane QC könnte auf eine wichtige Rolle bei der Entstehung der Alzheimerschen Erkrankung und anderer Amyloidosen hinweisen. Obwohl die Nachweise einer derartigen Beteiligung auf zellulärer Ebene noch ausstehen, sind die im Rahmen dieser Arbeit gewonnenen Erkenntnisse richtungweisend für nachfolgende Untersuchungen zur physiologischen und pathophysiologischen Funktion der QC und stellen einen Ausgangspunkt für die Entwicklung potentieller Wirkstoffe dar.

7 Literatur

Abraham, G. N. Podell, D. N. (1981). Pyroglutamic acid. Non-metabolic formation, function in proteins and peptides, and characteristics of the enzymes effecting its removal. Mol. Cell. Biochem. *38*, 181-190.

Agirregoitia, N., Gil, J., Ruiz, F., Irazusta, J., Casis, L. (2003). Effect of aging on rat tissue peptidase activities. J. Gerontol. A Biol. Sci. Med. Sci. *58*, 792-797.

Awade, A. C., Cleuziat, P., Gonzales, T., Robert-Baudouy, J. (1994). Pyrrolidone carboxyl peptidase (Pcp): an enzyme that removes pyroglutamic acid (pGlu) from pGlu-peptides and pGlu-proteins. Proteins *20*, 34-51.

Baker, J. O. und Prescott, J. M. (1983). *Aeromonas* Aminopeptidase: pH Dependence and a Transition-State-Analogue Inhibitor. Biochemistry *22*, 5322-5331.

Bateman, R. C., Temple, J. S., Misquitta, S. A., Booth, R. E. (2001). Evidence for essential histidines in human pituitary glutaminyl cyclase. Biochemistry *40*, 11246-11250.

Bateman, R. C. J. (1989). A spectrophotometric assay for glutaminyl-peptide cyclizing enzymes. J. Neurosci. Methods *30*, 23-28.

Bennett, B. und Holz, R. C. (1997). EPR studies on the mono- and dicobalt(II)-substituted forms of the aminopeptidase from *Aeromonas proteolytica*. Insight into the catalytic mechanism of dinuclear hydrolases. J. Am. Chem. Soc. *119*, 1923-1933.

Bockers, T. M., Kreutz, M. R., Pohl, T. (1995). Glutaminyl-cyclase expression in the bovine/porcine hypothalamus and pituitary. J. Neuroendocrinol. *7*, 445-453.

Busby, W. H. J., Quackenbush, G. E., Humm, J., Youngblood, W. W., Kizer, J. S. (1987). An enzyme(s) that converts glutaminyl-peptides into pyroglutamyl-peptides. Presence in pituitary, brain, adrenal medulla, and lymphocytes. J. Biol. Chem. *262*, 8532-8536.

Chen, G. J. und Russell, J. B. (1989). Transport of glutamine by *Streptococcus bovis* and conversion of glutamine to pyroglutamic acid and ammonia. J. Bacteriol. *171*, 2981-2985.

Cherny, R. A., Atwood, C. S., Xilinas, M. E., Gray, D. N., Jones, W. D., McLean, C. A., Barnham, K. J., Volitakis, I., Fraser, F. W., Kim, Y., Huang, X., Goldstein, L. E., Moir, R. D., Lim, J. T., Beyreuther, K., Zheng, H., Tanzi, R. E., Masters, C. L., Bush, A. I. (2001). Treatment with a copper-zinc chelator markedly and rapidly inhibits beta-amyloid accumulation in Alzheimer's disease transgenic mice. Neuron *30*, 665-676.

Chevrier, B., Schalk, C., Orchymont, H., Rondeau, J. M., Moras, D., Tarnus, C. (1994). Crystal structure of *Aeromonas proteolytica* aminopeptidase: a prototypical member of the co-catalytic zinc enzyme family. Structure *2*, 283-291.

Consalvo, A. P., Young, S. D., Jones, B. N., Tamburini, P. P. (1988). A rapid fluorometric assay for N-terminal glutaminyl cyclase activity using high-performance liquid chromatography. Anal. Biochem. *175*, 131-138.

Dahl, S. W., Slaughter, C., Lauritzen, C., Bateman, R. C. Jr., Connerton, I., Pedersen, J. (2000). Carica papaya glutamine cyclotransferase belongs to a novel plant enzyme subfamily: cloning and characterization of the recombinant enzyme. Protein Expr. Purif. *20*, 27-36.

El Moussaoui, A., Nijs, M., Paul, C., Wintjens, R., Vincentelli, J., Azarkan, M., Looze, Y. (2001). Revisiting the enzymes stored in the laticifers of Carica papaya in the context of their possible participation in the plant defence mechanism. Cell. Mol. Life Sci. *58*, 556-570.

Esch, F. S., Keim, P. S., Beattie, E. C., Blacher, R. W., Culwell, A. R., Oltersdorf, T., McClure, D., Ward, P. J. (1990). Cleavage of amyloid beta peptide during constitutive processing of its precursor. Science *248*, 1122-1124.

Fischer, W. H. und Spiess, J. (1987). Identification of a mammalian glutaminyl cyclase converting glutaminyl into pyroglutamyl peptides. Proc. Natl. Acad. Sci. U. S. A. *84*, 3628-3632.

Francis, R., McGrath, G., Zhang, J., Ruddy, D. A., Sym, M., Apfeld, J., Nicoll, M., Maxwell, M., Hai, B., Ellis, M. C., Parks, A. L., Xu, W., Li, J., Gurney, M., Myers, R. L., Himes, C. S., Hiebsch, R., Ruble, C., Nye, J. S., Curtis, D. (2002). aph-1 and pen-2 are required for Notch pathway signaling, gamma-secretase cleavage of betaAPP, and presenilin protein accumulation. Dev. Cell *3*, 85-97.

Fujiwara, K. und Tsuru, D. (1978). New chromogenic and fluorogenic substrates for pyrrolidonyl peptidase. J. Biochem. (Tokyo) *83*, 1145-1149.

Garden, R. W., Moroz, T. P., Gleeson, J. M., Floyd, P. D., Li, L., Rubakhin, S. S., Sweedler, J. V. (1999). Formation of N-pyroglutamyl peptides from N-Glu and N-Gln precursors in *Aplysia* neurons. J. Neurochem. *72*, 676-681.

Giordani, R., Cardenas, M. L., Moulin-Traffort, J., Regli, P. (1996). Fungicidal activity of latex sap from *Carica papaya* and antifungal effect of D(+)-glucosamine on Cundida albicans growth. Mycoses *39*, 103-110.

Glenner, G. G. und Wong, C. W. (1984a). Alzheimer's disease and Down's syndrome: sharing of a unique cerebrovascular amyloid fibril protein. Biochem. Biophys. Res. Commun. *122*, 1131-1135.

Glenner, G. G. und Wong, C. W. (1984b). Alzheimer's disease: initial report of the purification and characterization of a novel cerebrovascular amyloid protein. Biochem. Biophys. Res. Commun. *120*, 885-890.

Goate, A., Chartier, H., Mullan, M., Brown, J., Crawford, F., Fidani, L., Giuffra, L., Haynes, A., Irving, N., James, L. (1991). Segregation of a missense mutation in the amyloid precursor protein gene with familial Alzheimer's disease. Nature *349*, 704-706.

Goldgaber, D., Lerman, M. I., McBride, O. W., Saffiotti, U., Gajdusek, D. C. (1987). Characterization and chromosomal localization of a cDNA encoding brain amyloid of Alzheimer's disease. Science *235*, 877-880.

Gololobov, M. Y., Song, I., Wang, W., Bateman, R. C. J. (1994). Steady-state kinetics of glutamine cyclotransferase. Arch. Biochem. Biophys. *309*, 300-307.

Gololobov, M. Y., Wang, W., Bateman, R. C. J. (1996). Substrate and inhibitor specificity of glutamine cyclotransferase (QC). Biol. Chem. *377*, 395-398.

Haass, C., Koo, E. H., Capell, A., Teplow, D. B., Selkoe, D. J. (1995a). Polarized sorting of beta-amyloid precursor protein and its proteolytic products in MDCK cells is regulated by two independent signals. J. Cell Biol. *128*, 537-547.

Haass, C., Lemere, C. A., Capell, A., Citron, M., Seubert, P., Schenk, D., Lannfelt, L., Selkoe, D. J. (1995b). The Swedish mutation causes early-onset Alzheimer's disease by beta-secretase cleavage within the secretory pathway. Nat. Med. *1*, 1291-1296.

Harigaya, Y., Saido, T. C., Eckman, C. B., Prada, C.-J., Shoji, M., Younkin, S. G. (2000). Amyloid β protein starting pyroglutamate at position 3 is a major component of the amyloid deposits in the Alzheimer`s disease brain. Biochem. Biophys. Res. Commun. *276*, 422-427.

Hartmann, T., Bieger, S. C., Bruhl, B., Tienari, P. J., Ida, N., Allsop, D., Roberts, G. W., Masters, C. L., Dotti, C. G., Unsicker, K., Beyreuther, K. (1997). Distinct sites of intracellular production for Alzheimer's disease A beta40/42 amyloid peptides. Nat. Med. *3*, 1016-1020.

Hashimoto, T., Wakabayashi, T., Watanabe, A., Kowa, H., Hosoda, R., Nakamura, A., Kanazawa, I., Arai, T., Takio, K., Mann, D. M., Iwatsubo, T. (2002). CLAC: a novel Alzheimer amyloid plaque component derived from a transmembrane precursor, CLAC-P/collagen type XXV. EMBO J. *21*, 1524-1534.

He, W. und Barrow, C. J. (1999). The A beta 3-pyroglutamyl and 11-pyroglutamyl peptides found in senile plaque have greater beta-sheet forming and aggregation propensities in vitro than full-length A beta. Biochemistry *38*, 10871-10877.

Hook, V. Y. H. und Reisine, T. D. (2003). Cysteine proteases are the major β-Secretase in the regulated secretory pathway that provides most of the β-amyloid in Alzheimer`s Disease: Role of BACE1 in the constitutive secretory pathway. J. Neurosci. Res. *74*, 393-405.

Hosoda, R., Saido, T. C., Otvos, L. J., Arai, T., Mann, D. M., Lee, V. M., Trojanowski, J. Q., Iwatsubo, T. (1998). Quantification of modified amyloid beta peptides in Alzheimer disease and Down syndrome brains. J. Neuropathol. Exp. Neurol. *57*, 1089-1095.

Hung, A. Y. und Selkoe, D. J. (1994). Selective ectodomain phosphorylation and regulated cleavage of beta-amyloid precursor protein. EMBO J. *13*, 534-542.

Kang, J., Lemaire, H. G., Unterbeck, A., Salbaum, J. M., Masters, C. L., Grzeschik, K. H., Multhaup, G., Beyreuther, K., Muller, H. (1987). The precursor of Alzheimer's disease amyloid A4 protein resembles a cell-surface receptor. Nature *325*, 733-736.

Koger, J. B., Humm, J., Kizer, J. S. (1989). Assay of glutaminylpeptide cyclase. Methods Enzymol. *168*, 358-365.

Kuda, T., Shoji, M., Arai, H., Kawashima, S., Saido, T. C. (1997). Reduction of plasma glutamyl aminopeptidase activity in sporadic Alzheimer's disease. Biochem. Biophys. Res. Commun. *231*, 526-530.

Kuo, Y. M., Emmerling, M. R., Woods, A. S., Cotter, R. J., Roher, A. E. (1997). Isolation, chemical characterization, and quantitation of A beta 3-pyroglutamyl peptide from neuritic plaques and vascular amyloid deposits. Biochem. Biophys. Res. Commun. *237*, 188-191.

Levy, E., Carman, M. D., Fernundez, M., Power, M. D., Lieberburg, I., van De Bots, G. T., Luyendijk, W., Frangione, B. (1990). Mutation of the Alzheimer's disease amyloid gene in hereditary cerebral hemorrhage, Dutch type. Science *248*, 1124-1126.

Lowther, W. T. und Matthews, B. W. (2002). Metalloaminopeptidases: common functional themes in disparate structural surroundings. Chem. Rev. *102*, 4581-4608.

Messer, M. (1963). Enzymatic cyclization of L-glutamine and L-glutaminyl peptides. Nature *4874*, 1299.

Messer, M. und Ottesen, M. (1964). Isolation and properties of glutamine cyclotransferase of dried papaya latex. Biochim. Biophys. Acta *92*, 409-411.

Mori, H., Takio, K., Ogawara, M., Selkoe, D. J. (1992). Mass spectrometry of purified amyloid beta protein in Alzheimer's disease. J. Biol. Chem. *267*, 17082-17086.

Munger, J. S., Haass, C., Lemere, C. A., Shi, G. P., Wong, W. S., Teplow, D. B., Selkoe, D. J., Chapman, H. A. (1995). Lysosomal processing of amyloid precursor protein to A beta peptides: a distinct role for cathepsin S. Biochem. J. *311*, 299-305.

Oberg, K. A., Ruysschaert, J. M., Azarkan, M., Smolders, N., Zerhouni, S., Wintjens, R., Amrani, A., Looze, Y. (1998). Papaya glutamine cyclase, a plant enzyme highly resistant to proteolysis, adopts an all-beta conformation. Eur. J. Biochem. *258*, 214-222.

Pike, C. J., Overman, M. J., Cotman, C. W. (1995). Amino-terminal deletions enhance aggregation of beta-amyloid peptides in vitro. J. Biol. Chem. *270*, 23895-23898.

Pohl, T., Zimmer, M., Mugele, K., Spiess, J. (1991). Primary structure and functional expression of a glutaminyl cyclase. Proc. Natl. Acad. Sci. U. S. A. *88*, 10059-10063.

Prescott, J. M., Wagner, F. W., Holmquist, B., Vallee, B. L. (1985). Spectral and kinetic studies of metal-substituted *Aeromonas* aminopeptidase: nonidentical, interacting metal-binding sites. Biochemistry *24*, 5350-5356.

Prescott, J. M. und Wilkes, S. H. (1966). *Aeromonas* aminopeptidase: Purification and some general properties. Arch. Biochem. Biophys. *117*, 328-336.

Prescott, J. M. und Wilkes, S. H. (1976). *Aeromonas* aminopeptidase. Methods Emzymol. *45*, 530-543.

Prescott, J. M., Wilkes, S. H., Wagner, F. W., Wilson, K. J. (1971). *Aeromonas* aminopeptidase. Improved isolation and some physical properties. J. Biol. Chem. *246*, 1756-1764.

Russo, C., Saido, T. C., DeBusk, L. M., Tabaton, M., Gambetti, P., Teller, J. K. (1997). Heterogeneity of water-soluble amyloid beta-peptide in Alzheimer's disease and Down's syndrome brains. FEBS Lett. *409*, 411-416.

Russo, C., Violani, E., Salis, S., Venezia, V., Dolcini, V., Damonte, G., Benatti, U., Arrigo, C., Patrone, E., Carlo, P., Schettini, G. (2002). Pyroglutamate-modified amyloid beta-peptides--AbetaN3(pE)--strongly affect cultured neuron and astrocyte survival. J. Neurochem. *82*, 1480-1489.

Saido, T. C. (1998). Alzheimer's disease as proteolytic disorders: anabolism and catabolism of beta-amyloid. Neurobiol. Aging *19*, S69-S75.

Saido, T. C., Iwatsubo, T., Mann, D. M., Shimada, H., Ihara, Y., Kawashima, S. (1995). Dominant and differential deposition of distinct beta-amyloid peptide species, A beta N3(pE), in senile plaques. Neuron *14*, 457-466.

Saido, T. C., Yamao, H., Iwatsubo, T., Kawashima, S. (1996). Amino- and carboxyl-terminal heterogeneity of beta-amyloid peptides deposited in human brain. Neurosci. Lett. *215*, 173-176.

Scheuner, D., Eckman, C., Jensen, M., Song, X., Citron, M., Suzuki, N., Bird, T. D., Hardy, J., Hutton, M., Kukull, W., Larson, E., Levy, L., Viitanen, M., Peskind, E., Poorkaj, P., Schellenberg, G., Tanzi, R., Wasco, W., Lannfelt, L., Selkoe, D., Younkin, S. (1996). Secreted amyloid beta-protein similar to that in the senile plaques of Alzheimer's disease is increased in vivo by the presenilin 1 and 2 and APP mutations linked to familial Alzheimer's disease. Nat. Med. *2*, 864-870.

Schilling, S., Hoffmann, T., Rosche, F., Manhart, S., Wasternack, C., Demuth, H.-U. (2002a). Heterologous expression and characterization of human glutaminyl cyclase: evidence for a disulfide bond with importance for catalytic activity. Biochemistry *41*, 10849-10857.

Schilling, S., Hoffmann, T., Wermann, M., Heiser, U., Wasternack, C., Demuth, H.-U. (2002b). Continuous spectrometric assays for glutaminyl cyclase activity. Anal. Biochem. *303*, 49-56.

Schilling, S., Manhart, S., Hoffmann, T., Ludwig, H.-H., Wasternack, C., Demuth, H.-U. (2003a). Substrate specificity of glutaminyl cyclases from plants and animals. Biol. Chem. *384*, 1583-1592.

Schilling, S., Niestroj, A. J., Rahfeld, J.-U., Hoffmann, T., Wermann, M., Zunkel, K., Wasternack, C., Demuth, H.-U. (2003b). Identification of human glutaminyl cyclase as a metalloenzyme: Inhibition by imidazole derivatives and heterocyclic chelators. J. Biol. Chem. *278*, 49773-49779.

Schilling, S. und Demuth, H.-U. (2004). Continuous assays of glutaminyl cyclase: From development to application. Spectroscopy, in press.

Selkoe, D. J. (1998). The cell biology of beta-amyloid precursor protein and presenilin in Alzheimer's disease. Trends Cell Biol. *8*, 447-453.

Selkoe, D. J. (2001). Alzheimer's disease: genes, proteins, and therapy. Physiol. Rev. *81*, 741-766.

Selkoe, D. J., Podlisny, M. B., Joachim, C. L., Vickers, E. A., Lee, G., Fritz, L. C., Oltersdorf, T. (1988). Beta-amyloid precursor protein of Alzheimer disease occurs as 110- to 135-kilodalton membrane-associated proteins in neural and nonneural tissues. Proc. Natl. Acad. Sci. U. S. A. *85*, 7341-7345.

Sinha, S., Underson, J. P., Barbour, R., Basi, G. S., Caccavello, R., Davis, D., Doan, M., Dovey, H. F., Frigon, N., Hong, J., Jacobson, C., Jewett, N., Keim, P., Knops, J., Lieberburg, I.,

Power, M., Tan, H., Tatsuno, G., Tung, J., Schenk, D., Seubert, P., Suomensaari, S. M., Wang, S., Walker, D., John, V. (1999). Purification and cloning of amyloid precursor protein beta-secretase from human brain. Nature *402*, 537-540.

Song, I., Chuang, C. Z., Bateman, R. C. J. (1994). Molecular cloning, sequence analysis and expression of human pituitary glutaminyl cyclase. J. Mol. Endocrinol. *13*, 77-86.

Takasugi, N., Takahashi, Y., Morohashi, Y., Tomita, T., Iwatsubo, T. (2002). The mechanism of gamma-secretase activities through high molecular weight complex formation of presenilins is conserved in Drosophila melanogaster and mammals. J. Biol. Chem. *277*, 50198-50205.

Takasugi, N., Tomita, T., Hayashi, I., Tsuruoka, M., Niimura, M., Takahashi, Y., Thinakaran, G., Iwatsubo, T. (2003). The role of presenilin cofactors in the gamma-secretase complex. Nature *422*, 438-441.

Temple, J. S., Song, I., Burns K. H., Bateman, R. C. J. (1998). Absence of an essential thiol in human glutaminyl cyclase: implications for mechanism. Korean J. Biol. Sci. *2*, 243-248.

Terry, R. D. und Katzman, R. (1983). Senile dementia of the Alzheimer type. Ann. Neurol. *14*, 497-506.

Thinakaran, G., Harris, C. L., Ratovitski, T., Davenport, F., Slunt, H. H., Price, D. L., Borchelt, D. R., Sisodia, S. S. (1997). Evidence that levels of presenilins (PS1 and PS2) are coordinately regulated by competition for limiting cellular factors. J. Biol. Chem. *272*, 28415-28422.

Tomita, T., Watabiki, T., Takikawa, R., Morohashi, Y., Takasugi, N., Kopan, R., de Strooper, B., Iwatsubo, T. (2001). The first proline of PALP motif at the C terminus of presenilins is obligatory for stabilization, complex formation, and gamma-secretase activities of presenilins. J. Biol. Chem. *276*, 33273-33281.

Van Coillie, E., Proost, P., Van Aelst, I., Struyf, S., Polfliet, M., De Meester, I., Harvey, D. J., Van Damme, J., Opdenakker, G. (1998). Functional comparison of two human monocyte chemotactic protein-2 isoforms, role of the amino-terminal pyroglutamic acid and processing by CD26/dipeptidyl peptidase IV. Biochemistry *37*, 12672-12680.

Vassar, R., Bennett, B. D., Babu, K., Kahn, S., Mendiaz, E. A., Denis, P., Teplow, D. B., Ross, S., Amarante, P., Loeloff, R., Luo, Y., Fisher, S., Fuller, J., Edenson, S., Lile, J., Jarosinski, M. A., Biere, A. L., Curran, E., Burgess, T., Louis, J. C., Collins, F., Treanor, J., Rogers, G., Citron, M. (1999). Beta-secretase cleavage of Alzheimer's amyloid precursor protein by the transmembrane aspartic protease BACE. Science *286*, 735-741.

Vidal, R., Frangione, B., Rostagno, A., Mead, S., Revesz, T., Plant, G., Ghiso, J. (1999). A stop-codon mutation in the BRI gene associated with familial British dementia. Nature *399*, 776-781.

Wagner, F. W., Wilkes, S. H., Prescott, J. M. (1972). Specificity of *Aeromonas* aminopeptidase toward amino acid amides and dipeptides. J. Biol. Chem. *247*, 1208-1210.

Wilkes, S. H., Bayliss, M. E., Prescott, J. M. (1973). Specificity of *Aeromonas* aminopeptidase toward oligopeptides and polypeptides. Eur. J. Biochem. *34*, 459-466.

Xia, W., Zhang, J., Ostaszewski, B. L., Kimberly, W. T., Seubert, P., Koo, E. H., Shen, J., Selkoe, D. J. (1998). Presenilin 1 regulates the processing of beta-amyloid precursor protein C-terminal fragments and the generation of amyloid beta-protein in endoplasmic reticulum and Golgi. Biochemistry *37*, 16465-16471.

Yamada, K., Shimada, T., Kondo, M., Nishimura, M., Hara, N. (1999). Multiple functional proteins are produced by cleaving Asn-Gln bonds of a single precursor by vacuolar processing enzyme. J. Biol. Chem. *274*, 2563-2570.

Yan, R., Bienkowski, M. J., Shuck, M. E., Miao, H., Tory, M. C., Pauley, A. M., Brashier, J. R., Stratman, N. C., Mathews, W. R., Buhl, A. E., Carter, D. B., Tomasselli, A. G., Parodi, L. A., Heinrikson, R. L., Gurney, M. E. (1999). Membrane-anchored aspartyl protease with Alzheimer's disease beta-secretase activity. Nature *402*, 533-537.

Zerhouni, S., Amrani, A., Nijs, M., Smolders, N., Azarkan, M., Vincentelli, J., Looze, Y. (1998). Purification and characterization of papaya glutamine cyclotransferase, a plant enzyme highly resistant to chemical, acid and thermal denaturation. Biochim. Biophys. Acta *1387*, 275-290.

Zerhouni, S., Amrani, A., Nijs, M., Vundermeers, A., Looze, Y. (1997). Purification and characterization of the plant glutaminyl-peptide cyclotransferase isolated from papaya latex. Int. J. Bio-chromatography *3*, 189-206.

8 Angefügte Publikationen und Manuskripte

Schilling, S., Hoffmann, T., Rosche, F., Manhart, S., Wasternack, C., Demuth, H.-U. (2002a). Heterologous expression and characterization of human glutaminyl cyclase: evidence for a disulfide bond with importance for catalytic activity. Biochemistry *41*, 10849-10857.

Schilling, S., Hoffmann, T., Wermann, M., Heiser, U., Wasternack, C., Demuth, H.-U. (2002b). Continuous spectrometric assays for glutaminyl cyclase activity. Anal. Biochem. *303*, 49-56.

Schilling, S., Manhart, S., Hoffmann, T., Ludwig, H.-H., Wasternack, C., Demuth, H.-U. (2003a). Substrate specificity of glutaminyl cyclases from plants and animals. Biol. Chem. *384*, 1583-1592.

Schilling, S., Niestroj, A. J., Rahfeld, J.-U., Hoffmann, T., Wermann, M., Zunkel, K., Wasternack, C., Demuth, H.-U. (2003b). Identification of human glutaminyl cyclase as a metalloenzyme: Inhibition by imidazole derivatives and heterocyclic chelators. J. Biol. Chem. *278*, 49773-49779.

Schilling, S. und Demuth, H.-U. (2004). Continuous assays of glutaminyl cyclase: From development to application. Spectroscopy, im Druck.

Schilling, S., Hoffmann, T., Manhart, S., Hoffmann, M., Demuth, H.-U. Inhibition of glutaminyl cyclase prevents the formation of pGlu[3]-amyloid-β related peptides. Biochemistry, in Revision.

Heterologous Expression and Characterization of Human Glutaminyl Cyclase: Evidence for a Disulfide Bond with Importance for Catalytic Activity

Stephan Schilling,[‡] Torsten Hoffmann,[‡] Fred Rosche,[‡] Susanne Manhart,[‡] Claus Wasternack,[§] and Hans-Ulrich Demuth*,[‡]

Laboratory of Biochemistry, Probiodrug AG, Weinbergweg 22, 06120 Halle/Saale, Germany, and Leibniz Institute for Plant Biochemistry, P.O. Box 110432, 06120 Halle/Saale, Germany

ABSTRACT: Glutaminyl cyclase (QC, EC 2.3.2.5) catalyzes the formation of pyroglutamate residues from glutamine at the N-terminus of peptides and proteins. In the current study, human QC was functionally expressed in the secretory pathway of *Pichia pastoris*, yielding milligram quantities after purification from the supernatant of a 5 L fermentation. Initial characterization studies of the recombinant QC using MALDI-TOF mass spectrometry revealed correct proteolytic processing and N-glycosylation at both potential sites with similar 2 kDa extensions. CD spectral analysis indicated a high α-helical content, which contrasts with plant QC from *Carica papaya*. The kinetic parameters for conversion of H-Gln-Tyr-Ala-OH by recombinant human QC were almost identical to those previously reported for purified bovine pituitary QC. However, the results obtained for conversion of H-Gln-Gln-OH, H-Gln-NH₂, and H-Gln-AMC were found to be contradictory to previous studies on human QC expressed intracellularly in *E. coli*. Expression of QC in *E. coli* showed that approximately 50% of the protein did not contain a disulfide bond that is present in the entire QC expressed in *P. pastoris*. Further, the enzyme was consistently inactivated by treatment with 15 mM DTT, whereas deglycosylation had no effect on enzymatic activity. Analysis of the fluorescence spectra of the native, reduced, and unfolded human QC point to a conformational change of the protein upon treatment with DTT. In terms of the different enzymatic properties, the consequences of QC expression in different environments are discussed.

Besides proteolytic cleavage and C-terminal amidation, N-terminal formation of 5-oxoproline (pyroglutamate, pGlu) is a common post-translational event during the biosynthesis of a number of peptides. Examples of pyroglutamate containing peptides include the hormones thyrotropin-releasing hormone (TRH) and gastrin, the neuropeptide neurotensin, and the chemokines MCP-1 through MCP-4 (*1*, *2*). For peptides such as TRH and MCP-2, biological function has been shown to depend on the 5-oxoproline at their N-terminus. Loss or modification of this residue leads to a decrease in biological activity (*3*, *4*). The maturation of these peptide hormones, taking place in the regulated secretory pathway (RSP), is well understood, and many of the enzymes involved in the pro-hormone to hormone conversion have been identified and characterized (*5*, *6*). The enzyme glutaminyl cyclase (QC), however, responsible for formation of pyroglutamate from glutamine at the N-termini of hormones, is poorly understood.

First identified in the plant *Carica papaya* (*7*), QCs have been reported from a bovine (*8*), porcine (*9*), and human as well as other mammalian sources (*10*, *11*). Though the QCs from plants and mammals are similar in size (33 kDa and 38−40 kDa respectively), recent studies have revealed little or no sequence homology between them (*12*). A highly conserved primary structure, however, was reported for QCs from different mammalian species (*11*).

Due to the abundancy of QC in papaya latex and to a simple isolation procedure, the majority of biochemical data of QC has been collected for the papaya enzyme (*13−15*). To date, there has been only one report of QC purification to homogeneity from a natural mammalian source. On the basis of considerable effort, 38 μg of homogeneous QC could be recovered from 2000 bovine pituitaries (*16*). Subsequently, cDNAs encoding the bovine and human enzyme, respectively, have been isolated, and enzymological studies with recombinant human QC expressed intracellulary in *Escherichia coli* have been reported (*10*, *11*). Aggregation of the protein during bacterial expression, however, has necessitated protein refolding under denaturing conditions or expression of the QC as a fusion protein (N-terminal mannose binding protein or glutathione S-transferase) in order to recover the active protein.

These difficulties tempted us to express human QC in another host system, *Pichia pastoris*. This methylotrophic

---

* Corresponding author. Tel.: 49 345 5559900. Fax: 49 345 5559901. E-mail: Hans-Ulrich.Demuth@probiodrug.de.

‡ Probiodrug AG.

§ Leibniz Institute for Plant Biochemistry.

¹ Abbreviations: BMGY, buffered glycerol complex medium; BMMY, buffered methanol complex medium; DAHC, diammonium hydrogen citrate; DAP A, dipeptidyl aminopeptidase A; DHAP, 2′,6′-dihydroxyacetophenone; DTT, dithiothreitol; GdmCl, guanidinium chloride; GlcNAc, N-acetyl-D-glucosamine; H-Gln-AMC, L-glutaminyl-4-methylcoumarinylamide; H-Gln-βNA, L-glutaminyl-2-naphthylamide; IMAC, immobilized metal ion affinity chromatography; IPTG, isopropyl β-D-1-thiogalactopyranoside; Man, D-mannose; MCP, monocyte chemotactic protein; QC, glutaminyl cyclase; TFA, trifluoroacetic acid; TRH, thyrotropin releasing hormone

Table 1: Oligonucleotides Used in Cloning Procedures for Heterologous Expression of QC in *E. coli* and *P. pastoris*

oligonucleotiode	sequence (5′ → 3′), restriction sites (underlined)	restriction enzyme for cloning
QC−SDMCs	GCCGTGCCATGTGCAATGATGTTG	−
QC−SDMCas	CAACATCATTGCACATGGCACGGC	−
QC4	ATAGTCGACGCAGGCGGAAGACACCGGC	*Sal*I
QC5	ATAAAGCTTTTACAAATGAAGATATTCC	*Hin*dIII
pQCyc-1	ATATAGCATGCGGAGGAGAAGAATTACCACCAG	*Sph*I
pQCyc-2	ATATAAAGCTTACAAATGAAGATATTCCAACAC	*Hin*dIII
QC−Pic1	ATGCTAGCGCCTGGCCAGAGGAGAAGAAT	*Nhe*I
QC−Pic2	ATTCTAGAGTATTACAAATGAAGATATTC	*Xba*I
HPic-K1	GCTCATCATCATCATCATGCTAGCGGTAC	*Nhe*I
HPic-K2	CGCTAGCATGATGATGATGATGATGAGCTGCA	*Nhe*I

yeast shares the advantages of bacterial hosts, such as simple genetic manipulation, simple culture conditions and rapid growth, while facilitating post-translational modification in a manner more similar to that of higher eukaryotes (e.g., N-glycosylation, disulfide formation, fatty acylation and C-terminal methylation). Further, *P. pastoris* allows high-level expression of heterologous proteins either intracellulary or in secreted form (*17−19*), as well as allowing simple scale-up production using a fermenter.

Here, we describe the large-scale expression of human QC in *P. pastoris* and the subsequent identification of important enzymatic properties in contrast to those obtained from human QC expressed in *E. coli*.

EXPERIMENTAL PROCEDURES

Host strains and media. The *E. coli* strain JM109 was applied for all plasmid constructions and propagation. *P. pastoris* strain X33 (*AOX1, AOX2*), used for the expression of human QC was grown, transformed, and analyzed according to the manufacturer's instructions (Invitrogen). Media for propagation of *E. coli*, i.e., low salt LB, as well as the media required for *P. pastoris*, i.e., buffered glycerol (BMGY) complex or methanol (BMMY) complex medium, and the fermentation basal salts medium were prepared according to the manufacturer's recommendations.

Isolation of QC cDNA and site-directed mutagenesis. A full-length cDNA encoding the human QC was isolated from clone DKFZp566F243, obtained from the resource center of the human genome project at the Max-Plank-Institute for Molecular Genetics (Berlin, Germany). Sequencing (Seqlab GmbH, Göttingen) of the cDNA revealed three single base exchanges in the open reading frame, one in codon 15 replacing CTG (Leu) by CCG (Pro), a silent exchange in codon 98 (CTC instead of CTT), and in codon 164 TGT (Cys) was replaced by TGG (Trp). Site-directed mutagenesis was carried out to replace Trp with Cys at position 164. All amplifications were performed according to the instructions of the supplier of the *Pfu* polymerase utilized (New England Biolabs). In brief, the complementary oligonucleotides QC−SDMCs and QC−SDMCas (Table 1) were employed for amplification of two fragments of the cDNA with oligonucleotides QC4 and QC5, which cover the open reading frame of QC. Subsequently, a second PCR was performed using the two fragments as template and again Primers QC4 and QC5, yielding the cDNA encoding a Cys in codon 164. The open reading frame was subcloned into the pPCR−Script Cam SK(+) vector applying the manufacturer's recommendations (Stratagene).

Molecular cloning of plasmid vectors encoding the human QC. All cloning procedures were done applying standard molecular biology techniques (*20*). For expression in yeast, the vector pPICZαB (Invitrogen) was used that covers a coding sequence for the *S. cerevisiae* α-factor prepro-peptide upstream of a multiple cloning site. To express the QC with an N-terminal 6×histidine affinity tag, a cassette consisting of the oligonucleotides HPic-K1 and HPic-K2 (Table 1) was inserted in frame with the leader sequence using the restriction sites *Pst*I and *Kpn*I. In addition, with the cassette a novel restriction site for *Nhe*I was introduced. Finally, the cDNA encoding the mature QC starting with amino acid 33 was amplified by PCR using the primers QC−Pic1 an QC−Pic2 (Table 1). Subsequently, subcloning into the pPCRScript Cam SK (+) vector and insertion into the yeast expression plasmid via the *Nhe*I and *Xba*I restriction sites was performed.

The pQE−31 vector (Qiagen) was used to express the human QC in *E. coli*. The cDNA of the mature QC starting with codon 38 was fused in frame with the plasmid encoded 6×histidine tag. After amplification utilizing the primers pQCyc-1 and pQCyc-2 (Table 1) and subcloning, the fragment was inserted into the expression vector employing the restriction sites of *Sph*I and *Hin*dIII. All expression plasmids were sequenced using either vector- or cDNA-specific primers.

Transformation of P. pastoris and mini-scale expression. Plasmid DNA was amplified in *E. coli* JM109 and purified according to the recommendations of the manufacturer (Qiagen). In the expression plasmid used, pPICZαB, three restriction sites are provided for linearization. Since *Sac*I and *Bst*XI cut within the QC cDNA, *Pme*I was chosen for linearization. 20−30 μg plasmid DNA was linearized with *Pme*I, precipitated by ethanol, and dissolved in sterile, deionized water. A 10 μg sample of the DNA was then applied for transformation of competent *P. pastoris* cells by electroporation according to the manufacturer's instructions (BioRad). Selection was done on plates containing 150 μg/mL Zeocin. One transformation using the linearized plasmid yielded several hundred transformants.

To test the recombinant yeast clones for QC expression, recombinants were grown for 24 h in 10 mL conical tubes containing 2 mL BMGY. Afterward, the yeast was centrifuged and resuspended in 2 mL BMMY containing 0.5% methanol. This concentration was maintained by addition of methanol every 24−72 h. Subsequently, QC activity in the supernatant was determined. The presence of the fusion protein was confirmed by western blot analysis using an

antibody directed against the 6×histidine tag (Qiagen). Clones that displayed the highest QC activity were chosen for further experiments and fermentation.

Large-scale expression in a fermenter. Expression of the QC was performed in a 5 L reactor (Biostad B, B. Braun biotech), essentially as described in the "*Pichia* fermentation process guidelines" (Invitrogen). In brief, the cells were grown in the fermentation basal salts medium supplemented with trace salts, and with glycerol as the sole carbon source (pH 5.5). During an initial batch phase for about 24 h and a subsequent fed-batch phase for about 5 h, cell mass was accumulated. Once a cell wet weight of 200 g/L was achieved, induction of QC expression was performed using methanol applying the three-step feeding profile recommended by invitrogen for an entire fermentation time of approximately 60 h. Subsequently, cells were removed from the QC-containing supernatant by centrifugation at 6000g, 4 °C for 15 min. The pH was adjusted to 6.8 by addition of NaOH, and the resultant turbid solution was centrifuged at 37000g, 4 °C, for 40 min. In cases of continued turbidity, an additional filtration step was applied using a cellulose membrane (pore width 0.45 μm).

Purification of 6×histidine tagged QC expressed in P. pastoris. The His-tagged QC was first purified by immobilized metal ion affinity chromatography (IMAC). In a typical purification, 1000 mL of culture supernatant was applied to a Ni^{2+}-loaded Chelating Sepharose FF column (1.6 × 20 cm, Pharmacia) that was equilibrated with 50 mM phosphate buffer, pH 6.8, containing 750 mM NaCl, at a flow rate of 5 mL/min. After washing with 10 column volumes of equilibration buffer and 5 column volumes of equilibration buffer containing 5 mM histidine, the bound protein was eluted by a shift to 50 mM phosphate buffer, pH 6.8, containing 150 mM NaCl and 100 mM histidine. The resulting eluate was dialyzed against 20 mM Bis-Tris/HCl, pH 6.8, at 4 °C overnight. Subsequently, the QC was further purified by anion exchange chromatography on a Mono Q6 column (BioRad), equilibrated with dialysis buffer. The QC-containing fraction was loaded onto the column using a flow rate of 4 mL/min. The column was then washed with equilibration buffer containing 100 mM NaCl. The elution was performed by two gradients, resulting in equilibration buffer containing 240 and 360 mM NaCl in 30 or 5 column volumes, respectively. Fractions of 6 mL were collected and the purity was analyzed by SDS−PAGE. Fractions containing homogeneous QC were pooled and concentrated by ultrafiltration. For long-term storage (−20 °C), glycerol was added to a final concentration of 50%. Protein was quantified according to the methods of Bradford or Gill and von Hippel (*21, 22*).

Expression and purification of QC in E. coli. The construct encoding the QC was transformed into M15 cells (Qiagen) and grown on selective LB agar plates at 37 °C. Protein expression was carried out in LB medium containing 1% glucose and 1% ethanol at room temperature. When the culture reached an OD$_{600}$ of approximately 0.8, expression was induced with 0.1 mM IPTG overnight. After one cycle of freezing and thawing, cells were lysed at 4 °C by addition of 2.5 mg/mL lysozyme in 50 mM phosphate buffer, pH 8.0, containing 300 mM NaCl and 5 mM histidine for approximately 30 min. The solution was clarified by centrifugation at 37000g, 4 °C for 30 min, followed by

two filtration steps applying cellulose filters for crude and fine precipitates and an additional filtration using a regenerated cellulose membrane (0.45 μM pore width). The supernatant was applied onto the Ni^{2+}-affinity column according to the purification of QC expressed in *P. pastoris*. In contrast to the aforementioned preparation, one additional washing step with equilibration buffer containing 15 mM histidine was implemented. Elution of QC was carried out with 50 mM phosphate buffer containing 150 mM NaCl and 100 mM histidine. The QC-containing fraction was concentrated by ultrafiltration and immediately used for further experiments or stored as described for the QC expressed in *P. pastoris*.

Synthesis of H-Gln-Tyr-Ala-OH and H-Gln-His-Pro-NH$_2$. Semi-automated synthesis of the tripeptides was performed on a 0.5 mmol scale using a peptide synthesizer (Labortec SP650) and the standard Fmoc-protocol of solid-phase peptide synthesis. Cycles were modified by using double couplings (shaking 2 × 24 min) with a 2-fold excess of Fmoc-Tyr(tBu)-OH or Fmoc-His(Trt)-OH and Fmoc-Gln-(Trt)-OH, employing the preloaded Fmoc-Ala-Wang (substitution 1.1 mmol/g) in case of H-Gln-Tyr-Ala-OH or the Rink Amide MBHA resin (substitution 0.79 mmol/g) in case of H-Gln-His-Pro-NH$_2$. The Wang resin was preloaded in our laboratories according to standard procedures. Fmoc deprotection was carried out by using 20% piperidine in dimethylformamide (1 × 3 min, 1 × 7 min). The amino acid couplings were performed by 2-(1H-benzotriazole-1-yl)-1,1,3,3,-tetramethyluronium tetrafluoroborate (TBTU) (2 equiv)/diisopropyl ethylamine (4 equiv) activation in dimethylformamide. Cleavage from the resin was accomplished with a cocktail consisting of 95% trifluoroacetic acid (TFA), 2.5% water, and 2.5% tris-isopropylsilane and yielded 80% of the crude peptide containing approximately 4% of the pyroglutaminyl peptide. The crude peptides were precipitated by cold ether and separated from the pyroglutaminyl peptide by preparative HPLC with TFA free solvents in order to avoid further cyclization of the N-terminal glutamine. Preparative HPLC was performed with a linear gradient of acetonitrile in water (5−65% acetonitrile over 40 min) on a 250−21 Luna RP18 column. Lyophylization resulted in a white, fluffy substance. To confirm peptide purity and identity, analytical HPLC and ESI-MS were employed. CHN analysis of H-Gln-Tyr-Ala-OH was consistent with the glutaminyl peptide containing one molecule of TFA and one molecule of water per molecule of peptide.

Assays for glutaminyl cyclase activity. All measurements were performed with a BioAssay Reader HTS-7000Plus for microplates (Perkin-Elmer) at 30 °C. QC activity was evaluated fluorometrically using H-Gln-βNA, essentially as described (*23*). The samples consisted of 0.2 mM fluorogenic substrate and 0.25 U pyroglutamyl aminopeptidase (Unizyme, Hørsholm, Denmark) in 0.2 M Tris/HCl, pH 8.0, containing 20 mM EDTA (50 mM Tris/HCl, pH 8.0, containing 5 mM EDTA in case of determination of the kinetic parameters) and 40−400 ng QC in a final volume of 250 μl. Excitation/emission wavelengths were 320/410 nm. The assay reactions were initiated by addition of glutaminyl cyclase. QC activity was determined from a standard curve of β-naphthylamine under assay conditions. One unit is defined as the amount of QC catalyzing the formation of 1 μmol pGlu-βNA from H-Gln-βNA per minute under the described conditions.

The kinetic parameters for conversion of H-Gln-Gln-OH, H-Gln-NH$_2$ (both from Bachem), H-Gln-His-Pro-NH$_2$, and H-Gln-Tyr-Ala-OH by QC were determined spectrophotometrically using a continuous assay developed on basis of a previously described method (*24*) (manuscript in preparation).

Spectral analysis of QC and investigation of the disulfide bond status. CD spectra of human QC in 20 mM phosphate buffer, pH 6.8, were acquired with a Jasco J-715 spectropolarimeter using quartz cuvettes of 0.1 cm path length. The mean of 15 scans between 185 and 250 nm was calculated and corrected by subtraction of the buffer spectra. The percentage of secondary structure elements was calculated using the Jasco secondary structure estimation program based on the method of Yang et al. (*25*).

For investigation of the structural changes of QC, fluorescence emission spectra were recorded in the wavelength range between 300 and 400 nm using the luminescence spectrometer LS 50 B (Perkin-Elmer). The excitation wavelength was 295 nm. Spectra were recorded at 100 nm/min using slit widths of 3 nm for excitation and 6 nm for emission.

The disulfide bond status was investigated by SDS−PAGE using deglycosylated QC. Samples were prepared under reducing (5% 2-mercaptoethanol) and nonreducing conditions as described previously (*26*). Electrophoresis was carried out in 15% polyacrylamide gels (Mini-Protean 3, BioRad), at constant voltage (200 V) for 2 h. Additionally, the determination of mercaptans in proteins by a dye reagent, Bis(3-carboxy-4-nitrophenyl)disulfide, was performed as described by Ellman (*27*).

MALDI-TOF mass spectrometry and deglycosylation assay. Matrix-assisted laser desorption/ionization mass spectrometry was carried out using the Hewlett-Packard G2025 LD-TOF System with a linear time-of-flight analyzer. The instrument was equipped with a 337 nm nitrogen laser, a potential acceleration source (5 kV), and a 1.0 m flight tube. Detector operation was in the positive-ion mode, and signals were recorded and filtered using LeCroy 9350M digital storage oscilloscope linked to a personal computer. Samples (5 μl) were mixed with equal volumes of the matrix solution. For the matrix solution, we used 2′,6′-dihydroxyacetophenone (DHAP, Aldrich)/diammonium hydrogen citrate (DAHC, Fluka), prepared by solving 30 mg DHAP and 44 mg DAHC in 1 mL acetonitrile/0.1% TFA in water (1/1, v/v). A small volume (∼1 μl) of the matrix-analyte-mixture was transferred to a probe tip and immediately evaporated in a vacuum chamber (Hewlett-Packard G2024A sample prep accessory) to ensure rapid and homogeneous sample crystallization. For determination of the molecular mass of QC, bovine serum albumin was added as an internal standard. The deglycosylation experiments were performed after external calibration using bovine serum albumin. For the deglycosylation, 8 μg QC was treated with 4×10^{-5} (0.4 NEB units) units of endoglycosidase H$_f$ (New England Biolabs) in 0.05 M sodium citrate, pH 5.5, at room temperature, without denaturation of the protein. Aliquots were removed at different times, the deglycosylation process was stopped by addition of matrix (1:1 v/v), and the respective mass spectra were evaluated.
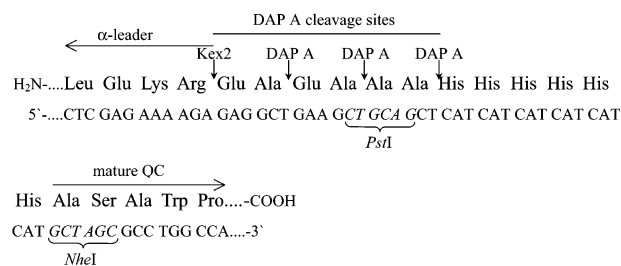

FIGURE 1: Partial sequences of the cDNA sense strand of the construct used for expression of QC in *P. pastoris* and its corresponding amino acid sequence. The cleavage sites of Kex2 and DAP A are indicated. The proteolytic processing results in a secreted, 6×histidine tagged QC, starting with alanine 33 of the native sequence.

RESULTS

Expression of human QC in P. pastoris. As demonstrated for QC from bovine pituitary and hypothalamus, the enzyme is directed to the secretory pathway caused by an N-terminal leader sequence and was colocalized in the secretory granules with its products of catalysis, e.g., TRH (*16*, *28*). Therefore, secretory expression should also be employed when QC is produced in *P. pastoris*. The N-terminal leader sequences of proteins of higher eucaryotes often yield only small quantities of secreted proteins in yeast. To improve the secretion efficiency in *P. pastoris*, the mature QC cDNA was fused to the plasmid-encoded sequence of the α-factor prepro-peptide from *S. cerevisiae*, capable of directing proteins efficiently to the secretory pathway (*29*). This sequence is extended by codons for two Glu−Ala and for one Ala−Ala that are post-translationally cleaved by dipeptidyl aminopeptidase A (DAP A). In addition, the Glu−Ala repeats are thought to favor the cleavage of the α-factor by Kex2. A coding sequence of a 6×histidine tag was attached to the 5′-end of the mature QC cDNA in order to facilitate the purification. Thus, expression of the construct should result in a secreted protein with 6 histidine residues at its N-terminus followed by mature QC starting with amino acid alanine 33, as illustrated in Figure 1.

To increase the integration frequency of the construct for overexpression, plasmids were linearized in the sequence of the *AOX1* promoter by an endonuclease treatment using the *Pme*I restriction site. Initially, transformants were checked for integration by PCR, immunodetection, and activity measurements. Since all clones tested were positive, additional recombinants were only checked by QC activity evaluation. Finally, three of 100 clones showing the highest expression level were chosen for scaled-up expression in a fermenter.

A typical fermentation procedure is documented in Fig. 2 by the time course of the optical density at 600 nm (OD$_{600}$), cell wet weight and QC activity appearing in the fermentation medium. The fermentation consisted of the three stages glycerol batch, glycerol fed batch, and methanol fed batch. The glycerol phases were marked by rapid growth of the yeast cells but lacked any QC activity. The production phase, starting upon depletion of glycerol and supply of methanol, was indicated by decreased cell growth and appearance of first QC activity, indicating that QC expression depended on activation of the *AOX* promoter. The enzymatic activity increased throughout the fermentation.
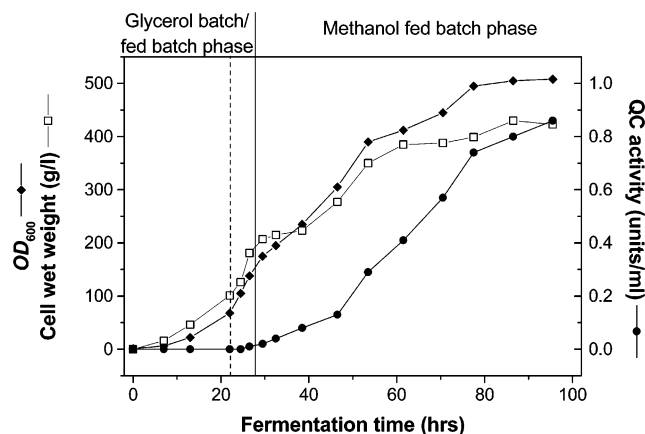
FIGURE 2: Time course of OD$_{600}$, cell wet weight and QC activity in fermentation of a recombinant strain of *P. pastoris* expressing human QC. The fermentation can be subdivided into three stages, the glycerol batch phase for about 24 h, followed by the glycerol fed batch phase for about 5 h, and finally by the methanol fed batch phase.
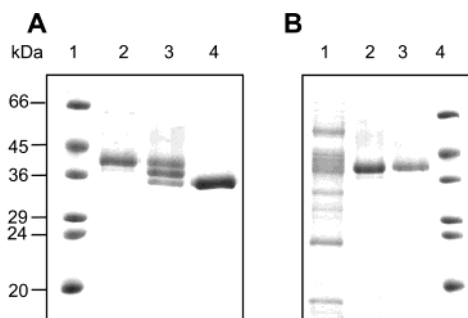

FIGURE 3: Characterization of human QC using SDS−PAGE. (A) SDS−PAGE analysis of QC-containing fractions of three different fermentations after IMAC. Lanes: 1, molecular mass standards (kDa); 2, 55 h fermentation; 3, after 75 h; 4, after 96 h. (B) SDS−PAGE illustrating the purification procedure of human QC. Lanes: 1, fermentation medium after expression; 2, the QC-containing fraction after IMAC; 3, purified QC after ion-exchange chromatography; 4, molecular mass standards. Electrophoresis was performed in 12% gels using reducing sample preparation as described elsewhere (*41*). Proteins were visualized by Coomassie staining.

Upon initial purification of the QC-containing fractions by affinity chromatography on immobilized nickel ions (IMAC), there were still apparent impurities by a protein of about 2 kDa less than the QC-containing band. Since impurities increased during fermentation, represented by an increase in this lower band, and appearance of a third band that became the sole band after 96 h of fermentation, the QC was purified from cultures grown after 60 h of fermentation. At this stage, only residual impurities were found (Figure 3A). Further purification was performed by chromatography using a strong anion-exchange resin and a very broad salt gradient. Despite a surprisingly small yield, 4 mg of pure QC was ultimately obtained from the 5 L fermentation. The purification procedure is shown in Figure 3B and Table 2.

Characterization of human QC expressed in P. pastoris. Western blot analysis following IMAC revealed that QC and both impurities contained a histidine tag (data not shown). Since the lowest band of the three species could be separated by lectin affinity chromatography (data not shown), two of the three protein species seemed to be less glycosylated forms

Table 2: Purification Scheme of Recombinant Human QC Following Expression in *P. pastoris*

purification step	protein (mg)	QC activity (units)	specific activity (units/mg)	yield (%)
fermentation broth	393.2	362.8	0.9	100
immobilized metal ion affinity chromatography (IMAC)	41.6	256.8	6.2	71
ion-exchange chromatography (IEC)	4.1	76.9	18.7	21

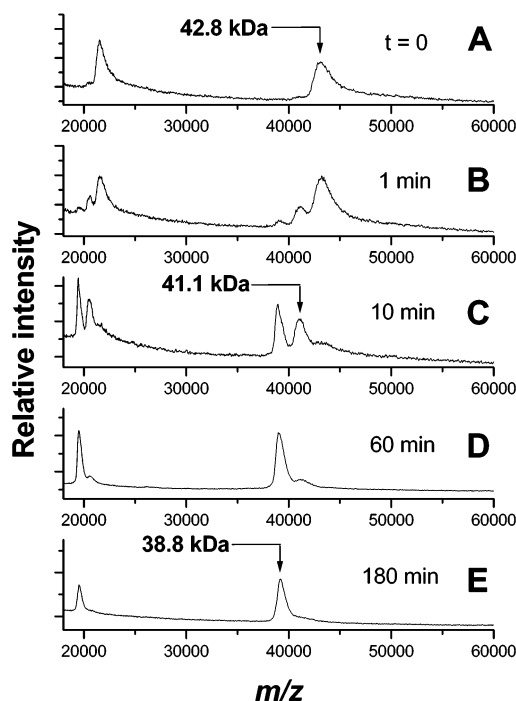

FIGURE 4: Deglycosylation of recombinant human QC, monitored by MALDI-TOF mass spectrometry. 8 μg of QC was treated with 4×10^{-5} units of endoglycosidase H$_f$ in 0.05 M sodium citrate, pH 5.5, at room temperature. At the times indicated, samples were removed and diluted with matrix and the mass spectra recorded. The peak at 42.8 kDa corresponds to the double glycosylated QC. The peaks at 41.1 and 38.8 kDa represent the less glycosylated QC forms. The 2-fold charged proteins correspond to the peaks around 20 kDa.

of QC. This conclusion was corroborated by MALDI-TOF mass spectrometry. The recombinant human QC displayed a relatively broad peak at a molecular mass of 42.8 kDa (Figure 4A). Upon deglycosylation with endoglycosidase H$_f$, two other protein species exhibiting molecular masses of 41.1 kDa and 38.8 kDa were formed consecutively (Figure 4B−E). The primary structure of QC reveals two potential N-glycosylation sites, located at asparagine residues 49 and 296 (*10*). Thus, in the recombinant QC, both asparagines were glycosylated with oligosaccharides of about 2 kDa per residue, suggesting that QC is also expressed as a glycoprotein in mammalian cells.

Using MALDI-TOF mass analysis with bovine serum albumin as an internal standard, from five independently recorded mass spectra, a molecular mass of 38,795 ± 19 Da was determined for the quantitatively deglycosylated enzyme (not shown). This mass corresponds well to the theoretical value of 38 745 Da, calculated from all amino acid residues and the two GlcNAc residues remaining after deglycosylation by endoglycosidase H$_f$. Therefore, post-translational modifications other than N-glycosylation are
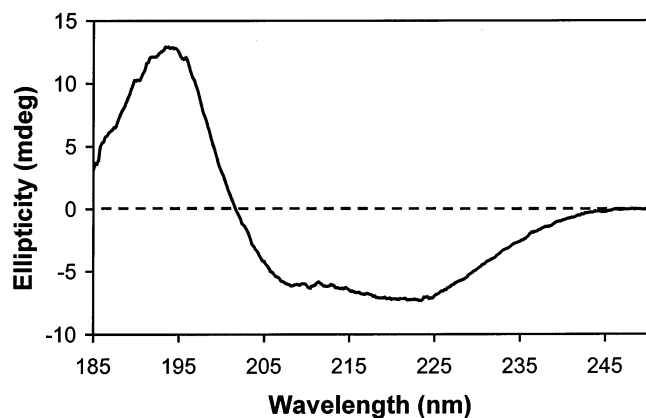
FIGURE 5: CD-spectroscopic analysis of the secondary structure of recombinant human QC. The protein was dissolved in 20 mM potassium phosphate buffer, pH 6.8. Estimation of the secondary structure revealed 47% α-helix, 14% β-sheet, and 14% β-turn content.

Table 3: Kinetic Parameters Determined for Human QC Expressed in *P. pastoris*[a]

QC substrate	Michaelis constant (μM)	turnover number (s^{-1})
H-Gln-Tyr-Ala-OH	101 ± 4	125 ± 1
H-Gln-His-Pro-NH$_2$	90 ± 4	83 ± 1
H-Gln-AMC	51 ± 3	5.4 ± 0.1
H-Gln-βNA	60 ± 6	18.8 ± 0.7
H-Gln-NH$_2$	409 ± 40	12.8 ± 0.5
H-Gln-Gln-OH	148 ± 5	20.7 ± 0.2

[a] Reactions were carried out at 30 °C in 0.05 M Tris/HCl, pH 8.0, containing 5 mM EDTA.

improbable during expression, and the N-terminus seems to be completely processed by Kex2 and DAP A, a frequent cause of inhomogeneities observed when foreign genes are expressed in *P. pastoris*.

Further characterization of recombinant human QC was performed by applying CD spectroscopy (Figure 5). The appearance of the spectrum indicates a dominant α-helix content. The two minima at 208 and 222 nm are characteristic for proteins that contain a high portion of α-helix in their overall secondary structure. A calculation of quantities of α-helix, β-sheet, turn, and random structure revealed an α-helix content of 47% for the human QC. This amount contrasts with the 5% content reported for the QC from papaya latex, indicating completely different folding patterns for both proteins.

Kinetic parameters were recorded for the recombinant human QC in order to characterize the catalytic competence of the enzyme. The values obtained at 30 °C with the substrates H-Gln-Tyr-Ala-OH, H-Gln-His-Pro-NH$_2$, H-Gln-AMC, H-Gln-βNA, H-Gln-NH$_2$, and H-Gln-Gln-OH as substrates are listed in Table 3. Upon examination at 37 °C, the kinetic parameters K_m and k_{cat} for conversion of H-Gln-Tyr-Ala-OH shifted to 153 ± 5 μM and 220 ± 2 s^{-1}, respectively.

Interestingly, the data found are in good agreement with values determined with QC from papaya latex. For instance, H-Gln-AMC and H-Gln-βNA were converted with K_m values of 52 ± 5 μM and 43 ± 4 μM and k_{cat} values of 31 and 46 s^{-1}, respectively (23). The kinetic parameters listed in Table 3 are in striking contrast, however, to those found by Song et al. for human QC, expressed in *E. coli* (10). In this study,
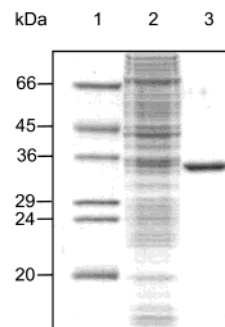

FIGURE 6: SDS−PAGE of the purification steps of human QC expressed in *E. coli*. Lanes: 1, molecular mass standards (kDa); 2, supernatant after lysis, 3, purified QC after IMAC. Electrophoresis was performed in 12% gels using reducing sample preparation as described elsewhere (41).

a K_m value of 0.64 mM and a k_{cat} of 50.9 min^{-1} were obtained for conversion of H-Gln-Gln-OH. Also, H-Gln-NH$_2$ was processed differently. The enzyme expressed in *P. pastoris* exhibits approximately 3-fold tighter binding and 30-fold faster turnover compared to recombinant human QC expressed in *E. coli* (30). Most strikingly, H-Gln-AMC was not converted at all by the human QC expressed in *E. coli* (10), while the recombinant human QC from *P. pastoris* cyclized H-Gln-AMC almost comparable to other substrates (Table 3).

Recombinant expression and characterization of human QC in E. coli. The remarkably different kinetic properties of human QC expressed in *P. pastoris* with that formerly described for QC expressed in *E. coli* (10) prompted a more detailed comparison. The cDNA starting with codon 38 was cloned into the pQE-31 vector and expressed in the cytosol with an N-terminal 6×histidine tag. Minimal enzymatic activity was detected upon expression at 37 °C using LB broth and induction with 0.1 mM IPTG for 5 h. After overnight expression at room temperature in LB medium supplemented with 1% glucose and 1% ethanol, however, a 50-fold increase in QC activity was found. Supernatants of enzymatically lysed bacteria were clarified by several centrifugation and filtration steps and the resulting soluble QC was purified to apparent homogeneity by IMAC in one step (Figure 6). Usually, about 5 mg QC could be purified per 2 L culture corresponding to an overall yield of 20%.

Applying H-Gln-βNA as substrate, a K_m value of 62 ± 5 μM and a k_{cat} of 7.5 ± 0.3 s^{-1} were found. Thus, compared to the human QC expressed in yeast, the enzyme expressed in *E. coli* showed an identical K_m value, but an approximately 3-fold lower turnover number. A frequent reason for reduced or abolished activity of proteins expressed heterologously in *E. coli* is the lack of post-translational modifications such as proper disulfide bond formation or N-glycosylation. Therefore, the presence of disulfide bonds in the recombinant QCs and the influence of glycosylation on the catalysis were tested. Interestingly, deglycosylation by endoglycosidase H$_f$ did not alter the kinetic parameters of QC expressed in yeast using Gln-βNA as substrate, indicating that the lower activity was not caused by lack of glycosylation (not shown). QC contains only two cysteine residues, one in position 139 and another one in 149. Thus, the disulfide status could be easily analyzed. In a one-dimensional SDS−PAGE after reducing and nonreducing sample preparation, disulfide-containing polypeptides migrate different from their reduced counter-
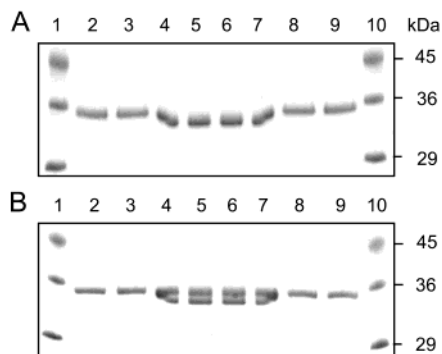
FIGURE 7: Disulfide-status of QC expressed in *P. pastoris* (A) and *E. coli* (B), examined using SDS−PAGE (*27*). Lanes: 1 and 10, molecular mass standards (kDa); 2, 3, 8, and 9, sample prepared under reducing conditions (5% β-mercaptoethanol); 4−7, sample prepared under nonreducing conditions. Electrophoresis was performed in 15% gels (6 × 8 cm) at constant voltage of 200V for 2 h and protein visualized by Coomassie staining. Due to diffusion of the reducing agent from lanes 3 and 8 into lanes 4 and 7, respectively, the band pattern was a mixed type.

parts, indicating the presence of intramolecular disulfide bonds (*26*). In the case of QC expressed in yeast and separated by SDS−PAGE after nonreducing sample preparation (Figure 7A, lanes 4−7), the protein clearly migrated faster than that after a reducing sample preparation (lanes 2 and 3 and lanes 8 and 9), providing evidence of a disulfide bond in native human QC. In contrast, two bands of similar strength were formed after nonreducing sample preparation in the case of QC expressed in *E. coli* (Figure 7B, lanes 4−7). This clearly indicates that not all of the QC expressed in *E. coli* contained a disulfide bond. Accordingly, color development using Ellman's reagent was only detected in the case of the QC that was expressed in *E. coli*. The portion of the protein being free of a disulfide bond was calculated to be 50% using an absorption coefficient of 13 600 M^{-1} cm^{-1} (*27*).

Effects of disulfide reduction on activity and structure of QC expressed in P. pastoris. Due to the obvious effect of the disulfide on the active structure of QC, the influence of reducing agents was examined. In the absence of a reducing agent, QC activity was constant at pH 6.8 and room temperature for 2 h (Figure 8). In contrast, QC was readily inactivated by 15 mM dithiotreitol (DTT) during this time. The loss of QC activity appeared exponentially and was independent of the initial amount, suggesting pseudo-first-order kinetics of inactivation. A shift of the pH from 6.8 to 8.0 accelerated the inactivation 10-fold (not shown), suggesting that the process is favored upon formation of the thiolate-anion of DTT.

To investigate how the structure of QC is affected by disulfide bond cleavage, fluorescence spectra of the native, reduced, and unfolded protein were recorded. Usually, upon denaturation the emission maximum of proteins exhibits a tryptophan-mediated shift from a shorter wavelength to about 350 nm which corresponds to the fluorescence maximum of tryptophan in aqueous solutions (*31*). The native QC exhibited its fluorescence maximum at 340 nm (Figure 9A). Upon complete unfolding of the protein in 6 M GdmCl, the fluorescence intensity decreased and the emission maximum shifted to 355 nm, indicating a more hydrophilic environment of the tryptophan residues compared to the folded state. Interestingly, reduction of the disulfide with 15
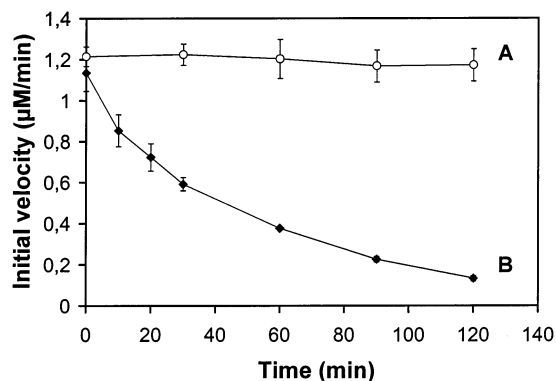

FIGURE 8: Inactivation of QC by 15 mM DTT (B). Reactions were carried out in 0.05 M potassium phosphate, pH 6.8, containing 0.3 M NaCl, and started by addition of 8 μg QC. At times indicated, samples were withdrawn and diluted 100-fold in 0.05 M Tris/HCl, pH 8.0, and the residual QC activity was determined using H-Gln-βNA as substrate. In absence of a reducing agent, enzyme activity remained constant (A).
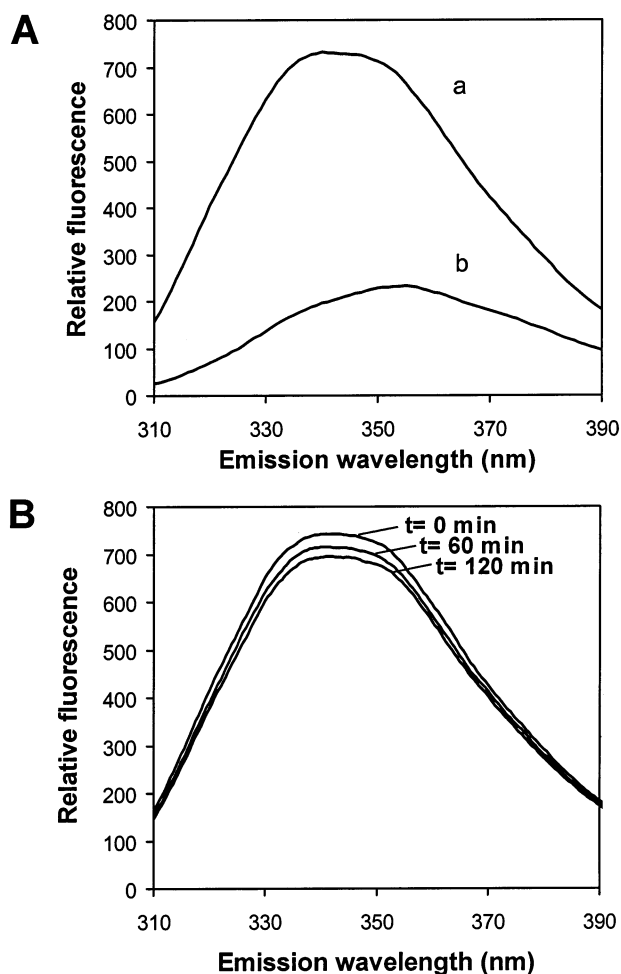

FIGURE 9: Fluorescence emission spectra of QC. (A) Spectra of 0.18 μM enzyme samples recorded in 0.05 M sodium phosphate, pH 6.8, containing 0.3 M NaCl in absence (a) and presence (b) of 6 M GdmCl after excitation at 295 nm. (B) Respective spectra recorded in the presence of 15 mM DTT at indicated times after addition of the reducing agent.

mM DTT at pH 6.8 decreased fluorescence intensity only slightly, and a change in the fluorescence maximum did not occur (Figure 9B). No change in fluorescence intensity was detected in the absence of DTT (not shown). The differences in the fluorescence spectra of the native, reduced, and

denatured QC indicate a small conformational change of the protein possibly caused by the reduction of the disulfide bond.

DISCUSSION

Many human proteins cannot be purified from natural sources in amounts necessary for functional analyses. Heterologous expression is often the only choice to get sufficient amounts of the protein of interest. Among the various expression hosts, the methylotrophic yeast *P. pastoris* has been used successfully for many human proteins (*29*). In the current study, we demonstrate functional expression of human QC in *P. pastoris*. During expression, the protein was directed to the secretory pathway by fusion to the α-leader of *S. cerevisiae* and purified from the culture supernatant by a two-step purification procedure. Although QC activity was readily detectable when the protein was expressed in shake flasks, the rate of expression was improved 40-fold by fermentation. The overall yield of expression, however, was accompanied by heterogeneities in the glycosylation pattern of QC during long-term fermentations. Because the different glycoforms could not be separated efficiently by lectin-affinity- and ion-exchange chromatography, a fermentation time was chosen in which the altered glycoforms appeared to be minimal (Figure 3A). For mammalian QCs glycosylation was first shown for the QC from porcine pituitary (*9, 16*). The contribution of post-translational modifications found (approximately 2−4 kDa) in the case of the bovine QC (*16*) corresponds to the extent of glycosylation when the human QC is expressed in yeast. This yield of glycosylation is also in agreement with the structure of N-linked oligosaccharides of an invertase expressed as a heterologous protein in *P. pastoris*, too. The recombinant invertase contains more than 85% oligosaccharides in the size range $Man_{8-14}GlcNAc_2$, thus comparable to high-mannose oligosaccharides synthesized by animal cells (*19*). In addition, hyperglycosylation that is frequently observed when heterologous proteins are expressed in *S. cerevisiae* is commonly not found with proteins expressed in *P. pastoris* (*17, 29*). Heterogeneities in glycosylation, however, have been previously reported for other proteins expressed in *P. pastoris*, for instance, interleukin-17 (*32*) and HIV-1 envelope protein (*33*). Here, the glycosylation pattern of QC shifted to deglycosylated forms at later stages of growth (Figure 2). Previously, for *S. cerevisiae* a deglycosidase activity was reported that increased in cells reaching the stationary phase (*34*). Possibly, the appearance of the glycoforms of QC could be due to a post-translational cleavage of the sugar moieties. The human QC expressed in *P. pastoris* was deglycosylated quantitatively by only very low amounts of endoglycosidase H_f (Figure 4). Thus, both glycosylation sites seem to be easily accessible for a putative deglycosidase, even in the native, folded structure of QC, and both are possibly exposed at the protein surface. Human and bovine QC contain putative glycosylation sites at positions 49 and at positions 296 and 183, respectively, and both proteins show an overall sequence identity of 86%. The glycosylation sites, however, are within less conserved regions, implying that the protein conformation around these sites are less important for the catalytic properties of the QC. This is strengthened by the fact that catalytic parameters were unaffected by deglycosylation of the enzyme.

The nearly identical kinetic parameters of bovine and recombinant human QC obtained with the peptide H-Gln-Tyr-Ala-OH also reflect the high degree of homology between the enzymes. To date, estimates of the Michaelis constant and the turnover number for a native mammalian QC can only be achieved for H-Gln-Tyr-Ala-OH from literature data. On the basis of a molecular weight of 38−40 kDa for the purified bovine pituitary protein, a k_{cat} value of 225−235 s^{-1} can be calculated for the conversion of H-Gln-Tyr-Ala-OH at 37 °C (*16*). The corresponding Michaelis constant of 132 μM was determined in an earlier study (*8*). Thus, the kinetic parameters determined using the recombinant human QC are in excellent agreement with these earlier results obtained applying the highly homologous QC from bovine pituitary. This suggests that the proteins have similar if not identical catalytic competence, despite of heterologous expression and the presence of an N-terminal affinity tag in the recombinant human QC.

Remarkable differences in enzymatic activity were found between human QC expressed in *E. coli* (*10, 11, 30*) and that expressed in yeast, as reported here. At least partially, these differences might be due to the glutathione S-transferase fused to the N-terminus of QC expressed in *E. coli* (*30*). In the current study, the major portion of the QC protein expressed in *E. coli*, however, was inactive, suggesting that the active structure of QC was not formed as also indicated by the absence of the disulfide bond. This could be an additional reason for the apparent reduction in QC activity reported previously. Whether inactive proteins were formed by improper folding or by a lack of disulfide formation was not investigated in detail. However, initial experiments to separate the active and inactive QC forms by ion exchange chromatography failed. Furthermore, enzymatic activity could not be restored by addition of oxidized and reduced glutathione, a method often used for refolding of proteins in order to facilitate the correct formation of the disulfide bonds (*35*). Additionally, QC activity could not be detected when QC cDNA was expressed with the single base exchange in codon 164, which led to a tryptophan residue instead of a cysteine in this position. Although these results could also be interpreted in terms of misfolding, the loss of the disulfide bond of QC could also be a reason for inactivation, as indicated by the treatment of QC with DTT. Reducing cytosolic conditions are known to hinder the formation of disulfides in proteins (*36*), and therefore, translocation of the QC into a less reducing environment seems to be important for efficient formation of the enzymatically active structure.

The fluorescence spectra obtained for native, reduced, and unfolded QC showed that reduction of the disulfide bond resulted in a relatively small change of the protein conformation, indicated by a reduced fluorescence intensity. The unchanged fluorescence emission maximum also pointed to minor conformational differences. The concomitant loss of the enzymatic activity, however, clearly indicate an important role of the disulfide bond for the stabilization of the active protein structure. Furthermore, the fluorescence maximum at 339 nm of native QC indicates that not all tryptophan residues are in a hydrophobic environment. In such cases, the fluorescence maximum can still shift further into the blue range, as shown for RNase T1 (*31*) or prolyl oligopeptidase (*37*).

The QCs from *C. papaya* and its mammalian counterparts seem to be very similar with respect to molecular weights, subunit composition, and catalytic properties (*30*, *38*). However, there was no sequence homology found between the enzymes (*12*), and their folding pattern was assumed to be different (*14*). Similarities were found between the predicted structure of human QC and bacterial zinc-dependent aminopeptidases that contain an α/β-structure (*30*). In addition, two different prediction methods (*39*, *40*) used to calculate the portions of secondary structure from the amino acid sequence yielded 43% and 52% of α-helix and 15% and 16% of β-sheet for the recombinant human QC. Thus, the calculated values from the CD spectroscopy data and the predicted values are in the same range. Similar characterization experiments performed with QC from papaya latex revealed that the protein adopts an all-beta structure (*14*). Although the β-sheet content cannot be calculated from CD spectra without uncertainties (*31*), helical contents are mostly well reflected. Thus, the mammalian QCs seem to contain a pronounced α-helical secondary structure, in stark contrast to papaya QC.

To our knowledge, this is the first mammalian QC expressed and purified from an eukaryotic host. Due to the post-translational modifications of QC taking place in *P. pastoris*, this expression system has proven to be more favorable than bacterial expression. This might have also implications for other disulfide containing proteins that are expressed heterologously in these organisms. The most important advantage is provided by the fact that the catalytic competence of the human QC expressed in yeast is identical to the highly homologous QC purified from bovine pituitary, providing evidence that the recombinant protein resembles native QC very well. Therefore, by this study detailed enzymological and structural studies of human QC can be initiated.

REFERENCES

1. Awade, A. C., Cleuziat, P., Gonzales, T., and Robert-Baudouy, J. (1994) *Proteins 20*, 34−51.
2. Garavelli, J. S. (2000) *Nucleic Acids Res. 28*, 209−211.
3. Abraham, G. N., and Podell, D. N. (1981) *Mol. Cell Biochem. 38 Spec No*, 181−190.
4. Van Coillie, E., Proost, P., Van Aelst, I., Struyf, S., Polfliet, M., De Meester, I., Harvey, D. J., Van Damme, J., and Opdenakker, G. (1998) *Biochemistry 37*, 12672−12680.
5. Steiner, D. F. (1998) *Curr. Opin. Chem. Biol. 2*, 31−39.
6. Nillni, E. A., and Sevarino, K. A. (1999) *Endocr. Rev. 20*, 599−648.
7. Messer, M. (1963) *Nature 4874*, 1299.
8. Fischer, W. H., and Spiess, J. (1987) *Proc. Natl. Acad. Sci. U.S.A. 84*, 3628−3632.
9. Busby, W. H. J., Quackenbush, G. E., Humm, J., Youngblood, W. W., and Kizer, J. S. (1987) *J. Biol. Chem. 262*, 8532−8536.
10. Song, I., Chuang, C. Z., and Bateman, R. C. J. (1994) *J. Mol. Endocrinol. 13*, 77−86.
11. Temple, J. S., Song, I., Burns K. H., and Bateman, R. C. J. (1998) *Korean J. Biol. Sci. 2*, 243−248.
12. Dahl, S. W., Slaughter, C., Lauritzen, C., Bateman, R. C., Jr., Connerton, I., and Pedersen, J. (2000) *Protein Expr. Purif. 20*, 27−36.
13. Gololobov, M. Y., Song, I., Wang, W., and Bateman, R. C. J. (1994) *Arch. Biochem. Biophys. 309*, 300−307.
14. Oberg, K. A., Ruysschaert, J. M., Azarkan, M., Smolders, N., Zerhouni, S., Wintjens, R., Amrani, A., and Looze, Y. (1998) *Eur. J. Biochem. 258*, 214−222.
15. Zerhouni, S., Amrani, A., Nijs, M., Smolders, N., Azarkan, M., Vincentelli, J., and Looze, Y. (1998) *Biochim. Biophys. Acta 1387*, 275−290.
16. Pohl, T., Zimmer, M., Mugele, K., and Spiess, J. (1991) *Proc. Natl. Acad. Sci. U.S.A. 88*, 10059−10063.
17. Romanos, M. (1995) *Curr. Opin. Biotechnol. 6*, 527−533.
18. Cregg, J. M., Vedvick, T. S., and Raschke, W. C. (1993) *Biotechnology (N.Y.) 11*, 905−910.
19. Grinna, L. S., and Tschopp, J. F. (1989) *Yeast 5*, 107−115.
20. Sambrook, J., Fritsch, E. F., and Maniatis, T. (1989) *Molecular Cloning: A Laboratory Manual*, Cold Spring Harbor Laboratory Press, Plainview, NY.
21. Bradford, M. M. (1976) *Anal. Biochem. 72*, 248−254.
22. Gill, S. C., and von Hippel, P. H. (1989) *Anal. Biochem. 182*, 319−326.
23. Schilling, S., Hoffmann, T., Wermann, M., Heiser, U., Wasternack, C., and Demuth, H.-U. (2002) *Anal. Biochem. 303*, 49−56.
24. Bateman, R. C. J. (1989) *J. Neurosci. Methods 30*, 23−28.
25. Yang, J. T., Wu, C. S., and Martinez, H. M. (1986) *Methods Enzymol. 130*, 208−269.
26. Allore, R. J., and Barber, B. H. (1984) *Anal. Biochem. 137*, 523−527.
27. Ellman, G. L. (1958) *Arch. Biochem. Biophys. 74*, 443−450.
28. Bockers, T. M., Kreutz, M. R., and Pohl, T. (1995) *J. Neuroendocrinol. 7*, 445−453.
29. Cereghino, J. L., and Cregg, J. M. (2000) *FEMS Microbiol. Rev. 24*, 45−66.
30. Bateman, R. C., Temple, J. S., Misquitta, S. A., and Booth, R. E. (2001) *Biochemistry 40*, 11246−11250.
31. Schmid, F. X. (1989) in *Protein Structure: A Practical Approach* (Creighton, T. E., Ed.) pp 251−285, IRL Press, Oxford.
32. Murphy, K. P., Gagne, P., Pazmany, C., and Moody, M. D. (1998) *Protein Expr. Purif. 12*, 208−214.
33. Scorer, C. A., Buckholz, R. G., Clare, J. J., and Romanos, M. A. (1993) *Gene 136*, 111−119.
34. Suzuki, T., Park, H., Kitajima, K., and Lennarz, W. J. (1998) *J. Biol. Chem. 273*, 21526−21530.
35. Rudolph, R., and Lilie, H. (1996) *FASEB J. 10*, 49−56.
36. Hannig, G., and Makrides, S. C. (1998) *Trends Biotechnol. 16*, 54−60.
37. Polgar, L. (1995) *Biochem. J. 312* (Partt 1), 267−271.
38. Gololobov, M. Y., Wang, W., and Bateman, R. C. J. (1996) *Biol. Chem. Hoppe Seyler 377*, 395−398.
39. Geourjon, C., and Deleage, G. (1995) *Comput. Appl. Biosci. 11*, 681−684.
40. Gibrat, J. F., Garnier, J., and Robson, B. (1987) *J. Mol. Biol. 198*, 425−443.
41. Laemmli, U. K. (1970) *Nature 227*, 680−685.

Continuous Spectrometric Assays for Glutaminyl Cyclase Activity

Stephan Schilling, Torsten Hoffmann, Michael Wermann, Ulrich Heiser,
Claus Wasternack,* and Hans-Ulrich Demuth[1]

*Laboratory of Biochemistry, probiodrug AG, Weinbergweg 22, 06120 Halle/Saale, Germany; and
Leibniz Institute for Plant Biochemistry, P.O. Box 110432, 06120 Halle/Saale, Germany

The enzymatic conversion of one chromogenic substrate, L-glutamine-*p*-nitroanilide, and two fluorogenic substrates, L-glutaminyl-2-naphthylamide and L-glutaminyl-4-methylcoumarinylamide, into their respective pyroglutamic acid derivatives by glutaminyl cyclase (QC) was estimated by introducing a new coupled assay using pyroglutamyl aminopeptidase as the auxiliary enzyme. For the purified papaya QC, the kinetic parameters were found to be in the range of those previously reported for other glutaminyl peptides, such as Gln-Gln, Gln-Ala, or Gln-*tert*-butyl ester. The assay can be performed in the presence of ammonia up to a concentration of 50 mM. Increasing ionic strength, e.g., potassium chloride up to 300 mM, resulted in an increase in enzymatic activity of about 20%. This is the first report of a fast, continuous, and reliable determination of QC activity, even in the presence of ammonium ions, during the course of protein purification and enzymatic analysis. © 2002 Elsevier Science (USA)

Several bioactive peptides and proteins (e.g., TRH,[2] IgG, GnRH) contain a pyroglutamate residue at their N-terminal position. This feature was assumed to result from a spontaneous cyclization reaction of the N-terminal glutamine residue. However, enzymatic conversion by glutaminyl cyclase (QC; EC 2.3.2.5) could be shown (1–3).

Up to now, papaya latex has been the only plant source, in which this enzyme is found to be abundant, whereas several mammalian tissues have been shown to express QC (4, 5).

Little is known about the biological role of QC. It has been suggested that QC is responsible for modification of storage proteins during seed germination (6), as well as *in vivo* modification of bioactive peptides such as glucagon, MCP-2, TRH, and GnRH (4, 7, 8). These findings support the idea that the QC-catalyzed reaction might be important for protection of the N-terminus of bioactive peptides against exopeptidases. Moreover, this enzymatically catalyzed N-terminal formation of a pyroglutamic acid residue could be important in developing the proper receptor binding conformation of such peptides.

Interestingly, a number of pyroglutamate peptides are formed in tissues, although no QC activity has been detected there thus far, indicating a need for more detailed investigations (9). As an initial step in elucidating the function of QC in plants or animals, expression studies for various tissues and enzyme purification for further characterization are essential, and both require a reliable assay. In previously applied methods, QC activity was determined either by analyzing the products formed using HPLC (3, 10) or radioimmunoassay (11) or by detecting the release of ammonia spectrophotometrically (12). In the latter assay, the QC-catalyzed cyclization of the N-terminal glutamine residue is quantified by coupling the reaction with the conversion of NADH/H$^+$ to NAD$^+$ by glutamate dehydrogenase. Avoidance of any ammonium traces is an essential prerequisite, making this assay difficult to handle in some enzyme purification steps. Although the aforementioned methods are sensitive, they are all

---

discontinuous and therefore time consuming and laborious. As a result of these disadvantages, we developed new continuous assays which allow determination of QC activity during purification and characterization. In contrast to the assays mentioned above, these new methods use the glutaminyl derivatives of p-nitroaniline, 7-amino-4-methylcoumarin, and 2-naphthylamine as substrates. Once cyclized into the respective pyroglutamic acid derivatives by QC, they are subsequently cleaved by pyroglutamyl aminopeptidase. The resulting liberation of p-nitroaniline, 7-amino-4-methylcoumarin, or 2-naphthylamine allows the reliable and convenient determination of QC activity.

MATERIALS AND METHODS

Materials

Lyophilized papaya latex and S-methylmethane thiosulfonate were purchased from Fluka (Seelze, Germany). Pyroglutamic acid p-nitroanilide and molecular mass standards for SDS–PAGE were provided by Sigma (Deisenhofen, Germany). Gln-AMC and Gln-βNA were from Bachem (Bubendorf, Switzerland). SP–Sepharose Fast Flow and Butyl–Sepharose 4 Fast Flow were obtained from Pharmacia Biotech (Uppsala, Sweden). Boc-L-glutamine was supplied by Bachem (Heidelberg, Germany). Pyroglutamyl aminopeptidase from *Bacillus amyloliquefaciens*, recombinantly expressed in *Escherichia coli*, was purchased from Unizyme Laboratories (Hørsholm, Denmark) and Tris as well as Tricine from Serva (Heidelberg, Germany).

Synthesis of Gln-pNA

Boc-Gln-pNA. Boc-Gln-OH (2.46 g; 10 mmol) was dissolved in THF (20 ml) by adding 0.81 ml (10 mmol) pyridine and 1.39 ml (10 mmol) TEA and solvation was completed by a brief warming of the solution. After the mixture was cooled down to −10°C, 1.23 ml (10 mmol) pivaloyl chloride was added, and the clear solution was stirred for 10 min at 0°C. Upon completed formation of the mixed anhydride, 1.311 g (9.5 mmol) p-nitroaniline was added. Subsequently, the mixture was stirred for 1 h at 0°C and left overnight at room temperature. In the usual workup the solvent was removed, and the residue was partitioned between ethyl acetate and aqueous HCl (15% in water), followed by a subsequent washing with brine, saturated aqueous solution of KHCO₃, and brine again. The organic layer was separated and the solvent was removed. Chromatography on silica gel using a CHCl₃:MeOH (1:3, v/v) gradient resulted in a pure Boc-Gln-pNA as a faint yellow oil. The overall yield was 2.93 g (80%).

*H-Gln-pNA*HCl.* Boc-Gln-pNA was treated with 20 ml HCl solution (4 N in dioxane) until the starting material was no longer detectable. After solvent removal, the resulting material was recrystallized from methanol/ether. The yield was 2.17 g (90%), HPLC purity 99.35% (water/ACN/TFA). ¹³C NMR (CD₃OD) δ 24.95 (CH₂), 30.11 (CH₂), 53.27 (CH—NH₃⁺), 121.55 (CH=phenyl), 122.4 (CH=phenyl), 143.87 (=C=phenyl), 147.23 (=C—NO₂), 161.65 (CONH), 173.88 (CONH).

Purification of QC from Papaya Latex

QC from papaya latex was prepared using the BioCAD 700E (Perceptive Biosystems, Wiesbaden, Germany) with a modified version of a previously reported method (13). Fifty grams of latex was dissolved in water and centrifuged as described (13). Inactivation of proteases was performed with S-methylmethane thiosulfonate, and the resultant crude extract was dialyzed (13, 23).

SP–Sepharose Fast Flow. After dialysis, the entire supernatant was loaded onto a (21 × 2.5-cm i.d.) SP–Sepharose Fast Flow column, equilibrated with 100 mM sodium acetate buffer, pH 5.0 (flow rate 3 ml/min). Elution was performed in three steps by increasing the sodium acetate buffer concentration at a flow rate of 2 ml/min. The first step was a linear gradient from 0.1 to 0.5 M acetate buffer in 0.5 column volume. The second step was a linear increase in buffer concentration from 0.5 to 0.68 M in 4 column volumes. During the last elution step, 1 column volume of 0.85 M buffer was applied. Fractions (6 ml) containing the highest enzymatic activity were pooled. Concentration and buffer changes to 0.02 M Tris/HCl, pH 8.0, were performed via ultrafiltration (Amicon; molecular mass cut-off of the membrane 10 kDa).

Butyl–Sepharose 4 Fast Flow. Ammonium sulfate was added to the concentrated papaya enzyme, obtained from the ion-exchange chromatography step to a final concentration of 2 M. This solution was applied onto a (21 × 2.5-cm i.d.) Butyl–Sepharose 4 Fast Flow column (flow rate 1.3 ml/min), equilibrated with 2 M ammonium sulfate, 0.02 M Tris/HCl, pH 8.0. Elution was performed in three steps with decreasing concentrations of ammonium sulfate. During the first step a linear gradient from 2 to 0.6 M ammonium sulfate, 0.02 M Tris/HCl, pH 8.0, was applied for 0.5 column volume at a flow rate of 1.3 ml/min. The second step was a linear gradient from 0.6 to 0 M ammonium sulfate, 0.02 M Tris/HCl, pH 8.0, in 5 column volumes at a flow rate of 1.5 ml/min. The last elution step was carried out by applying 0.02 M Tris/HCl at pH 8.0 for 2 column volumes at a flow rate of 1.5 ml/min. All fractions containing QC activity were pooled and concentrated by ultrafiltration. The resultant homogeneous QC was stored at −70°C. Final protein concentrations were determined using the method of Bradford (14),

compared to a standard curve obtained with bovine serum albumin.

Assays

All measurements were performed with the BioAssay Reader HTS 7000Plus for microplates (Perkin–Elmer) at 30°C.

Spectrophotometric assay for QC. The assay consisted of the chromogenic substrate Gln-pNA (1 mM), pyroglutamyl aminopeptidase (0.25 U), and an appropriate amount of QC in a final volume of 0.25 ml buffer (0.05 M Tricine/NaOH, pH 8.0). This pH was reported to be within the optimal range for the catalysis of both QC and pyroglutamyl aminopeptidase (9, 15). Due to the composition of the storage buffer of pyroglutamyl aminopeptidase, assay mixtures contained cysteamine (0.1 mM), sodium chloride (2 mM), EDTA (0.1 mM), and 2% (v/v) glycerol.

Reactions were initiated by addition of QC and preincubated for 2 min, and subsequently absorption was monitored at 405 nm for 8–15 min. QC activity was calculated using an absorption coefficient of 6710 L/mol, which was determined from a standard curve of p-nitroaniline under assay conditions.

Fluorometric assays for QC. Glutaminyl cyclase activity was evaluated fluorometrically using either Gln-AMC or Gln-βNA. The samples consisted of the fluorogenic substrate (0.05 mM), 0.25 U pyroglutamyl aminopeptidase in 20 mM Tris/HCl, pH 8.0, containing 200 mM potassium chloride, and an appropriately diluted aliquot of papaya glutaminyl cyclase. Excitation/emission wavelengths were 380/465 nm in the case of Gln-AMC and 320/410 nm in the case of Gln-βNA. The assay reactions were initiated by addition of glutaminyl cyclase. Monitoring of progress curves was started immediately after initiation. QC activity was determined from standard curves of 7-amino-4-methylcoumarin and β-naphthylamine under assay conditions.

Assay for pyroglutamyl aminopeptidase. Measurements of pyroglutamyl aminopeptidase activity were carried out using pGlu-pNA as substrate. In order to maintain conditions identical to those used in the QC assay, samples (250 μl) contained 0.1 mM cysteamine, 2 mM sodium chloride, 0.1 mM EDTA, 2 mM pGlu-pNA (stock solution in dimethyl sulfoxide), 2% (v/v) glycerol, and an diluted aliquot of pyroglutamyl aminopeptidase in 0.05 M Tricine/NaOH, pH 8.0. The final concentration of 1% (v/v) dimethyl sulfoxide did not interfere with the activity of pyroglutamyl aminopeptidase. One unit is defined as the amount of enzyme that hydrolyzes 1 μmol pGlu-pNA per minute under the conditions described. The activity was expressed in units using an absorption coefficient of 6690 L/mol, which was obtained from a standard curve. The specific activity of the enzyme preparation was approximately 4

units/mg. The pyroglutamyl aminopeptidase was stored in a solution consisting of Tris/HCl (6 mM), cysteamine (2 mM), sodium chloride (40 mM), EDTA (2 mM), 50% glycerol, pH 8.0. The enzyme was stable for several months at −20°C.

RESULTS AND DISCUSSION

Spectrophotometric Assay

The spectrophotometric assay is based on the detection of p-nitroaniline at 405 nm, one of the products generated in the coupled assay. The first reaction is the conversion of Gln-pNA into pGlu-pNA, catalyzed by QC. pGlu-pNA, in turn, is hydrolyzed in the second reaction by the abundant pyroglutamyl aminopeptidase, which leads to the terminal products pyroglutamate and pNA. Thus, QC is the enzyme being analyzed, and pyroglutamyl aminopeptidase represents the auxiliary enzyme. p-Nitroaniline is released in equimolar amounts to the Gln-pNA converted by QC. Hence, QC activity is directly related to the amount of p-nitroaniline released and can therefore easily be quantified. For estimation of the conversion rate from Gln-pNA to pGlu-pNA, this first step has to be rate determining for the complete assay. Previous theoretical investigations on the kinetics of irreversible coupled enzyme assays showed the possibility of calculating the required amount of an auxiliary enzyme for the development of a reliable method (16). The calculation was performed according to Eq. [1],

$$V_2 = -K_{m2} \times \ln(1 - [\text{pGlu-}p\text{NA}]_t/[\text{pGlu-}p\text{NA}]_{ss})/t,$$

[1]

where K_{m2} is the Michaelis constant and V_2 the maximal velocity of the reaction catalyzed by the auxiliary enzyme, pyroglutamyl aminopeptidase. [pGlu-pNA]$_t$ represents the concentration of pGlu-pNA at time t after initiation of the reaction. [pGlu-pNA]$_{ss}$ describes the steady-state concentration of pGlu-pNA under these conditions. Equation [1] is valid if the initial substrate concentration does not change significantly during the considered time and the second reaction follows a first-order rate law ([pGlu-pNA]$_{ss} \ll K_{m2}$). Using the known K_{m2}, the required amount of auxiliary enzyme can be calculated from V_2. We determined a K_{m2} value of 710 ± 50 μM for pyroglutamyl aminopeptidase and pGlu-pNA under the assay conditions, which corresponds to data obtained from the literature (17). Using this value and assuming that the definition of 1 unit of auxiliary enzyme refers to saturated substrate concentrations, we estimated 0.25 U pyroglutamyl aminopeptidase to be required in the sample volume to reach 95% of the steady-state concentration of pGlu-pNA after 130 s. Thus, linear progress curves
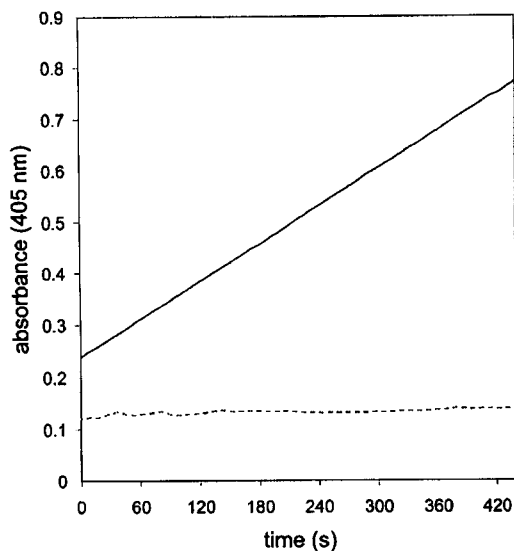
FIG. 1. Progress curves of pNA formation from Gln-pNA, monitored by the increase in absorption at 405 nm. No increase in absorption was detected in the absence of QC (dotted trace). Linear product formation was observed in the presence of QC (solid trace). Reactions were initiated by the addition of QC, preincubated for 2 min, and subsequently the absorption was monitored. The assay conditions were Gln-pNA (1 mM), pyroglutamyl aminopeptidase (0.25 U), and QC (3 × 10^{-3} U) in 50 mM Tricine/NaOH, at pH 8.0, 30°C. The final sample volume was 250 μl.

generated by only two separation steps. A rapid purification was reached by implementing a multilevel gradient in the initial ion-exchange chromatography followed by a hydrophobic interaction chromatography. Similar to the purification procedure described by Zerhouni et al. (13), QC was eluted among the last enzymes that can be purified from papaya by cation-exchange chromatography. This is somewhat surprising since the proteins should be eluted in the order of their increasing isoelectric points (pI). However, the QC of our preparation showed a pI of 9.4–9.6, determined by isoelectric focusing in agarose gels (data not shown). This value is more alkaline than the reported isoelectric point of papain (pI8.75), but noticeably more acidic than that of papaya proteinase A (pI11) (18), the most basic of the papaya proteinases (19). The reasons for the anomalous order of elution were not examined in detail, but the phenomenon might be explained by assuming that highly basic regions on the surface of QC may account for strong electrostatic interactions with the cation exchange resin. The high hydrophobicity reported previously (13) might be attributed to other regions, established in the correctly folded protein. Although the overall yield of the purification presented here was approximately 25%, three times less than that previously published (13), our strategy was much less time consuming. Hence, the reduced overall yield of the purification can be easily compensated by the yield of QC in the latex of C. papaya. Thirty-five milligrams of homogeneous QC was obtained from
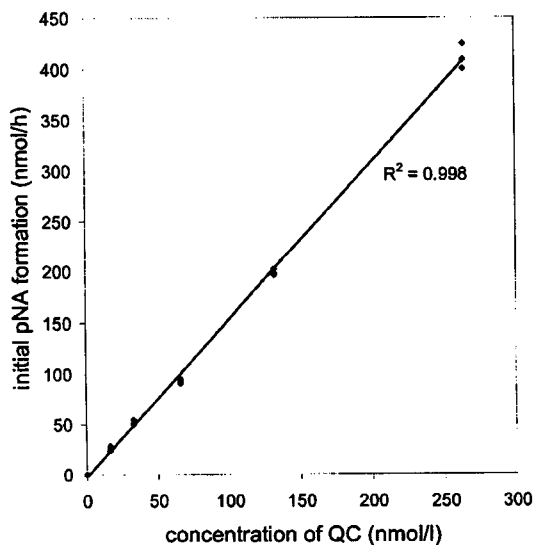
were expected after a lag time of 2 min, independent of the concentration of Gln-pNA.

As shown in Fig. 1, Gln-pNA is recognized as a substrate for QC, demonstrated by an increase in absorption at 405 nm. There was no increase in absorption without QC, indicating that formation of p-nitroaniline is dependent on the presence of QC. Linear product formation was observed at 0.25 U pyroglutamyl aminopeptidase and a preincubation time of 120 s, verifying the reliability of the assay and the calculation made above regarding the excess of pyroglutamyl aminopeptidase required. To counteract rapid substrate consumption during preincubation, the concentration of QC was adjusted precisely by dilution. Based on this, the assay was carried out at an activity concentration of 1 unit/ml pyroglutamyl aminopeptidase, giving reproducible progress curves of glutaminyl cyclase activity under the conditions used. Increasing the amount of pyroglutamyl aminopeptidase shortened the lag time, but had no influence on the slope of the progress curves.

In addition, there was a linear relationship between the initial velocity and the concentration of QC (Fig. 2). This confirms that the rate of catalysis is dependent on the QC-mediated conversion of Gln-pNA to pGlu-pNA.

The feasibility of the novel assay was tested during the QC purification from papaya latex, demonstrated here by determination of QC activity in fractions of the first purification step (Fig. 3). Highly purified QC was

FIG. 2. Dependence of pNA formation on the concentration of QC in the sample. The samples contained various amounts of QC between 16.5 and 264 nmol/L, prepared by the dilution of a stock solution. The protein concentration was assayed using the method of Bradford (14) and calculated using a molecular mass of 33 kDa for QC. For assay conditions, see Materials and Methods.
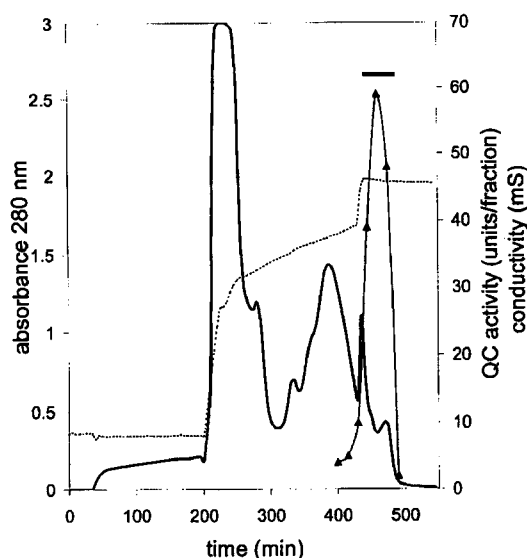
FIG. 3. Elution profile of QC during ion-exchange chromotography. Lyophilized papaya latex was dissolved, and proteases were inactivated using S-methylmethane thiosulfonate and centrifuged as described elsewhere (13, 23). The supernatant after centrifugation was applied onto a SP-Sepharose Fast Flow column and proteins were eluted as described under Materials and Methods. Absorption at 280 nm (solid trace) and conductivity (dotted trace) were measured directly in the column eluate. Assays of QC activity contained an appropriately diluted aliquot of the column eluate and were performed using conditions given under Materials and Methods. Enzymatic activity was determined and plotted as units/chromatographic fraction (▲). Pooled fractions, indicated by the bar, were concentrated and further purified by hydrophobic interaction chromatography.

absorption of the substrate Gln-pNA at 340 nm, a detection wavelength of 355 nm was found to be optimal when using this substrate. Kinetic parameters computed for the conversion of Gln-pNA correlate well with those obtained using the novel assay described above, e.g., K_m and k_{cat} were calculated to be 99 ± 6 μM and 27 ± 1 s^{-1}, respectively, thus indicating the validity of the continuous method.

In order to substantiate the feasibility of the new assay in more detail, the effect of ammonia concentration on the conversion rate of Gln-pNA to pGlu-pNA was recorded at constant ionic strength ($\mu = 0.071$ M). No change in activity could be observed in the range of ammonia concentration analyzed, indicating that the assay can be performed up to 50 mM ammonia. This suggests that QC lacks product inhibition by ammonia. Obviously, the release of ammonia is not the rate-limiting step in the catalysis by papaya QC.

Ionic strength was tested as another important parameter in establishing the new QC assay in enzyme characterization. As a prerequisite, constant activity of the auxiliary enzyme is necessary under the chosen conditions, e.g., time to reach steady-state conditions (Eq. [1]) is unaltered. This prerequisite was fulfilled, since activity of pyroglutamyl aminopeptidase was enhanced by increasing ionic strength (data not shown). As demonstrated in Fig. 5, activity of QC increased steadily up to 300 mM KCl and was almost constant up

150 g of lyophilized papaya latex using the new procedure.

Although Gln-pNA is a dipeptide surrogate, the kinetic parameters for its conversion by QC correspond to those of other dipeptides. Using the continuous spectrophotometric assay presented here, a Michaelis constant of 102 ± 4 μM was determined (Fig. 4). This corresponds to 90 ± 20 μM detected for Gln-Gln and 210 ± 40 μM for Gln-Ala under comparable conditions (6). Based on the assumption of a monomeric protein with a molecular mass of 33 kDa, determined by gel electrophoresis (13), a first-order rate constant for breakdown of the enzyme/substrate complex to the products (k_{cat}) of 28 ± 1 s^{-1} at 30°C was determined. This corresponds to the value of 50 s^{-1} at 37°C reported for Gln-$tert$-butyl ester (13).

In order to verify these parameters, they were evaluated by an alternative method (12). In this assay, detection of QC activity was accomplished by conversion of the ammonia formed into glutamate, catalyzed by glutamate dehydrogenase in the presence of α-ketoglutaric acid and NADH/H^{+}. In the subsequent reaction, consumption of NADH/H^{+} can be monitored spectrophotometrically at 340 nm. Due to the overlapping

FIG. 4. Dependence of initial pNA formation on the concentration of Gln-pNA due to conversion to pGlu-pNA by QC. Reactions were performed in a final volume of 250 μl at 30°C. The following component concentrations were used: 0.05–1 mM Gln-pNA, 0.25 U pyroglutamyl aminopeptidase, and 1 mU QC in 50 mM Tricine/NaOH, pH 8.0. For the determination of the rate constant, k_{cat}, a molecular mass of 33 kDa of the monomeric papaya glutaminyl cyclase was assumed (13).
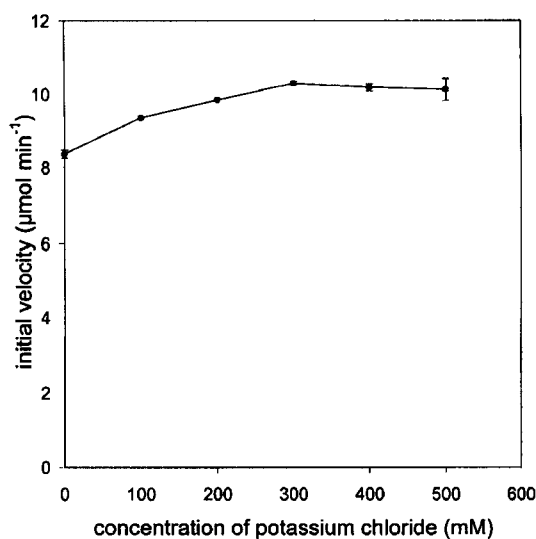
FIG. 5. Dependence of QC activity on ionic strength. Reactions were performed in 50 mM Tricine/NaOH, pH 8.0, at different concentrations of potassium chloride between 0 and 500 mM. This corresponds to an ionic strength of 0.02 to 0.52 M. Determinations were performed in triplicate. Error bars indicate the standard deviation. Other assay conditions were as described under Materials and Methods.

to 500 mM. The overall activation by increasing ionic strength was approximately 20%. A very similar dependence was observed for NaCl (not shown). Thus, within the QC assay a constant ionic strength is important to avoid activating effects of abundant ions. The effect of ionic strength on QC activity might be caused by (i) weakened salt bridges, leading to structural changes and higher enzymatic activity, and by (ii) altered dissociation constant of catalytic groups of the enzyme. Such altered constants at increasing ionic strength were reported previously for lysozyme (20).

Fluorometric Assays

Based on the results obtained with the spectrophotometric assay, two further assays using fluorometric detection were developed. For convenience, the commercially available fluorogenic substrates Gln-βNA and Gln-AMC were purchased and tested as substrates of papaya glutaminyl cyclase. As expected from data in the literature, pyroglutamyl-βNA and pyroglutamyl-AMC are potent substrates for the auxiliary enzyme (21, 22). In agreement with these reports, we determined V_{max}/K_m values for the fluorogenic substrates that were approximately 20-fold higher than that of pGlu-pNA. This potency of the auxiliary enzyme for hydrolysis of the potential intermediates emerging in the QC assay results in drastically reduced lag times when using the same concentration (1 U/ml) of pyroglutamyl aminopeptidase compared to the spectrophotometric assay based on release of pNA. The times required to reach steady-state conditions were calcu-

lated according to the method mentioned above and were found to be less than 5 s for Gln-AMC as well as Gln-βNA. Thus, steady-state conditions were reached within the time required for mixing and beginning of data monitoring. In fact, linear progress curves were obtained in the QC assay for the conversion of both fluorogenic substrates, immediately after initiation of the reaction (Fig. 6A). In the case of both substrates, the observed change in fluorescence was found to increase linearly during the time of incubation. There was no increase in fluorescence detected in the absence of QC or pyroglutamyl aminopeptidase.

As shown in Fig. 6B, linearity was observed between the reaction rate and the enzyme concentration when 0.05 mM substrate was used under these conditions, indicating that the compounds can be used as sensitive substrates for glutaminyl cyclase. Furthermore, in comparison to the chromogenic substrate Gln-pNA, the assays described here seem to be approximately 1000 times more sensitive and are capable of detecting enzyme concentrations as low as 0.4 ng/ml.

Kinetic analyses of the enzymatic conversion of both substrates revealed that the enzyme reactions fit Lineweaver–Burk plots (data not shown). The K_m values for conversion of the substrates were 43 ± 4 μM for Gln-βNA and 52 ± 5 μM in the case of Gln-AMC. Interestingly, these are the lowest values that were determined for payaya glutaminyl cyclase, and they are noticeably less than that of the chromogenic substrate Gln-pNA. The values of k_{cat} for conversion of Gln-βNA (46 s^{-1}) and Gln-AMC (31 s^{-1}) by QC are similar to that of Gln-pNA. As a consequence, it can be concluded that the chromogenic and fluorogenic substrates described here can be regarded as the best for papaya QC with respect to their k_{cat}/K_m values. Both fluorogenic substrates seemed to show weak substrate inhibition at concentrations higher than 10 K_m. However, at the concentrations used, this inhibition was minimal and did not interfere with the determination of the kinetic parameters.

A limitation of feasibility, also in the case of other assays of QC, is the susceptibility of the chromogenic and fluorogenic substrates to aminopeptidase attack. Thus, in some applications, addition of aminopeptidase inhibitors will be necessary. Accordingly, we tested three peptidase inhibitors, i.e., bestatin (100 μg/ml), aprotinin (50 μg/ml), and EDTA (5 mM), concerning their influence on the assay, using Gln-βNA as substrate. None of the three substances interfered with the assay, making them useful as additives to inhibit peptidases in crude samples.

Finally, the substrates were also tested upon conversion by human glutaminyl cyclase, recombinantly expressed in the yeast *Pichia pastoris* (published elsewhere). All three assays also worked with this enzyme
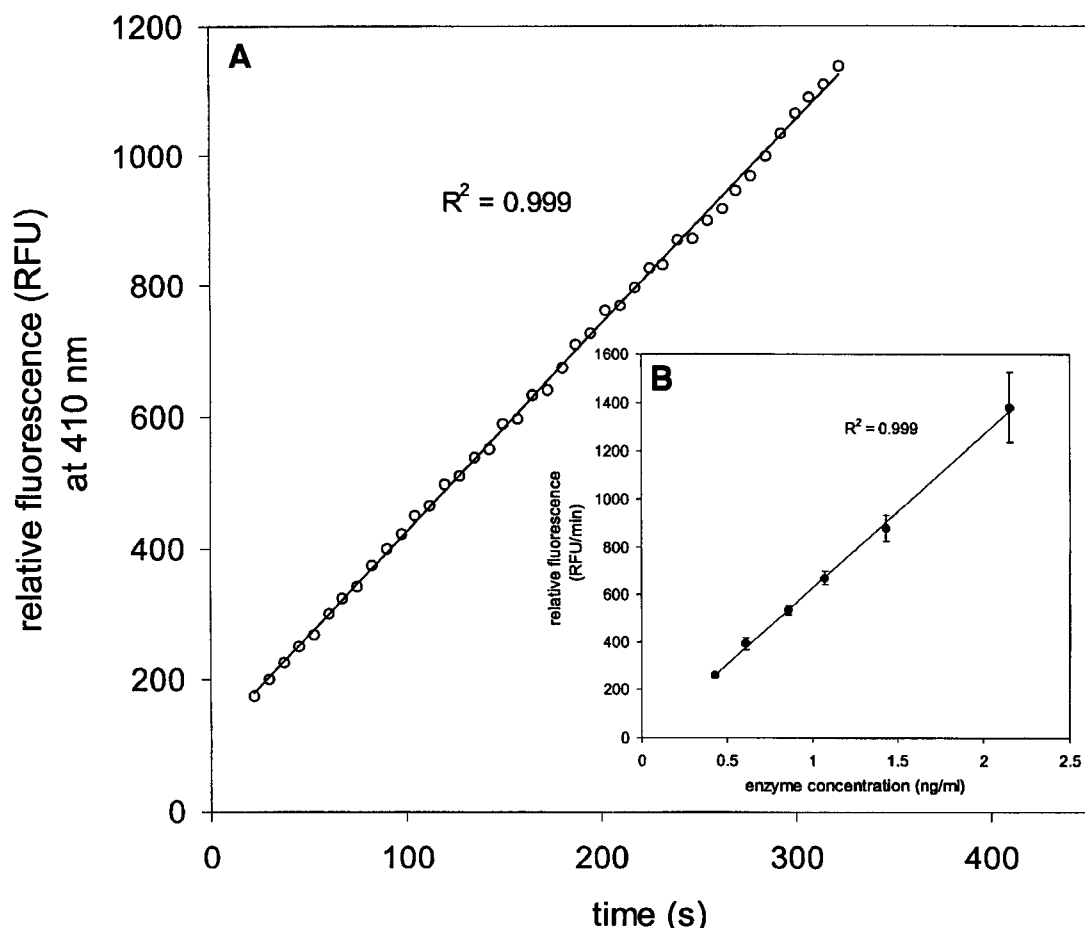
FIG. 6. (A) Progress curve of 2-naphthylamine formation from L-glutamine-2-naphthylamide (Gln-βNA) by catalysis of QC and pyroglutamyl aminopeptidase, monitored by measurement of the relative fluorescence at 410 nm. No increase in fluorescence was detected in the absence of QC (not shown). Product formation obeyed with high accuracy a straight line during the time of analysis. (B) Dependence of initial velocity on the concentration of QC, using Gln-βNA as the fluorogenic substrate. Determinations were carried out in the high sensitivity scale of the spectrofluorometer. Every data point is the mean value of four determinations, while error bars indicate the standard deviations. QC concentrations were achieved by dilution of a stock solution. The assay composition is described under Materials and Methods.

(data not shown), making the procedures applicable for plant and animal sources of QC.

To our knowledge, these are the first continuous assays described for QC that can be implemented during protein purification. Among the advantages of the presented methods, the continuous measurement and less time consumption make the methods more favorable compared to previously developed methods.

The most important advantage of the new methods, in comparison to a previously described assay (12), is the fact that these methods can be performed in the presence of ammonia. Thus, various protein purification steps using ammonium sulfate can be easily monitored.

ACKNOWLEDGMENTS

REFERENCES

1. Messer, M. (1963) Enzymatic cyclization of L-glutamine and L-glutaminyl peptides. *Nature* **4874**, 1299.

2. Busby, W. H. J., Quackenbush, G. E., Humm, J., Youngblood, W. W., and Kizer, J. S. (1987) An enzyme(s) that converts glutaminyl-peptides into pyroglutamyl-peptides: Presence in pituitary, brain, adrenal medulla, and lymphocytes. *J. Biol. Chem.* **262**, 8532–8536.

3. Fischer, W. H., and Spiess, J. (1987) Identification of a mammalian glutaminyl cyclase converting glutaminyl into pyroglutamyl peptides. *Proc. Natl. Acad. Sci. USA* **84**, 3628–3632.

4. Pohl, T., Zimmer, M., Mugele, K., and Spiess, J. (1991) Primary structure and functional expression of a glutaminyl cyclase. *Proc. Natl. Acad. Sci. USA* **88**, 10059–10063.

5. Sykes, P. A., Watson, S. J., Temple, J. S., and Bateman, R. C. J. (1999) Evidence for tissue-specific forms of glutaminyl cyclase. *FEBS Lett.* **455**, 159–161.

6. Gololobov, M. Y., Wang, W., and Bateman, R. C. J. (1996) Substrate and inhibitor specificity of glutamine cyclotransferase (QC). *Biol. Chem. Hoppe-Seyler* **377**, 395–398.

7. Hinke, S. A., Pospisilik, J. A., Demuth, H.-U., Manhart, S., Kühn-Wache, K., Hoffmann, T., Nishimura, E., Pedersen, R. A., and McIntosh, C. H. S. (2000) Dipeptidyl peptidase IV (DPIV/CD26) degradation of glucagon. *J. Biol. Chem.* **275**, 3827–3834.

8. Van Coillie, E., Proost, P., Van Aelst, I., Struyf, S., Polfliet, M., De Meester, I., Harvey, D. J., Van Damme, J., and Opdenakker, G. (1998) Functional comparison of two human monocyte chemotactic protein-2 isoforms, role of the amino-terminal pyroglutamic acid and processing by CD26/dipeptidyl peptidase IV. *Biochemistry* **37**, 12672–12680.

9. Awade, A. C., Cleuziat, P., Gonzales, T., and Robert-Baudouy, J. (1994) Pyrrolidone carboxyl peptidase (Pcp): An enzyme that removes pyroglutamic acid (pGlu) from pGlu-peptides and pGlu-proteins. *Proteins* **20**, 34–51.

10. Consalvo, A. P., Young, S. D., Jones, B. N., and Tamburini, P. P. (1988) A rapid fluorometric assay for N-terminal glutaminyl cyclase activity using high-performance liquid chromatography. *Anal. Biochem.* **175**, 131–138.

11. Koger, J. B., Humm, J., and Kizer, J. S. (1989) Assay of glutaminylpeptide cyclase. *Methods Enzymol.* **168**, 358–365.

12. Bateman, R. C. J. (1989) A spectrophotometric assay for glutaminyl-peptide cyclizing enzymes. *J. Neurosci. Methods* **30**, 23–28.

13. Zerhouni, S., Amrani, A., Nijs, M., Smolders, N., Azarkan, M., Vincentelli, J., and Looze, Y. (1989) Purification and characterization of papaya glutamine cyclotransferase, a plant enzyme highly resistant to chemical, acid and thermal denaturation. *Biochim. Biophys. Acta* **138**, 275–290.

14. Bradford, M. M. (1976) A rapid and sensitive method for the quantitation of microgram quantities of protein utilizing the principle of protein-dye binding. *Anal. Biochem.* **72**, 248–254.

15. Gololobov, M. Y., Song, I., Wang, W., and Bateman, R. C. J. (1994) Steady-state kinetics of glutamine cyclotransferase. *Arch. Biochem. Biophys.* **309**, 300–307.

16. McClure, W. R. (1969) A kinetic analysis of coupled enzyme assays. *Biochemistry* **8**, 2782–2786.

17. Fujiwara, K., Kobayashi, R., and Tsuru, D. (1979) The substrate specificity of pyrrolidone carboxylyl peptidase from Bacillus amyloliquefaciens. *Biochim. Biophys. Acta* **570**, 140–148.

18. Goodenough, P. W., and Owen, J. (1987) Chromatographic and electrophoretic analyses of papaya proteinases. *Phytochemistry* **26**, 75–79.

19. Kaarsholm, N. C., and Schack, P. (1983) Characterization of papaya peptidase A as an enzyme of extreme basicity. *Acta Chem. Scand. [B]* **37**, 607–611.

20. Parsons, S. M., and Raftery, M. A. (1972) Ionization behavior of the catalytic carboxyls of lysozyme: Effects of ionic strength. *Biochemistry* **11**, 1623–1629.

21. Tsuru, D., Fujiwara, K., and Kado, K. (1978) Purification and characterization of L-pyrrolidonecarboxylate peptidase from Bacillus amyloliquefaciens. *J. Biochem.* **84**, 467–476.

22. Fujiwara, K., and Tsuru, D. (1978) New chromogenic and fluorogenic substrates for pyrrolidonyl peptidase. *J. Biochem.* **83**, 1145–1149.

23. Wynn, R., and Richards, F. M. (1995) Chemical modification of protein thiols: Formation of mixed disulfides. *Methods Enzymol.* **251**, 351–356.

Substrate Specificity of Glutaminyl Cyclases from Plants and Animals

**Stephan Schilling[1], Susanne Manhart[1],
Torsten Hoffmann[1], Hans-Henning Ludwig[1],
Claus Wasternack[2] and Hans-Ulrich Demuth[1],***

[1] Probiodrug AG, Weinbergweg 22,
D-06120 Halle/Saale, Germany
[2] Leibniz Institute for Plant Biochemistry,
P.O. Box 110432, D-06120 Halle/Saale, Germany

*Corresponding author

Glutaminyl cyclases (QC) catalyze the intramolecular cyclization of N-terminal glutamine residues of peptides and proteins. For a comparison of the substrate specificity of human and papaya QC enzymes, a novel continuous assay was established by adapting an existing discontinuous method. Specificity constants (k_{cat}/K_m) of dipeptides and dipeptide surrogates were higher for plant QC, whereas the selectivity for oligopeptides was similar for both enzymes. However, only the specificity constants of mammalian QC were dependent on size and composition of the substrates. Specificity constants of both enzymes were equally pH-dependent in the acidic pH-region, revealing a pK_a value identical to the pK_a of the substrate, suggesting similarities in the substrate conversion mode. Accordingly, both QCs converted the L-βhomoglutaminyl residue in the peptide H-βhomoGln-Phe-Lys-Arg-Leu-Ala-NH₂ and the glutaminyl residues of the branched peptide H-Gln-Lys(Gln)-Arg-Leu-Ala-NH₂ as well as the partially cyclized peptide H-Gln-cyclo(Nε-Lys-Arg-Pro-Ala-Gly-Phe). In contrast, only QC from *C. papaya* was able to cyclize a methylated glutamine residue, while this compound did not even inhibit human QC-catalysis, suggesting distinct substrate recognition pattern. The conversion of the potential physiological substrates [Gln¹]-gastrin, [Gln¹]-neurotensin and [Gln¹]-fertilization promoting peptide indicates that human QC may play a key role in posttranslational modification of most if not all pGlu-containing hormones.
*Key words:* Glutamine cyclotransferase / βHomo-glutamine / 5-Oxo-L-proline / Pyroglutamic acid.

Introduction

Glutaminyl cyclases (QC, EC 2.3.2.5) catalyze the intramolecular cyclization of N-terminal glutamine residues into pyroglutamic acid (pGlu) with liberation of ammonia

(Figure 1). In 1963, the first QC was isolated from the latex of the tropical plant *Carica papaya* (Messer, 1963). Twenty four years later, a corresponding enzymatic activity was discovered in mammalian pituitary homogenates (Busby *et al.*, 1987; Fischer and Spiess, 1987). This enzyme is thought to be responsible for the generation of the N-termini of peptide hormones and proteins containing pGlu. The conversion of Gln into pGlu by a QC was demonstrated for the precursors of thyroid hormone-releasing hormone (TRH) and gonadotropin-releasing hormone (GnRH) (Busby *et al.*, 1987; Fischer and Spiess, 1987). Experiments revealed a colocalization of the QC with its putative catalytic products in bovine pituitary, thereby supporting a potential function in peptide hormone synthesis. The physiological function of plant QC is unknown. In case of QC from *C. papaya*, a role in plant defense reactions was suggested (El Moussaoui *et al.*, 2001). Putative QCs from other plants have been identified by sequence comparisons (Dahl *et al.*, 2000), but physiological functions of these enzymes are yet to be characterized.

An initial comparison of plant and animal QCs reveals several similarities. QCs from both sources are monomeric with similar molecular masses of 33 – 40 kDa (Pohl *et al.*, 1991; Zerhouni *et al.*, 1998). They are glycoproteins synthesized *via* the secretory pathway, and the carbohydrates contribute approximately 2 – 4 kDa to their molecular mass (Pohl *et al.*, 1991; Dahl *et al.*, 2000). Furthermore, all QCs show a strict specificity for L-glutamine at the N-terminal position of the substrates and their kinetic behavior was found to obey the Michaelis-Menten equation (Consalvo *et al.*, 1988; Pohl *et al.*, 1991; Gololobov *et al.*, 1996). Interestingly, the primary structures of QC from *C. papaya* and that of the highly conserved QC from mammals did not reveal any sequence homology (Dahl *et al.*, 2000). In addition, plant QC was described to contain extensive β-sheet structure (Oberg *et al.*, 1998), in contrast to a recent CD-spectral structure determination
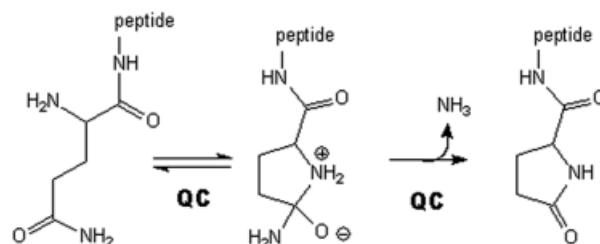
Fig. 1 The N-Terminal Cyclization of Glutaminyl Peptides by QC.

of the human enzyme (Schilling *et al.*, 2002a). The structure of the mammalian QCs is remarkably homologous to the bacterial aminopeptidases (Bateman *et al.*, 2001), whereas the plant QCs appear to belong to a separate enzyme family (Dahl *et al.*, 2000). This led to the conclusion that QCs from plants and animals have different evolutionary origins.

Due to the apparent divergence, different properties and consequently different functions are to be expected when comparing QC isoforms from plants and animals. To address this question, we performed a direct comparison of plant and animal QC by analysis of the QC from *C. papaya* and the recombinant human QC, including a detailed analysis of catalytic properties. Based on the previously used discontinuous assay methods, only limited information concerning substrate specificity and QC selectivity is currently known. So far, kinetic parameters have only been determined for amino acid derivatives or di- and tripeptides (Bateman, 1989; Song *et al.*, 1994; Gololobov *et al.*, 1996; Sykes *et al.*, 1999). Gonadotropin-releasing hormone and thyrotropin releasing-hormone have been investigated using HPLC as the only larger potential substrates of QC (Fischer and Spiess, 1987).

Here, we report the first comprehensive characterization of longer peptides as QC substrates using a novel continuous spectrophotometric assay. This method enabled a detailed investigation of the impact of N-terminal glutamate/glutamine modifications, of the nature of the C-terminal amino acids and the length of the substrates on QC-catalysis. Furthermore, kinetic parameters of QC-catalysis of potential physiological substrates were also determined for the first time.

Results

Spectrophotometric Assay

The discontinuous assay introduced by Bateman (1989) was modified to a continuous method, applicable for microplates. In the assay, glutamic dehydrogenase and its substrates α-ketoglutaric acid and NADH/H$^+$ are coupled to QC activity by liberation of ammonia from the glutamine residue. Accordingly, QC activity is reflected by a decrease in absorbance at 340 nm caused by the ammonia release and subsequent consumption of NADH/H$^+$ due to formation of glutamate from α-ketoglutaric acid. The amount of the auxiliary enzyme necessary to obtain a sufficiently short 'lag time', *i.e.* the time in which a steady-state is reached between the reaction catalyzed by the investigated enzyme and the reaction catalyzed by the auxiliary enzyme, was first calculated using a previously described method (McClure, 1969), an approach that was already used to develop fluorescence-based continuous assays for QC (Schilling *et al.*, 2002b). Under saturating concentrations of NADH/H$^+$ and α-ketoglutaric acid (McClure, 1969), 30 U/ml glutamic dehydrogenase
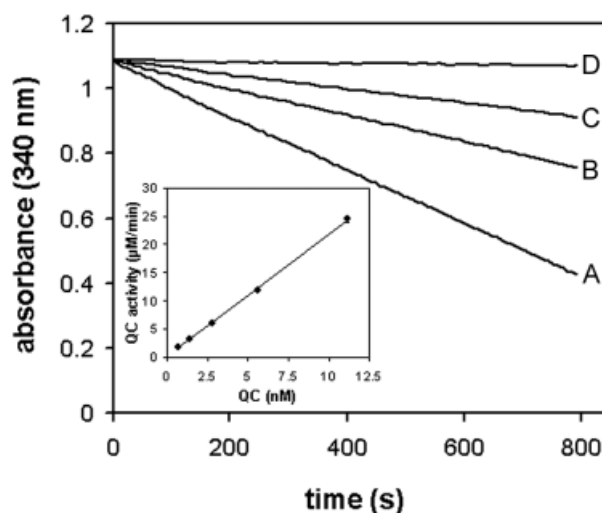
Fig. 2 Progress Curves of the Cyclization of H-Gln-Ala-OH, Catalyzed by Human QC.
The samples contained 0.3 mM NADH/H$^+$, 14 mM α-ketoglutaric acid, 30 U/ml glutamic dehydrogenase and 1 mM H-Gln-Ala-OH. For curves A-D, varying concentrations of QC were applied: A, 10 mU/ml, B, 5 mU/ml, C, 2.5 mU/ml. In case of curve D, QC was omitted. A linear relationship was obtained between the QC concentration and the observed activity (inset).

was calculated to be a sufficient excess to reach 95% of the steady-state concentration of ammonia after 20 s, *i.e.* a time required for starting the reaction and mixing of the assay constituents. Thus, linear progress curves should be observed upon starting data acquisition. Indeed, linear progress curves were detected under these conditions (Figure 2). A linear relationship was observed between the activity and the concentration of QC. The kinetic parameters obtained for H-Gln-Gln-OH in the continuous assay (Table 1) were in good agreement with those obtained with the discontinuous method ($K_m = 175 \pm 18$ μM, $k_{cat} = 21.3 \pm 0.6$ s^{-1}). In addition, the kinetic parameters for conversion of the substrates H-Gln-Ala-OH and H-Gln-NH$_2$ by the papaya QC (Table 1) correspond well to those determined with a direct method at pH 8.8 and 37 °C (Gololobov *et al.*, 1996).

pH Dependence

The pH dependence of catalysis of human and papaya QC was investigated under first-order rate law conditions, thus reflecting the impact of pH on the specificity constant k_{cat}/K_m. For this purpose, pyroglutamyl aminopeptidase was used as auxiliary enzyme with Gln-βNA as substrate in the coupled assay. Pyroglutamyl aminopeptidase was shown to be active and stable between pH 5.5 – 8.5 (Tsuru *et al.*, 1978), hence, this assay allowed QC analysis in this pH-range. The rate profiles obtained fit to classical bell-shaped curves (Figure 3). For human QC a very narrow pH dependence with an optimum at about pH 7.8 – 8.0 was observed (Figure 3A), and the rate

Table 1   Kinetic Parameters of the Conversion of Di-, Tri- and Tetrapeptides by Human and Papaya QC.

Substrate	Human QC				Papaya QC			
	K_m (µM)	k_{cat} (s^{-1})	K_i [a] (mM)	k_{cat}/K_m (mM^{-1} s^{-1})	K_m (µM)	k_{cat} (s^{-1})	K_i [a] (mM)	k_{cat}/K_m (mM^{-1} s^{-1})
H-Gln-OH	n.r.	n.r.	n.r.	n.r.	n.d.	n.d.	n.d.	0.23±0.1[b]
H-Gln-AMC	54±2	5.3±0.1	n.d.	98±2	42±1	39.4±0.4	n.d.	938±13
H-Gln-βNA	70±3	20.6±0.5	1.21±0.07	294±6	38±3	51.4±1.4	1.20±0.08	1353±70
H-Gln-OtBu	1235±74	6.7±0.2	n.i.	5.4±0.2	223±9	49.4±0.6	n.i.	222±6
H-Gln-NH$_2$	409±40	12.8±0.5	n.i.	31±2	433±13	44.8±0.4	n.i.	103±2
H-Gln-Gly-OH	247±10	13.2±0.2	n.i.	53±1	641±20	45.8±0.4	n.i.	71±2
H-Gln-Ala-OH	232±5	57.2±0.4	n.i.	247±4	158±8	69.8±1.0	n.i.	442±16
H-Gln-Gln-OH	148±5	20.7±0.2	n.i.	140±2	44±3	43.2±0.7	n.i.	982±51
H-Gln-Glu-OH	359±10	24.7±0.2	n.i.	58±1	106±5	50.3±0.6	n.i.	475±17
H-Gln-Val-OH	196±5	17.2±0.1	n.i.	88±2	n.d.	n.d.	n.d.	n.d.
H-Gln-Tyr-OH	211±5	94±1	n.i.	446±6	n.d.	n.d.	n.d.	n.d.
H-Gln-Glu-Tyr-NH$_2$	79±2	45.1±0.4	n.i.	524±8	103±4	53.6±0.7	n.i.	520±13
H-Gln-Gly-Pro-OH	130±5	25.3±0.2	n.i.	195±7	333±15	41.7±0.5	n.i.	125±4
H-Gln-Tyr-Ala-OH	101±4	125±1	n.i.	930±27	63±3	104.0±1.0	n.i.	1650±63
H-Gln-Phe-Ala-NH$_2$	69±3	109±1	n.i.	1811±64	111±5	132.1±0.6	n.i.	1190±48
H-Gln-Trp-Ala-NH$_2$	50±2	47.0±0.7	n.i.	940±24	78±5	151.8±2.6	n.i.	1946±91
H-Gln-Arg-Gly-Ile-NH$_2$	143±4	33.5±0.4	n.i.	234±4	123±10	49.2±1.7	n.i.	400±19
H-Gln-Asn-Gly-Ile-NH$_2$	172±5	56.6±0.5	n.i.	329±7	153±9	51.4±0.9	n.i.	336±14
H-Gln-Ser-Tyr-Phe-NH$_2$	55±3	52.8±0.8	n.i.	960±38	135±6	64.9±1.0	n.i.	481±14
H-Gln-Arg-Tyr-Phe-NH$_2$	55±2	29.6±0.3	n.i.	538±14	124±6	48.9±0.7	n.i.	394±13
H-Gln-Pro-Tyr-Phe-NH$_2$	1889±152	31.7±1.2	n.i.	17±1	149±14	18.8±0.6	n.i.	126±8
H-Gln-His-Tyr-Phe-NH$_2$	68±3	55.4±0.7	n.i.	815±26	92±7	75.9±1.4	n.i.	825±48
H-Gln-Gln-Tyr-Phe-NH$_2$	41±2	41.4±0.4	n.i.	1010±40	45±2	52.9±0.7	n.i.	1176±37
H-Gln-Glu-Tyr-Phe-NH$_2$	47±4	46±1	n.i.	979±62	100±4	54.6±0.6	n.i.	546±16
H-Gln-Glu-Ala-Ala-NH$_2$	77±4	46±1	n.i.	597±18	102±4	53.7±0.6	n.i.	526±15
H-Gln-Glu-Tyr-Ala-NH$_2$	69±2	42.1±0.4	n.i.	610±12	113±5	44.7±0.5	n.i.	396±13
H-Gln-Glu-Ala-Phe-NH$_2$	39±3	39±1	n.i.	1000±51	81±3	48.5±0.45	n.i.	599±17
H-Gln-Glu-Asp-Leu-NH$_2$	55±2	45.8±0.5	n.i.	833±21	107±6	58.5±0.4	n.i.	547±27
H-Gln-Lys-Arg-Leu-NH$_2$	54±3	33.4±0.5	n.i.	619±25	118±6	48.2±0.8	n.i.	408±14

Reactions were carried out in Tris/HCl, pH 8.,0 containing 5 mM EDTA or in 0.05 M Tricine/NaOH, pH 8.0, 5 mM EDTA, respectively, at 30 °C (n.r., not reactive; n.d., not determined; n.i., no inhibition).
[a] Substrate inhibition; [b] determined under first-order rate law conditions, *i.e.* at [S]<<K_m.

decreased at more basic pH. Also papaya QC exhibited optimal activity near pH 8.0. However, no drop of k_{cat}/K_m occurred up to a pH of 8.5 (Figure 3B). Evaluation of rate profiles revealed that at 23 °C, pK_a values were 7.17±0.02 and 7.15±0.02 for human QC and papaya QC, respectively. These pK_a values are identical to the pK_a of the substrate H-Gln-βNA (7.16±0.01). The respecitve pK_a values obtained by titration and kinetic analysis of the pH dependence shifted toward 6.97±0.01 and 7.03±0.02 at 30 °C. Thus, substrate binding and/or conversion by both QC forms seems to be dependent on an unprotonated α-amino group.

The shape of the pH-profile of human QC in the basic pH-range was obviously due to dissociation of a group with a pK_a of approximately 8.5. For papaya QC, the limited stability of the auxiliary enzyme resulted in collection of insufficient data under basic pH conditions. Consequently, a reliable determination of a potential second pK_a value could not be achieved. This is also reflected by

the fact that fitting the data to a single dissociation model gave a very similar result (pK_a 7.13±0.03) compared to a double dissociation model, indicating that both pK_a values are fairly separated.
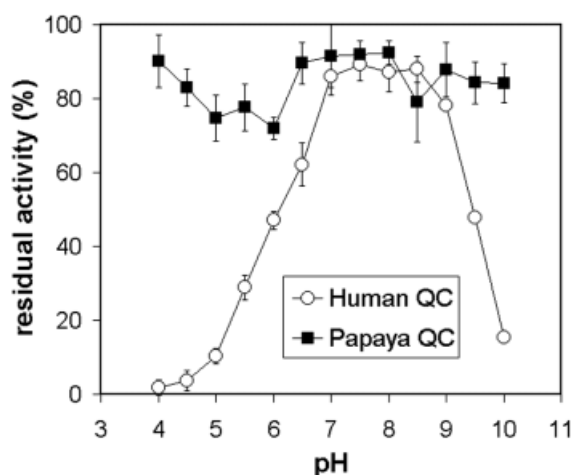
pH Stability

The stability of the QCs was analyzed by preincubating both enzymes at 30 °C for 30 min at different pH values between pH 4 and pH 10, followed by activity tests under standard conditions (Figure 4). The QC from papaya latex was found to be stable in the pH-range studied (Zerhouni *et al.*, 1998). In contrast, the human QC was stable only between pH 7 and 8.5, but exhibited a remarkable instability above pH 8.5 and below pH 6. Thus, pH 8 seemed to be optimal for activity and stability of plant and human QC. Consequently, this pH value was used to compare the substrate specificity of both QCs.
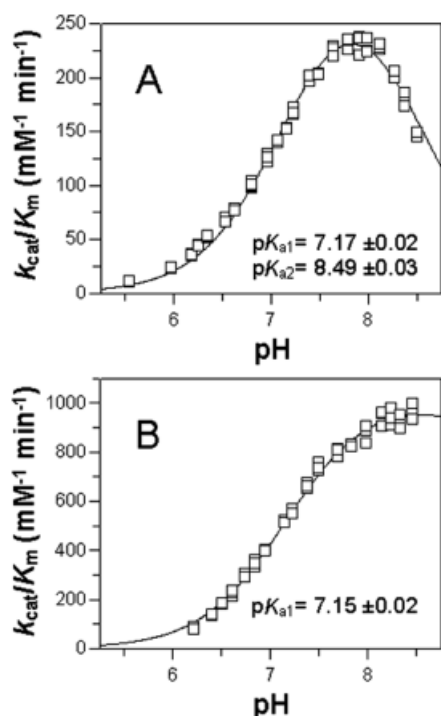
Fig. 3 pH Dependence of Human (A) and Papaya (B) QC.
Determinations were carried out under first-order rate conditions using Gln-βNA as substrate. In case of human QC, a buffer system providing a constant ionic strength according to Ellis and Morrison (1982) was used, consisting of 25 mм MES, 25 mм acetic acid and 50 mм Tris. Due to a slightly inhibiting effect of Tris, papaya QC was investigated using a 50 mм MOPS buffer. The ionic strength was adjusted to 0.05 м by addition of NaCl. The rate profiles were evaluated by fitting the data according to equations that account for two dissociating groups. In case of papaya QC, a pK_a value of 7.13 ± 0.03 was obtained by fitting the data according to a single dissociation model.

Fig. 4 Effect of pH on the Stability of the QC from Papaya Latex and Human QC.
An enzyme stock solution was diluted 20-fold in 0.1 м buffer of various pH values (pH 4 – 7, sodium citrate; pH 7 – 10, sodium phosphate). Enzyme solutions were incubated at 30 °C for 30 min, and subsequently enzymatic activity was analyzed according to the standard protocol.

Substrate Specificity

Di-, Tripeptides and Dipeptide Surrogates The substrate specificity of both QCs was analyzed with 30 potential substrates (Table 1). Nearly all of the short peptides were more efficiently converted by the papaya QC compared to the human QC. This is particularly obvious in case of the conversion of L-glutamine. Whereas the plant enzyme was able to react with L-glutamine, no reactivity of human QC was detected. Both enzymes were highly active toward substrates carrying large hydrophobic residues in the penultimate position of peptides, such as H-Gln-Tyr-Ala-OH, H-Gln-Phe-Ala-NH₂ and H-Gln-Trp-Ala-NH₂, or H-Gln-AMC and H-Gln-βNA, as compared to other tripeptides or dipeptide substrates. Plant as well as human QC were remarkably inhibited by H-Gln-βNA at high concentrations, revealing almost identical K_i values of about 1.2 mм (Table 1). Minor substrate inhibition was detected for H-Gln-AMC. Hence, low solubility of the substance hampered determination of the K_i value. A striking difference in specificity of the plant and the animal QC was observed for H-Gln-OtBu. Whereas the ester was converted by the papaya QC with similar specificity compared to dipeptide substrates, its turnover was more than one order of magnitude slower by human QC.

Oligopeptides In addition to several dipeptides and tripeptides, a number of putative oligopeptide substrates was tested with papaya and human QC (Table 1). Interestingly, the overall difference in the specificities between human and plant QC was not as large for tetrapeptides as was observed for dipeptide and tripeptide substrates. This indicates that the amino acids in the 3rd and 4th position still affect the kinetic behavior especially of human QC, leading to similar specificity constants. However, H-Gln-Pro-Tyr-Phe-NH₂, a tetrapeptide with proline in the penultimate position, yielded noticeably reduced k_{cat}/K_m values, providing an exception (Table 1). The reduction in the specificity was more pronounced for human QC, leading to an approximately 8-fold difference in the k_{cat}/K_m value as compared to papaya QC.

Slightly reduced specificity constants of human QC were also observed for the conversion of substrates with a positively charged amino acid on the C-terminal side of glutamine, such as H-Gln-Arg-Tyr-Phe-NH₂, H-Gln-Arg-Gly-Ile-NH₂ and H-Gln-Lys-Arg-Leu-NH₂, as compared to other tetrapeptides. Apparently, the reduced specificity was mainly due to a smaller turnover number. This effect was not observed for the plant enzyme.

In contrast to the selectivity of papaya QC for dipeptides, human QC was more selective for some tetrapeptides. The highest selectivity of human QC was recorded for peptides containing bulky hydrophobic residues in the 3rd and 4th amino acid position, which indicate hydrophobic interactions with the enzyme. Comparing the kinetic parameters for the respective peptides, the altered specificity seems to be mainly due to lower K_m values, since the turnover numbers for conversion of the

Table 2   Dependence of the Kinetic Parameters on the Substrate Size.

Substrate	Human QC			Papaya QC		
	K_m (µM)	k_{cat} (s^{-1})	k_{cat}/K_m (mM^{-1} s^{-1})	K_m (µM)	k_{cat} (s^{-1})	k_{cat}/K_m (mM^{-1} s^{-1})
H-Gln-Ala -NH$_2$	155±9	40.1±0.9	259±9	212±21	62.8±3.0	296±15
H-Gln-Ala-Ala-NH$_2$	87±3	76.3±0.7	877±22	164±6	83.2±1.0	507±12
H-Gln-Ala-Ala-Ala-Ala-NH$_2$	65±3	60.5±0.7	1174±43	197±8	74.6±1.0	379±10
H-Gln-Ala-Ala-Ser-Ala-Ala-NH$_2$	79±6	55.3±1.6	700±33	216±6	78.5±1.0	363±5

Reactions were performed under identical conditions as described in Table 1.

Table 3   Dependence of the Catalytic Parameters k_{cat} and K_m on the Ionic Strength for Substrates of Varying Length and Charge.

Substrate	K_m (µM)	k_{cat} (s^{-1})	k_{cat}/K_m (mM^{-1}s^{-1})	K_i [a] (mM)	K_m (µM)	k_{cat} (s^{-1})	k_{cat}/K_m (mM^{-1}s^{-1})	K_i [a] (mM)
Papaya QC	0.05 M Tricine-NaOH, pH 8.0				0.05 M Tricine-NaOH, pH 8.0, 0.5 M KCl			
H-Gln-NH$_2$	434±15	43.4±0.4	100±3	n.i.	446±10	45.2±0.3	101±2	n.i.
H-Gln-βNA	36±2	48.8±1.0	1356±50	1.14±0.05	32±2	47.2±0.8	1475±70	1.33±0.07
H-Gln-Ala-OH	137±7	69.7±.9	509±19	n.i.	143±5	68.1±0.6	480±12	n.i.
H-Gln-Glu-OH	98±5	45.0±0.5	459±18	n.i.	94±3	44.4±0.3	472±12	n.i.
H-Gln-Trp-Ala-NH$_2$	79±5	138±3	1747±73	n.i.	72±4	133±3	1847±61	n.i.
H-Gln-Arg-Gly-Ile-NH$_2$	106±8	52.9±1.2	499±26	n.i.	65±5	48.4±1.0	745±42	n.i.
H-Gln-Lys-Arg-Leu-NH$_2$	102±7	50±1	493±22	n.i.	53±2	58.1±0.7	1096±28	n.i.
H-Gln-Glu-Asp-Leu-NH$_2$	109±5	52.4±0.7	481±16	n.i.	94±3	53.6±0.5	570±13	n.i.
Human QC	0.05 M Tris-HCl, pH 8.0				0.05 M Tris-HCl, pH 8.0, 0.5 M KCl			
H-Gln-NH$_2$	442±30	12.8±0.3	29±1	n.i.	401±14	12.2±0.1	30±1	n.i.
H-Gln-βNA	76±4	21.7±0.5	285±8	1.39±0.08	63±3	20.0±0.4	318±9	0.97±0.04
H-Gln-Ala-OH	269±7	54.4±0.5	202±3	n.i.	357±12	47.6±0.6	133±3	n.i.
H-Gln-Glu-OH	373±15	21.4±0.3	57±2	n.i.	607±36	18.9±0.5	31±1	n.i.
H-Gln-Trp-Ala-NH$_2$	54±3	50.8±0.6	941±41	n.i.	56±2	50.0±0.4	893±25	n.i.
H-Gln-Arg-Gly-Ile-NH$_2$	166±13	31±1	187±9	n.i.	91±5	29.8±0.5	327±12	n.i.
H-Gln-Lys-Arg-Leu-NH$_2$	51±3	29.4±0.5	577±24	n.i.	34±1	31.6±0.3	929±19	n.i.
H-Gln-Glu-Asp-Leu-NH$_2$	60±2	46.6±0.5	777±18	n.i.	61±2	45.6±0.5	748±16	n.i.

Reactions were carried out at 30 °C.
[a] Substrate inhibition.

peptides were found to be similar. Obviously, the higher selectivity of human QC is due to stronger binding of the more hydrophobic substrates to the enzyme.

An increasing k_{cat}/K_m-ratio was also found for peptides of varying length consisting of the N-terminal glutamine residue and alanine residues as substrates of human QC (Table 2). While human QC was more selective for substrates of a length up to a pentapeptide, there was no such a trend with the papaya QC. Human QC was less active toward a serine-containing peptide, indicating that also the nature of the substrate side chains of the amino acids close to the reaction center is of importance.

Influence of Ionic Strength on Catalysis   To analyze the influence of ionic strength on the substrate specificity, the kinetic parameters for cyclization of several substrates were determined in presence and absence of 0.5 M KCl (Table 3). Interestingly, the specificity of both QCs

for substrates with uncharged backbone did not change significantly by salt addition. For substrates such as H-Gln-Ala-OH and H-Gln-Glu-OH, however, addition of KCl decreased specificity in case of the human enzyme. As indicated by the kinetic parameters, this effect was due to a higher K_m and a slightly reduced k_{cat} value. The papaya QC did not show altered kinetic parameters upon salt addition. The effect did not seem to be due to the negatively charged substrate as such, since similar kinetic parameters were found for the negatively charged peptide H-Gln-Glu-Asp-Leu-NH$_2$. With the positively charged substrates H-Gln-Arg-Gly-Ile-NH$_2$ and H-Gln-Lys-Arg-Leu-NH$_2$ addition of salt revealed a positive effect on catalysis for both QCs, as indicated by a lower K_m value and a slightly higher turnover number.

Physiological Substrates   Physiological substrates of papaya QC are unknown. For human QC the compounds

tested here can be regarded as putative substrates. In earlier studies, conversion of [Gln[1]]-thyrotropin releasing-hormone ([Gln[1]]-TRH) and [Gln[1]]-gonadotropin releasing-hormone ([Gln[1]]-GnRH) was shown for QC from bovine and porcine pituitary glands (Busby *et al.*, 1987; Fischer and Spiess, 1987). In addition to the previously studied hypophysiotropic hormones, the following three potential physiological substrates of human QC were synthesized and tested: [Gln[1]]-gastrin, [Gln[1]]-neurotensin, and [Gln[1]]-fertilization promoting peptide ([Gln[1]]-FPP) (Table 3). The glutaminyl peptides were converted to the respective pyroglutamyl peptides with increasing specificity in order of their size, *i.e.* the largest peptide [Gln[1]]-gastrin with 17 amino acids followed by [Gln[1]]-neurotensin, [Gln[1]]-GnRH, [Gln[1]]-TRH and [Gln[1]]-FPP.

Surprisingly, also the plant QC converted longer substrates with higher efficacy. Possibly there are secondary binding interactions between the substrate and the enzyme distant from the active site that may influence catalysis.

Peptides Comprising Modified Amino Acids The specificity of the QCs was further analyzed with peptides that contain either a modified N-terminal glutaminyl residue or a modified penultimate amino acid. The conversion of these peptides was investigated qualitatively by MALDI-TOF mass spectrometry. Due to the cyclization of the glutaminyl residue and its analog, respectively, a mass difference of the substrate and the product of catalysis was detected. If ammonia was liberated equimolarly, the conversion was also analyzed quantitatively using the spectrophotometric assay.

(1) H-Gln-Lys(Gln)-Arg-Leu-Ala-NH$_2$ This branched peptide contains two glutaminyl residues bound to a lysyl residue via a peptide- and partial isopeptide bond. Human QC (Figure 5) and papaya QC (not shown) converted this compound apparently in an identical manner. Both glutaminyl residues were cyclized into pyroglutamic acid, and the consistent substrate conversion (Figure 5) indicate the lack of any preference for one residue. Thus, the specificity of the QCs for the differently bound glutaminyl residues seems not to differ fundamentally.

(2) H-Gln(*N*Me)-Phe-Lys-Ala-Glu-NH$_2$ The methylated glutaminyl residue was only converted into a pyroglutamyl residue by papaya QC (not shown). An inhibition of human QC by the peptide was not detected, proving that the methylated residue is not recognized by human QC.

(3) H-Glu(*O*Me)-βNA and H-Glu-βNA Neither of these compounds were converted by papaya or human QC under the applied conditions. The *O*-methylated glutamic acid residue, however, showed a remarkable instability in both Tris and Tricine buffers leading to non-enzymatic cyclization, probably due to an increased polarity of the γ-ester. Furthermore, catalysis of both QC forms was not inhibited by the longer peptides H-Glu(*O*Me)-Phe-Lys-
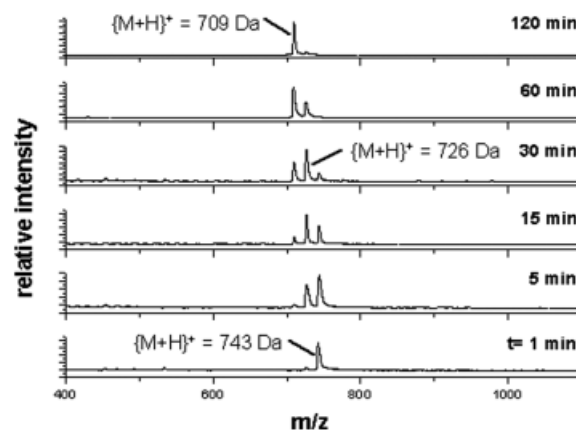
Fig. 5 Formation of pGlu-Lys(pGlu)-Arg-Leu-Ala-NH$_2$ from H-Gln-Lys(Gln)-Arg-Leu-Ala-NH$_2$ through Catalysis by Human QC. Substrate conversion was followed by monitoring by a time-dependent change in the m/z ratio due to the liberation of ammonia. The sample composition was 0.5 mM substrate, 38 nM QC in 40 mM Tris/HCl, pH 7.7. At the times indicated, samples were removed, mixed with matrix solution (1:1 v/v) and the mass spectra recorded. A very similar dependence was observed in case of papaya QC. There was no substrate conversion in samples without QC (not shown).

Arg-Leu-Ala-NH$_2$ or H-Glu-Phe-Lys-Arg-Leu-Ala-NH$_2$ up to 4 mM, demonstrating that glutamic acid or derivatives are not recognized by both QC forms.

(4) H-Gln-cyclo(Nε-Lys-Arg-Pro-Ala-Gly-Phe) The conversion of H-Gln-cyclo(Nε-Lys-Arg-Pro-Ala-Gly-Phe), which contains an intramolecular partial isopeptide bond was analyzed quantitatively, revealing K_m values of 240 ± 14 μM and 133 ± 5 μM for human and papaya QC, respectively. Due to the higher turnover number of conversion by the papaya QC (49.4 ± 0.6 s^{-1}) compared to the human QC (22.8 ± 0.6 s^{-1}), the plant enzyme exhibits with 372 ± 9 mM^{-1}s^{-1} an approximately 4-fold higher k_{cat}/K_m value than the human QC. Thus, the specificity constant is only slightly lower compared to substrates of similar size for papaya QC. The k_{cat}/K_m value for human QC was 95 ± 3 mM^{-1}s^{-1}, being about one order of magnitude lower than with substrates of similar size (Table 1). Possibly, the N-terminal glutaminyl residue is less accessible by the enzyme active site due to steric hindrance of the bulky ring and this may have a stronger effect on catalysis by human QC than in case of the plant enzyme.

(5) H-βhomoGln-Phe-Lys-Arg-Leu-Ala-NH$_2$ The N-terminal βhomoglutaminyl residue was converted into a five-membered lactam ring by catalysis of the human and the papaya QC. The concomitant liberation of ammonia was analyzed spectrophotometrically and by MALDI-TOF mass spectrometry as described before. There was no liberation of ammonia detected when QC was omitted or boiled, proving enzymatic catalysis of the cyclization. Interestingly, the QCs from *C. papaya* ($K_m = 3.1 \pm 0.3$ mM,

Table 4   Kinetic Parameters for Cyclization of Several Putative Physiological Substrates of Human QC.

Substrate	Human QC			Papaya QC		
	K_m (µM)	k_{cat} (s^{-1})	k_{cat}/K_m (mM^{-1} s^{-1})	K_m (µM)	k_{cat} (s^{-1})	k_{cat}/K_m (mM^{-1} s^{-1})
[Gln^1]-Gastrin	31±1	54.1±0.6	1745±36	33±2	31.6±0.9	958±40
[Gln^1]-Neurotensin	37±1	48.8±0.4	1318±24	23±2	37.7±0.6	1639±116
[Gln^1]-FPP	87±2	69.6±0.3	800±14	151±8	37.7±0.5	250±10
[Gln^1]-TRH	90±4	82.8±1.2	920±27	n.d.	n.d.	n.d.
[Gln^1]-GnRH	53±3	69.2±1.1	1305±53	54±3	72.4±1.0	1337±65

Reactions were carried out as described in Table 1 (n.d., not determined; TRH, thyrotropin releasing-hormone; FPP, fertilization promoting peptide; GnRH, gonadotropin releasing-hormone).

$k_{cat} = 4.0 ± 0.4$ s^{-1}) and human ($K_m = 2.5 ± 0.2$ mM, $k_{cat} = 3.5 ± 0.1$ s^{-1}) catalyze the conversion of this peptide with almost identical k_{cat}/K_m values of $1.4 ± 0.1$ and $1.3 ± 0.1$ mM^{-1}s^{-1}, respectively. Thus, the cyclization of the βhomoglutaminyl residue is catalyzed with an approximately 1000-fold reduced efficiency compared to peptides of similar size with N-terminal glutaminyl residue. This result suggests that the constitution of the α-carbon of the substrate is important for substrate recognition by both QC forms, but not essential. Possibly, the essential requirement for being a substrate is a γ-amide group and an unprotonated N-terminal amino group in a distance and angle suitable for cyclization, a requirement that is fulfilled by both, N-terminal glutaminyl and βhomoglutaminyl residues.

Discussion

Based on the elucidation of the primary structures of the enzyme from papaya latex, bovine and human pituitary, several different properties were detected for QCs of plant and animal origin (Pohl *et al.*, 1991; Song *et al.*, 1994; Dahl *et al.*, 2000). The sequence comparison revealed that the proteins have not much in common except the catalysis of pyroglutamyl formation. These findings prompted us to compare the substrate specificities of a plant and human QC in detail, in order to identify differences of the catalysis. Papaya QC, representing the first plant enzyme characterized, and human QC, representative for the highly homologous mammalian QCs, were chosen for this comparison. Papaya QC was purified from crude papain and the human enzyme was recombinantly expressed in *P. pastoris*. The recombinant QC was shown to have very similar characteristics and an identical specific activity compared to the highly homologous QC purified from bovine pituitary, suggesting that the recombinant enzyme resembles the native QC very closely (Schilling *et al.*, 2002a).

Due to difficulties in detecting pyroglutamyl formation directly, coupled enzymatic assays have been developed. Detection of ammonia liberated in a coupled assay with glutamate dehydrogenase is most suitable, since ammonia is formed by conversion of nearly all QC substrates (Bateman, 1989). Originally, the assay was developed as a time-consuming discontinuous method. An increase in the amount of the auxiliary enzyme, however, allowed a continuous data monitoring, suitable to determine the kinetic parameters for various substrates. With the continuous assay, the kinetic parameters for conversion of about 40 glutaminyl peptides by plant and human QC were determined. Both glutaminyl cyclases share obvious similarities in their catalytic properties (Table 1); they exhibited the highest turnover numbers with substrates containing an aromatic amino acid residue in the penultimate position, and similar specificities were observed for peptides that consist of more than two amino acids. Furthermore, both QC forms revealed substrate inhibition only for the fluorogenic substrates, and showed an overall similar dependence on the ionic strength. Finally, the pH dependence of the specificity constant k_{cat}/K_m reveals a dependence of the overall catalysis on an unprotonated substrate amino group, and both QC forms catalyze the cyclization of L-βhomoglutaminyl residues with identical competence. Obviously, the QCs from plants and animals catalyze the cyclization of the glutaminyl residue with very similar efficiency and probably by an identical overall mechanism, *i.e.* non-covalent catalysis, by facilitating the intramolecular cyclization of the glutaminyl residue. This was already suggested for papaya QC (Gololobov *et al.*, 1994). Initial data for the animal QC pointed to a nucleophilic influence by free thiol group(s), and subsequent formation of an acyl-enzyme during catalysis was suggested (Busby *et al.*, 1987). More recently, however, human QC was shown to carry no free thiol groups, and the inhibition by iodoacetamide previously observed could be explained by a side reaction (Bateman *et al.*, 2001; Schilling *et al.*, 2002a). Non-covalent catalysis by the human QC is also corroborated by the fact that this protein is assumed to possess a fold very similar to bacterial Zn-dependent aminopeptidases and that QC might be evolved from an ancestral aminopeptidase (Bateman *et al.*, 2001). Interestingly, also the related aminopeptidase from *Aeromonas proteolytica* (AAP), like human QC, showed a remarkably improved substrate specificity towards longer peptide substrates

possibly due to interactions between the P_1'- and P_2'-amino acid residue in the substrate and the enzyme (Wilkes *et al.*, 1973). Therefore, it is tempting to suggest that animal QCs evolved from a Zn-dependent aminopeptidase keeping the secondary substrate interaction sites, but underwent structural rearrangements of the active-site geometry accompanied by a switch in the catalytic mechanism.

In contrast to human QC, papaya QC did not show such a distinct secondary specificity (Table 2). This holds true for a relaxed selectivity pattern concerning substrate length and composition, as well as the different k_{cat}/K_m-ratio for the partially cyclized substrate H-Gln-cyclo(Nε-Lys-Arg-Pro-Ala-Gly-Phe). Moreover, substrates containing proline in the second position and the ester substrate H-Gln-OtBu are well accepted by plant QC but only weakly by human QC. A further striking difference is the inability of human QC to convert the methylated glutaminyl residue of H-Gln(*N*Me)-Phe-Lys-Ala-Glu-NH$_2$ into a pyroglutamyl residue. This property seems to be attributable to N-terminal substrate binding, since this peptide did not inhibit human QC. Furthermore, neither cyclization of, nor inhibition by, the peptide H-Glu(NH-NH$_2$)-Ser-Pro-Thr-Ala-NH$_2$ was detected for papaya QC. Human QC, however, was inhibited competitively by the N-terminal hydrazide peptide. The presented data suggest that both QCs differ in substrate binding. Obviously, there is more flexibility for substrate side-chain recognition by both enzymes. Interestingly, this is in great contrast to the strict requirement of an unprotonated substrate amino group for catalysis of both enzymes (Figure 3).

The conversion of the potential physiological substrates of human QC [Gln[1]]-gastrin, [Gln[1]]-neurotensin and [Gln[1]]-FPP, shown here for the first time, reflects the relatively broad substrate specificity of human QC. Possibly, the QC is physiologically active in the pGlu formation of most if not all N-terminally Gln-containing hormones. This implies that QC may occur in more tissues than detected to date (Pohl *et al.*, 1991; Sykes *et al.*, 1999). The QC could play a key role in the formation of the bioactive structure of pGlu-containing hormones.

Conclusion

The substrate specificity of human and papaya glutaminyl cyclase, enzymes that catalyze the same reaction but are not related in sequence, was analyzed in a comparative manner. Both enzymes reveal some analogy in their catalytic behavior, *i.e.*, they show

(i)   a dependence of catalysis on an unprotonated N-terminal substrate amino group,
(ii) a similar specificity towards oligopeptide substrates and
(iii) similar requirements for the distance between α-amino- and γ-amide group of the N-terminal glutaminyl residue.

Differences, however, are evident in

(iv) the conversion of short peptide substrates and dipeptide surrogates,
(v)   the dependence of size and amino acid composition of the substrate and
(vi) the recognition mode of the modified γ-amide group of the N-terminal glutamine of the substrate.

To our knowledge, this is first detailed analysis of substrate specificity of an animal QC and the first direct comparison of a plant and an animal QC. The continuous assay introduced allows the testing of a number of glutaminyl peptides revealing similarities in the overall potency for catalysis of glutamine cyclization, but also differences in the specificity of the QCs. Obviously, the differences are mainly based on dissimilar secondary binding sites for the substrates and a different recognition pattern of the N-terminal glutamine residue.

Materials and Methods

Materials

Papaya QC was purified from crude papain as described previously (Schilling *et al.*, 2002b). Human QC was expressed in *P. pastoris* and purified from the fermentation broth as described (Schilling *et al.*, 2002a). The QC substrates H-Gln-Gln-OH, H-Gln-Glu-OH, H-Gln-Gly-OH, H-Gln-βNA, H-Gln-AMC and H-Gln-Ala-OH were purchased from Bachem (Bubendorf, Switzerland) or Senn Chemicals (Dielsdorf, Switzerland). Pyroglutamate aminopeptidase from *Bacillus amyloliquefaciens* was supplied by Qiagen (Hilden, Germany). Glutamate dehydrogenase from bovine liver was purchased from Fluka (Seelze, Germany). NADH/H$^+$ and α-ketoglutaric acid were obtained from Sigma (St. Louis, USA). All other chemicals were of analytical or HPLC grade.

Peptide Synthesis

Oligopeptides   Peptides were synthesized semiautomatically at a 0.5 mmol scale using a peptide synthesizer (Labortec SP650, Bachem) as previously described (Schilling *et al.*, 2002a). Longer peptides were synthesized at a 25 µmol scale using the automated Symphony peptide synthesizer (Rainin Instrument Co., Emeryville, USA) as described (Manhart *et al.*, 2003). For all peptide couplings, modified Fmoc-protocols of solid-phase peptide synthesis were employed using 2-(1H-Benzotriazole-1-yl)-1,1,3,3,-tetramethyluronium tetrafluoroborate (TBTU; Novabiochem, Schwalbach, Germany)/base (diisopropyl ethylamine or N-methyl-morpholine; Merck, Darmstadt, Germany) or in case of difficult couplings *N*-[(dimethylamino)-1*H*-1,2,3,-triazolo[4,5-b]pyridin-1-ylmethylene]-*N*-methyl-methanammonium hexafluorophosphate *N*-oxide (4,5) (HATU; Applied Biosystems, Foster City, USA)/diisopropyl ethylamine as activating reagents were used. After cleavage from the resin by a trifluoroacetic acid (TFA; Merck) containing cocktail, the crude peptides were purified by preparative HPLC with acid free solvents in order to avoid further cyclization of the N-terminal glutamine. Preparative HPLC was performed with a linear gradient of acetonitrile in water (5 – 40% or 65% acetonitrile over 40 min) on a 250 – 21 Luna RP18 column (Phenomenex, Torrance, USA). To confirm peptide purity and identity analytical HPLC and ESI-MS was applied.

H-Glu(NH-NH$_2$)-Ser-Pro-Thr-Ala-NH$_2$ The linear precursor peptide (Fmoc-Glu-Ser-Pro-Thr-Ala-NH$_2$) was synthesized according to a standard Fmoc-procedure (Schilling *et al.*, 2002a) on Rink amide MBHA resin (Novabiochem). After cleavage of the Fmoc-protected peptide from the resin, the peptide was precipitated with diethyl ether, filtered and dried. HMBA-AM resin (1.16 mmol/g, Novabiochem) was used for coupling of the γ-carboxylic acid group of glutamic acid of the precursor peptide (3 eq.) in dichloromethane (DCM, Merck). Dicyclohexylcarbodiimide (DCC, Serva, Heidelberg, Germany) (4 eq.) and dimethylaminopyridine (DMAP, Aldrich, St. Louis, USA) (0.1 eq.) were used as coupling reagents. After 12 hours the resin was filtered, washed with DCM and the reaction was repeated. After deprotection of the N-terminal Fmoc-group by employing 20% piperidine in dimethylformamide (DMF) (3×5 min) the peptide resin was treated with a 5% hydrazine solution (20 ml/g) for 1.5 hours. The resin was filtered and washed with DMF and TFA. Following evaporation, the crude peptide was precipitated with ether giving 76% yield.

H-Gln-Lys(Gln)-Arg-Leu-Ala-NH$_2$ The linear peptide was synthesized according to standard Fmoc-procedure on Rink amide MBHA resin (Schilling *et al.*, 2002a) using Fmoc-Lys(Fmoc)-OH as penultimate amino acid coupling. After deprotection of the two amino protecting groups of lysine with 20% piperidine (Merck) in DMF, 4 eq. Fmoc-Gln(Trt)-OH were coupled. Standard cleavage procedure resulted in 95% yield.

H-Gln(*N*Me)-Phe-Lys-Ala-Glu-NH$_2$ Fmoc-Gln(NMe)-OH was synthesized starting from Fmoc-Glu-OtBu loaded on Fmoc-MI-AM (Novabiochem) resin. After swelling with DCM, the resin (0.5 g) was washed with DMF and deprotected with 20% piperidine solution in DMF. The resin was given into 5 ml DMF and 5 eq. Fmoc-Glu-OtBu, 5 eq. HATU and 10 eq. diisopropyl ethylamine were added subsequently and shaken for 6 hours. After filtration and washing, the product was cleaved according to standard TFA cleavage conditions. The peptide H-Gln(NMe)-Phe-Lys-Ala-Glu-NH$_2$ was synthesized as described (Schilling *et al.*, 2002a). Fmoc-Gln(NMe)-OH was coupled with HATU/diisopropyl ethylamine overnight. The standard cleavage procedure resulted in a yield of 78% of the crude peptide.

H-Glu(*OMe*)-β-naphthylamide, H-Gln-Val-OH, H-Gln-Tyr-OH Boc-protected dipeptides were synthezised applying standard mixed anhydride procedure by using isobutyl chlorocarbonate (Merck). The C-terminal methylesters Boc-Gln-Tyr-OMe and Boc-Gln-Val-OMe were saponified by 1 N NaOH in dioxane. The Boc-protected peptides were deprotected by HCl/dioxane solution for 10 min. After evaporation the residue was crystallized with several solvents giving 60–70% of a solid compound.

H-Gln-cyclo(Nε-Lys-Arg-Pro-Ala-Gly-Phe)   The linear precursor Boc-Gln(Trt)-Lys-Arg(Pmc)-Ala-Gly-Phe-OH was synthesized on acid sensitive 2-chlorotrityl resin. Coupling was carried out using a standard protocol of Fmoc-strategy using Fmoc-Lys(Mtt)-OH. After cleavage with 3% TFA solution in DCM (10 times 5 min), the solution was neutralized with 10% pyridine in methanol (MeOH; Merck), washed 3 times with DCM and MeOH, evaporated to 5% of the volume and the crude peptide was precipitated with ice-cold water. Following, the crude peptide was cyclized using DCC/*N*-hydroxybenzotriazole (HOBt; Aldrich) activation. The crude peptide was dissolved in dry dichloromethane (0.2 mmol/50 ml), 0.2 mmol N-methylmorpholine and 0.4 mmol 1-hydroxybenzotriazole were added. This solution was added dropwise to a solution of 0.4 mmol dicyclohexylcarbodiimide in 250 ml dichloromethane at 0°C. The reaction was completed by stirring overnight at room temperature. After filtration of *N,N´*-dicyclohexylurea, the solvent was removed by evaporation. The residue was dissolved in ethyl acetate and washed several times with 1 N HCl, saturated solution of NaHCO$_3$ and water. The solution was dried over anhydrous Na$_2$SO$_4$, filtered and evaporated to dryness in vacuum. The crude product was purified by RP-HPLC yielding 12% of the cyclic peptide.

Fluorometric Assays of QC

Human QC activity was evaluated using H-Gln-βNA at 30°C, essentially as described (Schilling *et al.*, 2002b). Briefly, the samples consisted of 0.2 mM fluorogenic substrate, 0.1 U pyroglutamyl aminopeptidase in 0.05 M Tris/HCl, pH 8.0 containing 5 mM EDTA and an appropriately diluted aliquot of QC in a final volume of 250 μl. In case of papaya QC, the Tris buffer was substituted by 0.05 M Tricine/NaOH, pH 8.0. Excitation/emission wavelength was 320/405 nm. The assay reactions were initiated by addition of QC. Enzymatic activity was determined from the amount of released βNA calculated using a standard curve of βNA under assay conditions. One Unit is defined as the amount of QC catalysing the formation of 1 μmol pGlu-βNA from H-Gln-βNA per minute under the described conditions. Reaction conditions were the same in case of H-Gln-AMC, except that the excitation/emission wavelength was adjusted to 380/460 nm. The measurements were performed with a Novostar (BMG Labtechnologies, Offenburg, Germany) or a SpectraFluor Plus reader for microplates (Tecan, Maennedorf, Switzerland).

Spectrophotometric Assay of QC

QC activity was analyzed spectrophotometrically using a continuous assay that was established by adapting a discontinuous method (Bateman, 1989) using glutamate dehydrogenase as auxiliary enzyme. Samples consisted of the respective QC substrate, 0.3 mM NADH, 14 mM α-ketoglutaric acid and 30 U/ml glutamate dehydrogenase in a final volume of 250 μl. Reactions were started by addition of QC and pursued by monitoring of the decrease in absorbance at 340 nm for 8–15 min. The initial velocities were evaluated and the enzymatic activity was determined from a standard curve of ammonia obtained previously under assay conditions. All samples were measured at 30°C, using either the SpectraFluor Plus or the Sunrise reader for microplates (both from Tecan). Kinetic data were evaluated using GraFit software (version 5.0.4. for windows, Erithacus Software Ltd., Horley, UK).

pH Dependence

The specificity rate constants (k_{cat}/K_m) at varying pH values were determined under first-order conditions, *i.e.*, at substrate concentrations lower than K_m, using H-Gln-βNA as substrate. The reactions were measured either in a three-component buffer system that provides a constant ionic strength over a wide pH-range consisting of 0.025 M MES, 0.025 M acetic acid and 0.05 M Tris, or in 0.05 mM MOPS (pH 6.2–8.2) buffer at a constant ionic strength of 0.05 M, adjusted by addition of NaCl. The buffers were titrated to the desired pH using HCl or NaOH. All measurements were performed with the Novostar reader (BMG Labtechnologies) for microplates at 23°C.

The pH-dependent rate data were evaluated by nonlinear regression utilising GraFit software. Measured rates were fitted to the following equation:

$$k_{cat}/K_m = k_{cat}/K_m(\text{limit})[1/(1 + 10^{pKI-pH} + 10^{pH-pKII})],$$

in which K_I and K_{II} are the dissociation constants of the catalytically important functional groups and k_{cat}/K_m(limit) is the pH-independent maximum rate constant.

MALDI-TOF Mass Spectrometry

Matrix-assisted laser desorption/ionization mass spectrometry was carried out using the Hewlett-Packard G2025 LD-TOF System (Palo Alto, USA) with a linear time-of-flight analyzer. The instrument was equipped with a 337 nm nitrogen laser, a potential acceleration source (5 kV) and a 1.0 m flight tube. Detector operation was in the positive-ion mode and signals were recorded and filtered using LeCroy 9350M digital storage oscilloscope linked to a personal computer. Samples (5 µl) were mixed with equal volumes of the matrix solution. For matrix solution we used DHAP/DAHC, prepared by solving 30 mg 2′,6′-dihydroxy-acetophenone (Aldrich) and 44 mg diammonium hydrogen citrate (Fluka) in 1 ml acetonitrile/0.1% TFA in water (1/1, v/v). A small volume (≈1 µl) of the matrix-analyte-mixture was transferred to a probe tip and immediately evaporated in a vacuum chamber (Hewlett-Packard G2024A sample prep accessory) to ensure rapid and homogeneous sample crystallization.

The enzymatic reactions were performed in samples of 100 µl consisting of QC (0.01–1 U) and 0.5 mM substrate in 0.04 M Tris/HCl, pH 7.7, at 30 °C. At the times indicated, aliquots were removed, diluted with matrix and analyzed as described.

Acknowledgments

References

Bateman, R. C. J. (1989). A spectrophotometric assay for glutaminyl-peptide cyclizing enzymes. J. Neurosci. Methods *30*, 23–28.

Bateman, R. C., Temple, J. S., Misquitta, S. A., and Booth, R. E. (2001). Evidence for essential histidines in human pituitary glutaminyl cyclase. Biochemistry *40*, 11246–11250.

Busby, W. H. J., Quackenbush, G. E., Humm, J., Youngblood, W. W., and Kizer, J. S. (1987). An enzyme(s) that converts glutaminyl-peptides into pyroglutamyl-peptides. Presence in pituitary, brain, adrenal medulla, and lymphocytes. J. Biol. Chem. *262*, 8532–8536.

Consalvo, A. P., Young, S. D., Jones, B. N., and Tamburini, P. P. (1988). A rapid fluorometric assay for N-terminal glutaminyl cyclase activity using high-performance liquid chromatography. Anal. Biochem. *175*, 131–138.

Dahl, S. W., Slaughter, C., Lauritzen, C., Bateman, R. C. Jr., Connerton, I., and Pedersen, J. (2000). *Carica papaya* glutamine cyclotransferase belongs to a novel plant enzyme subfamily: cloning and characterization of the recombinant enzyme. Protein Expr. Purif. *20*, 27–36.

El Moussaoui, A., Nijs, M., Paul, C., Wintjens, R., Vincentelli, J., Azarkan, M., and Looze, Y. (2001). Revisiting the enzymes stored in the laticifers of *Carica papaya* in the context of their possible participation in the plant defence mechanism. Cell Mol. Life Sci. *58*, 556–570.

Ellis, K. J. and Morrison, J. F. (1982). Buffers of constant ionic strength for studying pH-dependent processes. Methods Enzymol. *87*, 405–426.

Fischer, W. H. and Spiess, J. (1987). Identification of a mammalian glutaminyl cyclase converting glutaminyl into pyroglutamyl peptides. Proc. Natl. Acad. Sci. USA *84*, 3628–3632.

Gololobov, M. Y., Song, I., Wang, W., and Bateman, R. C. J. (1994). Steady-state kinetics of glutamine cyclotransferase. Arch. Biochem. Biophys. *309*, 300–307.

Gololobov, M. Y., Wang, W., and Bateman, R. C. J. (1996). Substrate and inhibitor specificity of glutamine cyclotransferase (QC). Biol. Chem. Hoppe-Seyler *377*, 395–398.

Manhart, S., Hinke, S. A., McIntosh, C. H., Pedersen, J., and Demuth, H.-U. (2003). Structure-function analysis of a series of novel GIP analogues containing different helical length linkers. Biochemistry *42*, 3081–3088.

McClure, W. R. (1969). A kinetic analysis of coupled enzyme assays. Biochemistry *8*, 2782–2786.

Messer, M. (1963). Enzymatic cyclization of L-glutamine and L-glutaminyl peptides. Nature *4874*, 1299

Oberg, K. A., Ruysschaert, J. M., Azarkan, M., Smolders, N., Zerhouni, S., Wintjens, R., Amrani, A., and Looze, Y. (1998). Papaya glutamine cyclase, a plant enzyme highly resistant to proteolysis, adopts an all-β conformation. Eur. J. Biochem. *258*, 214–222.

Pohl, T., Zimmer, M., Mugele, K., and Spiess, J. (1991). Primary structure and functional expression of a glutaminyl cyclase. Proc. Natl. Acad. Sci. USA *88*, 10059–10063.

Schilling, S., Hoffmann, T., Rosche, F., Manhart, S., Wasternack, C., and Demuth, H. U. (2002a). Heterologous expression and characterization of human glutaminyl cyclase: evidence for a disulfide bond with importance for catalytic activity. Biochemistry *41*, 10849–10857.

Schilling, S., Hoffmann, T., Wermann, M., Heiser, U., Wasternack, C., and Demuth, H.-U. (2002b). Continuous spectrometric assays for glutaminyl cyclase activity. Anal. Biochem. *303*, 49–56.

Song, I., Chuang, C. Z., and Bateman, R. C. J. (1994). Molecular cloning, sequence analysis and expression of human pituitary glutaminyl cyclase. J. Mol. Endocrinol. *13*, 77–86.

Sykes, P. A., Watson, S. J., Temple, J. S., and Bateman, R. C. J. (1999). Evidence for tissue-specific forms of glutaminyl cyclase. FEBS Lett. *455*, 159–161.

Tsuru, D., Fujiwara, K., and Kado, K. (1978). Purification and characterization of L-pyrrolidonecarboxylate peptidase from *Bacillus amyloiliquefaciens*. J. Biochem. (Tokyo) *84*, 467–476.

Wilkes, S. H., Bayliss, M. E., and Prescott, J. M. (1973). Specificity of aeromonas aminopeptidase toward oligopeptides and polypeptides. Eur. J. Biochem. *34*, 459–466.

Zerhouni, S., Amrani, A., Nijs, M., Smolders, N., Azarkan, M., Vincentelli, J., and Looze, Y. (1998). Purification and characterization of papaya glutamine cyclotransferase, a plant enzyme highly resistant to chemical, acid and thermal denaturation. Biochim. Biophys. Acta *1387*, 275–290.

Identification of Human Glutaminyl Cyclase as a Metalloenzyme

POTENT INHIBITION BY IMIDAZOLE DERIVATIVES AND HETEROCYCLIC CHELATORS*

Stephan Schilling‡, André J. Niestroj‡, Jens-Ulrich Rahfeld‡, Torsten Hoffmann‡, Michael Wermann‡, Katrin Zunkel‡, Claus Wasternack§, and Hans-Ulrich Demuth‡¶

From the ‡Probiodrug Aktiengesellschaft, Weinbergweg 22, and the §Leibniz Institute for Plant Biochemistry, Post Office Box 110432, 06120 Halle/Saale, Germany

Human glutaminyl cyclase (QC) was identified as a metalloenzyme as suggested by the time-dependent inhibition by the heterocyclic chelators 1,10-phenanthroline and dipicolinic acid. The effect of EDTA on QC catalysis was negligible. Inactivated enzyme could be fully restored by the addition of Zn^{2+} in the presence of equimolar concentrations of EDTA. Little reactivation was observed with Co^{2+} and Mn^{2+}. Other metal ions such as K^+, Ca^{2+}, and Ni^{2+} were inactive under the same conditions. Additionally, imidazole and imidazole derivatives were identified as competitive inhibitors of QC. An initial structure activity-based inhibitor screening of imidazole-derived compounds revealed potent inhibition of QC by imidazole N-1 derivatives. Subsequent data base screening led to the identification of two highly potent inhibitors, 3-[3-(1*H*-imidazol-1-yl)propyl]-2-thioxoimidazolidin-4-one and 1,4-bis-(imidazol-1-yl)-methyl-2,5-dimethylbenzene, which exhibited respective K_i values of 818 ± 1 and 295 ± 5 nM. The binding properties of the imidazole derivatives were further analyzed by the pH dependence of QC inhibition. The kinetically obtained pK_a values of 6.94 ± 0.02, 6.93 ± 0.03, and 5.60 ± 0.05 for imidazole, methylimidazole, and benzimidazole, respectively, match the values obtained by titrimetric pK_a determination, indicating the requirement for an unprotonated nitrogen for binding to QC. Similarly, the pH dependence of the kinetic parameter K_m for the QC-catalyzed conversion of H-Gln-7-amino-4-methylcoumarin also implies that only N-terminally unprotonated substrate molecules are bound to the active site of the enzyme, whereas turnover is not affected. The results reveal human QC as a metal-dependent transferase, suggesting that the active site-bound metal is a potential site for interaction with novel, highly potent competitive inhibitors.

Glutaminyl cyclases (QC)[1] (EC 2.3.2.5) are acyltransferases present in animals and plants that catalyze the conversion of N-terminal glutaminyl residues into pyroglutamic acid with the concomitant liberation of ammonia (Scheme 1). Several peptide hormones and proteins carry N-terminal pyroglutamyl residues. Previously, the formation of N-terminal pyrogluta-mate from glutamine was assumed to proceed spontaneously (1). However, the QCs were identified more recently as catalysts of the reaction in both mammals and plants (2–5). Generally, QCs from both mammalian and plant sources appear to be very similar monomeric proteins that are expressed in the secretory pathways and have similar molecular masses, ~33 and ~40 kDa, respectively (6, 7). Their primary structures, however, reveal no sequence homology, and the enzymes feature completely different folding patterns. Whereas plant QC consists almost solely of β-sheet structure, mammalian QCs are predicted to possess an α/β-fold (8–10). Furthermore, plant QC does not share sequence or structural homology to other plant enzymes, belonging, apparently, to a separate enzyme subfamily (4). Mammalian QCs, however, exhibit remarkable homology toward bacterial aminopeptidases, suggesting their evolutionary origin in this protein family (9).

Investigating the substrate specificity of both enzymes, we recently found differences between papaya and human QC (24). Although the catalysis of cyclization of and the inhibition by modified N-terminal residues were quite different, both enzymes catalyzed the cyclization of oligopeptides with similar specificity rate constants. Moreover, they also catalyzed the formation of a five-membered lactam ring from L-β-homoglutaminyl peptides. Based on the present state of knowledge, it is assumed that plant and animal QCs catalyze the formation of N-terminal pyroglutamic acid (pGlu) residues by enabling the intramolecular cyclization of the glutaminyl residue in a noncovalent manner (11, 12). However, the results of the substrate specificity study revealed differences in substrate recognition by both enzymes.

Thus, a more detailed analysis of the inhibition pattern of plant and human QCs should help to deepen our understanding of QC catalysis. To date, however, systematic inhibitor data exist only for plant QC, which is competitively inhibited by peptides containing an N-terminal proline residue (13), whereas human QC was shown to be inactivated by 1,10-phenanthroline and reduced 6-methylpterin (3). Thus, we investigated the inhibiting potency of heterocyclic compounds from different structural classes. Among them, imidazole and structurally related compounds were found to be the most efficient competitive inhibitors of human QC. The data provide the first insights into enzyme/inhibitor interactions, offer clues for further optimization of the inhibitory structure, and reveal novel aspects of human QC catalysis.
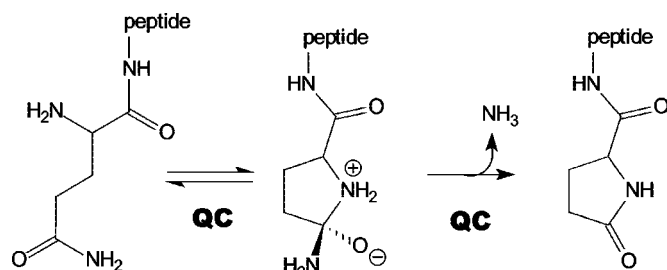
EXPERIMENTAL PROCEDURES

Materials—Human QC was recombinantly expressed in *Pichia pastoris* and purified as described previously (10). Chemicals were purchased as follows. Glutamate dehydrogenase was from Fluka, pyroglutamyl aminopeptidase came from Qiagen, H-Gln-AMC and H-Gln-Gln-OH were from Bachem, NADH/H$^+$ and α-ketoglutaric acid were from Sigma, and the imidazole derivatives were from Acros, Sigma-

---

[1] The abbreviations used are: QC, glutaminyl cyclase; AMC, 7-amino-4-methylcoumarin; Mes, 4-morpholineethanesulfonic acid.

Competitive Inhibition of Metal Enzyme Glutaminyl Cyclase

SCHEME 1. N-terminal cyclization of glutaminyl peptides by QC.

TABLE I
Inhibition constants of imidazole derivatives in the human QC catalyzed reaction
Assays were performed at 30 °C in 0.05 M Tris-HCl, pH 8.

Compound	K_i value
	μM
Core structures	
Imidazole	103 ± 4
Benzimidazole	138 ± 5
N-1 derivatives	
1-Benzylimidazole	7.1 ± 0.3
1-Methylimidazole	30 ± 1
1-Vinylimidazole	49 ± 2
Oxalic acid diimidazolidide	78 ± 2
N-Acetylimidazole	107 ± 3
N-(Trimethylsilyl)-imidazole	167 ± 7
N-Benzoylimidazole	174 ± 7
1-(2-Oxo-2-phenylethyl)-imidazole	184 ± 5
1-(3-Aminopropyl)-imidazole	410 ± 10
1-Phenylimidazole	No inhibition
1,1′-Sulfonyldiimidazole	No inhibition
C-4 (5) derivatives	
N-ω-acetylhistamine	17 ± 1
L-Histidinamide	560 ± 40
H-His-Trp-OH	600 ± 30
L-Histidinol	1530 ± 120
L-Histidine	4400 ± 200
4-Imidazole-carboxaldehyde	7600 ± 700
Imidazol-4-carbonic acid methylester	14500 ± 600
C-4,5 derivatives	
5-Hydroxymethyl-4-methyl-imidazole	129 ± 5
5-Amino-3H-imidazole-4-carboxylic acid amide	15500 ± 500
4,5-Diphenyl-imidazole	No inhibition
4,5-Dicyanoimidazole	No inhibition
C-2 derivatives	
2-Methyl-benzylimidazole	165 ± 4
2-Ethyl-4-methyl-imidazole	580 ± 40
2-Aminobenzimidazole	1800 ± 100
2-Chloro-1H-benzimidazole	No inhibition

FIG. 1. **Lineweaver-Burk plots for human QC catalyzed cyclization of H-Gln-AMC in presence of various concentrations of imidazole between 0.03 and 1 mM.** The *inset* shows a secondary plot of the obtained slopes of the Lineweaver-Burk evaluation *versus* the inhibitor concentrations. The conditions were 0.05 M Tris/HCl, pH 8.0, containing 5 mM EDTA at 30 °C.

Aldrich, Asinex, TimTec, and InterBioScreen. Papaya QC was purified from crude papain as described previously (14). All other chemicals were of analytical or high pressure liquid chromatography grade.

QC Assays—QC activity was assayed essentially as described elsewhere (14). Briefly, the assay reactions (250 μl) consisted of varying concentrations (~0.25–4 K_m) of H-Gln-AMC or H-Gln-Gln-OH in 0.05 M Tris-HCl, pH 8.0. In some cases, assay buffer also contained up to 5 mM EDTA, which has been shown to stabilize the auxiliary enzyme (15). K_i values of QC inhibition were not influenced by EDTA. In the case of the spectrophotometric assay, samples additionally contained 30 units/ml glutamic acid dehydrogenase, 0.25 mM NADH/H⁺, and 15 mM α-ketoglutaric acid. Reactions were started by the addition of QC, and activity was monitored by recording the decrease in absorbance at 340 nm. In contrast, the assay samples for the fluorometric detection of QC activity contained only buffer and 0.4 units/ml pyroglutamyl aminopeptidase as an auxiliary enzyme. The excitation/emission wavelengths were 380/460 nm. Reactions were started by the addition of QC. QC activity was determined from a standard curve of AMC under assay conditions. All determinations were carried out at 30 °C using either the TECAN SpectraFluor Plus or the BMG Novostar reader for microplates.

Inhibitor Assay—For inhibitor testing, the sample composition was the same as described above, except for the addition of the inhibitory compound. For rapid inhibitor screening, samples contained up to 4 mM of the respective imidazole derivative and a substrate concentration equal to the K_m value of the test substrate. For detailed investigations of the inhibition and determination of K_i values, the influence of the inhibitor on the auxiliary enzymes was investigated first. In no case was an influence on one of the auxiliary enzymes detected, enabling the reliable determination of the QC inhibition. The inhibition constants were evaluated by fitting the data of the obtained progress curves according to the general equation for competitive inhibition using

SCHEME 2. The constitution of the imidazole ring (A) and an imidazole N-1 derivative (B).

GraFit software (version 5.0.4. for windows, Erithacus Software Ltd., Horley, UK).

pH Dependence—For the investigation of the pH dependence of QC catalysis and inhibition, the previously developed fluorometric assay was used (14). Determinations were carried out at 30 °C in a buffer originally used by Ellis and Morrison consisting of 0.06 M acetic acid, 0.06 M Mes, and 0.12 M Tris (16). The buffer provides a constant ionic strength over the entire pH range chosen. Additionally, the activity of human QC acting on H-Gln-AMC has shown to be quite independent from variations in ionic strength. The resulting pH dependence data were fitted to single dissociation models for the inhibitors or to equations that account for two dissociating groups in the case of the kinetic parameter K_m using Grafit software. Because of the reduced stability and catalytic activity of the auxiliary enzyme pyroglutamyl aminopeptidase under acidic and basic conditions, the study was limited to the range between 5.5 and 8.5 pH.

Enzyme Inactivation/Reactivation Procedures—An aliquot of human QC (0.1–0.5 mg, 1 mg/ml) was inactivated overnight by dialysis against a 3000-fold excess of 5 mM 1,10-phenanthroline, or 5 mM dipicolinic acid in 0.05 M Bis-Tris/HCl, pH 6.8. Subsequently, the inactivating agent was carefully removed by dialysis (three cycles, 2000-fold excess) of the samples against 0.05 M Bis-Tris/HCl, pH 6.8, containing 1 mM EDTA.

TABLE II
Inhibition of human QC by N1 derivatives selected from compound databases
Determinations were carried out as described in Table I.

Compound	K_i-value	Structure
1-(6-phenoxyhexyl)-1*H*-imidazole	6.2 ±0.03 μM	
4-(2-imidazol-1-yl-ethoxy)-benzoic acid	2.3 ±0.03 μM	
N-(4-chlorophenyl)-*N'*-[2-(1*H*-imidazol-1-yl)ethyl]thiourea	1.2 ±0.03 μM	
3-[3-(1*H*-imidazol-1-yl)propyl]-2-thioxoimidazolidin-4-one	818 ±1 nM	
1,4-bis-(imidazol-1-yl)methyl-2,5-dimethylbenzene	295 ±5 nM	

Reactivation experiments were performed at room temperature for 15 min using Zn^{2+}, Mn^{2+}, Ni^{2+}, Ca^{2+}, K^+, and Co^{2+} ions at concentrations of 1, 0.5, and 0.25 mM in 0.025 M Bis-Tris, pH 6.8, containing 0.5 mM EDTA. QC activity assays were performed in 0.05 M Tris/HCl, pH 8, containing 2 mM EDTA to avoid a rapid reactivation by the traces of metal ions present in buffer solutions.

RESULTS

Inhibition by Imidazole—Because neither glutamic acid dehydrogenase nor pyroglutamyl aminopeptidase were inhibited by imidazole in the concentration range used, both the fluorometric as well as the spectrophotometric assay could be applied. The Lineweaver-Burk plot of the fluorometric assay data (Fig. 1) reveals competitive inhibition by imidazole (*inset* in Fig. 1). Thus, imidazole binds in the active site completely blocking substrate conversion. The K_i values of 103 ± 4 and 129 ± 8 μM obtained with the fluorometric and chromogenic assay, respectively, match very well. Interestingly, benzimidazole inhibits human QC similarly as does imidazole, also exhibiting linear competition and a K_i value of 138 ± 5 μM. Obviously, the condensed ring structure does not influence significantly the binding of the compound under the conditions used. Driven by the similar inhibitory characteristics of imidazole and benzimidazole, derivatives of both compounds were tested to identify secondary interactions that improve or diminish their inhibitory potency.

Imidazole Derivatives—Imidazole and benzimidazole derivatives carrying substituents at different positions of the ring system were tested, and the influence of the substituents was compared (Table I). The constitution refers to the imidazole ring (Scheme 2).
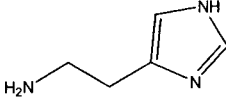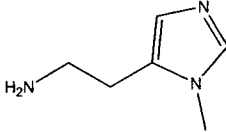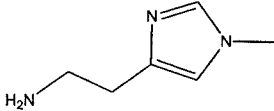
C-4 (5) and C-4,5 Derivatives—The compounds with substitutions either in the constitutionally equivalent 4 or 5 position of the imidazole ring or in both positions showed reduced inhibitory activity toward human QC. In contrast, *N*-ω-acetylated histamine proved to be a potent inhibitory compound. Small substituents in both positions (4 and 5) seemed to have only minor effects on binding, as indicated by the similar inhibition constants of 5-hydroxymethyl-4-methyl-imidazole and imidazole itself. Larger and more bulky groups attached to these sites diminished or abolished binding of the compounds to the enzyme. However, some of the substituents of the tested imidazole derivatives are known to exert negative inductive or mesomeric effects, thereby reducing the electron density within the imidazole ring. This could also contribute to poorer binding. The different K_i values detected for L-histidine and histidinamide also indicate an influence of the charge of the inhibitors on binding. Evidence for electrostatic repulsion of charged substrates was observed previously during an investigation of the substrate specificity of QC, *i.e.* glutaminamide was readily converted to products by human QC, but glutamine was not cyclized (24).

C-2 derivatives—All derivatives tested showed a diminished binding to the active site of QC relative to imidazole. Obviously, there is a strong impact on proper binding by any additional atom in this position. For instance, the simple addition of a methyl group to form 2-methyl-benzylimidazole reduces the

TABLE III
Inhibition of human QC by L-histamine and two derivatives

Assays were carried out as described in Table I. Another designation of the derivatives is *tele*-methylhistamine. They are *in vivo* occuring metabolites of histamine.

Compound	K_i-value (µM)	Structure
L-histamine	850 ± 40	
1-methyl-5-(β-aminoethyl)-imidazole	120 ± 4	
1-methyl-4-(β-aminoethyl)-imidazole	n.i.	

inhibition constant of the interaction by about one order of magnitude. A very similar relation becomes evident comparing the K_i values for benzimidazole and 2-amino-benzimidazole.

N-1 Derivatives—Among the imidazole derivatives tested as inhibitors of human QC, most compounds that had reduced K_i values compared with imidazole contained modifications at the N-1 nitrogen atom (Table I). Interestingly, only minor changes in the N-substituent were necessary for substantial loss of inhibitory power. This can be seen when comparing 1-benzylimidazole, 1-benzoylimidazole, and phenylimidazole as QC inhibitors. The data suggest, however, that steric hindrance for QC binding of N-1 derivatives is marginal, opening up the possibility for the development of even more potent QC inhibitors by structure optimization of N-1 modified imidazole compounds.

Compound Data Base Screening—The apparent improvement of the inhibitory power obtained by N-1 substitutions of the imidazole ring allowed us to identify highly potent inhibitors of QC by data base screening. Some of the most potent inhibitors are shown in Table II. In fact, the observed inhibition constants are one order of magnitude lower as compared with those determined in the initial structure-activity relationship experiments (Table I). This approach led finally to the identification of hit compounds exhibiting K_i values of the QC inhibition in the nM range.

Effect of 1,4 and 1,5 Derivatization—The inhibition constants obtained for the 4(5)-substituted imidazole derivatives already indicated that there are restrictions for efficient binding to the enzyme. An individual contribution of position 4 and 5, however, were undetectable, because both are identical with respect to substitutions at one carbon. The individual effect of substitutions in position 4 and 5 was analyzed by comparing the inhibitory constants of L-histamine and the two intermediates in the biological degradation of histamine, 1-methyl-4-histamine, and 1-methyl-5-histamine (Table III). Interestingly, whereas methylation of one nitrogen of histamine forming 1-methyl-5-histamine improved the inhibitory activity considerably, methylation of the other nitrogen (1-methyl-4-histamine) led to a near total loss of inhibitory potential. Thus, steric hindrance by the carbon atom adjacent to the basic nitrogen seems to occur, which provides further support for the key role of the basic nitrogen in binding of the imidazole derivatives to the enzyme.
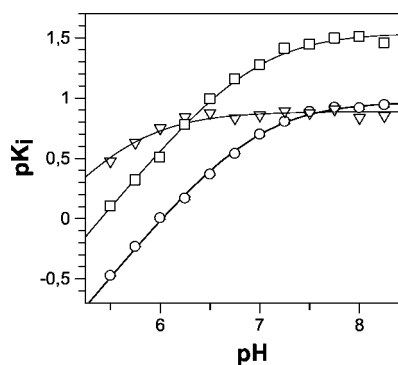

FIG. 2. **The pH-dependence of the inhibition constant of imidazole (*circles*), benzimidazole (*triangles*), and 1-methylimidazole (*squares*) inhibiting human QC catalyzed cyclization of H-Gln-AMC.** Data points were fitted to a single dissociation model and revealed pK_a values of 6.94 ± 0.02, 6.93 ± 0.03 and 5.60 ± 0.05 for imidazole, 1-methylimidazole, and benzimidazole, respectively. Reactions were carried out at 30 °C in 0.06 M acetic acid, 0.06 M Mes, and 0.12 M Tris adjusted to the respective pH by the addition of NaOH or HCl.

pH Dependence—The role of the basic nitrogen of imidazole was further characterized through an investigation of the pH-dependence of QC inhibition. Because of a limited catalytic activity as well as the reduced stability of the auxiliary enzyme pyroglutamyl aminopeptidase, this analysis was limited to a pH range between pH 5.5 and 8.5. Because imidazole has a pK_a value near neutrality, however, this range was assumed to be sufficiently wide for inspecting the influence of protonation and deprotonation of the inhibitor. The inhibition of the QC-catalyzed reaction showed a strict dependence on the pH value (Fig. 2). With decreasing pH, the K_i-value of imidazole increased drastically, exhibiting a 25-fold increase when moving from pH 8 to 5.5. Furthermore, in the basic pH region, K_i was constant, suggesting that the potency of QC inhibition depends on deprotonation of the imidazole derivatives. This was also corroborated by fitting of the data to a single dissociation model (Fig. 2). The dissociating group influencing the inhibitory properties of imidazole was characterized by a pK_a value that is in excellent agreement with the pK_a of the basic nitrogen of imidazole (Table IV). Similar pH dependences were obtained for QC in-

TABLE IV
Comparison of the dissociation constants of inhibitors and a substrate determined by the pH-dependence of inhibitory and Michelis-Menten constants as well as by acid/base titration

Assays were carried out at 30 °C in 0.06 M acetic acid, 0.06 M Mes, and 0.12 M Tris. The turnover number was found to be constant between pH 5.5 and 8.5. $K_{M(I)}$ reflects the dissociation of the substrate. $K_{M(II)}$ reveals a group of the enzyme.

Compound	Parameter	pK_a kinetic determination	pK_a titrimetric determination
Imidazole	K_i	6.94 ± 0.02	6.946 ± 0.003
Benzimidazole	K_i	5.60 ± 0.05	5.500 ± 0.010
1-Methylimidazole	K_i	6.93 ± 0.03	7.000 ± 0.003
H-Gln-AMC	$K_{M(I)}$	6.81 ± 0.04	6.830 ± 0.010
	$K_{M(II)}$	8.60 ± 0.10	—
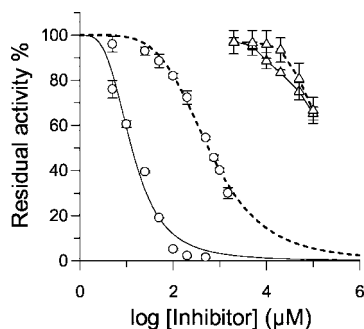
FIG. 3. **Inhibition of human QC by metal-chelating reagents.** Concentration dependence of inhibition by 1,10-phenanthroline (circles) and EDTA (*triangles*) is shown. Residual activity of QC in the presence of either compound was determined directly after the addition (*dotted traces*) or preincubation of QC with the respective reagent for 15 min at 30 °C (*continuous line*).

FIG. 4. **Reactivation of human QC with monovalent and divalent metal ions.** QC was nearly inactivated by the addition of 2 mM dipicolinic acid in 50 mM Bis-Tris, pH 6.8. Subsequently, the enzyme was subjected to dialysis against 50 mM Bis-Tris, pH 6.8, containing 1 mM EDTA. Reactivation of the enzyme was achieved by incubation of the inactivated enzyme sample with metal ions at a concentration of 0.5 mM in the presence of 0.5 mM EDTA to avoid an unspecific reactivation by traces of metal ions present in buffer solutions. Controls are given by enzyme samples that were not inactivated but also dialyzed against the EDTA solution as the inactivated enzyme (*+EDTA*) and by enzyme samples that were dialyzed against buffer solutions without added EDTA (*−EDTA*).

hibition by benzimidazole and 1-methylimidazole (Fig. 2). For both compounds, the kinetically determined pK_a values compare well with the pK_a values determined by titration (Table IV). The dependence of the kinetic parameters K_m and k_{cat} on the pH-value was also analyzed (data not shown). Whereas the turnover number for conversion of H-Gln-AMC was not affected in the pH range between 5.5 and 8.5, the Michaelis constant showed a simple pH dependence with an optimum between pH 7.5–8, tending to increase in the acidic and basic pH region. The pH dependence of K_m revealed a slope of 1 in the acidic pH range, reflecting the presence of a single underlying dissociative group. The kinetically determined pK_a value in the acidic range was nearly identical to the pK_a of the substrate H-Gln-AMC (Table IV). In the basic pH range, data revealed a pK_a value of 8.6 ± 0.1, apparently reflecting a dissociating group of the QC protein.

Inhibition by Heterocyclic Chelators—The inhibition of porcine QC by 1,10-phenanthroline has already been described (3). However, the fact that EDTA has been shown to have an activating effect on QC catalysis suggested that inhibition by phenanthroline is not due to metal chelation (3). Also, in addition to being inhibited by 1,10-phenanthroline, human QC-catalyzed substrate cyclization was abolished in presence of dipicolinic acid, another inhibitor of metalloenzymes. Both chelators inhibited QC in a competitive and time-dependent manner, *i.e.* initial activity that was already competitively inhibited was found to be further reduced after prolonged incubation with the compounds (Fig. 3). Interestingly, EDTA did not show remarkable inhibition regardless of incubation time or under any conditions.

Human QC was almost completely inactivated after extensive dialysis against 5 mM 1,10-phenanthroline or 5 mM dipicolinic acid. After repeated dialysis overnight against chelator-free buffer solutions, QC activity was partially reactivated up to 50–60% (data not shown). However, when dialyzed against buffers containing 1 mM EDTA, no reactivation was observed.

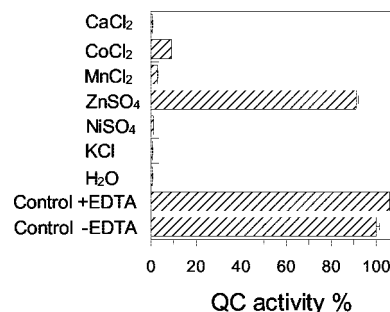Near-total restoration of QC activity after inactivation by either dipicolinic acid or 1,10-phenanthroline was achieved by incubating the protein for 10 min with 0.5 mM ZnSO$_4$ in presence of 0.5 mM EDTA (Fig. 4). Partial restoration of QC activity was similarly obtained using Co^{2+} and Mn^{2+} ions for reactivation. Even in the presence of 0.25 mM Zn^{2+}, a reactivation to 25% of the original activity was possible (data not shown). No reactivation was observed applying Ni^{2+}, Ca^{2+}, or K$^+$ ions. Similarly, incubation of fully active QC with these ions had no effect on the enzyme activity.

DISCUSSION

After a more detailed comparison, human QC does not seem to have much in common with its counterpart from the plant *Carica papaya* except for the catalyzed reaction. In a recent study of substrate specificity, we found a relatively similar proficiency for glutaminyl cyclization by both enzymes (24). However, differences were observed in binding and conversion of peptides bearing the modified N-terminal glutaminyl residues γ-hydrazide or γ-methylamide. Although human QC is inhibited by the hydrazide derivative (not papaya QC), only the methylamide derivative is recognized and cyclized by the plant enzyme. These results have already suggested differences in the recognition modes of the substrate glutaminyl residue by both enzymes. Additionally, we were unable to detect any inhibition of human QC by peptides containing N-terminal proline, which strongly inhibit papaya QC (13). Furthermore, in striking contrast to the prominent inhibition of human QC by imidazole derivatives, papaya QC was not influenced at all by any of these compounds.

Similarly as with metal-dependent aminopeptidases, human QC is inhibited by imidazole, 1,10-phenanthroline, and dipicolinic acid (17–19). In contrast to EDTA, these compounds all show a planar structure, possibly enabling the interaction with

```
hQC       MAGGRHRRVVGTLHLLLLVAALPWASRGVSPSASAWPEEKNYHQPAILNSSALRQIAEGT
SGAP      -----------------------------------------APDIPLANVKAHLTQLS
hGCP II   --------------------------ANEYAYRRGIAEAVGLPSIPVHPIGYYDAQ-K
                                                       *  *           ::  .


hQC       SISEMWQNDLQPLLIERYPGSPGSYAARQHIMQRIQRLQADWVLEIDTFLSQTPYGYRSF
SGAP      TIAAN--NGGN-----RAHGRPGYKASVDYVKAKLD--AAGYTTTLQQFTSGGATGYNLI
hGCP II   LLEKM--GGSAP---PDSSWRGSLKVPYNVGPGFTGNFSTQKVKMHIHSTNEVTRIYNVI
                  :       ..          .  .. :         :  .      .  .  *. :


hQC       SNIISTLNPTAKRHLVLACHYDSKYFSHWNNRVFVGATDSAVPCAMMLELAR---ALDKK
SGAP      ANWPG-GDP--NKVLMAGAHLDS--VSSG-----AGIMDNGSGSAAVLETAL---AVSRA
hGCP II   GTLRGAVEP--DRYVILGGHRDS-----W----VFGGIDPQSGAAVVHEIVRSFGTLKKE
          ..  .  :*  .: :: .  * **         *  *    .* : * .    ::.:


hQC       LLSLKTVSDSKPDLSLQLIFFDGEEAFLHWSPQDSLYGSRHLAAKMASTPHPPGARGTSQ
SGAP      GY--Q------PDKHLRFAWWGAEELGLIGS---KFY----------VNNLPSADR--SK
hGCP II   GW--R------PRRTILFASWDAEEFGLLGS---TEW------------AEENSR-LLQ
            :        *    : :  :..**   *   *    . :              *   :


hQC       LHGMDLLVLLDLIGAPNPTFPNFF--PNSARWFERLQAIEHELH---ELGLLKDHSLEGR
SGAP      LAG---YLNFDMIGSPNPGYFVYDDDPVIEKTFKNYFAGLNVPT---EIETEGDGRSDHA
hGCP II   ERG-VAYINADSSIEGNYTLRVDCT-PLMYSLVHNLTKELKSPDEGFEGKSLYESWTKKS
                *    :  *         *            *       ...   :        *      :    .


hQC       Y---FQNYSY----G-G-----VIQDD-HIPFLRRGVP-VLHLIPSPFPEVWHTMDDNEE
SGAP      P---FKNVGVP--VG-G-----LFTGAGYTKSAAQAQK-WGGTAGQAFDRCYHSSCDSLS
hGCP II   PSPEFSGMPRISKLGSGNDFEVFFQRLGIASGRARYTKNWETNKFSGYP-LYHSVYETYE
              *..          *  *        .:             :            . :   :*:  :. .


hQC       NLDESTID-N-LNKILQVFVLEYLHL----
SGAP      NINDTALDRNSDAAAHAIWTLSSGTGEPPT
hGCP II   -LVEKFYD--PMFKYHLTVAQVRGGMVFEL
          : :.   *                   .
```

FIG. 5. **Sequence alignment of human QC and other M28 family members of the metallopeptidase clan MH.** Multiple sequence alignment was performed using ClustalW at ch.EMBnet.org with default settings. The conservation of the zinc-ion ligating residues is shown for human QC (*hQC*; GenBank[TM] number X71125), the zinc-dependent aminopeptidase from *Streptomyces griseus* (*SGAP*; Swiss-Prot number P80561), and within the *N*-acetylated α-linked acidic dipeptidase (NAALADase I) domain (residues 274–587) of the human glutamate carboxypeptidase II (*hGCP II*; Swiss-Prot number Q04609). The amino acids involved in metal binding are set in *boldfaced type* and *underlined*. In the case of human QC, these residues are the putative counterparts to the peptidases. The shaded histidines (His-140 and His-330) indicate residues that were identified as being essential for QC catalysis (9).

the active site-bound metal ion. Because of the complete reactivation by the addition of Zn^{2+} ions to apo QC, one can conclude that human and probably all mammalian QCs are Zn^{2+}-dependent. Recently, a relationship of the tertiary structure of human QC and the aminopeptidase from *Vibrio proteolyticus*, a prominent member of the clan MH family M28 of metallopeptidases, was proposed (9). Comparing the sequence of human QC with those of two members of the clan MH (Fig. 5), the binding motif His-Asp-Glu-Asp-His of the two Zn^{2+} ions present in this clan of hydrolases is also conserved in human QC. Furthermore, as shown in another study (9), modification of two of the identified histidine residues, His-140 and His-330,

which are probably necessary for metal binding (Fig. 5), leads to a complete loss of catalytic activity. These data further substantiate the fact that mammalian QCs evolved from an ancestral metallo hydrolase and that at least one of the metal binding sites is conserved. It remains unclear, however, how the zinc ion(s) is involved in the catalysis of human QC. In the metallo peptidases, the catalytic mechanism leads to the formation of a non-covalent tetrahedral intermediate after the attack of a zinc-bound water molecule on the carbonyl group of the scissile bond. Either in parallel or subsequently, zinc binding stabilizes the oxanion of the formed tetrahedral intermediate. Zinc ions increase the nucleophilicity of the peptide bond-

attacking water molecule and polarize the scissile bond, making it susceptible to nucleophilic attack during transition state formation, with its progression to and the subsequent collapse of the tetrahedral intermediate followed by amid bond cleavage (20).

For the catalysis by human QC, the pH-dependence of substrate binding suggests that perhaps the metal ion could interact with the nitrogen of the *N*-terminal amino function of the substrate. Because QC catalyzes an intramolecular cyclization, the proper positioning of the substrate nitrogen in close proximity to the γ-carbonyl carbon is probably of essential catalytic importance. On the other hand, it seems likely that a metal ion in the active site of QC acts by polarizing the γ-amide group of the substrate glutaminyl residue, simultaneously stabilizing the oxanion formed by the nucleophilic attack of the α-nitrogen on the scissile γ-carbonyl carbon. Such an interaction of the γ-carbonyl group of the substrate and the active-site metal ion is also corroborated by the observed inhibition of human QC by γ-hydrazide residues. Furthermore, the interaction of one active site zinc ion with the α-amino group of the substrate and the polarization of the carbonyl group of the scissile peptide bond by another are proposed steps in the catalysis of the related aminopeptidase from *V. proteolyticus* (20). Accordingly, the metal ion(s) of QC might serve as a binding site for the imidazole-derived inhibitors and the substrate, with an unprotonated nitrogen interacting in analogy to the related peptidase.

In contrast to the aminopeptidase from *V. proteolyticus*, however, increasing Zn^{2+} concentrations in QC assays (0.1 mM and higher) considerably reduce QC activity, which also was observed in previous studies (3). Thus, it needs to be clarified whether QC also possesses two metal ions bound to the apoenzyme or whether, during evolution from an aminopeptidase to an acyltransferase, the already weak binding second Zn^{2+} ion was lost (20) because a further Zn^{2+} ion was not needed for exerting glutaminyl cyclization. The occupation of such a binding site at high concentrations of Zn^{2+} ions may block the intramolecular reaction of the substrate.

It should be also noted, in this respect, that we could not detect any proteolytic activity of QC. Moreover, 1-butaneboronic acid and peptide thiols (22, 23), potent inhibitors of *V. proteolyticus* aminopeptidase, did not inhibit human QC, supporting potential changes in the active site geometry of QC compared with the aminopeptidases. Because there have been extensive rearrangements during the evolution of the zinc hydrolase group, including remodeling of the active site upon changes in zinc ligation (20, 21), only the solution of the protein structure will finally clarify the binding modes of substrate and inhibitor.

In contrast to its mammalian counterparts, papaya QC is not inhibited by metal chelators, suggesting a metal-independent mechanism. However, for the cyclization reaction, the nitrogen of the α-amino group of the glutaminyl residue also needs to be deprotonated (Scheme 1), and both enzymes show a similar catalytic proficiency of catalysis. How the same catalytic reaction of such structurally divergent protein catalysts is maintained will remain obscure until the solution of the three-dimensional structures of both proteins.

In summary, we present here the first systematic structure-activity study of inhibitors for a mammalian QC. Because there is no reliable active site model for any QC available to date, there was only minimal information to identify the structural features that need to be incorporated into potent QC inhibitors. Besides the identification of N-1 imidazole derivatives as highly potent competitive inhibitors, the results revealed human QC as a metal-dependent enzyme as shown by the following: (*a*) the pH-dependence of inhibition by imidazole and imidazole derivatives; (*b*) the inactivation of QC by the metal-chelating reagents 1,10-phenanthroline and dipicolinic acid; (*c*) the reactivation of the QC-apoenzyme by bivalent metal ions; and (*d*) the conservation of metal-binding residues in the primary structure of QC. Finally, the observed impact of structural modifications of the imidazole derivatives on their QC-inhibitory potency can serve as a starting point for further, rationally driven inhibitor designs.

REFERENCES

1. Richter, K., Kawashima, E., Egger, R., and Kreil, G. (1984) *EMBO J.* **3,** 617–621
2. Messer, M. (1963) *Nature* **197,** 1299
3. Busby, W. H., Jr., Quackenbush, G. E., Humm, J., Youngblood, W. W., and Kizer, J. S. (1987) *J. Biol. Chem.* **262,** 8532–8536
4. Dahl, S. W., Slaughter, C., Lauritzen, C., Bateman, R. C. Jr., Connerton, I., and Pedersen, J. (2000) *Protein Expr. Purif.* **20,** 27–36
5. Fischer, W. H., and Spiess, J. (1987) *Proc. Natl. Acad. Sci. U. S. A.* **84,** 3628–3632
6. Pohl, T., Zimmer, M., Mugele, K., and Spiess, J. (1991) *Proc. Natl. Acad. Sci. U. S. A.* **88,** 10059–10063
7. Zerhouni, S., Amrani, A., Nijs, M., Smolders, N., Azarkan, M., Vincentelli, J., and Looze, Y. (1998) *Biochim. Biophys. Acta* **1387,** 275–290
8. Oberg, K. A., Ruysschaert, J. M., Azarkan, M., Smolders, N., Zerhouni, S., Wintjens, R., Amrani, A., and Looze, Y. (1998) *Eur. J. Biochem.* **258,** 214–222
9. Bateman, R. C., Jr., Temple, J. S., Misquitta, S. A., and Booth, R. E. (2001) *Biochemistry* **40,** 11246–11250
10. Schilling, S., Hoffmann, T., Rosche, F., Manhart, S., Wasternack, C., and Demuth, H.-U. (2002) *Biochemistry* **41,** 10849–10857
11. Gololobov, M. Y., Song, I., Wang, W., and Bateman, R. C., Jr. (1994) *Arch. Biochem. Biophys.* **309,** 300–307
12. Temple, J. S., Song, I., Burns K. H., and Bateman, R. C., Jr. (1998) *Korean J. Biol. Sci.* **2,** 243–248
13. Gololobov, M. Y., Wang, W., and Bateman, R. C., Jr. (1996) *Biol. Chem. Hoppe-Seyler* **377,** 395–398
14. Schilling, S., Hoffmann, T., Wermann, M., Heiser, U., Wasternack, C., and Demuth, H.-U. (2002) *Anal. Biochem.* **303,** 49–56
15. Tsuru, D., Fujiwara, K., and Kado, K. (1978) *J. Biochem. (Tokyo)* **84,** 467–476
16. Ellis, K. J., and Morrison, J. F. (1982) *Methods Enzymol.* **87,** 405–426
17. Czekay, G., and Bauer, K. (1993) *Biochem. J.* **290,** 921–926
18. Kelly, J. A., Slator, G. R., Tipton, K. F., Williams, C. H., and Bauer, K. (2000) *J. Biol. Chem.* **275,** 16746–16751
19. Aoyagi, T., Yoshida, S., Matsuda, N., Ikeda, T., Hamada, M., and Takeuchi, T. (1991) *J. Antibiot. (Tokyo)* **44,** 573–578
20. Lowther, W. T., and Matthews, B. W. (2002) *Chem. Rev.* **102,** 4581–4607
21. Wouters, M. A., and Husain, A. (2001) *J. Mol. Biol.* **314,** 1191–1207
22. Baker, J. O., and Prescott, J. M. (1983) *Biochemistry* **22,** 5322–5331
23. Huntington, K. M., Bienvenue, D. L., Wei, Y., Bennett, B., Holz, R. C., and Pei, D. (1999) *Biochemistry* **38,** 15587–15596
24. Schilling, S., Manhart, S., Hoffmann, T., Ludwig, H.-H., Wasternack, C., and Demuth, H.-U. (2003) *Biol. Chem.* **384,** in press

Continuous Assays of Glutaminyl Cyclase: From Development to Application

Stephan Schilling and Hans-Ulrich Demuth*

Probiodrug AG, Weinbergweg 22, 06120 Halle/Saale, Germany

*To whom correspondence should be addressed at probiodrug AG, Weinbergweg 22, 06120 Halle, Germany

tel.: 49 345 5559900 fax: 49 345 5559901 email: Hans-Ulrich.Demuth@probiodrug.de

Abstract

Glutaminyl cyclase (QC, EC 2.3.2.5) catalyses the formation of pyroglutamyl residues from glutamine at the N-terminus of peptides and proteins. In previously applied assays, QC activity was determined by either analysing the products formed using HPLC coupled with photometric or fluorometric detection, radioimmunoassay, or by detecting the release of ammonia spectrophotometrically. Although these methods are sensitive, they are all discontinuous and therefore time-consuming and laborious. To conduct detailed kinetic investigation of QC-catalysis, we developed coupled continuous assays suitable for microplates which allow now convenient determination of QC activity. The methods either use pyroglutamyl aminopeptidase or glutamate dehydrogenase as auxiliary enzymes, which results in the liberation of chromophores or fluorophores such as pNA, AMC, βNA or in the conversion of the chromophore NADH/H$^+$ into NAD$^+$, respectively.

The assays were applied in various enzyme isolation and characterization studies, using crude protein solutions as well as purified enzyme in pH-dependence, substrate and inhibitor specificity investigations. Depending on the respective analytical task, both assays complement each other. Therefore, different enzymatic properties could be explored in more detail. Since the employed strategy of assay development could be of interest also for the analysis of other enzymes, the methods are described here in a comprehensive manner.

Introduction

Several peptides and proteins contain pyroglutamic acid at their N-terminus. Initially, pyroglutamyl formation was assumed to result from a spontaneous cyclisation reaction of a *N*-terminal glutamine or glutamic acid residue. However, specific enzymatic conversion of glutamine by glutaminyl cyclase (EC 2.3.2.5) has been discovered in plant and animal tissues [1,2,3,4].

Although a QC was first explored in papaya latex, its physiological function in the plant is still enigmatic. More recently, however, QCs were also identified in several other plant species, suggesting a general physiological significance of this protein [5]. In contrast to plant QC, several physiological substrates and products of mammalian QC-activities could be identified. Pyroglutamic acid is present, for instance in the hormones Thyrotropin releasing hormone (TRH), gonadoliberin (GnRH) and gastrin, neurotensin and chemokines of the monocyte chemotactic protein (MCP) family. The formation of this *N*-terminal 5-oxoproline residue has shown to cause the bioactive structure of the hormones and to improve their stability towards N-terminal proteolysis [6,7,8]. Interestingly, plant and animal QCs seem to be very similar at a first glance. Both enzyme forms are expressed via the secretory pathway, carry carbohydrates and are monomeric proteins with similar molecular masses of 33-40 kDa [5,9,10]. Furthermore, all QCs are strictly specific for L-glutamine in the *N*-terminal position of the substrates and their kinetic behaviour was found to obey the Michaelis-Menten equation [10,11,12]. The primary and secondary structures of the QCs from *C. papaya* and that of the highly conserved QC from mammals, however, did not reveal homology [5,13,14]. Due to this apparent divergence, a detailed comparison of the catalytic properties of the QC forms could be helpful for deepening the understanding of pyroglutamyl formation and to identify, whether the different QC forms catalyse the pyroglutamyl formation by the same mechanism.

A detailed enzymatic characterisation of QC catalysis and inhibition, however, was hampered by the lack of handy assays. In previously applied methods, QC activity was determined by either

analysing the products formed using HPLC linked to photometric or fluorimetric detection [11,10] or radioimmunoassay [3,15] using antibodies directed against TRH, or by detecting the release of ammonia spectrophotometrically in a coupled enzymatic assay [16]. Although the methods are sensitive, they are all discontinuous and therefore time-consuming and laborious. Furthermore, some of these methods can be only applied for one certain substrate, thus hampering detailed substrate specificity studies. In another approach, the change in absorbance occurring due to the formation of an intramolecular amid bond during *N*-terminal pyroglutamyl formation by QC is detected [17]. Although this assay allows a continuous data monitoring, the observed changes in absorbance are very small, making the assay insensitive. Furthermore, due to measuring the absorbance change at 220 nm, at the wavelength characteristic for the n→π* electron transition of peptide bonds, enzyme activity in crude samples cannot be determined because of the huge background. Accordingly, also the high initial absorbance of large peptides hinders the determination of catalytic parameters for such QC substrates.

Due to these disadvantages, the development of new assays was triggered that allow a) the convenient and fast determination of QC activity, making it suitable during protein purification and characterization and b) to easily determine the specificity of QCs for an assortment of substrates of different size and structure. This flexibility was obtained by developing coupled continuous assays that utilize different auxiliary enzymes. The inability of detecting the intramolecular amid transferase reaction in buffered systems could be compensated by well-observable coupled reactions, enabling detailed QC-characterisation studies such as substrate and inhibitor specificity, influence of ionic strength and pH-dependence of the kinetic parameters.

Body of text

Coupled enzymatic assays - theoretical considerations. Enzyme catalysed reactions are most often analysed using spectrophotometric or fluorimetric detection, since the detectors, i.e. the photometers or fluorimeters, are relatively inexpensive and present in nearly all life science laboratories. However, many enzyme catalysed reactions cannot be monitored directly, since substrate conversion does not result in a change of the absorbance or fluorescence characteristics, as for instance the case in kinase-, phosphatase- or many transferase-catalysed reactions. Therefore, coupled enzymatic assays were established, using an auxiliary reaction that results in a change in absorbance or fluorescence. In the coupled reaction, one of the products of the reaction that should be analysed is consumed. The simplest case, which is also valid for the assays described below, can be represented schematically

$$A \xrightarrow{k_1} B \xrightarrow{k_2} C$$

primary enzyme   auxiliary enzyme
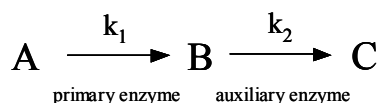
For a reliable assay, the following assumptions have to be fulfilled [18]: a) k_1 represents a zero-order rate constant, i.e. the concentration of A does practically not change during the observed reaction time, b) the second reaction is irreversible, and c) k_2 is a rate constant of first order, which requires that the concentration of B is always much lower than the Michaelis constant of the auxiliary enzyme for B ([B]$<<$ K_B). Based on these assumptions, the rate equation focussed on formation and consumption of B, which is the prerequisite of the observed spectroscopic changes, is

$$\frac{d[B]}{dt} = k_1 - k_2[B] \qquad\qquad (1)$$

which provides after integration

$$[B] = \frac{k_1}{k_2} (1 - e^{-k_2 t}) \qquad (2)$$

As can be seen from this equation, if time runs to infinity (t→∞), a constant concentration of B is reached, the so-called steady state concentration [B_{ss}], characterised by a linear progress of the formation of C. In a practical view, progress curves are usually indistinguishable from linearity, if 95 % of the intermediate steady-state concentration is reached, which is sufficient for providing reliable results. The time to reach this state is characterised by a "lag phase", the progress curve shows an exponential increase. After rearrangement of equation 2, substitution of $-V_{max2} t/K_B$ for $-k_2 t$ and [B_{ss}] for (k_1/k_2), the following equation is obtained, which offers the opportunity to calculate the time until reaching assay conditions that provide progress curves indistinguishable from linearity

$$V_{max2} = \frac{-K_B \ln(1 - [B]/[B_{ss}])}{t^*} \qquad . \qquad (3)$$

In this equation, t* denotes the time to reach a certain fraction of [B_{ss}] (i.e., [B]/[B_{ss}]), which is dependent on the concentration and specificity of the auxiliary enzyme for its substrate, indicated by V_{max2}/K_B. Therefore, with knowledge of the specificity of the respective auxiliary enzyme, one can calculate the amount of protein required to obtain a reliable assay, without consuming excessive protein quantities. As follows, equation 3 was applied for the development of two different continuous assays for determination of QC activity.

Coupling QC to Pyroglutamyl Aminopeptidase (pGAP) catalysis - development. Coupling the cyclising activity of QC to a peptidase was accomplished by use of dipeptide surrogates that are prone to cleavage after conversion by QC. Accordingly, potential assay substrates possessing *N*-

terminal glutamine are Gln-pNA, Gln-βNA or Gln-AMC. After cyclisation by QC, the respective intermediates pGlu-pNA, pGlu-βNA or pGlu-AMC are hydrolysed by pGAP, liberating a chromophoric or fluorogenic group. Since the spectrophores are liberated in equimolar amounts to the glutaminyl-substrate converted, QC-activity can be calculated from standard curves. The reactions are exemplified for the turnover of Gln-βNA in Figure 1.

For assay development, the bacterial pyroglutamyl aminopeptidase from *Bacillus amyloliquefaciens* was chosen. This well-characterised cysteine protease shows a broad substrate specificity, suitable stability and is commercially available. With regard to specificity, the potential intermediates in QC assay have shown to be among the best substrates of this enzyme [19,20,21,22]. The time to reach virtual steady state conditions in the QC assay, if 1 U/ml auxiliary enzyme is applied, were calculated according to equation 3 using the available specificity data of pGAP (table 1). Due to the relatively low specificity of pGAP towards the intermediate pGlu-pNA, the time until observation of linear progress curves is approximately 2 min for the chromophoric substrate Gln-pNA. In contrast, when using Gln-βNA as QC substrate, virtual steady state conditions are observed within one second after initiation of the reaction caused by the high specificity of pGAP for the intermediate pGlu-βNA.

In fact, linear progress curves were observed according to such calculation. They are exemplified for Gln-βNA and Gln-AMC in Figure 2. For all substrates, there was a linear relationship between the QC concentration and the observed rate, indicating the linear dependence of the assay on conversion of the QC substrate (not shown). Finally, the assay could be applied for recombinant human or mouse and purified papaya QC. The now possible characterisation studies enabled the comparison of the QC forms concerning differences and similarities of their catalysis. Due to the shorter lag times observed with the fluorogenic substrates (Table 1), the assays using Gln-AMC or Gln-βNA provide a higher flexibility. Small alterations in the activity of the auxiliary enzyme do not affect the assay, because the auxiliary enzyme activity is still excessive to provide reliable results, i.e. the "lag times" are always shorter than the time required for starting the reaction and

mixing of the samples. Therefore, most of the characterising studies shown below were carried out using the fluorogenic substrates.

Coupling QC to Pyroglutamyl Aminopeptidase (pGAP) catalysis – application. Applications of spectroscopic enzyme assays range from the identification of enzyme activity in tissues, quantification of enzymatic activity during protein purification, protein characterisation in terms of pH-dependence of catalysis, substrate specificity and for inhibitor screening. Recently, we applied the assay during purification of papaya QC [23]. Although the continuous data monitoring already accelerated the enzyme determination during the purification procedure, its application is much more important during characterisation studies, since many assay reactions have to be performed, thus favouring the continuous assays. Moreover, only the analysis of kinetic parameters investigating a wide substrate concentration range makes it possible to detect differences in kinetic mechanisms or models.

Hence, the plots of substrate concentration versus the respective velocities obtained for Gln-AMC and Gln-βNA follow different kinetic laws. Whereas the kinetic data for Gln-AMC readily resembled Michaelis-Menten kinetics in the concentration range limited by substrate solubility, Gln-βNA showed discernible substrate inhibition (Figure 3). Interestingly, papaya QC showed a higher selectivity for Gln-βNA, but was inhibited by the substrate with similar potency. To our knowledge, Gln-βNA is the only QC substrate showing differences to Michaelis-Menten-kinetics, which could be indicative for a similar catalytic action of both enzymes.

Subsequently, the pH-dependence of the catalytic parameters k_{cat} and K_M for conversion of Gln-AMC by human QC was investigated. The pH-range used was restricted to 5.5-8.5, due to the limited stability of QC and the auxiliary enzyme at more basic and acidic pH. Similar experiments were already performed with papaya QC using Gln-tBE as substrate [17], revealing that the catalytic activity depends only on changes of substrate binding. Apparently, the substrate having a protonated amino group was not bound by the active site. The rate constant k_{cat} did not change in

the investigated pH-range. Also human QC-catalysis exhibited only a dependence in terms of substrate binding, reflected by a pH-dependent change of K_M, and a pH-independent k_{cat} (Figure 4). Fitting of the pH-dependent kinetic data of K_M to an equation that accounts for two dissociating groups revealed a pK_a-value that is very close to the pK_a of the substrate amino group and a second pK_a, probably representing a dissociating group of the enzyme. Thus, human and papaya QC bind only *N*-terminally unprotonated substrate molecules in a catalytically productive manner, indicating some general similarity in the catalytic mechanism, in spite of a lack of structural homology. Differences, however, where observed in the binding of inhibitory compounds. Whereas papaya QC was inhibited by peptides bearing N-terminal proline [12], human QC was not. We found, however, competitive inhibition of human QC by peptides bearing *N*-terminal γ-glutamyl-hydrazide residues (Figure 5). Furthermore, human QC was also inhibited by imidazole derivatives which contrasts with plant QC (not shown). These results suggest differences of plant and human QC concerning substrate conversion, apparently due to differences in the substrate and inhibitor recognition modes. Although the described assays have shown to be suitable for many applications, there is one major disadvantage. Only QC substrates can be used, whose conversion yields finally chromophoric or fluorogenic groups. Thus, the substrate spectrum is limited to variations of the chromophores and fluorophores, which hampers a detailed substrate specificity investigation. Therefore, alternative assays were needed, that overcome this drawback without waiving a continuous data monitoring.

Coupling QC to glutamic dehydrogenase (GDH) catalysis – development and application of an alternative assay. This assay is based on quantification of ammonia, that is liberated by cyclisation of glutamine. The auxiliary enzyme in this assay is glutamic dehydrogenase, converting ammonia, α-ketoglutaric acid and NADH/H$^+$ into glutamic acid and NAD$^+$. Since the absorbance characteristics of NADH/H$^+$ changes by oxidation, its conversion can be followed at 340 nm. QC activity can be subsequently quantified by calculation of the liberated ammonia from standard curves of ammonia under assay conditions. The assay reactions are illustrated in Figure 6.

Originally, the assay was developed as a discontinuous method [16], probably due to the relatively low affinity of GDH towards ammonia. In turn, this low reactivity leads to very high auxiliary enzyme concentrations necessary to implement conditions that enable a continuous data monitoring according to equation 3. The usage of common cuvettes for spectrophotometers requiring sample volumes of 1-2 ml, however, causes the consumption of tremendous amounts of GDH, making the assay prohibitive. A calculation of the required auxiliary enzyme amount (equation 3) resulted in 30 U/ml GDH needed to reach a virtual steady state 20 s after initiation of the reaction (assuming a K_M of 3.2 mM of GDH for ammonia [24] and that one Unit of GDH refers to saturating concentrations of all substrates). Due to implementation of microplate readers for assay development, it was possible to reduce the assay volume to 250 µl, thus keeping the required auxiliary enzyme amount low, but still providing convenient volumes for pipetting. Furthermore, the use of the microplates, that were already applied in the fluorometric assays, enable a fast determination of QC activity in many samples at the same time, thus accelerating the determinations enormously. Finally, due to the detection of ammonia that is liberated from the QC-substrates the assay can be implemented for a fast examination of a variety of glutaminyl-peptides.

In fact, linear progress curves were obtained according to the predicted conditions, and most importantly there was a linear relationship between QC-concentration and initial velocity, indicating that the assay provides reliable results (Figure 7). Subsequently, a detailed substrate specificity investigation was performed using about 40 newly synthesised substrates (Schilling et al., submitted), showing that the assay is applicable independently from changes of substrate amino acid composition and peptide size. Moreover, since the auxiliary enzyme was not influenced significantly by potassium chloride concentrations up to 0.5 M, the method was also implemented to investigate the influence of ionic strength on conversion of different substrates. Interestingly, the observed changes of the specificity constant k_{cat}/K_M were substrate dependent (Figure 8). Neither papaya QC, nor human QC revealed altered activity by increasing ionic strength towards peptides with uncharged backbone and residues. Both enzymes, however, displayed a significant increase in

activity towards peptides comprising positively charged amino acid residues. Thus, besides the similar pH-dependence of catalysis for both enzymes, also the behaviour of the different QC-forms in environments with differing dielectric constants is similar, which could be also indicative for analogous catalytic mechanisms. Finally, this conclusion was also corroborated by the ability of both, human and papaya QC, to cyclise *N*-terminal β-homoglutaminyl residues with the same catalytic efficiency (not shown).

Conclusions

The application of theoretical deductions [18] facilitated the development of the first coupled enzymatic assays for Glutaminyl cyclase (QC) activity. Due to the use of different enzymatic reactions for coupling to QC catalysis, many characterisation studies could be performed including pH-dependence, inhibitory and substrate specificity. In this regard, the general differences in the coupling strategy, i.e. the consumption of the QC-products, either the pyroglutamyl peptide by pGAP or the liberated ammonia by GDH, led to a compensation of respective disadvantages of both assays. For instance, traces of ammonia in a sample hamper the QC-determination in the GDH-coupled assay, but show no effect in the assays using pGAP, resulting in the preferred usage of the latter enzyme for assays during enzyme purification. When investigating different peptide substrates, however, only the coupling to ammonia production provided satisfying results since a large substrate spectrum that can be investigated. Thus, the use of the different assay coupling strategies enabled the convenient determination of QC activity in different fields of protein characterisation.

Finally, the demonstrated strategy to develop continuous assay techniques could also be used to modify discontinuous assays for other enzymes or to develop new ways for their catalytic characterisation by implementing different coupling strategies.

Acknowledgement

References

[1]   M. Messer, Enzymatic cyclization of L-glutamine and L-glutaminyl peptides, Nature 4874 (1963), 1299.

[2]   M. Messer and M. Ottesen, Isolation and properties of glutamine cyclotransferase of dried papaya latex, Biochim Biophys Acta 92 (1964), 409-411.

[3]   W.H.J. Busby, G.E. Quackenbush, J. Humm, W.W. Youngblood, and J.S. Kizer, An enzyme(s) that converts glutaminyl-peptides into pyroglutamyl-peptides. Presence in pituitary, brain, adrenal medulla, and lymphocytes, J Biol Chem 262 (1987), 8532-8536.

[4]   W.H. Fischer and J. Spiess, Identification of a mammalian glutaminyl cyclase converting glutaminyl into pyroglutamyl peptides, Proc Natl Acad Sci U S A 84 (1987), 3628-3632.

[5]   S.W. Dahl, C. Slaughter, C. Lauritzen, R.C.Jr. Bateman, I. Connerton, and J. Pedersen, Carica papaya glutamine cyclotransferase belongs to a novel plant enzyme subfamily: cloning and characterization of the recombinant enzyme, Protein Expr Purif 20 (2000), 27-36.

[6]   E. Van Coillie, P. Proost, I. Van Aelst, S. Struyf, M. Polfliet, I. De Meester, D.J. Harvey, J. Van Damme, and G. Opdenakker, Functional comparison of two human monocyte chemotactic protein-2 isoforms, role of the amino-terminal pyroglutamic acid and processing by CD26/dipeptidyl peptidase IV, Biochemistry 37 (1998), 12672-12680.

[7]   G.N. Abraham and D.N. Podell, Pyroglutamic acid. Non-metabolic formation, function in proteins and peptides, and characteristics of the enzymes effecting its removal, Mol Cell Biochem 38 Spec No (1981), 181-190.

[8]   S.A. Hinke, J.A. Pospisilik, H.-U. Demuth, S. Manhart, K. Kühn-Wache, T. Hoffmann, E. Nishimura, R.A. Pedersen, and C.H.S. McIntosh, Dipeptidyl peptidase IV (DPIV/CD26) degradation of Glucagon, J Biol Chem 275 (2000), 3827-3834.

[9]   S. Zerhouni, A. Amrani, M. Nijs, N. Smolders, M. Azarkan, J. Vincentelli, and Y. Looze, Purification and characterization of papaya glutamine cyclotransferase, a plant enzyme highly resistant to chemical, acid and thermal denaturation, Biochim Biophys Acta 1387 (1998), 275-290.

[10] T. Pohl, M. Zimmer, K. Mugele, and J. Spiess, Primary structure and functional expression of a glutaminyl cyclase, Proc Natl Acad Sci U S A 88 (1991), 10059-10063.

[11] A.P. Consalvo, S.D. Young, B.N. Jones, and P.P. Tamburini, A rapid fluorometric assay for N-terminal glutaminyl cyclase activity using high-performance liquid chromatography, Anal Biochem 175 (1988), 131-138.

[12] M.Y. Gololobov, W. Wang, and R.C.J. Bateman, Substrate and inhibitor specificity of glutamine cyclotransferase (QC), Biol Chem Hoppe Seyler 377 (1996), 395-398.

[13] K.A. Oberg, J.M. Ruysschaert, M. Azarkan, N. Smolders, S. Zerhouni, R. Wintjens, A. Amrani, and Y. Looze, Papaya glutamine cyclase, a plant enzyme highly resistant to proteolysis, adopts an all-beta conformation, Eur J Biochem 258 (1998), 214-222.

[14] S. Schilling, T. Hoffmann, F. Rosche, S. Manhart, C. Wasternack, and H.U. Demuth, Heterologous expression and characterization of human glutaminyl cyclase: evidence for a disulfide bond with importance for catalytic activity, Biochemistry 41 (2002), 10849-10857.

[15] J.B. Koger, J. Humm, and J.S. Kizer, Assay of glutaminylpeptide cyclase, Methods Enzymol 168 (1989), 358-365.

[16] R.C.J. Bateman, A spectrophotometric assay for glutaminyl-peptide cyclizing enzymes, J Neurosci Methods 30 (1989), 23-28.

[17] M.Y. Gololobov, I. Song, W. Wang, and R.C.J. Bateman, Steady-state kinetics of glutamine cyclotransferase, Arch Biochem Biophys 309 (1994), 300-307.

[18] W.R. McClure, A kinetic analysis of coupled enzyme assays, Biochemistry 8 (1969), 2782-2786.

[19] K. Fujiwara, R. Kobayashi, and D. Tsuru, The substrate specificity of pyrrolidone carboxylyl peptidase from Bacillus amyloliquefaciens, Biochim Biophys Acta 570 (1979), 140-148.

[20] K. Fujiwara and D. Tsuru, New chromogenic and fluorogenic substrates for pyrrolidonyl peptidase, J Biochem (Tokyo) 83 (1978), 1145-1149.

[21] D. Tsuru, K. Fujiwara, and K. Kado, Purification and characterization of L-pyrrolidonecarboxylate peptidase from Bacillus amyloiliquefaciens, J Biochem (Tokyo) 84 (1978), 467-476.

[22] P.M. Cummins and B. O'Connor, Pyroglutamyl peptidase: an overview of the three known enzymatic forms, Biochim Biophys Acta 1429 (1998), 1-17.

[23] S. Schilling, T. Hoffmann, M. Wermann, U. Heiser, C. Wasternack, and H.-U. Demuth, Continuous spectrometric assays for glutaminyl cyclase activity, Anal Biochem 303 (2002), 49-56.

[24] C. Frieden, Glutamic Dehydrogenase, 234 (1959), 2891.

[25] K.J. Ellis and J.F. Morrison, Buffers of constant ionic strength for studying pH-dependent processes, Methods Enzymol. 87 (1982), 405-426.

Tables

Table 1: Times to reach virtual steady state conditions in QC assay by coupling to

pyroglutamyl aminopeptidase (1 U/ml), calculated according to equation 3. The

kinetic data for pGAP were obtained from references [20] and [21][a].

Substrate	K_B (mM)	V_{max2} (μmol mg^{-1} min^{-1})	time to reach 95 % [$B_{,ss}$] in QC assay at 1 U/ml
pGlu-*p*NA	0.69	0.56	2 min
pGlu-AMC	0.33	5.7	6 s
pGlu-βNA	0.13	20.0	< 1 s

<div align="center">**Figure captions**</div>

Figure 1: Representation of the coupled QC-assay using Gln-βNA as substrate. In the initial

reaction, Gln-βNA is converted by QC into pGlu-βNA. Subsequently, the intermediate is

cleaved by the abundant pyroglutamyl aminopeptidase into pyroglutamic acid and the

fluorophore 2-naphthylamine, resulting in an increase in the observed fluorescence.

Figure 2: Progress curves of the conversion of Gln-βNA and Gln-AMC by QC, investigated

by coupling the reaction to pGAP catalysis. According to a calculation (Equation

3), linear progress curves were observed directly after initiation of the reaction

(Gln-βNA and Gln-AMC). Assays were carried out in 0.05 M Tris/HCl, pH 8.0 at

30 °C. The substrate and QC concentrations were 0.25 mM and 0.9 nM,

respectively.

Figure 3: Dependence of the conversion-rate of Gln-βNA from the substrate concentration,

determined for human (α) and papaya QC (B). The resulting graphs were obtained by

fitting the data to the general equation of substrate inhibition. Human QC (K_M= 70

±3 μM, k_{cat}= 21 ±1 s^{-1}, K_i= 1.21 ±0.07 mM) showed a reduced specificity compared

to papaya QC (K_M= 36 ±2 μM, k_{cat}= 49 ±1 s^{-1}, K_i= 1.14 ±0.05 mM), but the

catalysis was inhibited to similar extends by the substrate. Reactions were carried

out in 0.05 M Tris/HCl, pH 8.0 (human QC) or 0.05 M Tricine/NaOH, pH 8.0

(papaya QC) at 30 °C.

---

[a] The unit definition refers to pGlu-*p*NA. One unit of pGAP is defined as 1 μmol substrate converted per min under the described conditions.

Figure 4: The pH-dependence of Gln-AMC conversion by human QC. At varying pH-values, the kinetic parameters K_M and k_{cat} were determined, and the logarithmic values plotted. Whereas the k_{cat}-value (B) was independent from pH, the K_M-values (α) increased in the acidic and basic pH-region. Fitting the data to an equation that accounts for two dissociating groups resulted in pKa-values of 6.81 ±0.04 and 8.6 ±0.1. The former value is in good agreement with the pK_a of the substrate whereas the latter probably reflects a dissociating group of the enzyme. Reactions were carried out in a buffer system providing a constant ionic strength over the entire pH-range, consisting of 0.06 M acetic acid, 0.06 M Mes and 0.12 M Tris [25] at 30 °C.

Figure 5: The array of curves obtained for the conversion of Gln-AMC by human QC in presence of varying concentrations of the inhibitory active peptide H-Glu(NH-NH_2)-Ser-Pro-Thr-Ala-NH_2. Data points were fitted according to the general equation for competitive inhibition. The resulting K_i-value was 0.697 ±0.003 mM. The assay was carried out in 0.05 M Tris/HCl, pH 8.0, containing 5 mM EDTA. The substrate concentrations ranged from 1 mM to 0.125 mM.

Figure 6: Representation of the QC-assay using GDH as auxiliary enzyme and an *N*-terminal Glutaminyl peptide as substrate. In the initial reaction, the respective pyroglutamyl peptide and ammonia are formed. Subsequently, ammonia, α-ketoglutaric acid and NADH/H^+ are converted into glutamic acid and NAD^+ catalysed by GDH. The consumption of NADH/H^+ can be observed at 340 nm.

Figure 7: Linear dependence of the initial rate of conversion on concentration of human QC using GDH as auxiliary enzyme. The inset shows two progress curves, in the sample containing human QC (12 nM), a linear decrease of absorbance was observed. Without added QC, the decrease in absorbance was negligible. Reactions were carried out in 0.05 M Tris/HCl pH 8.0, containing 5 mM EDTA.

Figure 8: The influence of ionic strength on the specificity constant k_{cat}/K_M for conversion of

various substrates by human and papaya QC. For most peptides, there was little effect of changes in ionic strength detected. However, human and papaya QC specificity towards positively charged peptides increased significantly by addition of 0.5 M KCl. Without additional salt added, the ionic strength was 0.029 M, corresponding to a 0.05 M Tris- or Tricine buffer.
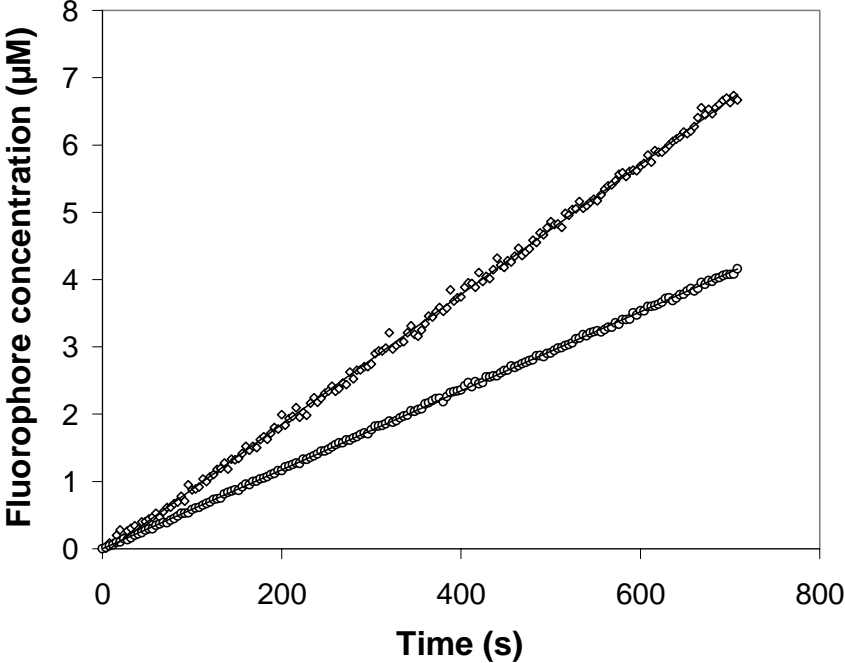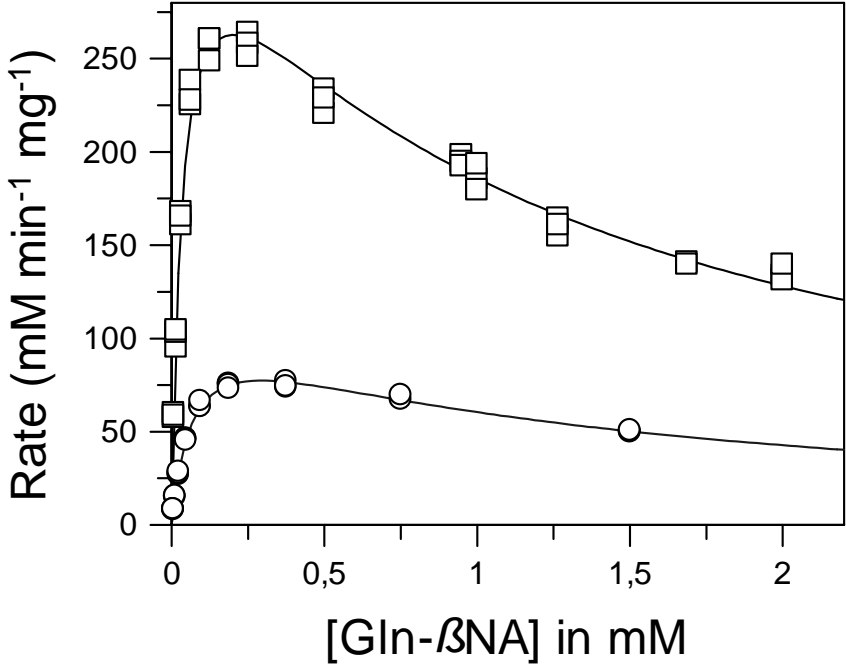
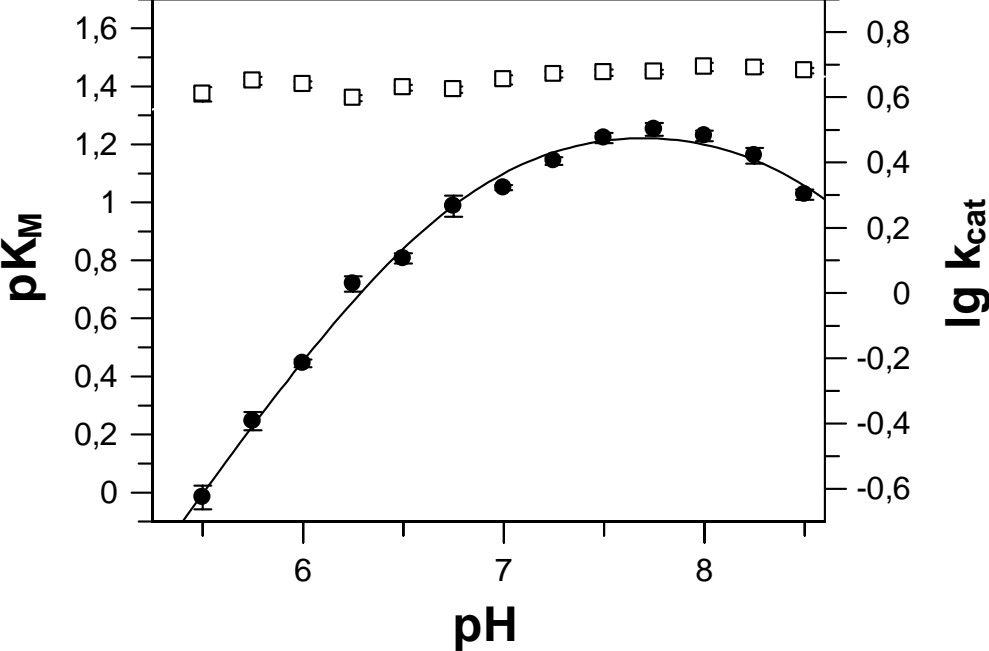Figure 1:
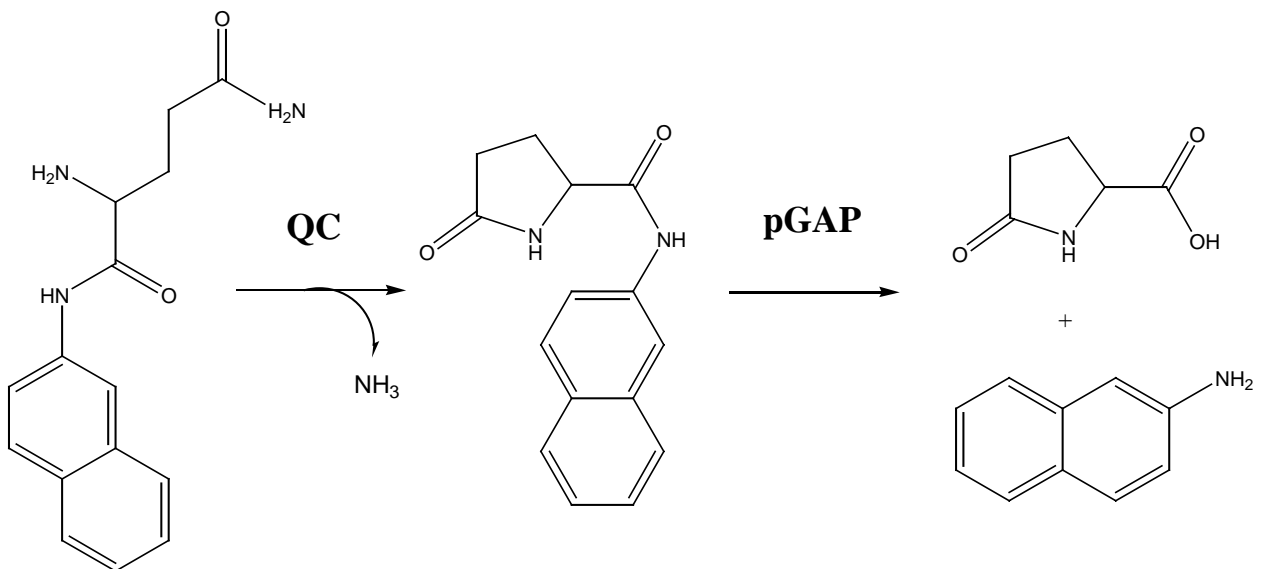
Figure 2:

Figure 3:

Figure 4:

Figure 5:

Figure 6:

NH$_3$ + NADH/H$^+$ + α–ketoglutaric acid $\xrightarrow{\textbf{GDH}}$ NAD$^+$ + glutamic acid
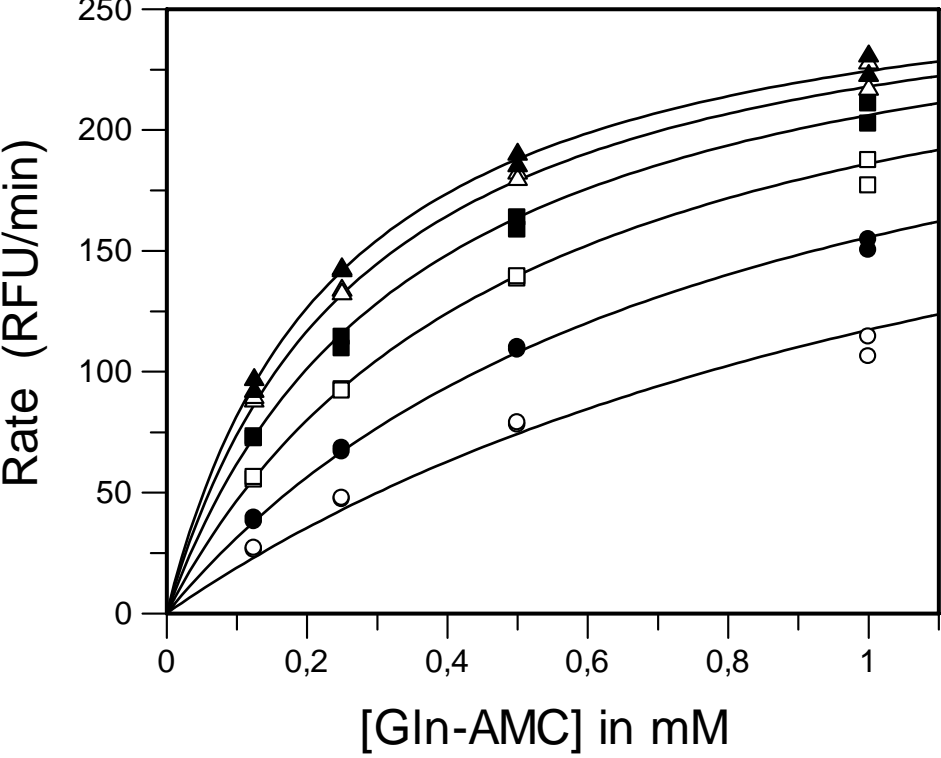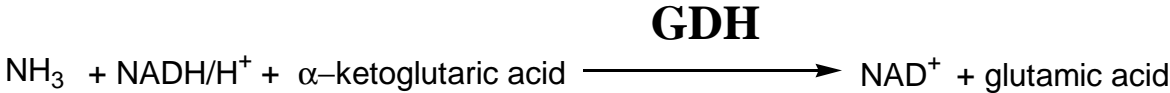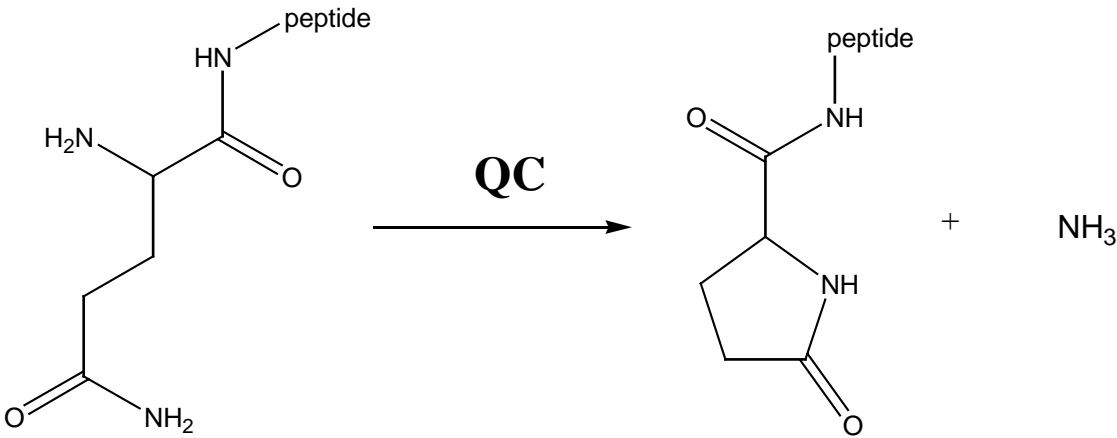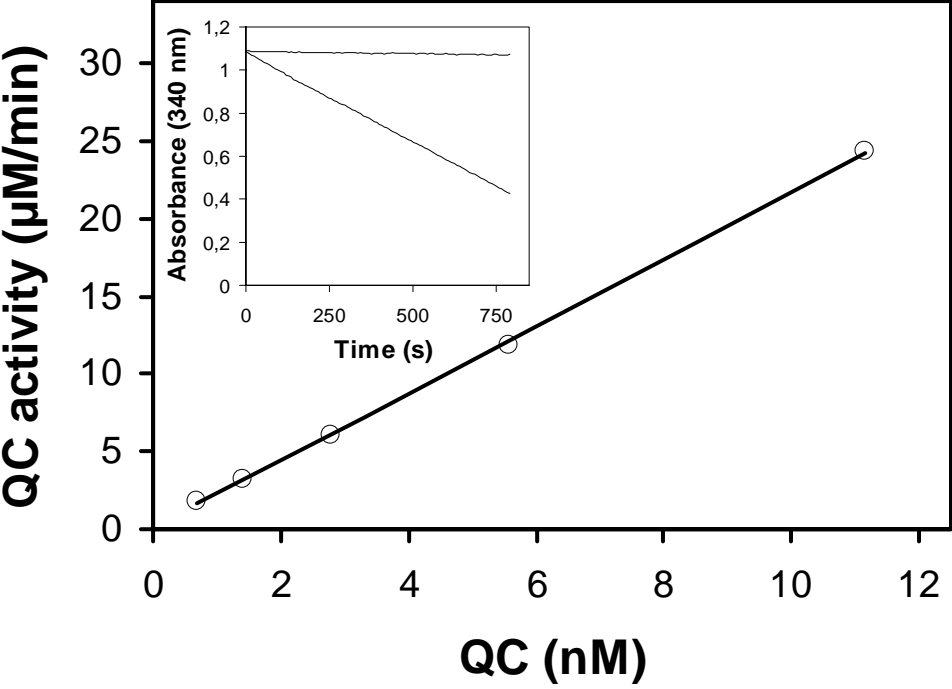
Figure 7:

Figure 8:

Inhibition of glutaminyl cyclase prevents the formation of pGlu[3]-amyloid-β related peptides

Stephan Schilling, Torsten Hoffmann, Susanne Manhart, Matthias Hoffmann, Hans-Ulrich Demuth[*]

Probiodrug AG, Weinbergweg 22, 06120 Halle/Saale, Germany

Running Title: Discovering the glutamate cyclase activity of glutaminyl cyclase

[*]To whom correspondence should be addressed at probiodrug AG, Weinbergweg 22, 06120

Halle, Germany tel.: +49 345 5559900 fax: +49 345 5559901

email: hans-ulrich.demuth@probiodrug.de

Abbreviations: AD, Alzheimer`s disease; APP, amyloid precursor protein; BACE, βNA, 2-naphthylamine; pGlu, pyroglutamic acid; QC, glutaminyl cyclase; EC, glutamyl cyclase; DP IV, dipeptidyl peptidase IV; Aβ(3-11)a, Amyloid β-peptide 3-11 amide, GnRH, Gonadotropin releasing-hormone; TRH, thyrotropin releasing-hormone

Abstract

N-terminal pyroglutamate (pGlu) has been identified as one of the major amyloid-β (Aβ) peptide components of plaques found in the brains of Alzheimer's disease (AD) patients. Several related Aβ peptides contain *N*-terminal glutamate residues at positions 3 and 11. In parallel or subsequent to posttranslational β- and γ-secretase cleavage of the Aβ precursor protein (APP), *N*-terminal processing generates pGlu-Aβ peptides, molecular species are much more resistant to further degradation by aminopeptidases. Such *N*-terminal pGlu-peptide formation can be facilitated by glutaminyl cyclase (QC), a metal-dependent enzyme abundant in the brain and thought to be responsible for the ultimate processing of bioactive neuropeptides such as TRH and neurotensin during their maturation in the secretory pathway. To clarify whether QC can also recognize Aβ-related peptides, the turnover of Gln^3-Aβ(1-11)a, Aβ(3-11)a, Gln^3-Aβ(3-11)a, Aβ(3-21)a, Gln^3-Aβ(3-21)a and Gln^3-Aβ(3-40) by the enzyme was investigated. Unexpectedly, we found that recombinant human QC as well as QC-activity from procine brain extracts catalyze both the *N*-terminal glutaminyl as well as glutamate cyclization. Most striking was the finding that cyclase-catalyzed Glu^1-conversion is favored around pH 6.0 while Gln^1-conversion to pGlu-derivatives occurs with a pH-optimum of around 8.0. Since the formation of pGlu-Aβ-related peptides can be suppressed by inhibition of recombinant human QC and QC-activity from porcine pituitary extracts, the enzyme QC is suggested as a novel target in drug development for AD-treatment.

Introduction

Regulatory peptides such as GnRH, TRH and neurotensin, and the cytokines MCP-1 through 4, require *N*-terminal pyroglutamate in order to exert their respective biological functions (1;2). Early studies have suggested that the formation of pyroglutamate at the *N*-terminus of glutaminyl peptides was a spontaneous reaction (3). Since this intramolecular reaction occurs only very slowly under physiological conditions, glutaminyl cyclase (QC; EC 2.3.2.5) was postulated and subsequently identified to be the catalyst responsible for the transformation of *N*-terminal glutamine residues during posttranslational maturation of peptides in the secretory pathway of mammals and plants (Scheme 1) (4-7).

The first QC was isolated by Messer from the latex of the tropical plant *Carica papaya* in 1963 (4). Later, in 1987, a corresponding enzymatic activity was discovered in animal pituitary. This mammalian QC was shown to convert the Gln^1-precursors of TRH and GnRH into the appropriate mature $pGlu^1$-peptides (5;7). In addition, QC was co-localized to the secretory pathway of the bovine pituitary together with its putative products of catalysis, supporting its processing role in peptide hormone biosynthesis (8).

Coincidently, in several neurodegenerative disorders pyroglutamate-containing peptides are thought to contribute to the pathogenesis by enhancing the proteolytic stability and neurotoxicity of hydrophobic, plaque-forming peptides (9). The most prominent severe dementia, Alzheimer's disease (AD), is characterized by abnormal accumulation of extracellular amyloidotic plaques closely associated with dystrophic neurons, reactive astrocytes and microglia (10-16). Amyloid-β peptides are generated by proteolytic processing of the β-amyloid precursor protein (APP), which is cleaved *N*-terminally by β-secretase (BACE) and *C*-terminally by γ-secretase in a subsequent step (17-19) (scheme 2). It should be mentioned that there is much controversy concerning the ultimate involvement of the γ-

secretase activity of the presenilins in the formation of Aβ(1-40/42) and their utility as targets in AD-therapy (20;21).

Within the widely heterogeneous *N*-terminus of the amyloid peptide found in senile plaques exists a dominant fraction of Aβ-peptides containing an amino terminal aspartate residue such as Asp[1]-Aβ(1-40) and Asp[1]-Aβ(1-42). These full-length Aβ-peptides are found predominantly in the plaque periphery. In contrast, a second dominant fraction of Aβ-peptides, those with an *N*-terminal pyroglutamine, e.g. pGlu[3]-Aβ(3-40/42) and pGlu[11]-Aβ(11-40/42), can be found preferentially in the core of senile plaques. These shortened peptides are reported to be more neurotoxic *in vitro* and to aggregate more rapidly than the full-length isoforms (9;22). *N*-terminally truncated peptides have been shown to be overproduced in early onset familial AD (FAD) subjects (23), to be dominant in diffuse plaques in the brains of patients with Down´s syndrome (DS) and AD (24), and to appear early and increase with age in Down's syndrome brains (25-28). Further, their quantity has been shown to correlate with disease severity (25).

Among all prominent Aβ peptides, the isoforms containing pyroglutamate at position 3, such as pGlu[3]-Aβ(3-40/42), represent the most abundant of the *N*-terminally truncated peptide species (~ 50 % of total Aβ protein), particularly in the core of senile plaques (29-31). The accumulation of pGlu-Aβ peptides is likely due to the structural modification that enhances aggregation and confers resistance to most aminopeptidases (23;32). This evidence provides clues for a pivotal role of pGlu-Aβ peptides in AD pathogenesis. Cyclization, which yields the pyroglutamate form of an amyloidogenic peptide (with an uncharged *N*-terminus), may contribute to the overall hydrophobicity of the structure (9).

There are four potential pathways, which could lead to such neurotoxic pGlu-compounds:

(i)   **spontaneous cyclization** of *N*-terminal glutamate residues following exposure by BACE and/or aminopeptidases

(ii)   **Glu to Gln mutations** and/or posttranslational esterification or amidation of Aβ-glutamates buried within the APP-chain and subsequent **spontaneous cyclization** of the glutamines after *N*-terminal exposure by BACE and/or aminopeptidase processing

(iii)   **enzymatic cyclization** of *N*-terminally uncovered glutamate

(iv)   **Glu to Gln mutations** and/or posttranslational amidation of the Aβ-glutamates buried within the APP-chain **and enzymatic cyclization** after *N*-terminal exposure by BACE and/or aminopeptidase processing.

So far, there is no experimental evidence that is supportive of pathways (i) and (ii). The enzymatic conversion of Glu[1]-peptides into pGlu[1]-peptides by an unknown glutamyl cyclase (EC) corresponding to pathway (iii) was recently proposed (30). However, to date, no such enzyme activity has been identified, capable of cyclizing Glu[1]-peptides which are *N*-terminally protonated and possess a negatively charged Glu[1] γ-carboxylate moiety. Hence, the remaining postulated path to *N*-terminal pGlu formation (iv) may involve glutaminyl cyclase activity as speculated previously (33). However, QC-activity against Gln[1]-substrates is dramatically reduced below pH 7.0 (Schilling et. al., 2003a[1]). Interestingly, Glu[1]-conversion has been reported to occur at acidic reaction conditions (24-30).

In order to prove whether QC is able to recognize and to turnover amyloid-β derived peptides under mild acidic conditions, we synthesized and investigated Gln[3]-Aβ(1-11)a, Aβ(3-11)a, Gln[3]-Aβ(3-11)a, Aβ(3-21)a, Gln[3]-Aβ(3-21)a and Gln[3]-Aβ(3-40) as potential substrates of the

---

[1] Schilling, S., Manhart, T., Hoffmann, T., Ludwig, H.-H., Wasternack, C. and Demuth, H.-U., Substrate Specificity of Glutaminyl Cyclases from Plants and Animals, *Biol. Chem.* (2003) **384**, in press

enzyme. These sequences were designed according to the sequences of naturally occuring *N*-terminally and *C*-terminally truncated Glu^3-Aβ peptides and Gln^3-Aβ peptides which could occur due to posttranslational Glu-amidation.

Another objective of the study was to compare the fate of the amyloid-β derived peptides using either porcine pituitary homogenate as source of native QC, purified recombinant human QC alone, or QC in combination with an aminopeptidase, under the rationale that aminopeptidase cleavage of full length Aβ peptide is a pre-requisite to QC cyclization of Glu/Gln at position three from the N-terminus. Finally, it was of interest whether human QC-activity processing of the above amyloid-β peptides can be suppressed by recently characterized QC-inhibitors (Schilling et al., 2003b[2]).

Experimental Procedures

QC Isolation

Human QC was expressed in *P. pastoris* or *E. coli* and purified as described (34). Papaya QC was purified from papaya latex essentially as described elsewhere (35) with the addition of a third chromatography step on an UNO S (BioRad) column.

Oligopeptide synthesis

Amyloid-β peptide fragments Gln^3-Aβ(1-11)a, Aβ(3-11)a, Gln^3-Aβ(3-11)a, Aβ(3-21)a and Gln^3-Aβ(3-21)a were synthesized as *C*-terminal amides both semi-automatically in a 0.5 mmol scale on a peptide synthesizer (Labortec SP650, Bachem) as previously described (34) or using an automated Symphony peptide synthesizer (Rainin Instrument Co.) in a 50μmol scale. Amyloid-β peptide Gln^3-Aβ(3-40) was synthesized in 25 μmol scale on Fmoc-Val-

[2] Schilling, S., Niestroj, A.J., Rahfeld, J.-U., Hoffmann, T., Wermann, M., Zunkel, K., Wasternack, C. and Demuth, H.-U., Identification of Human Glutaminyl Cyclase as a Metalloenzyme: Potent Inhibition by

NovaSyn®TGA resin (0.15 mmol/g) or on the NovaSyn®TGR resin (0.23mmol/g) using the automated Symphony peptide synthesizer. For all peptide couplings modified Fmoc-protocols of solid-phase peptide synthesis were employed using 2-(1H-Benzotriazole-1-yl)-1,1,3,3,-tetramethyluronium tetrafluoroborate (TBTU; Novabiochem)/*N*-methyl-morpholine; (NMM; Merck) as coupling regents. The coupling reaction was carried out by using 5 eq of Fmoc-amino acid, 5 eq TBTU and 10 eq NMM employing double coupling (twice 30 min and twice 1h from the 21st coupling onwards). Deprotection was carried out by using 20% piperidine in DMF (twice 5 min, then from the 21st coupling step onwards, once 5 min and once 12 min). After cleavage from the resin by a trifluoroacetic acid (TFA; Merck) containing cocktail, the crude peptides were purified by preparative HPLC with acid free solvents in order to avoid further cyclization of the *N*-terminal glutamine. Preparative HPLC was performed with a gradient of acetonitrile in water (20 % to 65 % acetonitrile over 40 min) on a 250-10 Luna RP18, WP300 column (MERCK). To confirm peptide purity and identity analytical HPLC and ESI-MS were performed.

Assays of QC

QC activity was evaluated fluorometrically using Gln-βNA at 30 °C, essentially as described (35). Glu-βNA was employed for observation of glutamate cyclization catalyzed by papaya QC. Spontaneous cyclization of Glu-βNA and Gln-βNA (2 mM) was investigated for 30 days in 20 mM MES-buffer, pH 6.0, 30°C. Samples were removed for determination of pGlu-content, diluted 10-fold and fluorometrically analyzed (35).

For the pH-dependence studies under first-order rate-law conditions (i.e. substrate concentrations far below K_M-values), a buffer was prepared consisting of 0.05 M acetic acid, 0.05 M pyrophosphoric acid and 0.05 M Tricine. The pH-value was adjusted by addition of NaOH. In order to compensate for differences in ionic strength between buffers, constant

conductivity was maintained by addition of NaCl to the different buffers prepared at different pH-values. The spectrophotometric assay of QC was applied as described elsewhere (Schilling et al., 2003a). Enzyme kinetic data was analyzed using Grafit software (version 5.0.4. for windows, Erithacus software Ltd., Horley, UK).

MALDI-TOF mass spectrometry

Matrix-assisted laser desorption/ionization mass spectrometry was carried out using a Hewlett-Packard G2025 LD-TOF System. Enzymatic reactions using the Gln-peptides were performed in samples of 100 μl consisting of QC (0.01- 1 U) and 0.5 mM substrate in 0.04 M Tris/HCl, pH 8.0, at 30 °C or at pH- and buffer conditions described further in the text. At the times indicated, samples were removed, diluted with matrix and analyzed as described previously (34).

For long-term testing of Glu[1]-cyclization, Aβ-derived peptides were incubated in 100μl 0.1 M sodium acetate buffer, pH 5.2 or 0.1 M Bis-Tris buffer, pH 6.5 at 30°C. Peptides were applied in 0.5 mM [Aβ(3-11)a and other synthetic peptides] or 0.15 mM [Aβ(3-21)a] concentrations, and 0.2 U QC was added all 24 hours. In the case of Aβ(3-21)a, the assays contained 1 % DMSO. At the times indicated in the Figures 1-3, samples were removed from the assay tube, peptides were extracted using ZipTips (Millipore) according to the manufacturer`s recommendations, mixed with matrix solution (1:1 v/v) and subjected to mass spectrometry. Negative controls did either contain no QC or heat deactivated enzyme. For the inhibitor studies the sample composition was the same as described above, with exception of the inhibitory compound added (5 mM benzimidazole or 2 mM 1,10-phenanthroline).

Results

Synthesis of Aβ peptides

The synthesis of Aβ(1-40/42) peptides is known to be difficult due to excessive hydrophobicity in the *C*-terminal region which leads to aggregation or secondary structure formation during stepwise solid-phase peptide synthesis. Several attempts have been made to overcome these difficulties for instance by using stronger coupling reagents such as HATU or more efficient base for deprotection like DBU (36;37). To increase coupling yields during synthesis of Gln^3-Aβ(3-40) we used a low pre-loaded resin (Fmoc-Val-NovaSyn$^®$TGA, 0.15 mmol/g). Furthermore, we introduced a pseudoproline unit (Fmoc-Gly-Ser(Ψ^{Me,Me}pro)-OH instead of Gly^{25}-Ser^{26} to disrupt aggregation of the peptide chain (38). The introduction of this pseudoproline unit resulted in a significant improvement in the purity and the yield of the crude amyloid peptide.

Turnover of Gln^3-Aβ peptides 3-11a, 3-21a and 3-40 by recombinant human QC

In previous work we characterized more than 30 Gln^1- and Glu^1-peptides of different chain lengths as potential substrates of glutaminyl cyclase (Schilling et. al., 2003a). While H-Gln-βNA, H-Gln-Phe-Lys-Arg-Leu-NH$_2$ and even H-β-homoGln-Phe-Lys-Arg-Leu-Ala-NH$_2$ were recognized and *N*-terminally cyclized by human QC, compounds such as H-Glu(OMe)-Phe-Lys-Arg-Leu-Ala-NH$_2$, H-Glu-βNA or H-Glu-Phe-Lys-Arg-Leu-Ala-NH$_2$ neither served as substrates nor as inhibitors of the enzyme under the basic pH-conditions applied.

However, Glu(OMe)-Phe-Lys-Arg-Leu-Ala-NH$_2$ demonstrated a tendency towards spontaneous formation of pGlu-Phe-Lys-Arg-Leu-Ala-NH$_2$. Consistent with these findings, Glu(OMe)^3-Aβ(3-11)a was also found to cyclize spontaneously (data not shown).

All Gln^3-Aβ derived peptides tested were efficiently converted by human QC into the corresponding pyroglutamyl forms (Table 1). Due to the poor solubility of Gln^3-Aβ(3-21)a and Gln^3-Aβ(3-40) in aqueous solution, the determinations were carried out in the presence of 1% DMSO. The higher solubility of Gln^3-Aβ(3-11)a, however, enabled kinetic analysis both

in the presence and absence of DMSO (Table 1). Taken together, the investigation of the Aβ peptides as QC-substrates with chain-length of 8, 18 and 37 amino acids (see Table 1) confirmed our previous observation that human QC-activity increases with the length of its substrates. Accordingly, Gln^1-gastrin, Gln^1-neurotensin, Gln^1-GnRH are among the best QC-substrates when taking the specificity constants into account (Schilling et. al., 2003a). Similarly, Gln^3-Aβ(3-40) and glucagon, the largest QC-substrates investigated thus far, exhibited high second order rate constants (449 $mM^{-1}s^{-1}$ and 526 $mM^{-1}s^{-1}$ respectively) even in the presence of 1% DMSO (Table 1).

Interestingly, the kinetic parameters for the conversion of the investigated amyloid peptides did not change dramatically with increasing size, suggesting only moderate effects of the *C*-terminal part of Aβ on QC catalysis. Therefore, due to better solubility and experimental handling, the further investigations concerning *N*-terminal aminopeptidase processing of these peptides were performed using the smaller fragments of Aβ, Gln^3-Aβ(1-11)a, Gln^3-Aβ(3-11)a and Aβ(3-11)a.

Processing of Gln^3-Aβ(1-11)a by purified DP IV and QC present in porcine pituitary homogenate

After β-secretase post-methionine cleavage at position 670 of APP, further *N*-terminal degradation of the resulting Aβ peptide(s) occurs until the decomposition is halted by formation of *N*-terminal pGlu *in vivo* (22-28). Such concerted posttranslational processing mediated by aminopeptidases, dipeptidyl peptidase IV (DP IV) and glutaminyl cyclase has been already proposed for the formation of mature neuropeptides (39). Since full length Aβ(1-42) starts with the dipeptide Asp-Ala (a DP IV-recognition sequence) before the Glu in position 3, we investigated whether purified DP IV or aminopeptidases of porcine pituitary homogenate were able to remove this sequence from our sample peptides.

Incubation of the model peptides Gln^3-Aβ(1-11)a with DP IV and Gln^3-Aβ(3-11)a with porcine pituitary homogenate resulted in the formation of Gln^3-Aβ(3-11)a and $pGlu^3$-Aβ(3-11)a, respectively (see Figure 1A, 1C).

When the reaction was conducted in the presence of the DP IV-inhibitor Val-Pyrr, no further turnover of Gln^3-Aβ(1-11)a was observed (Figure 1B). Similarly, in the presence of the QC-inhibitor 1,10-phenanthroline, no final *N*-terminal pGlu-formation occurred, resulting in build-up of Gln^3-Aβ(3-11) as the final reaction product (Figure 1D).

When Gln^3-Aβ(1-11)a was incubated with porcine pituitary homogenate in the absence of both inhibitors, a slow stepwise removal of both amino acids by brain aminopeptidases and final cyclization to $pGlu^3$-Aβ(3-11)a by porcine pituitary QC and by DP IV-containing pituitary homogenate takes place (Figure 2A).

In the presence of the QC-inhibitor however, only the slow processing by brain aminopeptidases can be observed, yielding the intermediates Gln^3-Aβ(2-11)a and Gln^3-Aβ(3-11)a (Figure 2B). By incubating Gln^3-Aβ(1-11)a with DP IV-containing porcine pituitary homogenate in the presence of the DP IV-inhibitor Val-Pyrr only the formation of Gln^3-Aβ(2-11)a was detectable (Figure 2C).

Turnover of Aβ(3-11)a and Aβ(3-21)a by recombinant human QC

The incubation of Aβ(3-11)a and Aβ(3-21)a in the presence of QC revealed that in contrast to previous work, glutamate-containing peptides can also serve as QC-substrates (Figures 3C and D). The QC-catalyzed formation of $pGlu^3$-Aβ(3-11)a and $pGlu^3$-Aβ(3-21)a was investigated at pH 5.2 and 6.5, respectively. If the QC-inhibitor benzimidazole was added to the solution before starting the assay by the addition of QC, substrate conversion resulting in $pGlu^3$-Aβ(3-11)a or $pGlu^3$-Aβ(3-21)a was suppressed (Figures 3E and F). If QC was boiled before addition, formation of the pGlu-peptides was negligible (Figures 3A and B).

pH-dependency of the papaya QC-catalyzed cyclization of Gln-βNA and Glu-βNA

The plant QC from *C. papaya*, an analogous but non-homologous enzyme of the mammalian QCs, has been shown to possess a very similar substrate specificity pattern to human QC (Schilling et al., 2003a). Accordingly, plant QC cyclized Aβ(3-11)a at pH 5.2 (not shown). In contrast to human QC, however, we also observed the conversion of the short fluorogenic substrate Glu-βNA, which enabled us to apply a continuous coupled fluorometric assay (35). Since a different impact of substrate protonation on QC-catalysis was expected, higher amounts of QC were applied in the model reactions (34;35). Papaya QC converted Glu-βNA in a concentration range up to 2 mM (which was limited by substrate solubility) in accordance with Michaelis-Menten kinetics (Figure 4). Inspection of turnover versus substrate concentration diagrams for the conversion of Glu-βNA between pH 6.1 and 8.5 revealed that both K_M and k_{cat} changed in a pH-dependent manner (Figure 4). This is in contrast to the previously described QC-catalyzed glutamine cyclization, for which only changes in K_M were observed over the given pH range (40).

Subsequently, to study the impact of the proton concentration during Glu- and Gln-cyclization by QC, we investigated the pH-dependence of cyclization of Glu-βNA and Gln-βNA under first-order rate-law conditions (i.e. substrate concentrations far below K_M-values) (Figure 5). As expected the cyclization of glutamine has a pH-optimum at pH 8.0, in contrast to the cyclization of glutamic acid which showed a pH-optimum of pH 6.0. While the specificity constants at the respective pH-optima differ approximately 80,000-fold, the ratio of QC versus EC activity around pH 6.0, is only about 8,000.

The non-enzymatic pGlu-formation from Gln-βNA investigated at pH 6.0, was followed for 4 weeks and revealed a first-order rate constant of $1.2*10^{-7}$ s^{-1}. However, during the same time

period, no pGlu-βNA was formed from Glu-βNA enabling estimation of a limiting rate constant for turnover of $1.0*10^{-9}$ s^{-1}.

Discussion

Since spontaneous formation of pGlu^3-Aβ(3-40) occurs neither *in vitro* nor *in vivo*, only enzymatic cyclization of Glu-Aβ by a putative glutamyl cyclase (EC) or of Gln-Aβ peptides by the known glutaminyl cyclase (QC) is conceivable. Here, we have shown that papaya and human QC catalyze both glutaminyl and glutamyl cyclization (Schemes 1 and 3, Figures 1-5). The subcellular localization of these reactions remains unclear. Neurons can maintain in the cytosol pH values between 5.5 and 7.2 and cytosolic proteins of nerve cell enzymes are optimized for function at acidic pHs (41-43). Hence, under mildly acidic conditions preferred QC-catalyzed EC-reactions as observed in our study can occur in the cytosol.

However, Glu-Aβ peptides have been found to be preferentially generated by β-secretase processing in the endopasmatic reticulum as Aβ(1-40/42) and in the trans-golgi network as Aβ(11-40/42) most likely within secretory vesicles (44;45). Interestingly, QC is also localized in the secretory pathway (4-7) and by coincidence the major pGlu-Aβ peptides pGlu^3-Aβ(3-40/42) and pGlu^{11}-Aβ(11-40/42) have been found in senile plaques of aged and Down syndrome brains (46).

The primary physiological function of QC is likely terminal hormone processing (maturation) in endocrine cells by glutamine cyclization prior to, or during the hormone secretion process. Such secretory vesicles are known to be acidic in pH. Thus, an auxillary/additional function of the enzyme in the narrow pH-range from 5.0 to 7.0 could be its newly discovered glutamyl cyclase activity (Scheme 3) transforming Glu-Aβ peptides. However, due to the relatively inefficient rate of Glu-cyclization compared to Gln-conversion, it is questionable whether the

glutamyl cyclization plays a significant physiological role. In the etiology of neurodegenerative disorders, however, glutamyl cyclization may be of relevance providing that accumulation of peptidase resistant substrate, and appropriate QC-concentration and compartment acidity, coincide.

Investigating the pH-dependency of this enzymatic reaction, we found that the unprotonated *N*-terminus was essential for the cyclization of Gln[1]-peptides and accordingly that the pK_a-value of the substrate was identical to the pK_a-value for QC-catalysis (see Figure 5 and Schilling et. al., 2003a). These results support the view that QC stabilizes the intramolecular nucleophilic attack of the unprotonated α-amino moiety on the γ-carbonyl carbon electrophilically activated by amidation (Scheme 1).

In contrast to the monovalent charge present on *N*-terminal glutamine containing peptides, the *N*-terminal Glu-residue in Glu-containing peptides is predominantly bivalently charged around neutral pH. Glutamate exhibits pK_a-values of about 4.2 and 7.5 for the γ-carboxylic and for the α-amino moiety, respectively. I.e. at neutral pH and above, although the α-amino nitrogen is partially or fully unprotonated and nucleophilic, the γ-carboxylic group is unprotonated, and so exercising no electrophilic carbonyl activity. Hence, intramolecular cyclization is impossible.

However, in the pH-range of about 5.2-6.5, between their respective pK_a-values, the two functional groups are present both partially non-ionized, in concentrations of about 1-10% (-NH_2) or 10-1% (-COOH) of total *N*-terminal Glu-containing peptide. As a result, over a mildly acidic pH-range species of *N*-terminal Glu-peptides are present which carry both groups uncharged, and, therefore, it is possible that QC could stabilize the intermediate of intramolecular cyclization to pGlu-peptide. I.e. if the γ-carboxylic group is protonated, the carbonyl carbon is electrophilic enough to allow nucleophilic attack by the unprotonated α-amino group. At this pH the hydroxyl ion functions as a leaving group (Scheme 3). These assumptions are corroborated by the pH-dependence data obtained for the QC catalyzed

conversion of Glu-βNA. In contrast to glutamine conversion of Gln-βNA by QC, the pH-optimum of catalysis shifts to the acidic range to around pH 6.0, i.e. the pH-range in which substrate molecule species are simultaneously abundant carrying a protonated γ-carboxyl and unprotonated α-amino group. Furthermore, the kinetically determined pK_a-value of 7.55 ±0.02 is in excellent agreement with that of the α-amino group of Glu-βNA, determined by titration (7.57 ±0.05).

Physiologically, at pH 6.0 the second-order rate constant (or specificity constant, k_{cat}/K_M) of the QC-catalyzed glutamate cyclization might be in the range of 8,000fold slower than the one for glutamine cyclization (compare data in Figure 4). However, the non-enzymatic turnover of both model substrates Glu-βNA and Gln-βNA is negligible, which corroborates with the observed negligible pGlu-peptide formation in our study. Hence, for the pGlu-formation by QC an acceleration of at least 10^8 can be estimated from the ratio of the enzymatic versus non-enzymatic rate constants (comparing the second-order rate constants for the enzyme catalysis with the respective nonenzymatic cyclization first-order rate constants the catalytic proficiency factor is about 10^9 and 10^{10} M^{-1} for the Gln- and the Glu-conversion, respectively). The conclusion from these data is, that *in vivo* only an enzymatic path resulting pGlu-formations seems conceivable.

Since QC is highly abundant in the brain and taking into account the high turnover rate of 0.9 min^{-1} recently found for the maturation of 30 μM of (Gln-)TRH-like peptide (47), one can predict a cyclization half-life of about 100 hours for an appropriate glutamate-substrate, providing similar reaction conditions. Moreover, given compartmentalization and localization of brain QC/EC in the secretory pathway, the actual *in vivo* enzyme and substrate concentrations and reaction conditions might be even more favorable for the enzymatic cyclization in the intact cell. In addition, if *N*-terminal Glu is transformed to Gln a much more

rapid pGlu-formation mediated by QC could be expected. *In vitro*, we were able to suppress both reactions by applying inhibitors of QC/EC-activity (Figures 2 and 3).

Whether *N*-terminal processing of the tested Aβ-derived peptides takes place *in vivo* by a combination of aminopeptidase, dipeptidyl peptidase and glutaminyl/glutamyl cyclase activity and whether its selective blockage as achieved in our experiments is of physiological relevance begs further investigation. Previously, such *N*-terminal processing in an analog fashion was suggested for the immature neuropeptide Antho-RFamide precursors of coelenterates (39). Similarly, impaired post-translational proteolytic processing of Aβ peptides by aminopeptidases has been suggested as a causative event in AD (48). An imbalance between anabolic and catabolic processes of the APP-biosynthesis and the Aβ peptide degradation could cause the accumulation of Aβ(1-42) and other Aβ-peptides which are normally further degraded. According to this hypothesis, such an imbalance would occur through a reduced aminopeptidase activity which would not sufficiently process the *N*-terminus of Aβ resulting in a negligible iso-Asp[1]-Aβ(1-42) formation as compared to a significant accumulation of pGlu-Aβ peptides (23-29;46).

Recent reviews on potential AD treatment do not propose inhibition of pyroglutamate formation as potential therapeutic intervention (9;17;18;48). Since pGlu-Aβ peptides appear highly abundant, because they are even more hydrophobic and neurotoxic than the *N*-terminally charged amyloid peptides and since pGlu-Aβ formation prevents intracellular aminopeptidase-mediated disposal of such improperly generated peptides (44;46), inhibition of brain glutaminyl cyclase QC- and EC-activity could prove a valuable tool to combat the onset and progression of neurodegenerative disorders. In addition, a combination of the inhibition of QC/EC and aminopeptidases might be a suitable experimental approach to further investigate the site of the plaque-formation resulting from pGlu-Aβ peptides *in situ* and *in vivo*.

In summary, our results indicate that human QC/EC, which is highly abundant in the brain, is a likely catalyst to the formation of the amyloidogenic pGlu-Aβ peptides (from Glu-Aβ and Gln-Aβ precursors), major constituents of the senile plaques found in AD. In addition to their contribution towards our basic understanding of peptide processing during hormone maturation, these findings identify QC/EC as a potential player in plaque formation and thus as a novel drug target in the treatment of AD.

References

1. Awade, A. C., Cleuziat, P., Gonzales, T., and Robert-Baudouy, J. (1994) *Proteins 20*, 34-51.

2. Garavelli, J. S. (2000) *Nucleic Acids Res 28*, 209-211.

3. Richter, K., Kawashima, E., Egger, R., and Kreil, G. (1984) *EMBO J 3*, 617-621.

4. Messer, M. (1963) *Nature 4874*, 1299.

5. Busby, W. H., Quackenbush, G. E., Humm, J., Youngblood, W. W., and Kizer, J. S. (1987) *J Biol Chem 262*, 8532-8536.

6. Dahl, S. W., Slaughter, C., Lauritzen, C., Bateman, R. C., Connerton, I., and Pedersen, J. (2000) *Protein Express Purif 20*, 27-36.

7. Fischer, W. H. and Spiess, J. (1987) *Proc Natl Acad Sci U S A 84*, 3628-3632.

8. Bockers, T. M., Kreutz, M. R., and Pohl, T. (1995) *J Neuroendocrinol 7*, 445-453.

9. Saido, T. C. (2002) *Med Hypotheses 54*, 427-429.

10. Terry, R. D. and Katzman, R. (1983) *Ann Neurol 14*, 497-506.

11. Glenner, G. G. and Wong, C. W. (1984) *Biochem Biophys Res Commun 120*, 885-890.

12. Itagaki, S., McGeer, P. L., Akiyama, H., Zhu, S., and Selkoe, D. (1989) *J Neuroimmunol 24*, 173-182.

13. Funato, H., Yoshimura, M., Kusui, K., Tamaoka, A., Ishikawa, K., Ohkoshi, N., Namekata, K., Okeda, R., and Ihara, Y. (1998) *Am J Pathol 152*, 1633-1640.

14. Selkoe, D. J. (2001) *Physiol Rev 81*, 741-766.

15. Borchelt, D. R. (1998) *Lab Anim Sci 48*, 604-610.

16. Mann, D. M. and Iwatsubo, T. (1996) *Neurodegeneration 5*, 115-120.

17. Citron, M. (2002) *Nat Neurosci 5* Suppl: 1055-1057.

18. Wolfe, M. S. (2002) *Nat Rev Drug Discov 1*, 859-866.

19. Kimberly, W. T., Esler, W. P., Ye, W., Ostaszewski, B. L., Gao, J., Diehl, T., Selkoe, D. J., and Wolfe, M. S. (2003) *Biochemistry 42*, 137-144.

20. Thinakaran, G. (1999) *J Clin Invest 104*, 1321-1327.

21. Wilson, C. A., Doms, R. W., Zheng, H., and Lee, V. M. (2002) *Nat Neurosci 5*, 849-855.

22. Pike, C. J., Overman, M. J., and Cotman, C. W. (1995) *J Biol Chem 270*, 23895-23898.

23. Saido, T. C., Iwatsubo, T., Mann, D. M., Shimada, H., Ihara, Y., and Kawashima, S. (1995) *Neuron 14*, 457-466.

24. Iwatsubo, T., Saido, T. C., Mann, D. M., Lee, V. M., and Trojanowski, J. Q. (1996) *Am J Pathol 149*, 1823-1830.

25. Russo, C., Saido, T. C., DeBusk, L. M., Tabaton, M., Gambetti, P., and Teller, J. K. (1977) *FEBS Lett 409*, 411-416.

26. Russo, C., Salis, S., Dolcini, V., Venezia, V., Song, X. H., Teller, J. K., and Schettini, G. (2001) *Neurobiol Dis 8*, 173-180.

27. Tekirian, T. L., Saido, T. C., Markesbery, W. R., Russell, M. J., Wekstein, D. R., Patel, E., and Geddes, J. W. (1998) *J Neuropathol Exp Neurol. 57*, 76-94.

28. Russo, C., Violani, E., Salis, S., Venezia, V., Dolcini, V., Damonte, G., Benatti, U., DArrigo, C., Patrone, E., Carlo, P., and Schettini, G. (2002) *J Neurochem 82*, 1480-1489.

29. Hosoda, R., Saido, T. C., Otvos, L., Jr., Arai, T., Mann, D. M., Lee, V. M., Trojanowski, J. Q., and Iwatsubo, T. (1998) *J Neuropathol Exp Neurol 57*, 1089-1095.

30. Garden, R. W., Moroz, T. P., Gleeson, J. M., Floyd, P. D., Li, L. J., Rubakhin, S. S., and Sweedler, J. V. (1999) *J Neurochem 72*, 676-681.

31. Harigaya, Y., Saido, T. C., Eckman, C. B., Prada, C. M., Shoji, M., and Younkin, S. G. (2000) *Biochem Biophys Res Commun 276*, 422-427.

32. Tekirian, T. L., Yang, A. Y., Glabe, C., and Geddes, J. W. (1999) *J Neurochem 73*, 1584-1589.

33. Shirotani, K., Tsubuki, S., Lee, H. J., Maruyama, K., and Saido, T. C. (2002) *Neurosci Lett 327*, 25-28.

34. Schilling, S., Hoffmann, T., Rosche, F., Manhart, S., Wasternack, C., and Demuth, H.-U. (2002) *Biochemistry 41*, 10849-10857.

35. Schilling, S., Hoffmann, T., Wermann, M., Heiser, U., Wasternack, C., and Demuth, H.-U. (2002) *Anal Biochem 303*, 49-56.

36. Tickler, A. K., Barrow, C. J., and Wade, J. D. (2001) *J Pept Sci 7*, 488-494.

37. Fukuda, H., Shimizu, T., Nakajima, M., Mori, H., and Shirasawa, T. (1999) *Bioorg Med Chem Lett 9*, 953-956.

38. Mutter, M., Nefzi, A., Sato, T., Sun, X., Wahl, F., and Wohr, T. (1995) *Pept Res 8*, 145-153.

39. Schmutzler, C., Darmer, D., Diekhoff, D., and Grimmelikhuijzen, C. J. (1992) *J Biol Chem 267*, 22534-22541.

40. Gololobov, M. Y., Song, I., Wang, W., and Bateman, R. C. (1994) *Arch Biochem Biophys 309*, 300-307.

41. Nachshen, D. A. and Drapeau, P. (1988) *J Gen Physiol 91*, 289-303.

42. Drapeau, P. and Nachshen, D. A. (1988) *J Gen Physiol 91*, 305-315.

43. Ruscak, M., Orlicky, J., Zubor, V., and Hager, H. (1982) *J Neurochem 39*, 210-216.

44. Huse, J. T., Liu, K., Pijak, D. S., Carlin, D., Lee, V. M., and Doms, R. W. (2002) *J Biol Chem 277*, 16278-16284.

45. Haass, C., Lemere, C. A., Capell, A., Citron, M., Seubert, P., Schenk, D., Lannfelt, L., and Selkoe, D. J. (1995) *Nat Med 1*, 1291-1296.

46. Atwood, C. S., Martins, R. N., Smith, M. A., and Perry, G. (2002) *Peptides 23*, 1343-1350.

47. Prokai, L., Prokai-Tatrai, K., Ouyang, X., Kim, H. S., Wu, W. M., Zharikova, A., and Bodor, N. (1999) *J Med Chem 42*, 4563-4571.

48. Saido, T. C. (1998) *Neurobiol Aging 19*, 69-75.

Tables

Table 1: Kinetic parameters for conversion of N-terminally Gln-containing peptides by recombinant human QC in buffer solution containing 1% DMSO

Peptide	K_M (μM)	k_{cat} (s^{-1})	k_{cat}/K_M (mM^{-1}s^{-1})
Gln^3-Aβ(3-11)a	87 ±3$^{\#}$	55 ±1$^{\#}$	632 ±10$^{\#}$
Gln^3-Aβ(3-11)a	155 ±4	41.4 ±0.4	267 ±4
Gln^3-Aβ(3-21)a	162 ±12	62 ±3	383 ±10
Gln^3-Aβ(3-40)	89 ±10	40 ±2	449 ±28
Glucagon(3-29)	19 ±1	10.0 ±0.2	526 ±17

$^{\#}$ Determined in absence of DMSO

Schemes

Scheme 1:   *N*-terminal cyclization of glutaminyl peptides by QC
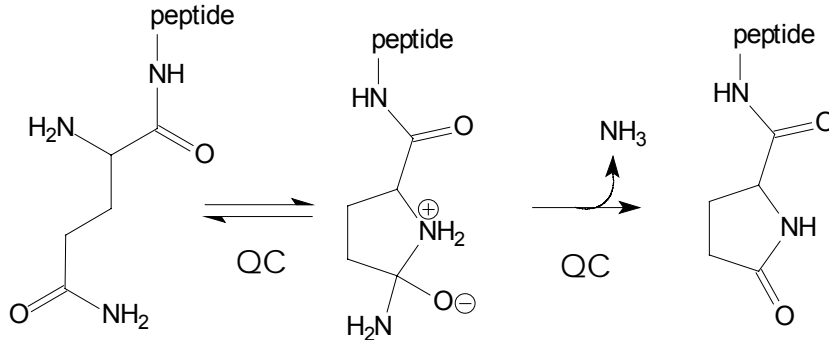
Scheme 2:   Sequence fragment of human amyloid precursor protein (APP 770)

661   Ile Lys Thr Glu Glu Ile Ser Glu Val Lys Met **β** *Asp Ala* **Glu** Phe   675
$$ 1 \quad 2 \quad 3 \quad 4$$

676   Arg His Asp Ser Gly Tyr **Glu** Val His His Gln Lys **α** Leu Val Phe   690
$$ 5 \quad 6 \quad 7 \quad 8 \quad 9 \quad 10 \quad 11 \quad 12 \quad 13 \quad 14 \quad 15 \quad 16 \quad 17 \quad 18 \quad 19$$

691   Phe Ala Glu Asp Val Gly Ser Asn Lys Gly Ala Ile Ile Gly Leu   705
$$ 20 \quad 21 \quad 22 \quad 23 \quad 24 \quad 25 \quad 26 \quad 27 \quad 28 \quad 29 \quad 30 \quad 31 \quad 32 \quad 33 \quad 34$$

706   Met Val Gly Gly Val Val Ile Ala **γ** Thr Val Ile Val Ile Thr Leu   720
$$ 35 \quad 36 \quad 37 \quad 38 \quad 39 \quad 40 \quad 41 \quad 42$$

- Full length Aβ peptide sequence 1-42 corresponding to amino acids 672-713 of APP in black.
- α-, β-, γ-secretase cleavage sites marked bold and underscored
- Glu^3 and Glu^{11} of the Aβ peptide marked bold and underscored.
- *N*-terminal aminopeptidase processing site Asp-Ala are in italics.

Scheme 3:   *N*-terminal cyclization of uncharged glutamyl peptides by QC (EC)
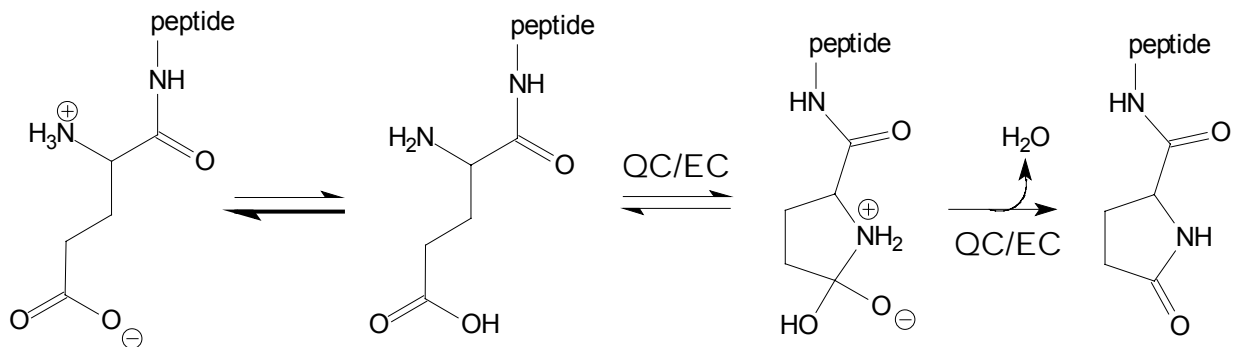
<h1 style="text-align:center"><u>Figure Legends</u></h1>

Figure 1: **A** Mass spectra of Gln³-Aβ(1-11)a incubated with DP IV catalyzing the *N*-terminal truncation yielding Gln³-Aβ(3-11)a. **B** Mass spectra of Gln³-Aβ(1-11)a incubated with DP IV and the DP IV-inhibitor Val-Pyrrolidide (Val-Pyrr) preventing *N*-terminal truncation of the peptide. **C** Mass spectra of Gln³-Aβ(3-11)a incubated with porcine pituitary homogenate catalyzing the formation of pGlu³-Aβ(3-11)a. **D** Mass spectra of Gln³-Aβ(3-11)a incubated with QC and the QC-inhibitor 1,10-phenanthroline preventing the formation of pGlu³-Aβ(3-11)a.

Figure 2: **A** Mass spectra of Gln³-Aβ(1-11)a incubated with DP IV-containing porcine pituitary homogenate resulting in the formation of pGlu³-Aβ(3-11)a after consecutive catalysis by both enzymes. **B** Mass spectra of Gln³-Aβ(1-11)a in the presence of DP IV-containing porcine pituitary homogenate and the QC-inhibitor 1,10-phenanthroline preventing pGlu³-Aβ(3-11)a formation. **C** Mass spectra of Gln³-Aβ(1-11)a in the presence of DP IV-containing porcine pituitary homogenate and the DP IV-inhibitor Val-Pyr suppressing the formation of pGlu³-Aβ(3-11)a.

Figure 3: **A** and **B** Mass spectra of Glu³-Aβ(3-11)a and Glu³-Aβ(3-21)a incubated with recombinant human QC which was boiled for 10 min before use. **C** and **D** Mass spectra of Glu³-Aβ(3-11)a and Glu³-Aβ(3-21)a in the presence of active human QC resulting in the formation of pGlu³-Aβ(3-11)a and pGlu³-Aβ(3-21)a, respectively. **E** and **F** Mass spectra of Glu³-Aβ(3-11)a and Glu³-Aβ(3-21)a in the presence of active QC and 5 mM Benzimidazole suppressing the formation of pGlu³-formation.

Figure 4: Reaction rates of papaya QC- catalyzed Glu-βNA-conversion plotted against the substrate concentration. The initial rates were measured in 0.1 M pyrophosphate buffer, pH 6.1 (squares), 0.1 M phosphate buffer, pH 7.5 (circles) and 0.1 M borate buffer, pH 8.5 (triangles). The kinetic parameters were as follows: K_M= 1.13 ±0.07 mM, k_{cat}= 1.13 ±0.04 min^{-1} (pH 6.1); K_M= 1.45 ±0.03 mM, k_{cat}= 0.92 ±0.01 min^{-1} (pH 7.5); K_M= 1.76 ±0.06 mM, k_{cat}= 0.56 ±0.01 min^{-1} (pH 8.5).

Figure 5: pH-dependence of the conversion of Gln-βNA (circles) and Glu-βNA (squares), determined under first-order rate-law conditions (S<<K_M). Substrate concentration were 0.01 mM and 0.25 mM, respectively. For both determinations, a three-component buffer system was applied consisting of 0.05 M acetic acid, 0.05 M pyrophosphoric acid and 0.05 M Tricine. All buffers were adjusted to equal conductivity by addition of NaCl, in order to avoid differences in ionic strength. The data were fitted to equations that account for two dissociating groups revealing pK_a-values of 6.91 ±0.02 and 9.5 ±0.1 for Gln-βNA and 4.6 ±0.1 and 7.55 ±0.02 for Glu-βNA. The pK_a-values of the respective substrate amino groups, determined by titration, were 6.97 ±0.01 (Gln-βNA) and 7.57 ±0.05 (Glu-βNA). All determinations were carried out at 30 °C.
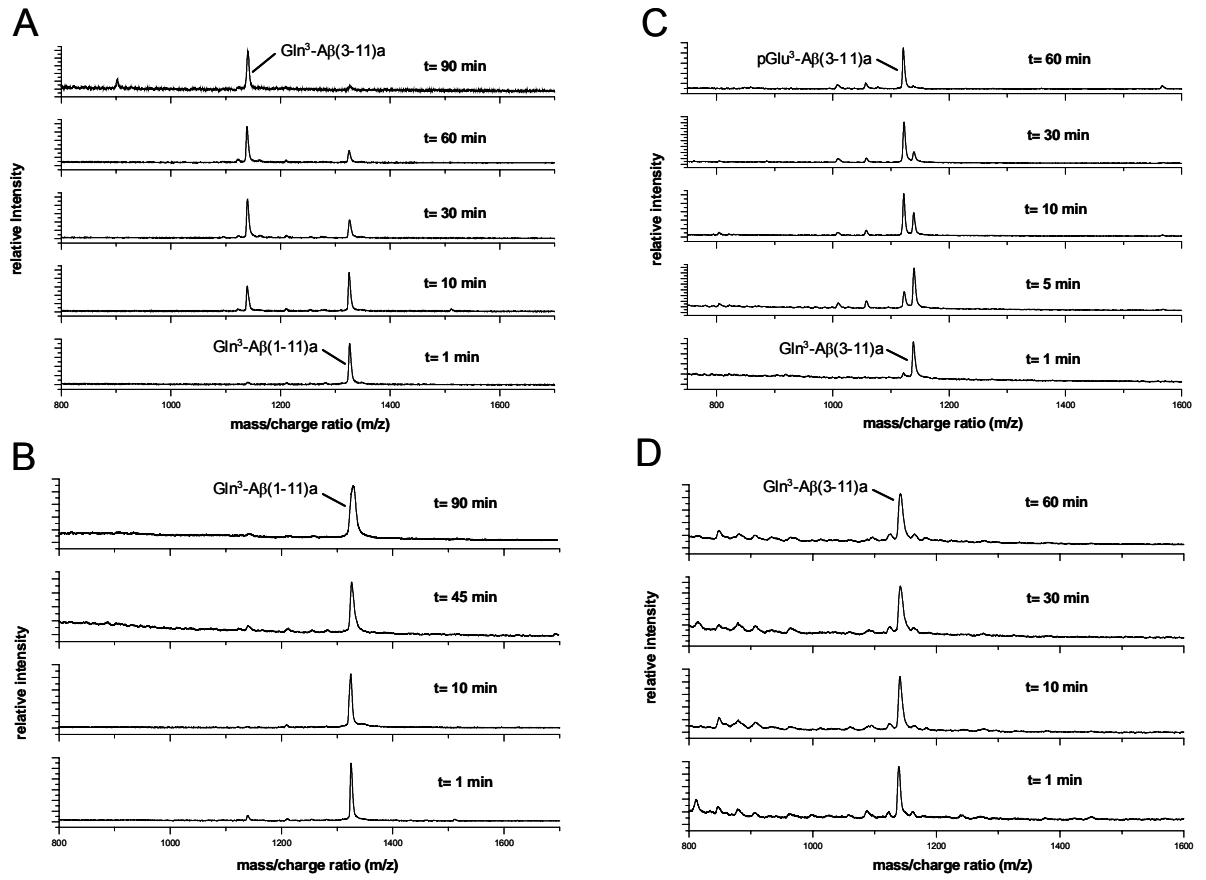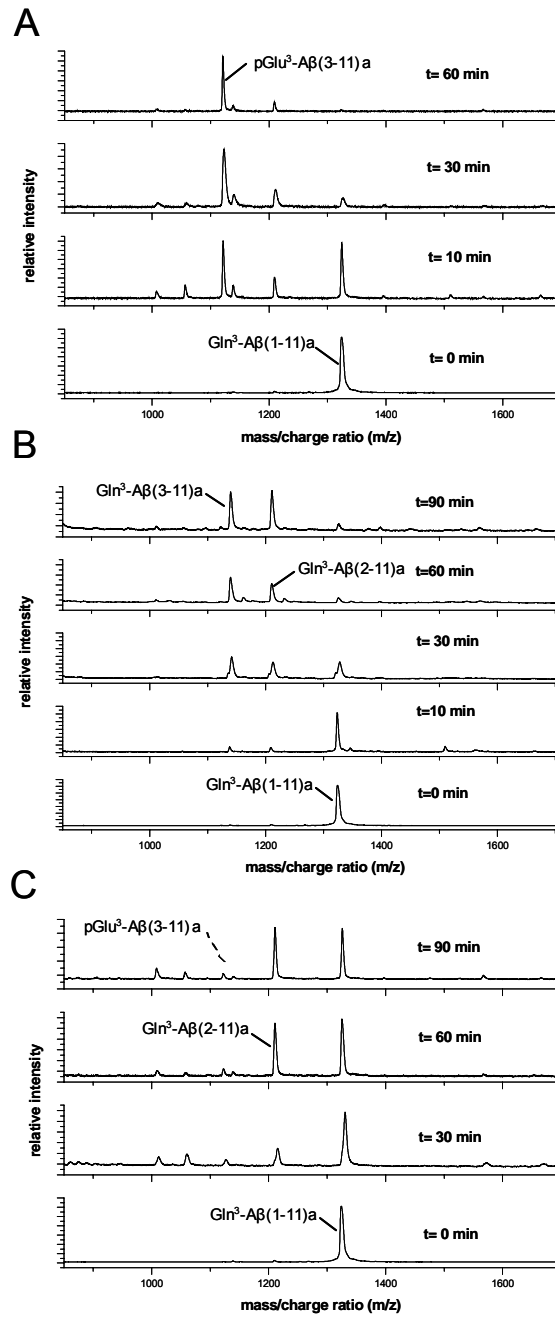
Figure 1
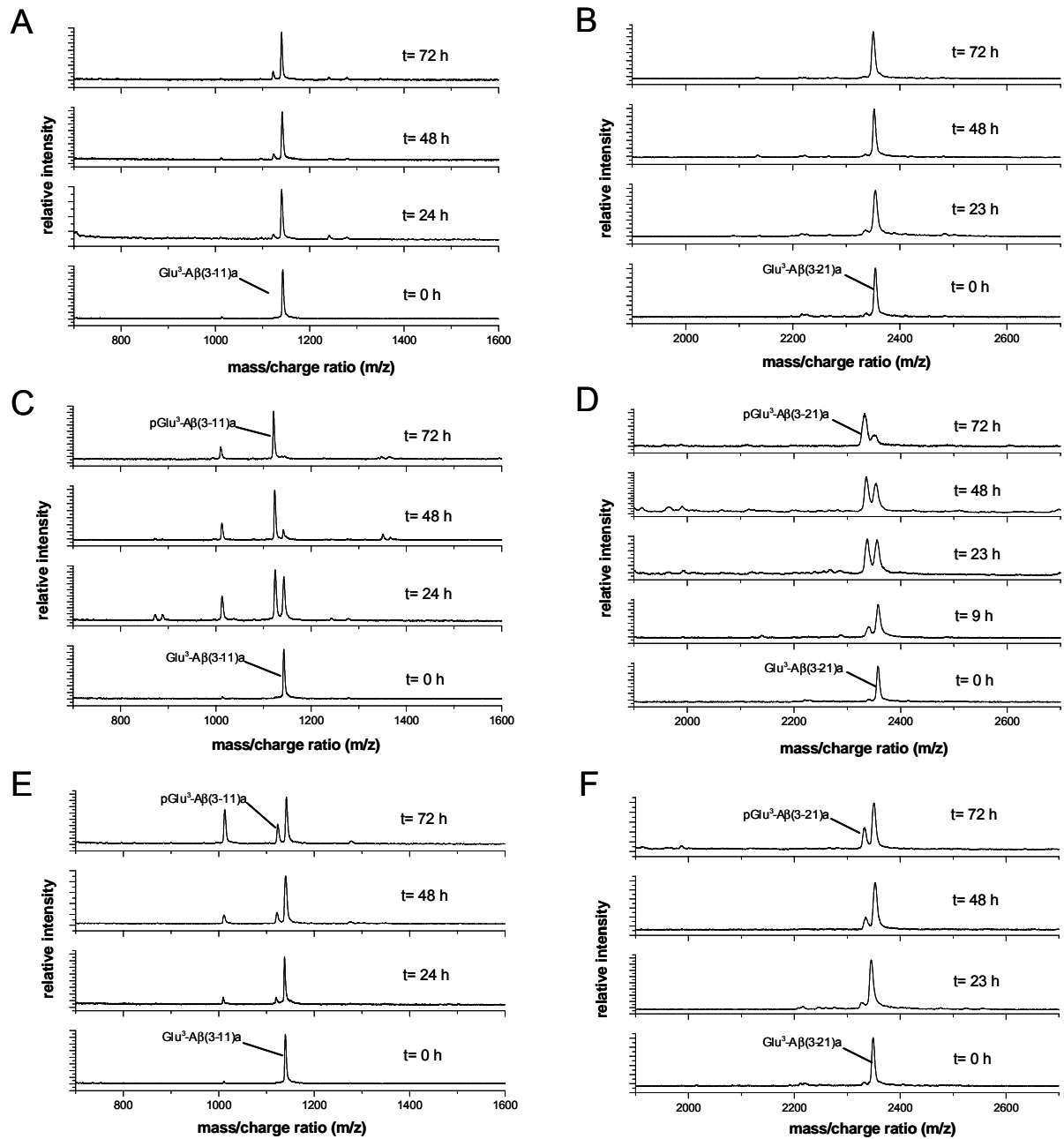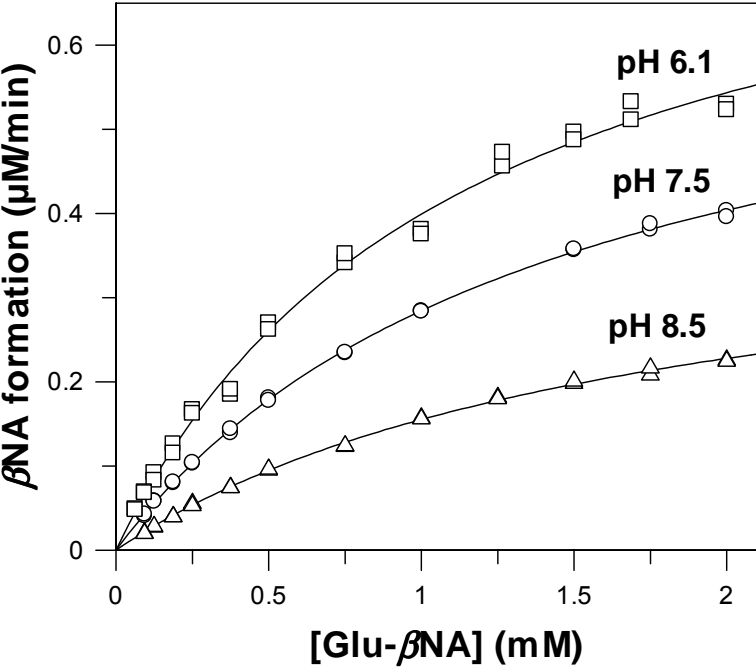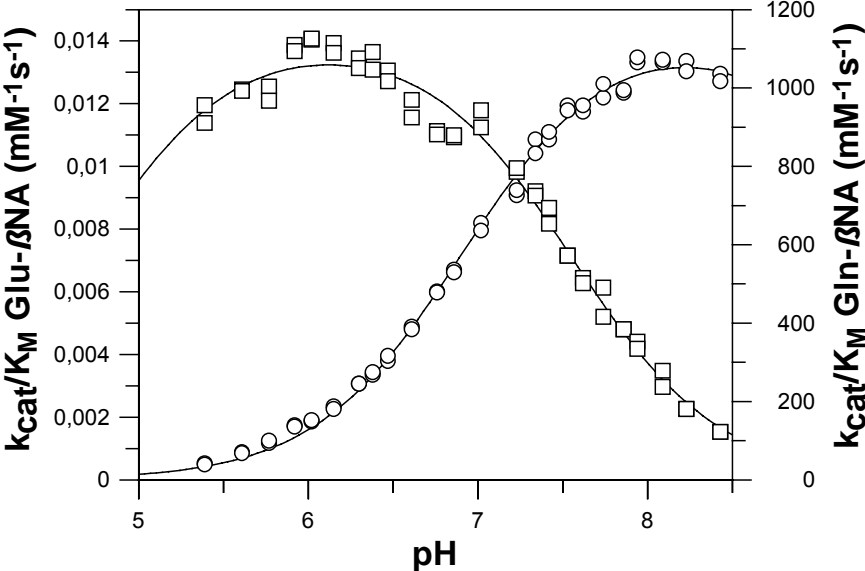
Figure 2

Figure 3

Figure 4

Figure 5

Danksagung

Mein besonderer Dank gilt Herrn PD Dr. Demuth für die Überlassung des interessanten Themas, das entgegengebrachte Vertrauen, das rege Interesse an der Fertigstellung der Dissertation und die Unterstützung bei der Bearbeitung des Projektes.

Herrn Prof. Dr. Wasternack danke ich für wertvolle Anregungen und die Unterstützung bei der Anfertigung der Dissertation und der Publikationen.

Herrn Dr. Hoffmann danke ich für wertvolle Diskussionen und seine tatkräftige Unterstützung bei der Bearbeitung des Themas.

Bei den MitarbeiterInnen der probiodrug AG, insbesondere bei Frau Dr. Manhart, Herrn Dr. Rahfeld und Herrn Wermann, bedanke ich mich für die angenehme Zusammenarbeit.

Meiner Familie danke ich für die mir entgegengebrachte Geduld und Unterstützung, was maßgeblich zur Entstehung dieser Arbeit beigetragen hat.

Lebenslauf

Angaben zur Person

Name: Stephan Schilling

Geburtsdatum/-ort: 30.05.1976, Halle (Saale)

Staatsangehörigkeit: deutsch

Familienstand: verheiratet, 1 Kind

Ausbildung

1982-1990	Polytechnische Oberschule „M. W. Frunse", Halle
1990-1994	Gymnasium „Adolf Reichwein", Halle, Abschluss Abitur
1994-1997	Grundstudium Biochemie, Martin-Luther-Universität Halle-Wittenberg, dazwischen 1995-1996 Zivildienst, ev. Kirchgemeinde Halle-Silberhöhe
1997-2000	Hauptstudium Biochemie, Martin-Luther-Universität Halle-Wittenberg, Abschluss 10/2000 Diplom-Biochemiker, Diplomarbeit: "Isolierung und Charakterisierung von Glutaminyl-Cyclase aus tierischem und pflanzlichem Material", Institut für Pflanzenbiochemie, Prof. Dr. C. Wasternack
1998-2000	Probiodrug GmbH, wissenschaftliche Hilfskraft
seit 10/2000	Probiodrug AG, wissenschaftlicher Mitarbeiter
seit 4/2001	Promotionsstudent der Martin-Luther-Universität Halle-Wittenberg

Erklärung

Hiermit erkläre ich an Eides statt, dass ich die vorliegende Arbeit selbständig und ohne fremde Hilfe verfasst, andere als die angegebenen Quellen und Hilfsmittel nicht benutzt und die den benutzten Werken wörtlich oder inhaltlich entnommenen Stellen gekennzeichnet habe.

Die Arbeit wurde nur an der Mathematisch-Naturwissenschaftlichen Fakultät der Martin-Luther-Universität Halle-Wittenberg eingereicht.

Die der Dissertation angefügten Publikationen umfassen den Inhalt der eigenen Arbeiten und wurden von mir verfasst.

Halle,